DEPARTMENT OF CIVIL AND ENVIRONMENTAL ENGINEERING
IMPERIAL COLLEGE LONDON

The Microwave Induced Pyrolysis of Problematic Plastics Enabling Recovery and Component Reuse

Steven James Goodman BSc.(Hons), MSc., ACSM, DIC

30/09/13

A Thesis submitted for the degree of Doctor of Philosophy of Imperial College London

I, Steven Goodman, confirm that the work presented in this PhD thesis is my own original work.

Signature: Steven James Goodman
Date: 9th June 2013

Supervisor:

Dr G. D. Fowler
Department of Civil & Environmental Engineering
Imperial College London
South Kensington
SW7 2AZ

Copyright

The copyright of this thesis rests with the author and is made available under a Creative Commons Attribution Non-Commercial No Derivatives licence. Researchers are free to copy, distribute or transmit the thesis on the condition that they attribute it, that they do not use it for commercial purposes and that they do not alter, transform or build upon it. For any reuse or redistribution, researchers must make clear to others the licence terms of work

ABSTRACT

Recent trends toward the effective utilisation of petroleum derived materials to increase the sustainability of their use (both for economic and environmental reasons), has resulted in an increased interest in the development of recycling methods for plastics including Acrylonitrile-co-Butadiene-co Styrene and Poly Vinylchloride. The recycling of these waste plastics that include mixed monomer compositions and halogens poses a great problem, with their decomposition making them hard to recycle due to loss of their material properties or through the production of problematic compounds e.g. HCl, PCBs, PCDD, and PCDF etc.

This work has investigated the microwave induced decompositions of these plastics and explored the potential of a carbon (a microwave absorber) assisted microwave decomposition process. This culminated in the examination of the carbon assisted microwave decomposition of ABS and the potential of a one and two step process for the de-hydrochlorination, then pyrolysis of PVC, which is an untried and novel approach for PVC recycling. . The influence of microwave power, exposure time, along with the effect of the proportion of carbon, was investigated for its influence upon the yields of gases, oils, chars and product components. The proportions of gases, oils and chars were quantified in terms of their product distribution and subsequently analysed for their properties/composition by TGA, FT-IR, GCMS, Py-GCMS and bomb calorimetry. From their analyses product distributions in the oils and gases were derived and decomposition mechanisms evaluated.

From these investigations it was found that the microwave decomposition process of both plastics was possible and demonstrated great versatility, with oil yields for ABS of between 2wt.% to 70wt.% and gas yields of 28wt.% to 77wt.% achieved in processing times as little as 3 minutes. From this it was also possible to identify that high quantities of monomer were also able to be recovered, significantly greater than that of a thermal process (39.5%TiC as to 34.5%TiC respectively for styrene monomer).

For PVC, it was identified by initial investigations that the de-hydrochlorination of PVC was possible, confirming results of Ito et al., (2006) and Moriwaki et al., (2006). However, the discovery of amplitude dependent heating was of significant interest, not previously identified in any microwave decomposition process.

It was also recognized that pyrolysis was not possible after de-hydrochlorination of PVC occurred as a result of the reduction in the materials ability to absorb microwaves (lesser dielectric constant), due to chlorine was removal. Hence it was necessary to investigate the use carbon additive to enable achieving sufficient temperatures to induce the pyrolysis of the remaining polyene structure.

The identification of key parameters and ensuing relationships with microwave power, heating rate and temperatures was identified herein, giving the first detailed account of the relationship between specific polymer types and microwaves during a pyrolysis process.

ACKNOWLEDGEMENTS

I would like to acknowledge the Engineering and Physical Sciences Research Council for the financial backing of this PhD. I would also like to thank Symphony Energy for their collaborative efforts. I would especially like to thank my supervisor Dr Geoff Fowler for the opportunity to undertake this PhD programme and his continuing support throughout. It has been a greatly enjoyable experience.

I would like to thank the inhabitants of Room 409, Cheokeroo, The German and Smithers for their support throughout the years and providing me with many varied discussions, jokes and missions to retrieve food. We spent 4 great years together and I shall certainly miss you all.

To Eliana (Bertrude) Athanassiades, and Fei (FeiFei) Zhang, many thanks for the support and company, it was greatly appreciated.

I would like to say a special thanks to Carol Edwards for watching over me in the lab.

I would also like to thank my parents and parents in law for their support throughout the years.

Finally, I would like to say a very special thank you to my dear wife Alice. Without your continuing support I would not have made it this far, I only hope I can do the same for you. You have been my rock!

CONTENTS

1 INTRODUCTION 19

1.1 Background 19

1.2 Motivation and Objectives 24

1.3 Investigation structure 26

2 LITERATURE REVIEW 28

2.1 Plastic Waste Legislation 28

2.2 Current Status of Plastic Recycling within the EU 30

2.3 Plastics 31
2.3.1 Polymer Structure 32
2.3.2 Commodity Plastics 34
2.3.3 Plastics additives 36

2.4 Plastic Recycling and Waste Management 36
2.4.1 Introduction 36
2.4.2 Municipal and Industrial Plastic Waste 37
2.4.3 Recycling Techniques 37
2.4.4 Sorting and Separation Techniques 39
2.4.4.1 Specific Gravity 40
2.4.4.2 Air Clarification 41
2.4.4.3 Triboelectric Separation 41
2.4.4.4 Fourier transform near infrared (FT-NIR) and X-ray detection Separation 42
2.4.5 Primary Recycling (Re-extrusion) 43
2.4.6 Secondary Recycling 43
2.4.7 Tertiary Recycling 45
2.4.7.1 Cracking/pyrolysis 45
2.4.7.2 Partial Oxidation/Gasification 48
2.4.7.3 Chemical Depolymerisation 49
2.4.8 Thermal and Catalytic Decomposition Mechanisms 49
2.4.8.1 Unzipping Mechanism and Random Chain Scissions 50
2.4.8.2 Chain Stripping Mechanism 51
2.4.8.3 Cross Linking 52
2.4.8.4 Effect of Polymer Side Chains 52
2.4.8.5 Mechanisms of Catalytic Degradation 52
2.4.9 Chemical Depolymerisation 53
2.4.10 Quaternary Recycling: Energy Recovery 53

2.5 Microwaves 54
2.5.1 Introduction 54
2.5.2 Dipolar Polarisation Mechanism 56
2.5.3 Effect of Phase 57
2.5.4 Conduction Mechanism 57
2.5.5 Loss Angle 58
2.5.6 Microwave Effects on Matter 59
2.5.6.1 Reaction Temperature and Rate 59
2.5.6.2 Inverted Temperature Profiles 60
2.5.6.3 Accelerated Heating/Thermal Runaway 60
2.5.6.4 Self Limiting Heating 60
2.5.6.5 Superheating Effect 61
2.5.7 Summary 61

3 MICROWAVE EXPERIMENTAL DEVELOPMENT AND DESIGN 62

3.1 Introduction 62

3.2 Experimental Parameters 63

3.3 Reactor Development 64
3.3.1 Microwave Parameters 64
3.3.1.1 Frequency 64
3.3.1.2 Mode 66
3.3.2 Reaction Vessel Design 70
3.3.2.1 Temperature Measurement 70
3.3.2.2 Reactor Material 73
3.3.2.3 Reactor Configuration 74

3.4 Product Capture: Oil/Gas 77

3.5 Conclusion 79

4 EXPERIMENTAL METHODS AND ANALYTICAL TECHNIQUES 80

4.1 Introduction 80

4.2 Materials 81

4.3 Microwave Batch Reactor 82
4.3.1 Experimental Equipment 82
4.3.2 Experimental Procedure 83
4.3.2.1 Polymer Sample Preparation 83
4.3.2.2 Carbon Additive Preparation 84
4.3.2.3 Microwave Pyrolysis 85
4.3.3 Experimental Calculations 87

4.3.3.1 Mass Balances 87

4.4 Model Thermal Pyrolysis 89
4.4.1 Thermal Gravimetric Analysis (TGA/DSC) 89
4.4.2 Pyrolysis Gas Chromatography/Mass Spectrometry 90

4.5 Char Analysis 93
4.5.1 Thermal Gravimetric Analysis/Differential Scanning Calorimetry (TGA/DSC) 93
4.5.2 Carbon Hydrogen Nitrogen Analysis (CHN) 93
4.5.3 Scanning Electron Microscopy (SEM) 94
4.5.4 Fourier Transform Infrared Spectroscopy 94
4.5.5 Pyrolysis-Gas Chromatography/Mass Spectrometry 94

4.6 Oil Analysis 94
4.6.1 Gas Chromatography/Mass Spectrometry (GC/MS) 94
4.6.2 Gas Chromatography/Flame Ionisation Detection - Simulated Distillation (GC/FID-SimDis) 95
4.6.3 Fourier Transform Infrared Spectroscopy 96
4.6.4 Carbon Hydrogen Nitrogen Ration Analysis 96
4.6.5 Bomb Calorimetry 96

4.7 Gas Compositional Analysis 96

5 INVESTIGATION OF THE MICROWAVE DECOMPOSITION OF ACRYLONITRILE-CO-BUTADIENE-CO-STYRENE AND STYRENE 97

5.1 Introduction 97

5.2 Conventional Thermal Decomposition of ABS 98
5.2.1 Thermal Gravimetric Analysis 98
5.2.2 Py-GC/MS 100

5.3 Microwave Decomposition of ABS 104

5.4 Microwave-receptor Induced Pyrolysis 107
5.4.1 Microwave Receptor 107
5.4.1.1 Chemical and Structural Characterisation 107
5.4.1.2 Microwave Response 110
5.4.1.3 Carbon Catalytic Activity 113
5.4.2 Thermal Profiles 114
5.4.3 Product Yield 117
5.4.4 Product Composition 120

5.5 Conclusions 124

6 MICROWAVE DECOMPOSITION OF POLY VINYL CHLORIDE 126

6.1 Introduction 126

6.2 Conventional Thermal Decomposition of Polyvinylchloride 129
6.2.1 Thermal Gravimetric Analysis 129
6.2.2 Py-GC/MS 134

6.3 Microwave Decomposition 142
6.3.1 Introduction 142
6.3.2 Microwave Power 143
6.3.2.1 Thermal Runaway 146
6.3.2.2 Power/Heating Anomalies 152
6.3.3 Optimal Sample Mass 155
6.3.4 Decomposition Residue Analysis 168
6.3.5 Conclusions 172

6.4 Microwave Induced Pyrolysis 174
6.4.1 Carbon Assisted Microwave Pyrolysis of PVC 174
6.4.1.1 Thermal Profiles 174
6.4.1.2 Average Heating Rate 176
6.4.1.3 Product Yields 179
6.4.1.4 Char yield 181
6.4.1.5 Oil Yield 183
6.4.1.6 Gas Yield 188
6.4.2 Product Analysis 191
6.4.2.1 Solid Residue 191
6.4.2.2 Oil 194
6.4.3 Conclusions 205

7 CONCLUSIONS AND DISCUSSIONS 207

7.1 Reactor Design and Methodology 207

7.2 Decomposition of Acrylonitrile-co-Butadiene-co-Styrene 209

7.3 Decomposition of Polyvinylchloride 213

7.4 Concluding Comments 215

8 FUTURE WORK 216

9 REFERENCES 220

10 APPENDIX A 236

11 APPENDIX B 237

LIST OF FIGURES

Figure 2-1 Uses of Celluloid Plastics, the Bakelite phone and billiard balls..... 31
Figure 2-2 World plastic consumption by polymer type (Aguado et al., 2008, Gupta et al., 1998) 32
Figure 2-3 Quantities of Plastics used per Application (Shent et al., 1999). 34
Figure 2-4 Material Chains in the recycling and disposal of plastic waste streams (Tukker, 2002)..... 39
Figure 2-5 Triboelectric charging sequence of plastics on different metal drum types (Diaz and Felix-Navarro, 2004)..... 41
Figure 2-6 Summary of General Decomposition Mechanisms (Beyler and Hirschler, 2002)..... 50
Figure 2-7 End Chain Scission/Unzipping – this is the process by which a single monomer unit can be removed from the end of a polymer chain(Beyler and Hirschler, 2002). 51
Figure 2-8 Random Chain Scission by Hydrogen Transfer Mechanism (Beyler and Hirschler, 2002). 51
Figure 2-9 Chain Stripping Mechanism..... 52
Figure 2-10 Advantages and Disadvantages of Microwaves in materials processing 54
Figure 2-11 Microwave and microwave components (Hayes, 2002) 56
Figure 2-12 Dipolar Polarisation Mechanism..... 56
Figure 2-13 Microwave Conduction Mechanism 57
Figure 2-14 (A) Phase difference which results when energy is converted to heat. (B) The relationship between ε' and ε'', tanδ = ε''/ ε'. (Taken from Lindstrom et al,. 2001)..... 59
Figure 3-1 Pulse Width Modulation achieving a time averaged power application of 250W 65
Figure 3-2 Constant power application by inverter technology..... 66
Figure 3-3 Schematic design of multimode and single mode microwave chambers (Kuhnert, 2002) 67
Figure 3-4 Thermal distribution of water within a single mode microwave cavity after 1 seconds microwave exposure: modelled (top) and measured (bottom) (Sturm et al., 2012). 67
Figure 3-5 Changes in field distribution within a 2.45 GHz microwave oven with ε' = 6.25 (left) and ε' = 9.00 from Santos et al. (2010) 68
Figure 3-6 IR pyrometers optical sight paths for differing models (Calex PyroUSB model number 151 (left), 301 (centre) and CF (right)..... 75
Figure 3-7 IR viewing window design accommodating sight path of Calex PyroUSB-CF (not to scale) 76
Figure 3-8 Final design of microwave reactor enabling measurement of temperature/heating rate by IR pyrometer, maintenance of an inert atmosphere by N_2 purge and evacuation of pyrolysis gases 77
Figure 4-1 Microwave Reactor Design: A) Quartz Reactor with Infrared Sensor Sight Path, B) Quartz Reactor with Gas Flow, C) Microwave Reactor Final Setup 82
Figure 4-2 Retcsh Cryo-mill: Schematic of Cryo-mill (Left) and cutaway of grinding jar (right) (Retsch, 2012)..... 84
Figure 4-3 Microwave Pyrolysis Experiment Glassware: A.) Quartz IR Viewing Window, B.) Quartz Joining Collar, C.) Quartz Bulb Flask and D.) Quickfit Cold Trap 85
Figure 4-4 1.) Rheometric Scientific STA 1500 TGA/DTA and 2.) Schematic of Rheometric STA1500 furnace (Russell et al., 1998), a. hangdown, b. crucible, c. Furnace winding, d. Sample thermocouple and e. Microenvironment cup 90
Figure 4-5 CDS 5200 Pyroprobe, pyrolysis unit 91

Figure 4-6 Pyrolysis units heated coil with quartz sample tube *92*
Figure 4-7 Py-GC/MS final polyethylene test method result *93*
Figure 5-1 Generic Structure of Acrylonitrile-co-butadiene-co-styrene (x,y and z = integers) (Sigma-Aldrich, 2013) *97*
Figure 5-2 Thermal Degradation profiles of ABS under nitrogen atmosphere at 1, 10, 30 and 50°C/min. *99*
Figure 5-3 Differential Thermal Gravimetric Analysis of ABS at 1, 10, 30 and 50°C presented as wt.%/°C vs Temperature *99*
Figure 5-4 Py-GC/MS trace of ABS at when pyrolysed to 500°C at 20°C/min *101*
Figure 5-5 Major organic components structures, as formed during Py-GC/MS of ABS in excess of 500°C at 20°C/min: 1). Styrene, 2). 3-methyl-3-phenyl-azetidine, 3). benzenebutanitrile, 4). 1,1'-(propanediyl)bis-benzene and 5). 1,5-Diphenylhex-3-ene *103*
Figure 5-6 Speciated products of ABS pyrolysis at a maximum temperature of 600°C (by major organic group) *103*
Figure 5-7 Semi quantification of product distribution by TiC of compounds produced from Py-GC/MS to 600°C at 20°C/min *104*
Figure 5-8 Measurements of (a) relative permittivity and (b) loss tangent for ABS and PVC at 11GHz for temperatures between 100 and 400°C (Polli et al., 2009) *105*
Figure 5-9 ABS dielectric properties as derived by Yarlagadda and Chai (1998) for frequencies of 0.5Ghz to 20GHz *105*
Figure 5-10 Mean temperature profile for 5g of ABS exposed to microwave powers of 440, 600 and 850W (standard deviation too low to be displayed) *106*
Figure 5-11 2Θ diffractogram of powdered carbon receptor (as produced in Section 4.3.2.2) *108*
Figure 5-12 Typical FT-IR spectrum of chars produced from coconut husk. *108*
Figure 5-13 Micrographs of carbonised coconut of particle sizes between 500µm and 250µm (after size reduction) at 70x (left) and 1000x (right) magnification *109*
Figure 5-14 Thermal behaviour of carbon char when heated from 0-1000°C at 10°C/min under nitrogen atmosphere (TGA) for raw carbon additive and that which has been exposed to 850W microwave radiation for 10 minutes. *110*
Figure 5-15 Average heating rates (left) and maximum temperatures (right) of 0.5g - 3.0g carbon when exposed to 440W, 600W and 850W microwave power *111*
Figure 5-16 Thermal profiles of 3g carbon samples when exposed to microwave powers of 440W, 600W and 850W *112*
Figure 5-17 Thermal profiles for 5g ABS with either 0.5, 1.0, 2.0 and 3.0g carbon receptor exposed to microwave irradiation at 440W, 600W and 850W *116*
Figure 5-18 Thermal profiles for 5 g samples ABS/carbon receptor with 10, 30, 50, 70 and 90wt% carbon receptor exposed to microwave irradiation at 850W *117*
Figure 5-19 Char, oil and gas yields for 0g-3g carbon, PVC samples exposed to 440W, 600W and 850W *118*
Figure 5-20 ABS oil and gas yields for pyrolysis over the microwave powers of 440W, 600W and 850W for 10wt.% to 90wt.% carbon receptor of a total 5g mass *118*
Figure 5-21 Relationship between maximum temperature and oil/gas yield, as derived from both fixed mass and ratio experiments *119*
Figure 5-22 Semi quantification of product distribution by TiC of compounds produced in a microwave process achieving 414°C *121*
Figure 5-23 Semi quantification of product distribution by TiC of compounds produced in a microwave process achieving 490°C *122*

Figure 5-24 Semi quantification of product distribution by TiC of compounds produced in a microwave process achieving 553°C *122*
Figure 5-25 Speciated products of ABS microwave pyrolysis at a maximum temperatures of 414, 490 and 553°C (by major organic group) *124*
Figure 6-1 Polychlorinated dibenzodioxin (PCDD), Polychlorinated dibenzofurans (PCDF) and Polychlorinated biphenyl (PCB) *127*
Figure 6-2 Generalised model of PVC decomposition from Thermal Gravimetric Analysis (TGA) under nitrogen purge gas at 10°C/min from 0-1000°C *129*
Figure 6-3 Thermal Degradation profiles of PVC under nitrogen atmosphere at 1, 10, 30 and 50°C/min *130*
Figure 6-4 Differential Thermal Gravimetric Analysis of PVC at 1, 10, 30 and 50°C presented as wt.%/°C vs Temperature *133*
Figure 6-5 Differential Thermal Gravimetric Analysis of PVC at 1, 10, 30 and 50°C presented as wt.%/sec vs Temperature *133*
Figure 6-6 Common aromatic species produced during the decomposition of PVC by Py-GCMS *138*
Figure 6-7 Speciated products of PVC pyrolysis at differing maximum temperatures of 200, 300, 400, 500 and 800°C (by major organic group) *139*
Figure 6-8 Semi quantification of product distribution by TiC of Py-GC/MS at 200, 300, 400, ... *141*
Figure 6-9 Change in tan δ of PVC with temperature (Moriwaki et al., 2006a) *143*
Figure 6-10 Mean temperature profile for 5g ± 0.01g of PVC exposed to microwave powers of 440W with standard deviation shown (n=5) *144*
Figure 6-11 Mean temperature profile for 5g ± 0.01g of PVC exposed to microwave powers of 600W with standard deviation shown (n=5) *144*
Figure 6-12 Mean temperature profile for 5g ± 0.01g of PVC exposed to microwave power of 850W with standard deviation shown (n=5) *145*
Figure 6-13 Variation in thermal runaway initiation point as demonstrated by (A.) PVC (Moriwaki et al., 2006a) in which runaway initiates at temperatures between 84°C and 105°C and (B.) Ceramics (Ahmed and Siores, 2001) *145*
Figure 6-14 Heating rates for 5g ± 0.01g of PVC exposed to microwave powers if 440W, 600W and 850W over 18 minutes *146*
Figure 6-15 S- shaped model of thermal runaway as a function of power and temperature profile (Hill and Marchant, 1996) *147*
Figure 6-16 The progressive decomposition of 5g ± 0.01g of PVC when exposed to powers of 440W, 600W and 850W *148*
Figure 6-17 Percentage weight loss of 5g ± 0.01g of PVC on microwave irradiation over increasing duration *149*
Figure 6-18 Percentage weight loss for 5g ± 0.01g of PVC vs. total applied energy in kilojoules *149*
Figure 6-19 A-C: Microwave thermal profiles and decomposition rates of 5g ± 0.01g of PVC for (A.) 440W, (B.) 600W, and (C.) 850W. D: Heating rates as derived from the inflection from the first stage of heating to 200°C vs. decomposition rate from 5g ± 0.01g of PVC at powers of 440W, 600W and 850W *151*
Figure 6-20 Heating rates of PVC samples of 1.25g ± 0.25g at differing microwave powers, from Moriwaki et al. (2006a) *152*
Figure 6-21 The (a) simplified structure of a one dimensional organic polymer ferromagnet and (b) arrangement of spin as illustrated by Zhao and Yao (2000) *153*
Figure 6-22 Microwave power absorption with respect to increasing microwave field strength showing critical threshold behaviour (h_c) (Sparks, 1965) *154*

Figure 6-23 Temperature profile for 10g ± 0.01g of PVC exposed to microwave powers of 440W, 600W and 850W over 10 minutes..... 155
Figure 6-24 Decreasing thermal gradient across PVC sample with increased microwave duration..... 156
Figure 6-25 Temperature profile for 15g ± 0.01g of PVC exposed to microwave powers of 440W, 600W and 850W over 10 minutes..... 157
*Figure 6-26 Percentage weight loss for samples of A.) 5g, B.) 10 g and C.) 15g of PVC when exposed to increasing microwave power and duration for microwave experiments as shown in Figure 4-1 (**Trend given to aid the eye**) 160*
Figure 6-27 Total energy required per gram of weight lost vs. percentage weight loss for microwave experiments utilising 5g PVC at 440W, 600W and 850W..... 161
Figure 6-28 Total energy required per gram of weight lost vs. percentage weight loss for microwave experiments utilising 10g PVC at 440W, 600W and 850W..... 162
Figure 6-29 Total energy required per gram of weight lost vs. percentage weight loss for microwave experiments utilising 15g PVC at 440W, 600W and 850W..... 162
*Figure 6-30 Percentage weight loss for samples of A.) 5g, B.) 10 g and C.) 15g of PVC when exposed to increasing microwave power and duration for microwave Milestone Rotosynth based experiments (**Trend given to aid the eye**)..... 165*
Figure 6-31 Total energy required per gram of weight lost vs. percentage weight loss for microwave experiments utilising 5g PVC at 300W 600W, 900W and 1200W for microwave Milestone Rotorsynth based experiments..... 166
Figure 6-32 Total energy required per gram of weight lost vs. percentage weight loss for microwave experiments utilising 10g of PVC at 300W 600W, 900W and 1200W for microwave Milestone Rotorsynth based experiments..... 166
Figure 6-33 Total energy required per gram of weight lost vs. percentage weight loss for microwave experiments utilising 15g PVC at 300W 600W, 900W and 1200W for microwave Milestone Rotorsynth based experiments..... 167
Figure 6-34 Decomposition rate for 15g samples exposed to 600W, 900W and 1200W utilising the Milestone Rotosynth microwave reactor system 167
Figure 6-35 Liquid decomposition residue formed during the microwave decomposition of PVC analysed by GC/MS..... 168
Figure 6-36 Top ten compounds found in PVC decomposition residue by %TiC..... 170
Figure 6-37 Cumulative speciated liquid decomposition products (by %TiC) from the microwave decomposition of PVC..... 171
Figure 6-38 Simplified typical thermal profile of PVC during microwave induced pyrolysis run..... 175
Figure 6-39 Average heating rates during the thermal runaway phase of PVC pyrolysis over the microwave powers of 440W, 600W and 850W for masses of carbon receptor from 0g to 3g 176
Figure 6-40 Average heating rates during the thermal runaway phase of PVC pyrolysis over the microwave powers of 440W and 600W for 20wt.% to 80wt.% carbon receptor of a total 5g mass..... 177
Figure 6-41 Comparison of equivalent carbon masses average heating rates for fixed and percentage ratio results..... 178
Figure 6-42 Char, oil and gas yields for pyrolysis over the microwave powers of 440W and 600W for 20wt.% to 80wt.% carbon receptor of a total 5g mass 179
Figure 6-43 Char, oil and gas yields for 0g-3g carbon, PVC samples exposed to 440W, 600W and 850W 181
Figure 6-44 Gas yield vs char yield for both fixed carbon receptor masses and ratios, for 440W, 600W and 850W where applicable..... 182

Figure 6-45 Char yield vs maximum temperature yield for both fixed carbon receptor weights and ratios, for 440W, 600W and 850W where applicable 183
Figure 6-46 Oil yields and maximum achieved temperatures vs. weights of carbon between 0 to 3g carbon additive at 440W, 600W, and 850W. 184
Figure 6-47 Oil yields and maximum achieved temperatures vs. percentage weights for pyrolysis over the microwave powers of 440W and 600W for 20wt.% to 80wt.% carbon receptor of a total 5g mass..... 184
Figure 6-48 The relationship between oil yield, maximum temperature and heating rate from 390^{o}C to 480^{o}C for experiments utilising 0-3g carbon additive at 440W, 600W, and 850W (Red = Max. Temp. vs Oil Yield, Blue = Max. Temp. vs Heating Rate, Green = Oil Yield vs Heating Rate, Black = x,y,z co-ordinate).. 185
Figure 6-49 The relationship between oil yield, maximum temperature and heating rate from 1st inflection to 250^{o}Cfor experiments utilising 0-3g carbon additive at 440W, 600W, and 850W (Red = Max. Temp. vs Oil Yield, Blue = Max. Temp. vs Heating Rate, Green = Oil Yield vs Heating Rate, Black = x,y,z co-ordinate)..... 187
Figure 6-50 Yields of oil and gas vs. heating rates from 1st inflection to 250^{o}C for pyrolysis over the microwave powers of 600W for 20wt.% to 80wt.% carbon receptor of a total 5g mass 188
Figure 6-51 Gas yields and heating rates between 1st inflection and 250^{o}C vs. Mass of carbon additive (0-3g) at 440W, 600W, and 850W. 189
Figure 6-52 Arc discharge and quasi spherical plasmas, formed during the microwave pyrolysis process of PVC 190
Figure 6-53 Heating rate vs. gas yield of 5g PVC containing between 0 to 3g carbon additive at 440W, 600W, and 850W. 190
Figure 6-54 Thermal gravimetric analysis of char residues from microwave pyrolysis experiments at 440W for the ratios of 80, 40, 50, 20wt.% carbon with resulting heating rates of 43.48, 176.47, 181.82 and 352.94^{o}C, respectively 191
Figure 6-55 Residual chars form PVC pyrolysis for 80wt.% carbon at 440W under SEM. Top (left): 70x, Top (right): 1000x and Bottom (centre): 4000x magnification..... 192
Figure 6-56 Thermal gravimetric of char residues from microwave pyrolysis experiments at 600W for the ratios of 30, 50, 60, 80wt.% carbon with resulting heating rates of 236.84, 720.00, 782.61 and >1000.00^{o}C, respectively..... 193
Figure 6-57 Residual chars form PVC pyrolysis for 80wt.% carbon at 600W under SEM. Top (left): 70x, Top (right): 1000x and Bottom (centre): 4000x magnification..... 193
Figure 6-58 Semi quantification of product distribution by TiC of oil produced from 440 W carbon ratio experiments, ordered by heating rates as derived from 1st inflection to 250^{o}C (lowest to highest)..... 195
Figure 6-59 Semi quantification of product distribution by TiC of oil produced from 600 W ratio experiments, ordered by heating rates as derived from 1st inflection to 250^{o}C (lowest to highest)..... 196
Figure 6-60 Boiling point distribution of oils derived from the 440W carbon ratio experiments with derived heating rates of 43.48, 176.47, 181.82, 352.94^{o}C/min from 1st inflection to 250^{o}C for 80, 40, 50 and 20wt.% carbon, respectively..... 198
Figure 6-61 Boiling point distribution of oils derived from the 600W carbon ratio experiments with derived heating rates of 236.84, 720.00, 782.61, >1000^{o}C/min from 1st inflection to 250^{o}C for 80, 60, 50 and 30wt.% carbon, respectively..... 199
Figure 6-62 Typical FTIR spectrum of PVC oils from 440W (blue) and 600W (black) ratio experiments. 200
Figure 6-63 Speciated oil constituents with increasing heating rate for 440W ratio experiments semi quantified by %TiC (branched aromatic structures relate to right hand y-axis)..... 202
Figure 6-64 Speciated oil constituents with increasing heating rate for 600W ratio experiments semi quantified by %TiC (branched aromatic structures relate to right hand y-axis)..... 203

Figure 6-65 Formation of aliphatic segments during the dehydrochlorination of PVC (Lattimer and Kroenke, 1982)..... 203
Figure 6-66 Production of volatile aliphatic species (Lattimer and Kroenke, 1982)..... 204
Figure 11-1 Thermal Degradation Profiles of ABS Chars Post Experiments for the Powers of 440W, 600W and 850W 237
Figure 11-3 Thermal Degradation Profiles of PVC Chars Post Experiments for the Powers of 440W, 600W and 850W 238
Figure 11-4 Typical py-GC/MS (0-1000oC at 10,000^{o}C/min) of ABS char residue after microwave exposure 238

LIST OF TABLES

Table 2-1 Structural Formulas of Some Plastics (Shent et al., 1999) 33
Table 3-1 Independent Variables (indicates variable that does not lend itself easily to experimental variation) 63*
Table 3-2 Dependent Variables..... 64
Table 3-3 Properties of 2.45GHz electromagnetic wave (Hokuto Electronics Corporation, 2012) 65
Table 3-4 Material and electrical properties of fused quartz (National-Scientific-Company, 2013)..... 74
Table 3-5 Water condensation yield by the differing condensation system arrangements tested..... 78
Table 4-1 Plastic Polymers..... 81
Table 4-2 List of Solvents 81
Table 4-3 List of Gases..... 82
Table 5-1 Pyrolysis products from the Py-GC/MS of ABS at 500^{o}C or greater under a heating rate of 20^{o}C/min semi-quantified by Total Ion Count (TiC) 102
Table 5-2 Mass loss from 5g of ABS exposed to microwave powers of 440, 600 and 850W 106
Table 5-3 Carbon, Hydrogen and Nitrogen content of coconut and coconut char (n=3) 109
Table 5-4 Theoretical heating rates of differing masses of carbon at microwave powers of 440W, 600W and 850W (assuming no losses of energy) 111
Table 5-5 1-Octenyl-benzene (left) and 1-(Phenylmethylene)-1H-indene..... 121
Table 5-6 Top ten products during the microwave decomposition of ABS attaining a maximum temperature of 414^{o}C..... 122
Table 5-7 Top ten products produced during the microwave decomposition of ABS attaining a maximum temperature of 490^{o}C..... 123
Table 5-8 Top ten products produced during the microwave decomposition of ABS attaining a maximum temperature of 553^{o}C..... 123
Table 6-1 Effect of heating rate on 1st stage of PVC decomposition with decomposition start/finish temperatures, total mass loss, temperature of peak mass loss and mass loss rate..... 131
Table 6-2 Effect of heating rate on the 2nd stage of PVC decomposition with start/finish temperatures, total mass loss, temperature of peak mass loss and mass loss rate 131
Table 6-3 Pyrolysis products from the Py-GC/MS of PVC at 200, 300, 400, 500 and 800^{o}C under a heating rate of 20^{o}C/min semi-quantified by Total Ion Count (TiC) 136

Table 6-4 -3 Pyrolysis products from the Py-GC/MS of PVC at 200, 300, 400, 500 and 800°C under a heating rate of 20°C/min semi-quantified by Total Ion Count (TiC) 137
Table 6-5 Proportion of HCl in mass lost during the initial decomposition of PVC under the microwave powers of 440W, 600W and 850W..... 150
Table 6-6 Summary heating rates and points of inflection as derived from 10g ± 0.01g thermal profiles (Figure 6-23) 158
Table 6-7 Summary heating rates and points of inflection as derived from 15g ± 0.01g thermal profiles (Figure 6-25) 159
Table 6-8 Decomposition products formed during the exposure of PVC to microwave radiation 169

LIST OF EQUATIONS

Equation 2-1 The loss equation..... 58
Equation 2-2 The microwave power absorbed by the dielectric (theoretical formula)..... 59
Equation 3-1 Measurement of microwave power output by the IEC 705-88 method 70
Equation 4-1 Mass Balance..... 87
Equation 4-2 Solid Mass Calculation..... 87
Equation 4-3 Oil Mass Calculation 88
Equation 4-4 Mass of Gases Calculated by Difference..... 88
Equation 4-5 Mass Fractions..... 88
Equation 4-6 Calculated Error (addition and subtraction)..... 88
Equation 4-7 Calculated Error (multiplication and division) 89
Equation 6-1 Radical formation resulting from cleavage of C-Cl bonds on the PVC polymer; as proposed byBockhorn et al. (1999b) and Marongiu et al. (2003). 131
Equation 6-2 Radical Chain Propagation step for de-hydrochlorination as per Montaudo and Puglisi (1991) and Marongiu et al. (2003) 131
Equation 6-3 Microwave power absorption 142

ABBREVIATIONS

ABS	Acrylonitrile-co-Butadiene-co-Styrene
CFCs	Chlorofluorocarbons
CHN	Carbon-Hydrogen-Nitrogen
DCM	Di Chloromethane
DEFRA	Department of Food and Rural Affairs
DSC	Differential Scanning Calorimetry
EfW	Energy from Waste
EU	European Union
FT-IR	Fourier Transform Infrared Spectroscopy
GC/MS	Chromatography/Mass Spectrometry
GC-FID	Gas Chromatography – Flame Ionisation Detection
HDPE	High Density Poly Ethylene
IPW	Industrial Plastic Waste
IR	Infrared
IWM	Integrated Waste Management
LCA	Life Cycle Assessment
LDPE	Low Density Poly Ethylene
LLDPE	Low Low Density Poly Ethylene
MDPE	Medium Density Poly Ethylene
MS	Mass Spectroscopy
MSW	Municipal Solid Waste
PAH	Poly Aromatic Hydrocarbons
PCB	Poly Bi-Phenyls
PCDD	Polychlorinated Dibenzodioxins
PCDF	Polychlorinated Dibenzofurans
PET	Poly Ethylene Terephthalate
PICs	Products of Incomplete Combustion
PM	Particulate Matter
PP	Poly Propylene
PS	Poly Styrene
PSW	Plastic Solid Waste
PTFE	Poly Tetra Fluoro Ethylene
PVC	Poly Vinyl Chloride
PWM	Pulse Width Modulation
Py-GC/MS	Pyrolysis Gas Chromatography/Mass Spectrometry
S.D.	Standard Deviation
SEM	Scanning Electron Microscopy
TG	Thermo Gravimetric
TGA	Thermal Gravimetric Analysis
UK	United Kingdom
UV	Ultra Violet
XRD	X-Ray Diffraction
%TiC	Percentage Total Ion Count

µm	Micro Metres
cm	centimetres
Cm	Column Minutes
eV	Electron Volt
FT-NIR	Fourier Transform Near Infra Red
G	grams
g/cm3	Grams per Cubic Centimetre
g/mol	Grams per Mole
GHz	Giga Hertz
Hrs	Hours
Hz	Hertz
J/Kg	Joules per Kilogram
K	Degrees Kelvin
KJ/mol	Kilojoules per Mole
l/min	Litres per Minute
LN2	Liquid Nitrogen
m	metres
mg	Milligrams
MHz	Mega Hertz
MJ/Kg	Mega Joules per Kilogram
ml	Millilitres
ml/min	Millilitres per Minute
mm	millimetres
MPa	Mega Pascals
Mt	Mega Tonnes
mW	Milliwatts
ng/m3	Nanograms per metre cubed
NOx	Nitrous Oxides
^{o}C	Degrees Celsius
^{o}C/min	Degrees Celsius per Minute
TiC	Total Ion Count
V/m	Volts per Metre
W	Watts
wt.%	Percentage Weight

CHAPTER ONE

1 Introduction

1.1 Background

The development of plastics has had a prolific effect on modern day man, providing the equivalent leap forward as that of metal in the Stone Age. Plastics have provided the perfect material to satisfy almost all mankind's material needs and as such, affected every aspect of our lives. Their continual development has resulted in a vast array of materials with very different physical and chemical properties; however, these attributes have also created a considerable environmental and technological challenge in dealing with the resultant waste generated.

The continual increase of the human population, development of new technology and the modernisation of the Developing World, have all resulted in a dramatic increase in the demand for plastics over the past fifty years. In 1950, the global production of all plastic types was estimated to be 1.5 million tonnes, since this, a year on year growth of approximately 9% has occurred, until 2008, whereby manufacture hit 245 million tonnes a year (Association of Plastics Manufactures in Europe, 2009). This trend is set to continue, if not increase, with accelerating demand from Asian nations, as they develop further and their internal markets for goods increase.

Inevitably the increase in plastic manufacture has gone hand in hand with the production of Plastic Solid Waste (PSW); with most plastic products entering the waste stream within a year of manufacture (Al-Salem *et al.*, 2010). As such society is presented with a growing problem, not only from a logistical view but also an environmental perspective (Zheng *et al.*, 2005).

Within the UK waste stream alone, households and industry generate 1.68 million tonnes of plastic packaging waste each year, all of which has the potential to be completely recycled (Ambrose *et al.*, 2002). As a proportion of plastics in the waste stream, High Density Polyethylene (HDPE) and Low Density Polyethylene (LDPE) represent ~17wt.% and ~12wt.% respectively, Poly Propylene (PP) ~19wt.%, Polyvinyl Chloride (PVC) ~13wt.%, Polystyrene (PS)

~7wt.%, Polyethylene Terephthalate (PET) ~7wt.%, Acrylonitrile-co-Butadiene-co-Styrene (ABS) ~2wt.% and others ~23wt.% (Aguado, 1999, Gupta *et al.*, 1998).

The end of life disposal of these plastics poses a significant problem, due to both the quantities that have been produced and their physical/chemical properties which make them attractive in the first place (Siddiqui and Redhwi, 2009).

The most common ways in which plastics have been disposed of within the Western World has been through the Municipal Solid Waste (MSW) stream. This has most commonly entailed landfill or incineration (Gentil *et al.*, 2009). However, both methods are recognised as posing negative impacts on the environment and are ultimately unsustainable (Denison, 1996).

Until now landfill has been the predominant method of disposing of PSW (Mølgaard, 1995). However, the low specific gravity of plastics presents a considerable problem, with their high volume, low density resulting in a disproportionally large volume of landfill being occupied (Ambrose *et al.*, 2002). This coupled with diminishing viable landfill capacity, plastics' environmental persistence and loss of chemical/calorific value, makes the landfilling of plastic an undesirable, unsustainable option which poses a considerable problem to future generations, if not our own (Lea, 1996).

Within the European Union a steady shift from landfill to incineration and recycling has been observed, being driven by both rising gate fees at landfill sites and increased regulation of the waste sector (Gentil *et al.*, 2009).

This has resulted in incineration taking preference in the elimination of plastics from the waste stream. The plastics themselves are not only considered a waste but provide a rich source of energy within incinerators. With calorific values ranging from 75 to 160 MJ/kg they act as a fuel, enabling operators to run incinerators more cost efficiently (del Remedio Hernández *et al.*, 2007). As such, current incineration methods require plastic in the waste stream to allow for their cost efficient running (Lea, 1996, Wollny *et al.*, 2001). It is further recognised that through incineration the destruction of potentially environmentally damaging chemicals, such as chlorofluorocarbons (CFCs) and other blowing agents can also be achieved (Council, 1999).

Incineration does however present potentially serious health and environmental consequences. The issue of health has been widely discussed and centres primarily on the products of combustion that are emitted from the incineration process; these include but are not limited to dioxins, furans, poly aromatic hydrocarbons (PAH), polychlorinated bi-phenyls (PCB), acid gases, heavy metals and particulate matter (PM) (Buekens and Huang, 1998, Dyke *et al.*, 2003).

However, it has been proven with sufficient legislation and stringent control measures, these emissions can be reduced to concentrations which no longer pose a threat to the environment and human health (Buekens and Huang, 1998, Damgaard *et al.*, 2010). This aside, incineration cannot be seen as a sustainable approach to dealing with the problem of PSW, as it essentially amounts to the combustion of fossil fuels; contributing to the production of the green house gas carbon dioxide (CO_2) and from an energy/solid waste perspective, does not compete with recycling in its ultimate efficiencies (Denison, 1996).

With this in mind, the last decade has seen governments across the globe introducing laws, regulations and targets in the aim of working towards a more sustainable future with regard to PSW. Within the EU regulators have set increasingly stringent standards to reduce the impact of waste plastics. These regulations cover a wide range of sectors. Recent publications such as Directive 2005/20/EC on Waste Packaging and the Directive 1999/31/EC on the Landfill of Waste (Hernandez *et al.*, 2006) have been developed to force industry to reduce the amount of plastic it produces, encouraging more efficient use or diversification away from plastic materials. Nevertheless, plastic still forms a large proportion of the municipal solid waste stream. Ergo, a multifaceted approach to the recovery/maintenance of energy and chemicals from plastics is required.

To achieve this, industry and government continue to develop a vast array of technologies to realise these goals. Nevertheless, as with any industrial process, technical, economic and commercial viability dominate the approach that we take when dealing with PSW when utilising advanced recycling methods. However, short sighted economic gain does not take into consideration the environmental benefits of material recovery/recycling and potential whole system savings.

The resultant methods developed to accomplish this goal are numerous, but they can be readily banded in to four main categories:

1. Primary recycling – the re-extrusion of waste plastics from the plastic manufacturing process.
2. Secondary – mechanical methods are used to separate, sort and reduce the size of single polymer plastic wastes to be fed back into the re-extrusion method.
3. Tertiary – chemical processes which can be used to recover monomer units or produce chemical intermediates of plastics and fuels
4. Quaternary – plastic is incinerated so that the energy can be recovered

Of these methods, primary and secondary recycling has been developed predominantly to efficiently process single type plastic wastes. As such, these processes can only be used to recover material from manufacturing industry; whereby single plastic waste types can easily be collected without fear of contamination or through household recycling in which selective collection has occurred (Wollny *et al.*, 2001).

Nevertheless, these processes do not lend themselves to be easily applied to mixed waste streams, in which issues of polymer quality (by degradation and heterogeneity) and contamination with foreign materials prevails (Ávila and Duarte, 2003). When this occurs, the resultant product is often of inferior chemical and structural properties rendering it unfit for purpose.

As a result, significant interest has been expressed in tertiary recycling to provide a possible solution to the recovery of the chemical resource held within PSW. From this the development of several methods has been pioneered, including chemical depolymerisation, gasification, pyrolytic and catalytic degradation (Aguado, 1999, Tukker, 2002).

The products from tertiary recycling are often hugely varied, dependent on the process and process parameters used (Scheirs and Kaminsky, 2006). As such, much research has been performed to ascertain the conditions which produce the highest value product yields. However, it has been found that current technology is limited in its feasibility, often resulting from, but not limited to, the following factors:

- Plastics have a low thermal conductivity – this results in large amounts of energy required to heat the PSW sufficiently to recover useful hydrocarbon fractions. Further to

this, heating is often slow and wide product distributions are formed, requiring further processing to make a useful product (Kaminsky *et al.*, 1996).

- Heteroatom (non-carbon/hydrogen species) content in specific types of plastics is detrimental to product quality and contaminates chemical intermediates (Cai *et al.*, 1993).
- Often, large volumes of fuel need to be stored on site as a fuel for heating of the reactors, resulting in a large land footprint due to the nature of the technology (Shang *et al.*, 2006).

Despite the aforementioned limitations, these technologies show the greatest potential for the development of methods which could provide a cost and energy effective process for the recovery of petrochemicals from plastics (Bockhorn *et al.*, 1999a, Shang *et al.*, 2006). Of particular interest is the thermal decomposition of organic material under an inert (non-oxidising) atmosphere: pyrolysis.

The pyrolysis of plastic has gained increasing attention in recent years, as it provides a route for the recovery of polymers by converting them into a hydrogen rich blend of oils and gas (Al-Salem *et al.*, 2010). This process can be further manipulated through the adjustment of process parameters or the addition of catalyst so that the production of specific molecular weight compounds can be achieved (Scheirs and Kaminsky, 2006).

Although a viable option, pyrolysis often proves costly, with a requirement for the collection, categorisation and the pre-treatment of plastic waste before entering the pyrolysis process. The pyrolytic stage itself is highly energy intensive (Appleton *et al.*, 2005), resulting from the low thermal conductivity of plastics (Zhou *et al.*, 2006), limitations of current reactor design and the need to attain temperatures of up to 700^{o}C to achieve decomposition of all components in PSW (Scheirs and Kaminsky, 2006).

For pyrolysis to become more widespread, it is necessary to overcome the need for the pre-processing of PSW, reduce the overall energy requirement and minimise the plant footprint. As a first step in attaining this, a revolution is required in the way that energy is transferred to PSW. Ergo, an ideal process would transfer energy directly to the PSW, resulting in better energy efficiencies and moving away from current technology, which is reliant on conductive mechanisms.

A logical step in achieving this outcome would be to utilise electromagnetic radiation, heating the plastic on a molecular level. One approach to realising this proposed process would be to employ the extant technology of microwaves.

Microwaves present several possible advantages over conventional heating methods. These include:

- Volumetric heating: reducing thermal gradients across the material undergoing irradiation with the resulting reductions in product distribution and overall processing time (Ludlow-Palafox and Chase, 2001).
- Direct heating: reducing the energy requirement by eliminating thermal losses in the conduction of heat from reactor to plastic/minimising thermal losses (Appleton *et al.*, 2005, Ludlow-Palafox and Chase, 2001).

  And

- rapid heating: reducing the possibility of secondary reactions occurring during the decomposition process (Al-Salem *et al.*, 2010, Miura *et al.*, 2004).

If this were to be achieved, it would result in the reduction of energy needed per unit of waste processed, decreased plant size and increased energy efficiencies. The subsequent process would then be significantly more cost effective and economically viable. However, little work has been undertaken to investigate this.

As a result of these potential benefits over thermal decomposition, it was proposed to undertake a rigorous examination of the application of microwaves to decompose plastics to produce fuel oils and/or chemical intermediates.

1.2 Motivation and Objectives

The inherently complex nature of plastic waste (alongside its current contribution to global warming and environmental damage), means it poses a significant challenge for society on a personal and global level.

Consequentially, it is crucial that alternatives are found to the current avenues of incineration and landfilling. Hence, the work undertaken in this research has been designed to explore the feasibility of using a microwave process to decompose plastic solid waste (PSW) for the recovery of its chemical and calorific value. With this, the envisaged advantages of increased energy efficiency and liquid product yield, will result in an industrial process with a significant reduction in its environmental impact and increased economic viability; as indicated from the works of Ludlow-Palafox and Chase (2001), Ito *et al.* (2006) and Moriwaki *et al.* (2006a) which the direct volumetric transfer of energy from electromagnetic radiation to heat is observed, with the resultant decrease in product distributions.

Primarily, the work undertaken set out to explore the effect of manipulating the fundamental parameters of microwaves on the decomposition of two major plastic fractions within the PSW stream; these being Acrlonitrile-co-Butadiene-co-Styrene (ABS) and Polyvinylchloride (PVC), representing approximately 21 wt.% of PSW.

Due to the low microwave dielectric properties of each plastic (the ability to absorb the energy from a microwave) at 2.45GHz, research focused on the addition of a microwave receptive material as an initiating agent in the decomposition process, so that the full potential of microwave pyrolysis could be realised.

In the course of investigations experimental parameters have been varied, with the aim of establish ensuing trends. Further to this, the solid/liquid products will be examined for their physical and chemical properties. This included establishing the energetic values of solid/liquid products and identifying product distributions/compositions. This was subsequently compared with the model 'thermal' decomposition of each plastic type; as defined from experimentation and literature, identifying differences/similarities in the underlying chemistry of each process.

1.3 Investigation structure

The structure of the work undertaken consisted of a number of stages. Initially the review of current literature was performed establishing the current state of knowledge and techniques employed in the recycling of plastics. From this it was possible to determine the current state of technology employed in the pyrolysis and gasification processes of plastic waste, determining the application of the technology, it advantages and limitations.

It was the attempted to understand the potential of microwaves and correct use in the pyrolysis of plastics. However, very limited information was available as little research had been performed, with the main authors of Ludlow-Palafox and Chase (2001) and Moriwaki *et al.* (2006a) having looked at the microwave irradiation of plastic waste and PVC, respectively. As such, there is little information available to produce baseline for comparison of results. This is compounded further as little investigation has been performed via conventional thermal pyrolysis on single plastic types as well.

Hence, the first stage of research was to produce a microwave pyrolysis system capable of measuring accurate temperature, collect and condense liquid/gaseous products so that the determination of mass balances can be performed. This is discussed at length in Section 3.

The initial testing took place in which the plastics of PBT, PET, PP, PVC, PS and ABS. These were irradiated with microwave radiation to determine whether it was possible to decompose any of these plastics without the addition of any further material. It was quickly found that only PVC underwent any form of decomposition and that an additive was required to assist in attaining higher temperatures in which decomposition could occur. As such, the inert materials of silicon carbide and carbon were examined for the microwave responses and potential use as an additive to aid in the initiation of plastics decomposition when exposed to microwaves. It was quickly determined that silicon carbide was not suitable as it was unable to heat past 180°C. As such, carbon (char) was used as a microwave receptive additive.

Further testing was performed using carbon with the aforementioned plastics. From this it was discovered that the reactor design and process was not suitable for testing of PBT, PET and PP due to complications arising around the re-polymerisation of these plastics in the condensation system resulting in blockage through the formation of waxes. This also presented the issue that

the correct analytical methods were not available to examine the higher molecular weight re-polymerised material. As such, it was decided that the examination of PVC and ABS would be undertaken with the current experimental setup.

To establish a baseline of the thermal decomposition of these polymers work was performed using the methods of py-GC/MS and TGA to look at the decomposition behaviour and product distribution relating to both heating rate and maximum achievable temperature.

As part of this phase, work was also undertaken to establish the stability of the carbon additive and also its chemical/catalytic activity when mixed with these two plastics. Hence, a good baseline was established.

Experimentation was then performed looking at the microwave decomposition of ABS. It was quickly determined that additives necessary to perform this and as such experiments were designed and undertaken utilising different proportions of additive to the mass of plastic was also the examining the effect of microwave power. The results gained were then used to establish correlations between microwave power amount of additives added, the derived heating rates, maximum temperature and the subsequent mass yields/composition.

The same method was used to then look at polyvinylchloride. However the initial investigations found that polyvinylchloride decomposed eliminating the chlorine from the structure without the need of additive. As such, the initial investigations examined to what extent this could be achieved, hence, the products produced during this. As decomposition could only be achieved while chlorine was on polyvinylchloride, additive was then tested to establish the full decomposition of the polymer and the products attained.

These investigations provided a significant insight into the possibility of using the microwave pyrolysis process for the decomposition of plastics two oil and gas for potential and reuse. Further to this, it provided significant insight to the potential advantages and disadvantages of a microwave pyrolysis process.

CHAPTER TWO

2 Literature Review

2.1 Plastic Waste Legislation

Plastic Solid Waste (PSW) accounts for 12-25% of Municipal Solid Waste (MSW) (Lee, 2006). Within the Western European community it is estimated that the annual consumption of plastic products is almost 100kg per person, totalling 39.1 million tonnes (Aguado *et al.*, 2007). Worldwide the consumption of plastic has reached 250Mt, which is currently growing at 4-8% a year. Of this, approximately 78% wt.% is from thermoplastics (low and high density polyethylene (LDPE and HDPE), polypropylene (PP), polyvinylchloride (PVC) and polyethylene terephthalate (PET). The remaining 23% by weight consists of the thermoset plastics (epoxy resins and polyurethane) (Aguado *et al.*, 2007)

Plastic waste is generated at several points during its life cycle. Initially, they are produced during the plastics manufacture, its use and at the end of its lifecycle. A considerable volume of plastic waste is produced in the pre consumer manufacture of virgin plastics from their raw materials (oil, gas and some natural organic sources). These waste streams are composed of floor sweepings, surface scum from waste water treatment, waste products from the polymerisation process and other such materials. This waste is added to by off-cuts from the industrial manufacturing processes, in laboratory characterisation and development.

The volume of plastic waste generated is still considerably less than that manufactured. This is due to a great deal of plastic being used in long term applications, such as construction, home and office appliances, furniture etc. These plastics may be used over a period of years if not decades before their disposal and as such have not entered into the current waste stream, although will at the end of their useful life.

Nevertheless, the municipal solid waste (MSW) stream does contain large volumes of plastic, arising largely from industrial packaging (agriculture, construction and demolition, electronics etc), household wares, automotive, electronic, and medical waste (Al-Salem *et al.*, 2009, Howell, 1992, Tukker, 2002)

With growing concern from the governing bodies, environmental pressure groups and the general public on the sustainability of current waste disposal practices, legislation has been brought in to control both the volume and type of wastes that can be disposed of. The aim of the legislation is to divert PSW from landfill, reuse when possible end of lifecycle plastics, reduce the production of plastics or diversify away from more environmentally damaging plastics. These instruments are doing this by making it either mandatory to recycle these materials or discourage their use/disposal by making the more inappropriate end of life fates more expensive.

The main instruments in achieving this with the European Union are as follows:

- Waste Framework Directive 2008/98/EC
- Packaging and Packaging Waste Directive 94/62/EC
- End of Life Vehicles Directive 2000/53/EC
- Electronic and Electronic Waste: WEEE Directive 2000/96 /EC
- Restriction of Hazardous Substances Directive 2000/95/EC

All the directives aim to provide a high level of environmental protection whilst ensuring the function of the internal markets. It is intended to be achieved through the use of a hierarchal system which drives resource efficiency and diversion from landfill. This is underpinned by a 5 step waste hierarchy introduced in the Waste Framework Directive 2008/98/EC, in which lifecycles are examined to decide upon the best environmentally viable way of managing waste, considering both its economic and technical viability.

The hierarchy is described in ascending order of importance as:

- Reduce – to not generate the waste in the first place
- Reuse – reuse an item over and over again, for the same function e.g. milk crate
- Recycle – recycling chemical building blocks as a raw material
- Recover – energy / chemical recovery
- Disposal

This provides the opportunity for the European Community to examine and explore new ways of using resources more efficiently than the methods of recovery and disposal. This is further supported/enforced by the introduction of targets which will reduce the amount of waste produced by reduction of materials at source and by the enforcement of recycling targets.

One of the largest changes within all the legislation is that it not only tackles industrially produced waste, but imposes recycling targets upon household and demolition waste, making their scope much more demanding. Further to this, efficient Energy from Waste (EfW) is now classified as recovery rather than disposal, although this is still controversial as it amounts to the burning of fossil fuels. It is not a materials recovery technology.

In conclusion, the legislative frameworks will encourage the development of more efficient practices for the reduction of items which will ultimately become waste. This will inevitably lead to the use of alternative materials and the further development of better recycling practices, both mechanical and chemical. Currently, it may also have the possible negative impact that high calorific value plastics will be diverted to EfW facilities. This will permanently destroy their chemical value and potential for reuse, with the subsequent effect of adding large quantities of CO_2 to the atmosphere and other possible harmful organic chemicals e.g. dioxins.

2.2 Current Status of Plastic Recycling within the EU

As of 2004, statistics indicated that the annual consumption of plastics was almost 100kg per person, resulting in a total of 39.1 million tonnes (A.P.M.E, 2011, Aguado *et al.*, 2008).Of this there is estimated to be a total of 78wt.% corresponding to thermoplastics, primarily low and high density polyethylene, polypropylene, polyvinyl chloride and polyethylene terephthalate. The remaining 22%wt is attributed to the thermosets such as epoxy resins and polyurethane (A.P.M.E, 2011).

When examined through their production, rather than a percentage of waste, it is seen as a world trend that as percentages of plastics are represented as 31wt.% polyethylene (PE), 17 wt.% polyvinyl chloride (PVC), 15 wt.% thermosets, 14 wt.% polypropylene (PP), and 9wt.% polystyrene (PS), with a further 14wt.% comprising of other plastics (Aguado *et al.*, 2008).

The current recovery and recycling rates of plastics are increasing year on year within the EU. Although the statistics that are reported are not necessarily accurate due to the nature in which they are recorded, recording the weight of plastics that are recovered at the kerbside. These can then be exported to a number of locations outside of the EU e.g. China and India. (Aguado *et al.*, 2008).

2.3 Plastics

Plastics have been in use in one form or another from approximately 1600BC. Plastic like material was first discovered by the ancient Mesoamericans when processing rubber into figurines, bands etc (Hosler *et al.*, 1999, Scheirs and Kaminsky, 2006). In time the human race has learnt to manipulate natural polymers from horn, waxes, natural rubber and resin. However, it was only in the 19th Century that modern thermoplastics were discovered and used (Andrady and Neal, 2009)

In 1839, Goodyear discovered vulcanised rubber and Eduard Simon discovered polystyrene (PS) (Scheirs and Kaminsky, 2006). Development continued throughout the 19th Century with the further discovery of natural/synthetic polymers, these included polyvinylchloride (PVC) and viscose (rayon) and celluloids used in such applications as the Bakelite phone, billiard balls etc (see Figure 2-1) (Andrady and Neal, 2009, Scheirs and Kaminsky, 2006) the development of plastics accelerated in the last 50 years of the 20th Century with at least 15 new classes of polymers synthesised and a myriad of subclasses resulting (Hosler *et al.*, 1999).



Figure 2-1 Uses of Celluloid Plastics, the Bakelite phone and billiard balls

The success of plastics has been unprecedented, replacing a vast number of more traditional materials as a result of their versatility in a vast range of applications.

Plastics are currently categorised into natural polymers, natural modified polymers, thermosetting plastics, thermoplastics and biodegradable plastics. Within this wide range, plastics possess a unique range of properties dependent upon their polymeric structure; they are able to be used in a very wide range of temperatures, are chemically and light resistant, strong, durable and can easily be moulded into shape. It is these factors which have driven our ever increasing dependence on plastics, with an annual worldwide demand of 280 million tonnes (A.P.M.E, 2011).

As previously mentioned, there are numerous plastic types available, however, only a handful of these make up the vast quantity produced. Most plastics are currently derived from the thermoplastics due to their high volume and low price. Of these, plastics six plastics account for 75% of the total world demand. These being Low density polyethylene (LDPE), high density polyethylene (HDPE), polypropylene (PP), polyvinyl chloride (PVC), polystyrene (PS) and polyethylene terephthalate (PET). Their relative proportions are shown in Figure 2-2.

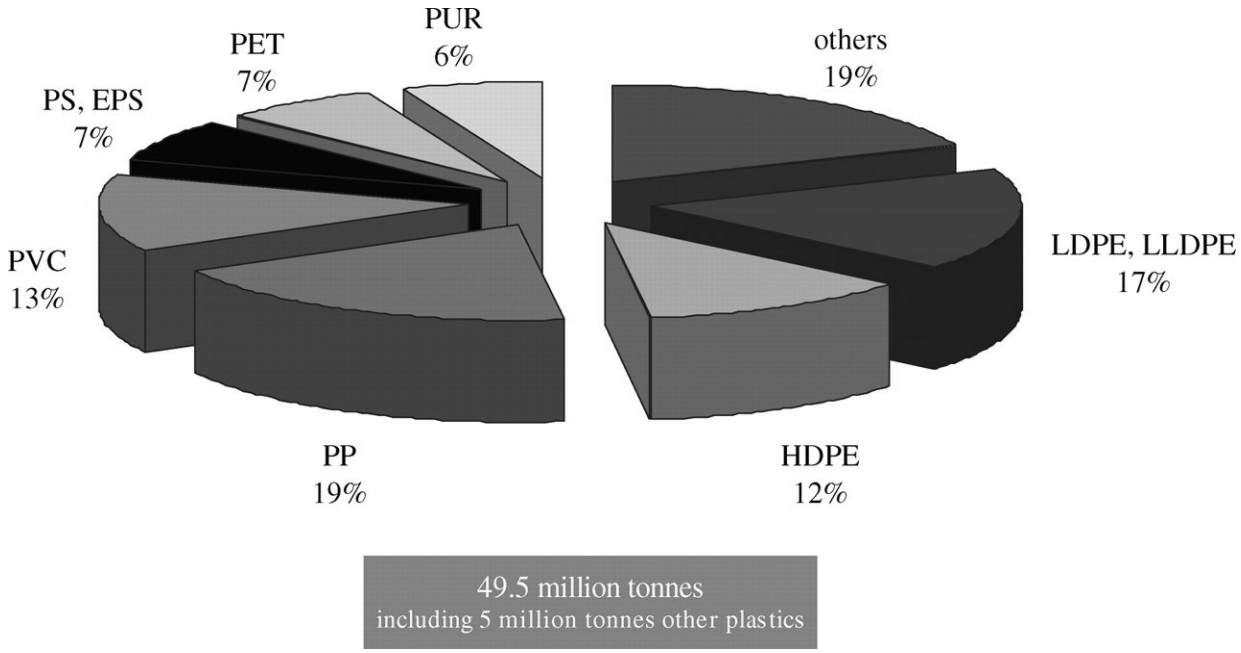


Figure 2-2 World plastic consumption by polymer type (Aguado *et al.*, 2008, Gupta *et al.*, 1998)

2.3.1 Polymer Structure

The typical thermoplastics molecular weights range is 20,000 – 500,000 g/mol, whereas thermosetting plastics are thought to have almost infinite molecular weights (Andrady and Neal, 2009). Plastic is comprised of repeating monomer units making a chain, with each polymer chain containing several thousand units. Thus, mainly contain a small number of elements; these can be carbon and hydrogen alone or with oxygen, nitrogen, chlorine or sulphur in the backbone. The backbone is the main part of the polymer which is constructed by linking together repeating units. The different types of plastic are usually formed by varying the molecular groups "hanging" from

the backbone. The ability to change the side groups on a plastic enable the physical and chemical properties to be readily modified, hence making plastics an indispensable material. The main types of plastics and there monomer units are displayed in Table 2-1.

A number of plastics exhibit crystalline and amorphous structures, giving them a melting point and one or more glass transitions. The plastics which are considered to be semi crystalline in nature include PE, PP, PVC and polyamides, polyesters and polyurethane (Scheirs and Kaminsky, 2006, Shent *et al.*, 1999).

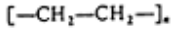
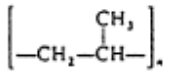
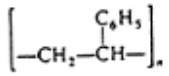
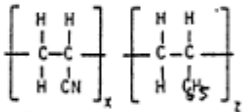
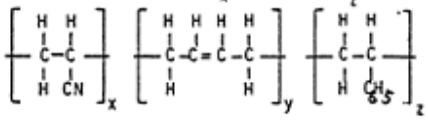
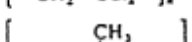
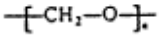
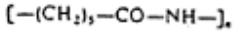
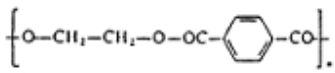
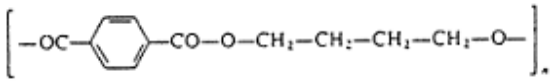
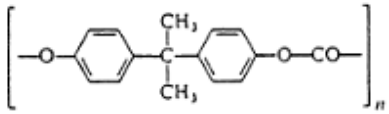
Polymer	Abbreviation	Molecular Category	Formula
Polyethylene	PE	Polyolefin	
Polypropylene	PP	----------	
Polystyrene	PS	Polystyrene	
Polystyrene-acrylonitrile	SAN	Copolymer	
Acrylonitrile-butadiene-styrene	ABS	----------	
Polyvinylchloride	PVC	Vinylchloride	
Polymethyl-methacrylate	PMMA	Polyacrylate	
Polyoxymethylene	POM	Polyether	
Nylon 6	PA6	Polyamide	
Polyethylene-terephthalate	PET	Polyester	
Polybutylene-terephthalate	PBT	----------	
Polycarbonate	PC	Aromatic polymer	

Table 2-1 Structural Formulas of Some Plastics (Shent *et al.*, 1999)

2.3.2 Commodity Plastics

Commodity plastics encompass PP, PE, PVC, PS and PET. Polypropylene is the single most widely used plastic worldwide. It is a cost effective polymer, which can easily be extruded and moulded into a variety of products. It is often used to make crates, storage boxes, blow moulded bottles, caps, window and door frames etc (Brydson, 1999, Andrady and Neal, 2009). A full breakdown of commodity plastics consumption and uses is shown in Figure 2-3**.**

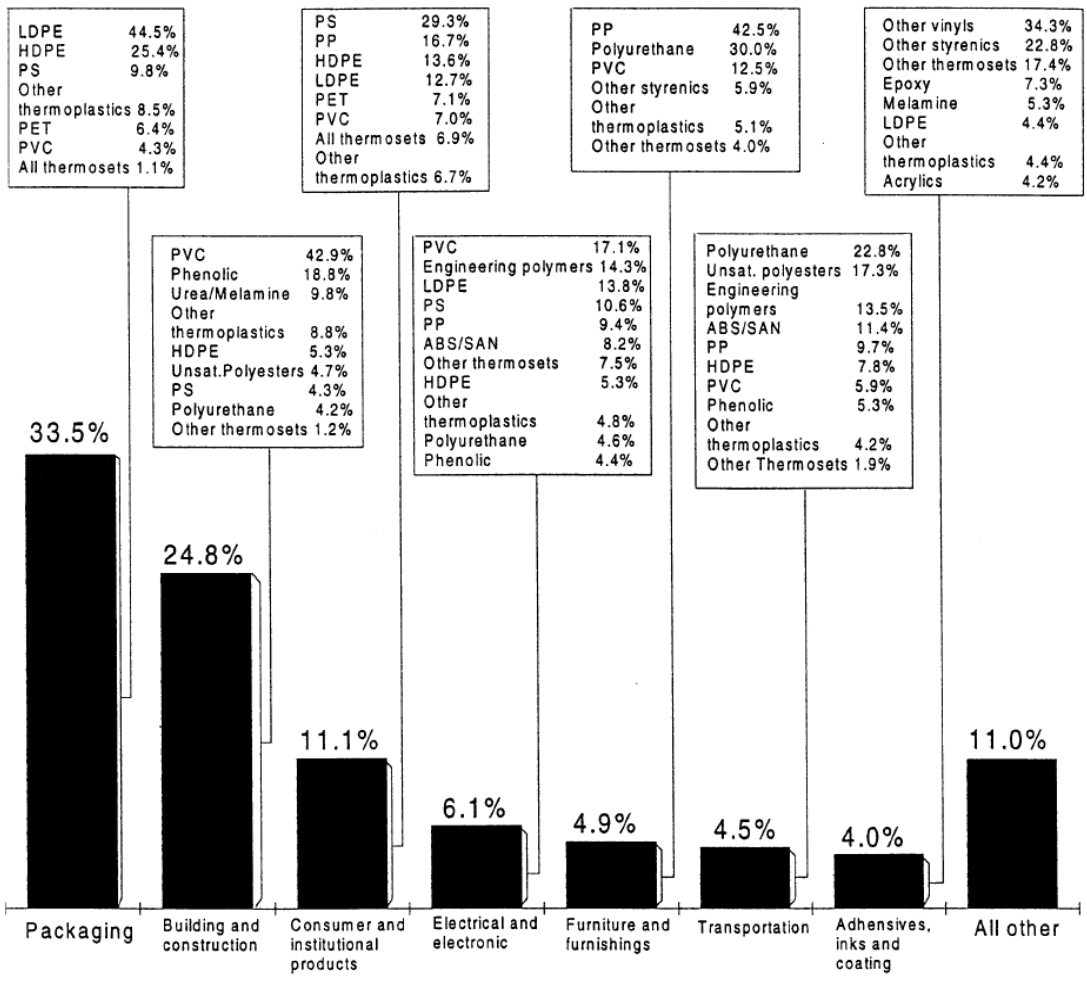


Figure 2-3 Quantities of Plastics used per Application (Shent *et al.*, 1999).

Polyethylene is a similarly structured material to polypropylene. It is the second most widely used plastic globally. It is currently manufactured in 25 different processes making a wide range of polyethylene ranges. One variant of the process involves the use of metallocene to catalyse

polyethylene in its production process. This results in the formation of a much tougher plastic. Polyethylene takes four forms, classified on the density of the resin. These are:

- LLDPE – 0.930 to 0.935g/cm^3
- LDPE – 0.925g/cm^3
- MDPE – 0.93 to 0.945g/cm^3
- HDPE – 0.945 to 0.965g/cm^3

(Brydson, 1999, Scheirs and Kaminsky, 2006, Andrady and Neal, 2009)

Approximately half of all PE produced throughout the world (35 million tonnes) is used to make plastic film, with a further 13-14% used in blow moulded products. The Asian, European and American market consume approximately 25-30wt.% each of the globally produced PE film. Polyethylene is predominantly used in the production of containers ranging from milk cartons to chemical storage barrels. It is also often used as a dielectric insulator in electrical cables (Andrady and Neal, 2009).

Polyvinyl Chloride makes up approximately 13wt.% of the world market of plastic products. It differs greatly from all other plastics due to its chemical composition, containing approximately 57wt.% of chlorine as well as carbon and hydrogen. It is normal practice to blend PVC with a number of ingredients to give a formulation most suitable to the intended use. The chemical properties of PVC make it, to all practical purposes, non-combustible. As such is used greatly in buildings, furniture, pipes etc. Currently world production of PVC is estimated to be at 35million tonnes (Andrady and Neal, 2009, Shent *et al.*, 1999).

Polystyrene takes two forms, general purpose grade and high impact grade. High impact grade PS is modified with polybutadiene hence is chemically different to general purpose grade. PS is widely used as an insulator for buildings and mouldable packaging. It is most commonly used for high value goods, especially electrical e.g. TV's, washing machines, microwaves etc.

PET was first used extensively in the 1970s as a replacement material for glass bottles. Its properties of being highly transparent, glossy, lightweight and resistant to penetration by carbon dioxide made it highly desirable for the fizzy drinks industry. This has resulted in the near full replacement of glass in Europe apart from those applications that require both oxygen and UV

resistance. World demand for PET is currently 14.5 million tonnes per annum and increasing (A.P.M.E, 2011)

2.3.3 Plastics additives

In most plastic applications there is a requirement for addition of chemicals to enhance their performance. These are referred to as additives. Additives can take many forms both organic and inorganic. Inorganic fillers such as carbon and silica are used as reinforcing agents and thermal stabilisers, allowing plastics to be processed at higher temperatures. Further additives include plasticisers to render the material more pliable, fire retardants to discourage ignition and burning, and UV stabilisers to prevent degradation when they are exposed to sunlight. Also additives are added as colorants or matting agents, opacifiers and lusture agents. Additives are often the most expensive component of a formulation, and the minimum quantity needed to achieve a given level of performance is generally used. The additives are intimately mixed with the polymer or 'compounded' into a formulation that is processed into the shape of the final product (Scheirs and Kaminsky, 2006, Aguado *et al.*, 2008, Mølgaard, 1995).

2.4 Plastic Recycling and Waste Management

2.4.1 Introduction

The growing cost and reduction in space available within landfills has increased demand to reduce the volume of plastic waste. This has been further driven by the implementation of the 5 step waste hierarchy as outlined in the Waste Framework Directive 2008/98/EC (previously mentioned in section 2.1). To achieve these targets the application of the combined strategy of reduction at source, valorisation for energy recovery and the application of technologies for the economically viable reuse, recovery and recycling of plastic materials have been developed and implemented for the treatment of plastic solid waste (PSW). Industry has identified a number of key workable technologies for the treatment, recycling and recovery of plastic wastes. These have been demonstrated in the recovery of polyethylene waste for use within the textile industry, where of 388,000 tonnes of required material, 378,000 tonnes were sourced from recovered plastic in 2002 (Al-Salem *et al.*, 2009) and by industry as a whole within the UK, where 95% of all PSW arising from production/manufacturing were recycled in 2007 (Environment-Agency, 2008).

2.4.2 Municipal and Industrial Plastic Waste

Plastic Solid Waste (PSW) can be categorised as either industrial plastic waste (IPW) or municipal plastic waste (MPW). Industrial plastic wastes are plastics which arise from construction and demolition companies (which provide mainly polyvinylchloride waste), electrical/electronics industries and automotive industries. Industrial plastic waste is often advantageous for recovery as it is of high purity and sufficiently free of contamination, and is also available in large quantities.

Industrial plastic waste is highly homogenous in comparison to municipal plastic waste, lending itself towards primary recycling techniques in which re-extrusion and pelletisation can be the most energy and economically efficient method of recycling. However, a lesser percentage of this waste takes a heterogeneous form, which is only viably recyclable by thermal cracking into hydrocarbons (tertiary recycling).

Municipal plastic waste is collected from the households, in which they form multiple plastic waste types. Its composition is highly variable and contains all types of domestic items (TVs, food packaging, electronic equipment cases, drain pipes etc), agricultural plastic waste (hessian sacks, tarpaulin etc), electrical waste (wires, switch casings, light fittings etc), automotive waste etc. As such, plastics in municipal solid waste (MSW) form multiple types (PE, PP, PET, ABS, PVC etc) and are extremely complex mixtures, varying seasonally in their proportions and compositions. Within municipal solid waste, plastics make up 15 – 25% of the total weight (Miskolczi *et al.*, 2004).

Municipal plastic waste is required to be separated from MSW. When dealing with mixed plastics initial separation can be performed using floatation techniques, with those parts having a greater density than water sinking and those with a lesser density than water floating. The plastics which float are usually polyethylene, polypropylene and expanded polystyrene. However, it is not possible to mechanically sort MSW, with no marketable fractions able to be produced to date (Panda *et al.*, 2010).

2.4.3 Recycling Techniques

There are four types of PSW recycling and reuse, categorised as primary (re-extrusion), secondary (mechanical), tertiary (chemical) and quaternary (energy recovery). The type of recycling used is dependent upon a number of factors, varying from location, to physical and

chemical requirements (these are summarised in Figure 2-4). The recycling of plastics can not only be tackled through the development of technologies but also through integrated waste management schemes (IWM).

Integrated waste management is largely based on life cycle assessments (LCA), with them aiding in the selection of suitable technologies and management techniques in the achievement of the goals set out in recovery strategies. In an IWM scheme the main goals set out to control waste generation through reduction in production, decreasing waste generation during manufacturing and recovering chemical/energy value from unavoidable waste arising, whilst maintaining efficient production that will meet the needs of society with minimal environmental impact. Within plastic waste management this is usually achieved through tackling six stages:

1. Waste Generation
2. Waste Handling and Sorting
3. Collection
4. Separation and Processing
5. Transfer Station Handling and Waste Transport
6. Disposal

(Al-Salem et al., 2009)

Within current plastic recycling the overriding factors controlling the methods used are technical and economic feasibility. In this context the overall chain of recycling must be viewed from collection to re-marketing for successful chemical recycling or energy recovery. As such this section will examine each individual form of recycling and recovery on their individual merits and their possible use in future applications.

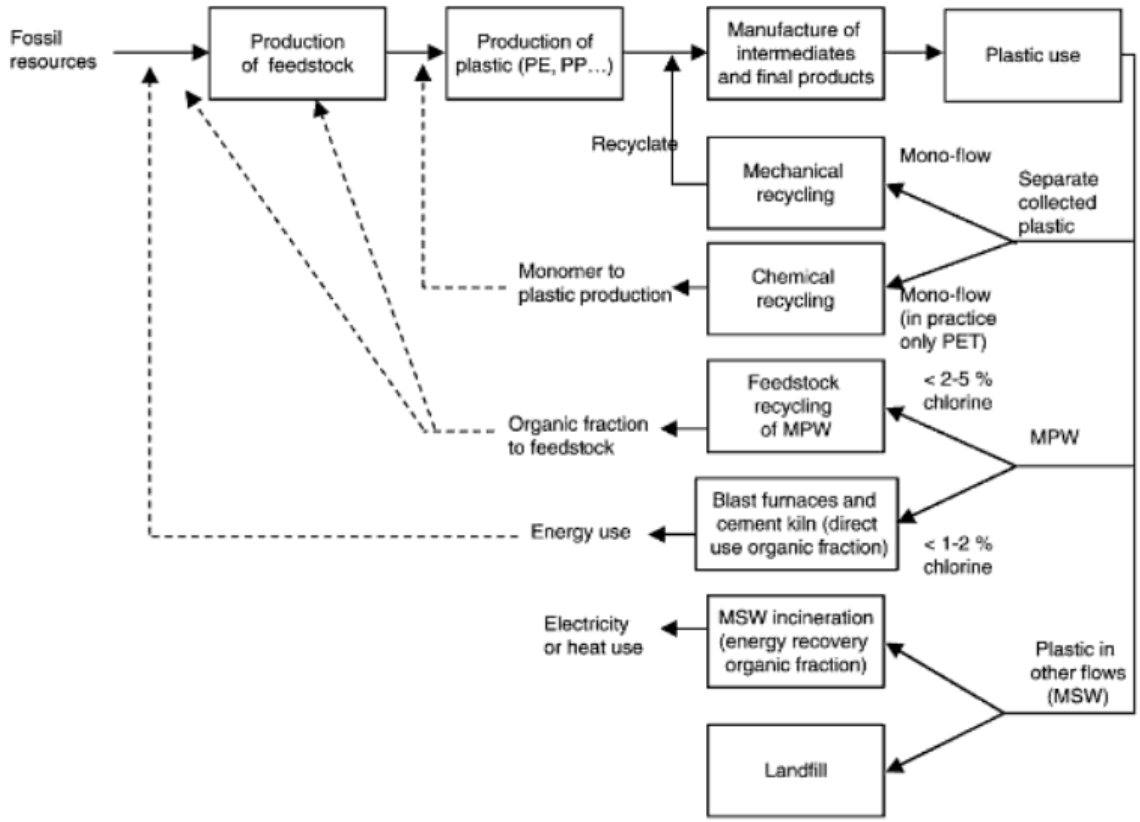


Figure 2-4 Material Chains in the recycling and disposal of plastic waste streams (Tukker, 2002)

2.4.4 Sorting and Separation Techniques

The reuse of plastic is preferable to its recycling; hence a drive has been made to the development and use of multiple uses items, leading to the overall reduction of plastic solid waste (PSW). This can be seen in the UK, where recyclable and returnable plastic crates have quadrupled from 8.5 million tonnes in 1992 to 35.8 million tonnes in 2002. This reduction in the overall demand for virgin plastic also has a number of resulting benefits.

These being:

- the reduction/conservation of fossil fuel
- reduction of energy consumed and PSW generated
- reduction of carbon dioxide (CO_2), nitrogen oxide (NO_x) and sulphur dioxide (SO_2) emissions

(Perdan, 2005)

With the reduction in plastics produced, techniques have also been further developed to recycle the chemical and calorific value of plastic. If the chemical value is to be recovered from plastic waste it must first be separated and sorted. Within these steps the accurate identification of primary plastics and further manual or automated sorting must be performed so that chemical feedstock can be kept as pure as possible.

Sorting is both performed manually and with automated systems. The aim of sorting is to remove glass, metal and paper from the plastic waste stream and any further impurities which will cause contamination of the end product or damage to the processing equipment.

The separation of mixed plastic waste into its constituent types is often limited by the differences in shape, size and the presence of paints/coatings, which can cause problems in their identification and separation both in automated and manual sorting. This results in a greater economic cost to the company trying to recycle plastic and can often turn a potentially economically viable process to one that is not.

A number of methods have been developed to try and reduce the amount of time and investment in the initial sorting step. The most apparent of these can be classified into six different strategies:

- Specific gravity
- Air clarification
- Triboelectric separation
- Fourier transform near infrared (FT-NIR) Separation
- X-ray detection

2.4.4.1 Specific Gravity

Specific gravity separation relies upon plastics having different densities to separate them when in a liquid. However, density sorting methods are limited, because most plastics are similar in density (see Section 2.3.2). However, it is employed in separating PSW arising from electronics (Kang and Schoenung, 2005). The method is still highly limited by variation in density from porosity, fillers, pigments, etc, shape factors of size-reduced particles, and the level of liberation from other materials (MBA-Polymers, 1998). Separation can be assisted by the addition of modifiers to the water to enhance wet ability of the plastics, although this often results in the

contamination of the end plastic and is also very costly. Hydrocyclones are often used within this process to aid in the plastics separation (Kang and Schoenung, 2005).

2.4.4.2 Air Clarification

Air clarification is also used in plastics separation. However, this is a very sensitive process requiring plastics to be prepared extensively so that the shape and size is within given limits. This can be very costly and is not always easy, requiring expensive machinery to achieve it. Air separation has many similarities with specific gravity separation techniques, in that the close range of plastic densities causes numerous problems. Although, this can be easily overcome as the density of air is ~1000 times less than water and much finer tuning of the process can take place.

2.4.4.3 Triboelectric Separation

A more efficient way of sorting PSW is through the method of triboelectric separation. This method relies upon surface charge transfer when plastics are rubbed together. The surface charging sequence of plastics is shown in Figure 2-5.

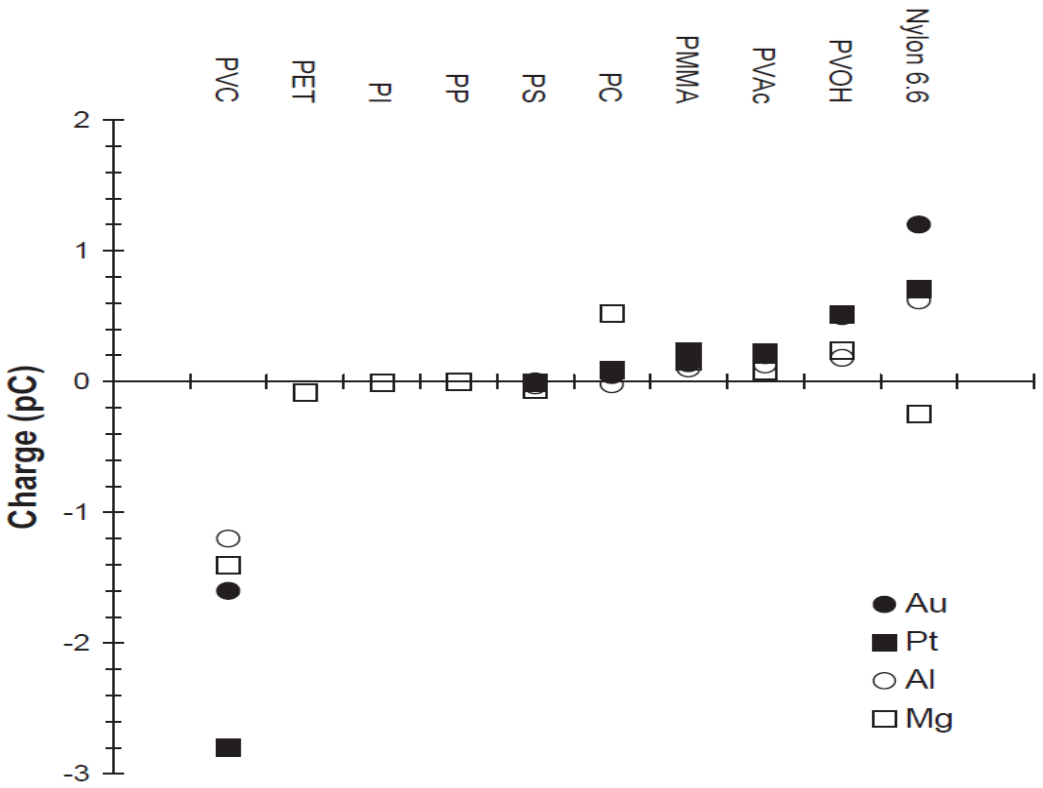


Figure 2-5 Triboelectric charging sequence of plastics on different metal drum types (Diaz and Felix-Navarro, 2004).

In this process one material becomes positively charged and the other negatively or neutrally charged. These can then be separated depending upon this charge. This process is found to work best when dealing with particle sizes of between 2 and 4 millimetres (Xiao *et al.*, 1999). Although the method it limited due to:

- Additives in the same plastic causing it to change position in the charging sequence
- Contamination can work adversely to the charging process
- Mixtures of more than two plastics can result in inefficiency in the charging and separation process
- It is difficult to separate plastics with too slight a charge difference

2.4.4.4 Fourier transform near infrared (FT-NIR) and X-ray detection Separation

Fourier transform near infrared detection relies upon a single waste stream of plastic. It is then used to separate a plastic based on colour recognition. An air conveyor system and system of air nozzles are used to blow the plastics into different hoppers and hence their separation (Hopewell *et al.*, 2009).

In a similar way X-ray systems are used to detect PVC in a waste stream and separate it in the same fashion as above. These techniques are both useful when dealing with a relatively clean waste stream in which they are either devoid of non plastic or wet waste. These are vulnerable though to the multilayer laminated or painted plastics (Al-Salem *et al.*, 2009, Hopewell *et al.*, 2009)

2.4.5 Primary Recycling (Re-extrusion)

Primary recycling is the technique whereby waste plastic polymers of a single type or origin, are reintroduced in to the extrusion cycle to produce similar materials or products(Al-Salem *et al.*, 2009). For this process to be technically and economically feasible, clean plastic waste is required. If not clean the resulting plastics will be contaminated chemically or by debris, often rendering the final product unfit for purpose.

As such, this process is most popular in the industrial plastics manufacturing sector, whereby process scrap which is largely uncontaminated by chemicals or debris can easily be re-introduced to the extrusion cycle. Of 250,000 tonnes of process scrap approximately 95% is recycled through the re-extrusion process (Parfitt, 2002).

Plastics found in municipal solid waste are often not suitable for use in the primary recycling process due to contamination. However, it is possible for plastic household waste to be recycled if they are selectively segregated for collection, although this requires the education and participation of the general public (Al-Salem *et al.*, 2009).

2.4.6 Secondary Recycling

Also known as mechanical recycling, it is the process of recovering PSW by mechanical means. The process can only be performed on single plastic types, for example, polypropylene, polyethylene etc. The waste must be free of any contamination, be it chemical or solid waste. This is essential as it will affect the reformation of the plastic, decreasing its quality, clarity and homogenous nature which are much needed within most industries.

A large problem affecting the quality of mechanically recycled plastic is the inclusion of degraded polymers. These are often as a result of plastics which have been exposed to heat or light, upon which oxidation can occur. In this same process polymer breakdown can occur, with embirtlement from crosslinking of oxidants/radical formation (Fossey *et al.*, 1995).

With mechanical recycling being a costly process, it is essential that the industry reduces the amount of steps required and man hours so that the costs of running the recycling plants are kept to a minimum. With this in mind, the minimum number of stages required can be classified into 8 steps, these are as follows:

1. Cutting/shredding – large plastics are reduced to flakes using shears or saws

2. Contaminant removal – municipal solid waste (paper, dust etc) are usually separated using a cyclone/air clarifiers
3. Floatation – plastics are subsequently separated into there different types using specific gravity flotation.
4. Milling – separated single type polymer plastics are milled to homogenise and size reduce the larger flakes.
5. Washing and drying – the milled flakes are washed to remove any further contamination, with chemicals being added to remove glue and binding agents. This is subsequently rinsed with water and dried.
6. Agglutination – the processed material is collected and pigments/additives added.
7. Extrusion – Plastic is extruded into long strands and pelletised to produce a single polymer plastic.
8. Quenching – plastic is cooled after extrusion and pelletisation.

(Al-Salem *et al.*, 2009, Aznar *et al.*, 2006)

In terms of mechanical recycling there are often variations to the scheme as previously presented but in essence the steps are true to all. There are a number of schemes which recover the value from plastics with a greater economic value than others, the most common of which are applied to polyvinylchloride (PVC) and polyethylene terephthalate (PET).

Polyvinylchloride is mechanically recycled to achieve two forms; rigid and flexible. To achieve this PVC must be sorted properly. It is initially shredded, metals mechanically removed and then classified into its rigid and flexible forms. The rigid form is often used in pipes, garden furniture etc, whereas its flexible counterpart is reduced to a fine powder and used in floor coverings, traffic cones etc (Al-Salem *et al.*, 2009).

Polyethylene terephthalate is recycled in a similar way to other mechanically recovered plastics, apart from during extrusion when it is added to virgin resin so that a clear grade of high quality PET can be produced to compete with virgin polymer. Technology has also been employed so that lesser grades of PET can be re-used via multilayering of plastics, where lower quality PET is not in contact with the contents of a container i.e. food. In applying new recovery techniques, for the use of lower grades in the production of high grade polymer, almost all PET polymer can be recycled through mechanical means (Al-Salem *et al.*, 2009, Hopewell *et al.*, 2009). PET bottles which are collected from households follow a different route to that of industrial PET waste. These require larger amounts of processing to remove impurities, after which they are cleaned, separated and turned in to flakes or granules. These can subsequently be used within the textile industry or made into sheet products via moulding techniques (Al-Salem *et al.*, 2009, Hopewell *et al.*, 2009).

2.4.7 Tertiary Recycling

Also known as chemical recycling, the process refers to the use of advanced technologies to convert plastic materials by depolymerisation to smaller units either in the form of monomers or partial degradation to secondary valuable materials.

These are normally useful for the production of new petrochemicals and plastics (Arena and Mastellone, 2000, Achilias *et al.*, 2008). There are a number of techniques used which are categorised as chemical recycling:

2.4.7.1 Cracking/pyrolysis

Pyrolysis is a form of tertiary recycling. It is the process by which materials are heated under an inert atmosphere to exclude oxygen, product quality and yield (Scheirs and Kaminsky, 2006). In the process of pyrolysis the macromolecular structure of polymeric materials is broken down into smaller molecules, oligomers and monomeric units. These molecules can be further degraded dependent upon the reaction conditions of the system. These can include heating rates, residence time and final temperatures (this is discussed further below).

The pyrolysis process produces a number of products; these are separated into gases, oils/waxes (distillates) and in some cases a char. These products are controlled by the reaction mechanisms and decomposition products in pyrolysis which are dependent upon a number of variables; these being:

- **Plastic composition** – Pyrolysis products relate directly to the composition and structure of the original plastic, and the mechanism by which it decomposes. For this an inert atmosphere must be maintained.
- **Reactor type** – there are two main effects of the reactor type. The first is concerned with heat transfer. With plastics having a low thermal conductivity it is critical that high rates of thermal conduction are achieved. The second effect is concerned with gas and liquid residence time. The residence time of primary products is critical as re-polymerisation of trapped monomers can occur within the reactor.
- **Reaction temperature and heating rate** – it would seem logical to consider these separately, although they both have essentially the same effect; greater temperature and/or heating rate results in higher rates of bond breakage, also discouraging re-polymerisation, hence smaller molecular products are formed.
- **Reaction time –** if products of pyrolysis are in the presence of each other for prolonged periods (greater residence time), then there is a greater chance of re-polymerisation of the

primary products. This results in the formation of aromatic hydrocarbons and coke, all of which are more thermally stable.

- **Operating Pressure** – Lower pressures decrease the number of molecules present for a given volume, decreasing the likelihood of molecular interactions which would form coke and heavier molecules, favouring the formation of lighter and more volatile products.
- **Presence of reactive gases** – this produces heat, reduces the product density, influencing equilibrium, reaction kinetics and mechanisms**.**
- **Additives** – Influence reaction mechanisms and kinetics but generally evaporate or decompose
- **Reaction phase –** Liquid phase pyrolysis reduces the rate at which evolving products escape, increasing the chances that secondary reactions might occur.
- **Catalysts –** provide an alternate pathway in which the energy of activation is less and/or a pathway that favours the formation of a specific chemical or chemicals

(Williams and Williams, 1997, Manos *et al.*, 2000, Scheirs and Kaminsky, 2006, Siddiqui and Redhwi, 2009)

Pyrolysis is largely an endothermic process, requiring large amounts of energy to break bonds; hence the application of heat is often the rate determining property. The process can be split in to three major categories, being:

1. Hydrocracking

Polymers are reacted with hydrogen over a catalyst in a stirred batch system autoclave at ~423-673K and 3-10MPa of Hydrogen. In this process polymer such as polyethylene, polyethylene terephthalate, polystyrene or polyvinylchloride are used, with examples also including mixing with coal, tyres, cattle manure, tyres and waste oil (Achilias *et al.*, 2008, Scheirs and Kaminsky, 2006). With this a number of studies have been performed investigating the effect of transition metal catalysts supported on an acidic solid. With this combination the catalysts perform both hydrogenation and cracking activities. This has resulted in gasoline range products (Scheirs and Kaminsky, 2006).

2. Thermal Cracking

Otherwise known as pyrolysis, the process involves the degradation of polymeric materials in the absence of oxygen. The process takes place between the temperatures of 350^{o}C and 900^{o}C. The 3 product categories formed are solids (in the form of carbonised char), volatile products (which may be condensed to form hydrocarbon oils) and non condensable high-calorific value gases. The proportions in which they form is dependent upon multiple variables e.g. final heating temperature, heating rate, residence time, composition of feed material etc. The process is limited in its use and normally results

in a very broad product range, also requiring high temperatures to achieve the degradation of polymers to the lower molecular weights (Scheirs and Kaminsky, 2006).

The thermal pyrolysis of polyolefin type plastics is a highly endothermic process. It is typically performed at three different temperature ranges; <400^{o}C, 400-600^{o}C and >600^{o}C (Aguado *et al.*, 2008). Higher temperatures are sometimes required to achieve greater product yield. All of which are undertaken normally at atmospheric pressure. A great deal of work has been performed on the less complex structured polyethylene, polypropylene and polystyrene, but with very few pieces of work on the more complex structured materials e.g. polyvinylchloride, polyethylene terephthalate, polyurethane etc (Al-Salem *et al.*, 2009, Panda *et al.*, 2010, Achilias *et al.*, 2008, Siddiqui and Redhwi, 2009). The process results in the poor production of polyolefins within the octane range, favouring higher residue fractions which are of little use as fuels. Further to this the gases produced from the process are unsuitable as fuel (Al-Salem *et al.*, 2009, Panda *et al.*, 2010).

Pyrolysis products are directly linked to the original polymer structure of the feedstock with primary products formed from bond breakage and secondary products from molecular and free radical rearrangements. The secondary processes convert the unstable primary products to more stable, less reactive forms. Hence the products are highly dependent upon temperature, residence time, heating rate, reactor shape etc, with all such parameters effecting reaction kinetics (Scheirs and Kaminsky, 2006).

The products generated can be used in several ways; mainly as fuels, petrochemicals and monomers. These are produced in different fractions dependent upon the mixtures of plastics fed, the fillers incorporated within the plastics and pyrolysis conditions of the reactor. As such the liquid and gaseous fractions, along with upgrading them to commercial specifications, are dependent upon each individual process developed. Most plastics begin pyrolysis at ~300^{o}C. The pyrolysis process is heavily influenced by the presence of additives such as stabilisers, plasticisers and pigments. Most processes are performed at medium temperatures (~500^{o}C) in which the plastics are in the liquid phase (Achilias *et al.*, 2008, Aguado, 1999, Kaminsky *et al.*, 2004, Scheirs and Kaminsky, 2006).

Reaction time is normally controlled relative to reaction temperature with the formation of primary products requiring shorter residence times; more complex/thermodynamically stable structures requiring longer times. The process can be further adjusted using low pressure in which primary products are favoured with secondary products being formed under higher pressure (Scheirs and Kaminsky, 2006, Shent *et al.*, 1999).

The type of reactor plays a critical role in the products formed within the pyrolysis process. However, this is normally dictated by technical considerations i.e. heat transfer and feedstock handling characteristics. In many examples of pyrolysis, polymer is dissolved into a molten bath of polymer or dispersed in a bed of salt, reducing its viscosity. Greater efficiencies in heat transfer reduces the possibility of thermal gradients throughout the polymer feedstock, hence reducing the possibility of wide product distributions (Al-Salem *et al.*, 2010, Panda *et al.*, 2010).

Pyrolysis is advantageous to other processes through its operation, environmental and financial benefits. This is due to the products of pyrolysis; char, oil and gas. The char which is produced can be fed back into the process and used to provide a large proportion of the energy required. Further to this the gases produced require little or no cleaning due to the process itself. Pyrolysis also produces high value calorific fuels which are easily marketed as gas fuels for the production of energy for electricity and heat. A number of disadvantages do arise in the process, mainly pertaining to the handling of chars produced and refinement of oils (Al-Salem *et al.*, 2010, Kiran Ciliz *et al.*, 2004).

3. Catalytic Cracking

With the advantages this method provides it lends itself to the development of a commercially viable process.

Catalytic pyrolysis is essentially the same as conventional thermal pyrolysis except for the addition of catalysts. The catalysis results in an alternative pathway which can provide a different decomposition route of lower activation energy and/or a decomposition route which favours a particular product or products. This can be used to favour the formation of lighter carbon number products with spread of carbon numbers, all formed at a lower temperature (Allred and Busselle, 2000, Gulab *et al.*, 2010, Kumar *et al.*, 2011).

Catalysts are also able to reduce the pyrolysis temperatures and reaction time for a large number of polymers. Further it produces a significantly smaller distribution of resulting chemicals, often reducing the spread from $C_5 - C_{28}$ to products within the gasoiline range of $C_5 - C_{12}$. There is also a tendency for a shift to olefinics being increasingly branched and aromatic formation. It is also seen that the gaseous yield is increased (Aguado *et al.*, 2008, Aguado, 1999, Audisio *et al.*, 1984).

2.4.7.2 Partial Oxidation/Gasification

The partial oxidation by oxygen or steam of plastic waste at high temperatures can result in the production of a mixture of hydrocarbons and synthesis gas (CO and H_2). The quantity of gases and

polyolefin's produced is dependent upon a number of parameters but most importantly the type and proportion of polymer/polymers used. This has advantages over the normal process of combustion due to some of the calorific value being derived from the plastic as heat and also useful fuels/chemical intermediates. It also reduces the production of detrimental gases, such as light hydrocarbons, nitrous oxides, sulphur oxides and dioxins (Al-Salem *et al.*, 2010).

2.4.7.3 Chemical Depolymerisation

A number of plastics can be depolymerised via reversible synthesis reactions, resulting in the production of diacids, diols and/or diamines. Common depolymerisation reactions are glycolysis, and hydrolysis. The resulting yields of monomers are extremely high. This process is often used in the recycling of polyamides, polyesters, nylons and polyethylene terephthalate. However, it is not suitable for polyolefins, which have no functional group and hence are not able to be chemically disassembled in a predictable manner. Hence, approximately 70% of MSW derived plastics cannot be recycled by reverse synthesis (Panda *et al.*, 2010).

2.4.8 Thermal and Catalytic Decomposition Mechanisms

When plastics undergo thermal decomposition they tend to follow radical chain mechanism decomposition (Gao *et al.*, 2003, Kelen *et al.*, 1969, Zhou *et al.*, 2006). This consists of four steps, initiation, propagation, intermolecular hydrogen transfer and termination. In most plastics this process is initiated by random chain scissions, which occur on the backbone of the polymer yielding free radical segments. Although in a number of cases scissions occur at precise points on the polymer chain, resulting in monomers being produced which can be recovered (Ballice, 2001). Only certain plastics, being PS and PTFE, are feasible for monomer recovery (Kaminsky, 1991). Non-chain scission reactions involving elimination of small molecules and double bond formation also occur. After the initial process of random cleavage, further intra and intermolecular reactions and secondary reactions occur in the gas phase, which can lead to the formation of a broad carbon chain distribution (Ballice, 2001, di Cortemiglia *et al.*, 1985, Gao *et al.*, 2003, Kiran Ciliz *et al.*, 2004).

Under isothermal decomposition conditions, activation energies are observed to be a strong, decreasing function of conversion. This was explained by (Mamleev *et al.*, 2000). He stated that the initial stages of polymer decomposition were accompanied by softening, which can be controlled by the process of formation of the gas phase within the solid and by nucleation/nucleus growth. The concentration of nuclei at fast heating rates is very low, resulting in isothermal decomposition being limited by nucleation only (Vyazovkin, 1996). In non isothermal decomposition this is limited by nuclei growth only as heating rates are low, therefore in the initial stages in depolymerisation the activation energies may increase or decrease, for non isothermal and isothermal respectively. It has also been reported by a number of authors, that the gaseous products play an important role in the

reduction of activation energies in the course of decomposition (Flammersheim and Opfermann, 1999, Vyazovkin, 1996).

In non-isothermal decomposition the two opposite effects of nuclei growth and gas diffusion make the activation energy a weak function of polymer conversion, being attributed to the formation of porous solid which allows for the diffusion of gases at a higher rate (Saha *et al.*, 2006).

The thermal decomposition of polymeric substances cannot be easily described by simple empirical formulas due to the complex nature of the reactions occurring. Thus the mechanisms of decomposition have been simplified and proposed as a number of basic steps. These are summarised in Figure 2-6.

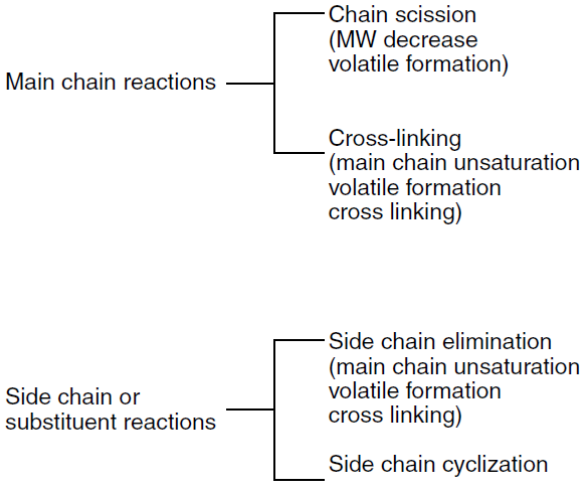


Figure 2-6 Summary of General Decomposition Mechanisms (Beyler and Hirschler, 2002)

2.4.8.1 Unzipping Mechanism and Random Chain Scissions

In simple thermoplastics, the most common thermal decomposition mechanism is a result of breakages in the main polymer backbone (main carbon chain). These can occur randomly within the chain (random chain scissions), or at the end which will result in the formation of monomer units. End chain scissions are often referred to as chain unzipping due to it being the reverse of the polymerisation process, with single monomer units being removed from the end of the chain. There is no transferral or re-arrangement of material in and/or between polymer chains (see Figure 2-7).

Random Chain scission/fragmentation occurs within and between simple polymers and more complex chain structures. The random nature of the breakage is a result of bond strengths being equal along the length of the hydrocarbon chain. The decomposition can follow two mechanisms (see Figure 2-8):

1. An ‘intramolecular’ hydrogen transfer occurs between an end chain radical site and the nearest available hydrogen. This normally occurs between one and four monomer units away dependent upon steric hindrances (Beyler and Hirschler, 2002)

2. An intermolecular hydrogen transfer can occur between polymer chains. The original radical abstracts a hydrogen from another polymer chain. The likelihood that the radical site will abstract hydrogen from within the polymer chain results in chain breakage. (Beyler and Hirschler, 2002).

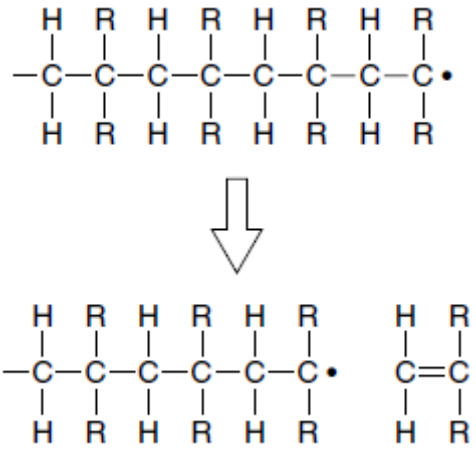


Figure 2-7 End Chain Scission/Unzipping – this is the process by which a single monomer unit can be removed from the end of a polymer chain(Beyler and Hirschler, 2002).

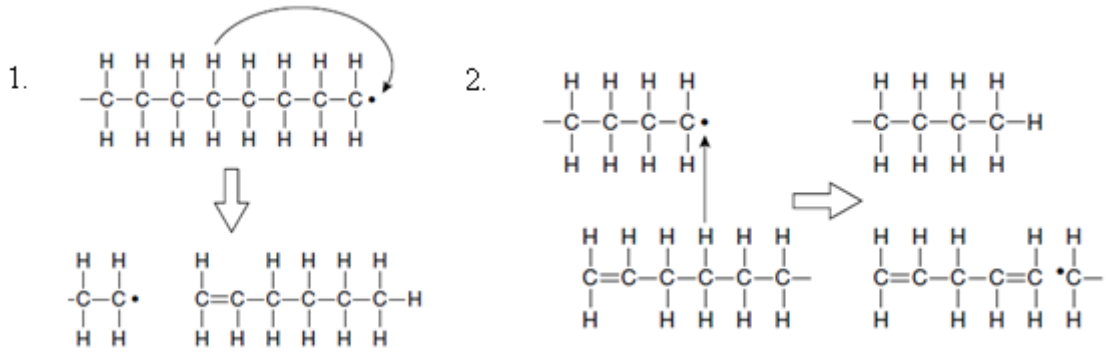


Figure 2-8 Random Chain Scission by Hydrogen Transfer Mechanism (Beyler and Hirschler, 2002).

2.4.8.2 Chain Stripping Mechanism

The mechanism of chain stripping/elimination is responsible for the formation of a vast number of products formed during pyrolysis. It is the process by which atoms or side chains are cleaved from the polymer backbone. This occurs when the bond strengths of side chains are considerably less than that

found in the polymer backbone. When the polymer is heated the side groups break off at a critical temperature leaving the polymer backbone untouched (Kiran Ciliz *et al.*, 2004, Bockhorn *et al.*, 1999c). This is shown in Figure 2-9.

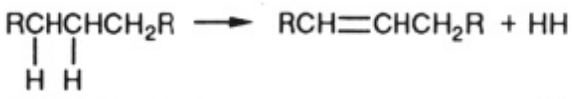


Figure 2-9 Chain Stripping Mechanism

2.4.8.3 Cross Linking

The last type of decomposition mechanism which is considered to be of greatest influence in the thermal decomposition of polymers is cross linking. Cross linking occurs in thermosetting polymers when they are heated to high temperature and thermal stripping occurs. The stripped polymer backbone can form linking bonds which result in a chain network of a higher molecular weight, for example char (Panda *et al.*, 2010).

2.4.8.4 Effect of Polymer Side Chains

Polymer side chains are highly influential in the product distribution from polymer thermal decomposition. These groups can act in two different ways, by elimination reactions or by cyclisation reactions. In an elimination reaction the side chain is cleaved from the polymer backbone with the bond breakage and the side groups will often reacting with other eliminated side groups. The resulting products are often highly volatile. When cyclisation occurs, two adjacent polymer side groups react to form a bond between them, resulting in a cyclic structure (Kiran Ciliz *et al.*, 2004, Tsuchiya and Sumi, 1969).

2.4.8.5 Mechanisms of Catalytic Degradation

A number of studies have examined the effect of catalytic pyrolysis. The catalysts which have been investigated and presented the most promising results were all acidic in nature. The mechanism by which the chemistry occurred was related to carbonium ions, with different steps seen to occur including hydrogen transfer, chain (beta) scissions, isomerisation, oligomerisation/alkylation and aromatisation, all of which are controlled by the acid site strength, density and distribution (Corma, 1995). The acidity of the catalyst has been characterised using Bronsted and Lewis theory by a number of authors, examining the effects on polyolefinic materials. This has been further examined for the microcrystalline structure of zeolitic materials, where the acidic sites are contained within the microporous structure of the solid. Hence the porosity of the solid catalyst is critical in its function (Armaroli *et al.*, 2000, Cerqueira *et al.*, 2000).

It has been also proposed that free radical mechanisms of catalytic degradation can occur. This was observed by Sekine and Fujimoto (2003) during the catalytic pyrolysis of polypropylene. During the decomposition it was observed that methyl primary and secondary radicals were formed, with hydrogen abstractions and recombination of radical units forming methane, olefins and monomers.

Catalyst type is a critical factor in the decomposition of polymeric materials, although a number of 'process' factors also heavily influence the products produced. These include: the composition of feedstock; the effect of catalyst loading; the catalyst contact mode; the catalyst particle size and the type of reactor. These factors are discussed extensively by (Panda *et al.*, 2010) and consultation of this study is advised for further information.

2.4.9 Chemical Depolymerisation

Chemical depolymerisation is the process by which a polymer is reacted with a reagent to break linkages to produce (ideally) the starting monomers. Five main methods are employed in achieving this, Hydrolysis, Glycolysis, Alcoholysis, Franctionation and Aminolysis (Zia *et al.*, 2007)

The process is limited to a number of polymers known as the condensation polymers, primarily the polyesters like PET. It cannot be used on such polymers as polyethylene, polypropylene or polyvinylchloride (Aguado *et al.*, 2000).

Problems occurring with these technologies are primarily concerned with the presence of impurities in the raw plastics. These are found to interfere with the depolymerisation mechanisms or take part in the subsequent reactions affecting the final outcome of the recovered product (Aguado *et al.*, 2000)

There are several examples of chemical depolymerisation being used in European industry, these being the PETCORE system, the Eastman Chemical Company and the Du Pont Process. All of these processes require a pre-treatment step to remove unwanted chemicals and impurities from the collected plastics. The acid hydrolysis (phosphoric acid) of Nylon 6 is also utilised by the German company, Zimmer and Lurgi (Tukker, 2002).

2.4.10 Quaternary Recycling: Energy Recovery

Energy recovery is a process most often reserved for heterogeneous waste streams, where methods of separation are too costly and time consuming to make the treatment of individual waste types viable. For this reason the only method currently available for recovering the value of PSW from the municipal solid waste stream is through the method of combustion. Plastic solid waste is derived from

crude oil and therefore has a high calorific value. This makes it a particularly attractive and convenient source of energy for incineration facilities.

Upon combustion of PSW the volume is reduced considerably, approximately by 90-99%. This has the advantage of reducing the volume of waste being sent to landfill. Incineration has the added advantage that it is able to destroy production agents such as CFCs which were used as a blowing agent in expanding foams that would otherwise escape into the atmosphere propagating ozone depletion (Denison, 1996, Dyke *et al.*, 2003, Wollny *et al.*, 2001)

Many governments are encouraging the use of incineration as a viable option for a disposal route of PSW, this is demonstrated by the UK Government whereby the Department of Environment, Food and Rural Affairs (DEFRA) set targets in 2006 that 25% of MSW (which includes PSW) to be incinerated by Energy from Waste (EfW) plants by 2020. With current waste compositions this equates to approximately 700MW of reliable electrical capacity (DEFRA, 2006).

2.5 Microwaves

2.5.1 Introduction

Microwave heating is currently used within a number of industrial fields/processes. These consist of mainly meat tempering, bacon cooking and rubber vulcanisation (Clark and Sutton, 1996). Microwave heating holds a number of advantages and disadvantages for industrial applications, these are summarised in Figure 2-10.

Advantages

- Reduction in time and energy used
- Precise, controlled heating
- Selective heating
- Rapid heating of thermal insulators
- Volumetric uniform heating
- Short processing times
- Reduction of hazardous emissions
- Self limiting heating in some materials
- Synthesis of new materials

Disadvantages

- Accelerated thermal runaway
- Heating low in poor absorbing materials
- Self limiting heating in some materials
- Ineffective transfer of microwave energy
- Arcing and control of plasmas

Figure 2-10 Advantages and Disadvantages of Microwaves in materials processing

Within industry, microwaves have been used in a limited number of applications. This has not been due to limitations of the equipment, but more related to the fact that up until now energy costs (fossil fuels) have been relatively cheap. The most common application to date has been in the vulcanisation of rubber. In the 1980s an increase in microwave research occurred whereby a number of investigations were performed on ceramics and polymers (Sutton *et al.*, 1988). Within some of these investigations the "microwave effect" was first discovered. This indicated that microwaves could be used in the sintering of Al_2O_3, but at much lower temperatures than in electric resistance heating, apparently reducing activation energies. This has been seen as a common effect in materials processing with microwaves, causing much controversy within the scientific community. It is still at argument whether the results are correct or are limitations being seen in temperature reading equipment (Wallace *et al.*, 2006b).

Microwaves are electromagnetic waves created when high frequency electrical disturbances occur of 300MHz – 300GHz or wavelengths between 1mm and 300mm. Microwaves are commonly used for heating, telecommunication and radar equipment. These applications are strictly regulated to stop interference with communication equipment. For microwave heating the frequency of 12.2 cm or 2.450 (±0.050) GHz (household) and 31.56 cm or 0.95 GHz (largely industrial) is used (Lidström *et al.*, 2001). There are also a number of frequencies which are reserved for industrial, scientific and medical applications (Zong *et al.*, 2003).

Microwaves obey the basic laws of optics and can be transmitted, absorbed or reflected, but differin the fact that they are coherent and polarising. A material's ability to absorb microwave energy is directly related to its conductive properties, hence materials which are poor conductors are effectively transparent to the incident waves and do not store any of the energy in the form of heat (Xia and Picklesi, 2000). Metallic materials merely reflect microwaves hence no appreciable heating occurs, although a current can be induced. However, at room temperature materials with a conductivity of typically 1-10Sm^{-1}, such as semiconductors, can be heated effectively. Although, if the temperature of the system is increased, insulators can couple with microwaves more effectively (Lidström *et al.*, 2001). To understand why this phenomenon occurs we must consider the mechanisms of microwave dielectric heating further.

Microwave radiation can be divided into its individual components; the electric and the magnetic field components (See Figure 2-11). The electric field component is responsible for the microwave heating of materials through two mechanisms, the dipolar polarisation mechanism and the conduction mechanism (Baden Fuller, 1979).

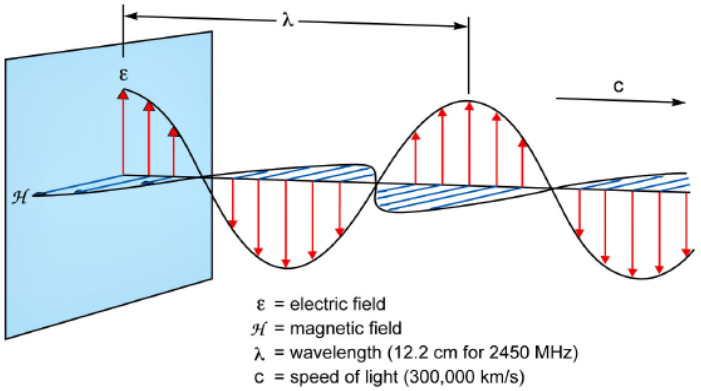


Figure 2-11 Microwave and microwave components (Hayes, 2002)

2.5.2 Dipolar Polarisation Mechanism

When a substance is exposed to microwave radiation it may heat due to the dipolar polarisation mechanism. For this to occur, the molecules within a substance being exposed to microwaves must have some charge separation (usually because the molecule is polar), thus it is said to possess a dipole moment. The dipole moment is described as a vector from the positive to negative charge on the molecule. They are usually classified as permanent, with the positive and negative centres of charge never cancelled (even if exposed to an external electric field).

The dipolar polarisation mechanism causes polar molecules to rotate, attempting to align them with the passing electric field. In this process the electric field gives the energy for the rotation of the molecule, this is shown in Figure 2-12 (Clark and Sutton, 1996)

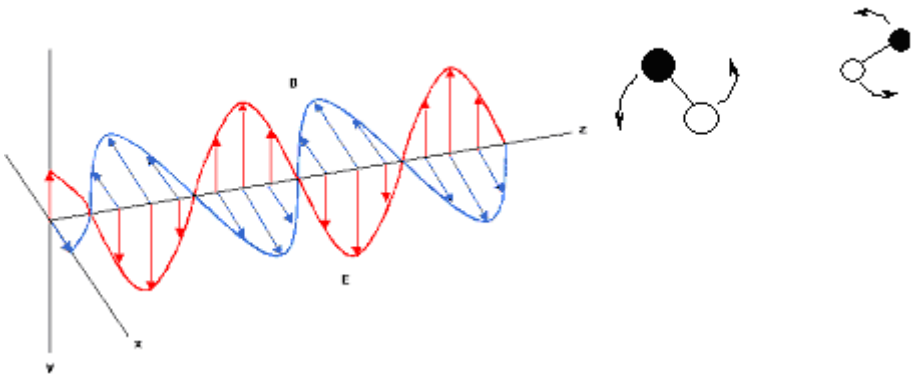


Figure 2-12 Dipolar Polarisation Mechanism

The rotation and alignment of the molecules is dependent upon their polarity, their phase and the frequency of microwaves applied.

2.5.3 Effect of Phase

Within a gas, the molecules are able to move rapidly, aligning with the microwave field. Within a liquid this differs, being highly dependent upon the frequency of the microwaves applied and the liquid's viscosity. The instantaneous alignment is prohibited due to the presence of surrounding molecules (Katz, 1992, Strauss and Trainor, 1995).

When a low frequency microwave field is applied to a dipolar liquid the molecules in the liquid are able to rotate in phase with the oscillating electric field, with only a little energy being gained by the full alignment being achieved. Contrary to this, at high frequencies the dipoles are unable to react to the oscillating electric field and little or no movement is induced. As a result no energy transfer takes place between the molecule and the wave, hence no heating occurs. If a frequency occurs between these extremes, then the effect of dielectric heating occurs. In this process the frequency of the radiation is low enough that the dielectric molecule is able to orientate itself following the electric field, although the radiation frequency is high enough that the dielectric molecule is not able to stay completely in phase and a phase difference arises. This causes energy to be lost through molecular friction and collisions resulting in dielectric heating (Clark and Sutton, 1996, Katz, 1992, Lidström *et al.*, 2001).

2.5.4 Conduction Mechanism

The conduction mechanism is related to the movement of ions or an ion with a hydrogen bonded cluster. The mechanism relies upon the movement of ions through a solution under the influence of the electric field. The increased movement of ions results in an increased collision rate causing the conversion of kinetic to thermal energy, as shown in Figure 2-13. The conduction mechanism has a much stronger interaction with the electric field than the dipolar heating mechanism, with a greater generation of heat.

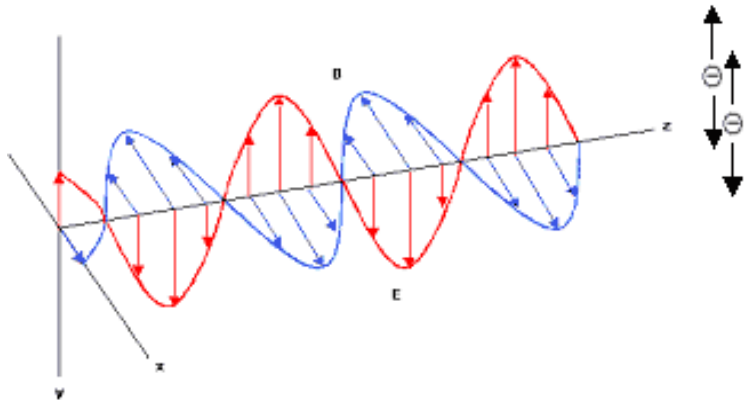


Figure 2-13 Microwave Conduction Mechanism

2.5.5 Loss Angle

The ability of a material to adsorb microwaves and convert the absorbed energy to heat is described mathematically through its loss angle (б) expressed as a tangent of the dielectric constant/relative permittivity (ε') and the loss factor (ε''), this is shown in Equation 2-1.

$$\tan б = ε'' / ε'$$

Equation 2-1 The loss equation

The dielectric constant represents the ability of a material to store electrical potential energy when exposed to an electric field. When a material is exposed to a static electric field at room temperature, ε' will be equal to the dielectric constant, $ε_s$. The loss factor, ε'', quantifies the energy efficiency of converting the absorbed energy to heat. When materials have low values of tan б and ε' the loss factor, ε'', can be used to estimate the rates at which they will heat due to better coupling (Lidström *et al.*, 2001).

With the re-orientation of dipoles and the displacement of electric charge this is equivalent to an electric current. This current would be observed to be at 90^o out of phase with the electric field, if the dielectric were to follow the field without being hampered by surrounding molecules. If the dielectric were not to follow the electric field precisely, a phase difference would occur between the dielectric and the field. The displacement of the phase is described by the component, *I* sin б, which is in phase with the field.

The result of this is that energy is adsorbed from the electric field and converted to heat. The relationship between tan б and ε' and ε'' can be described simply by trigometric methods (Lidström *et al.*, 2001). This is shown in Figure 2-14.

Within this equation, P is the power dissipation in W/cm^3, K is a constant equal to 55.61×10^{-14}, f is the applied frequency in Hz, E is the electric field strength in V/cm, ε' is the dielectric constant and tanб is dependent on the frequency and the sample temperature. The field energy dissipated as unit volume is proportional to the dielectric loss factor (ε'tanб), the square of the field strength (E^2) and the frequency (f) of the applied field. Equation 2-2 demonstrates that the power absorbed relates linearly to the frequency, the dielectric constant, loss tangent and the square of the electric field.

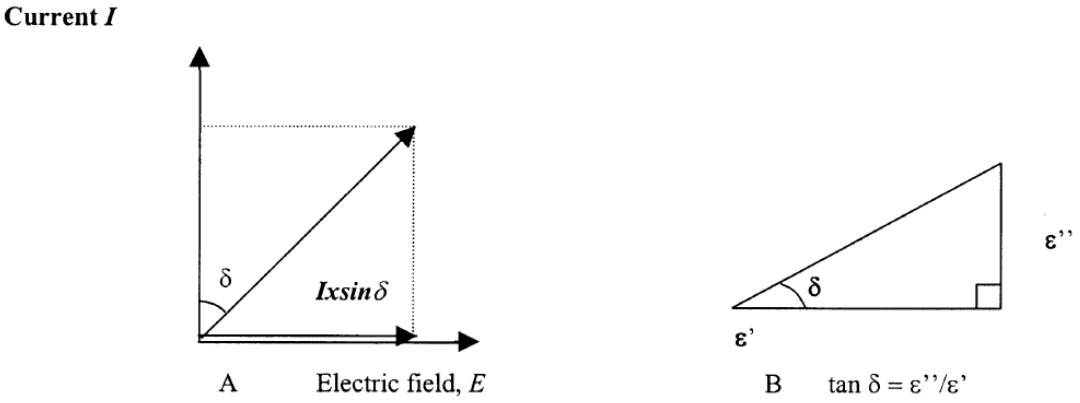


Figure 2-14 (A) Phase difference which results when energy is converted to heat. (B) The relationship between ε' and ε'', tanδ = ε''/ ε'. (Taken from Lindstrom et al,. 2001)

The dielectric power adsorption of a material is described in (Equation 2-2).

$$P = KfE^2\ \varepsilon' \tan\delta$$

Equation 2-2 The microwave power absorbed by the dielectric (theoretical formula)

The relative dielectric constant and the loss tangent are the parameters that describe the behaviour of a dielectric material under the influence of the microwave field. During heating the relative dielectric constant and the loss tangent change with temperature (Chen *et al.*, 1993, Das *et al.*, 2009, Sutton *et al.*, 1988).

2.5.6 Microwave Effects on Matter

Microwaving has a number of fundamental differences from conventional thermal heating. These include; inverted temperature profiles, accelerated and self limiting heating and lowered activation energies.

2.5.6.1 Reaction Temperature and Rate

Key differences occur in reaction mechanisms (through microwave heating) with different pathways either occurring or being preferred to that of conventional heating. This often results in increased reaction rates and sometimes differing reaction products.

In previous investigations, temperature measurement has been questioned since most methods are limited to measuring surface temperature. Problems arise if this is a bulk material in which temperature gradients may occur. To mitigate against bulk effects, temperature measurements were performed in a number of experiments using 10μm thick samples by Wallace *et al.* (2006a) in which increased reaction rates were observed at lower temperatures.

Further effects are seen in ionic materials where reactions are accelerated as a result of driving force rather than diffusion gradient or capillary stress. This was observed to be as a result of a non thermal driving force; i.e. an induced voltage gradient by the microwave field due to asymmetry in defect fields on the surface of crystalline structures, causing spatial charge polarisation that further couples with the microwave field (Clark and Sutton, 1996).

2.5.6.2 Inverted Temperature Profiles

An inverted temperature profile occurs due the mechanisms of microwave heating. It is normally seen that the internal temperature of a sample is greater than that of the external, the opposite of conventional thermal heating.

This is caused by materials with sufficient values of relative permittivity allowing the deep penetration of the microwaves into the sample. The bulk of the sample is normally heated to the same degree as the internal of the sample, with the thermal gradient being caused by the loss of radiated heat at the surface.

2.5.6.3 Accelerated Heating/Thermal Runaway

When a material is processed in a non uniform electromagnetic field, localised variations in temperature arise. If this localised area of increased heat reaches a critical temperature before the rest of the material being heated, it begins to heat more rapidly. This results in thermal runaway occurring (also referred to as hot spotting) (Das *et al.*, 2009). Abrupt rapid increases of temperature arise when relative permittivity increases with rising temperatures. The temperature at which this abrupt increase in relative permittivity occurs is called the critical temperature (T_c). The inverted temperature profile that occurs with microwave heating can also result in the non uniform heating between internal and external surfaces of a sample, hence thermal runaway can occur but not as a result of a non uniform microwave field. These properties can be used in the microwave processing of many materials which are poor receptors at ambient temperatures, but better receptors at elevated temperatures (Clark and Sutton, 1996). This is often achieved by preheating the material to its critical temperature before exposing it to a microwave field.

2.5.6.4 Self Limiting Heating

The relative permittivity of a material can also decrease with rising temperature, reaching a critical temperature at which the relative permittivity drops significantly. As a result, heating becomes self limiting. This effect is used to advantage in many aspects of materials science, specifically in polymer

processing in which polymerised materials are less susceptible to microwaves than the un-reacted monomer (Wallace *et al.*, 2006a).

2.5.6.5 Superheating Effect

Within a polar molecule, its relaxation time, τ, is defined as the time taken for one molecule to return to 36.8% of its original situation when the electric field is turned off (Lidström *et al.*, 2001). The relaxation time is temperature dependant, decreasing as temperature rises. Since ε'' and ε' are dependent upon τ, the material being heated will not only be dependent upon the microwave frequency to control its heating rate but on the temperature of the material as well. It is therefore often seen that the heating rate of organic chemicals will increase with temperature as the loss tangent increases. This can result in the boiling points of solvents being raised by up to 26^{o}C above their conventional value (Lidström *et al.*, 2001).

2.5.7 Summary

Microwaves present a different way of heating and decomposing a material to that of traditional pyrolysis. This is largely due to the effect of highly polar regions of a molecule (which tend to decompose first), super and self limited heating, accelerated heating and inverted temperature profiles resulting in product distributions that are likely to differ from conventional thermal pyrolysis. As such they offer an opportunity for research into alternative methods of recycling plastic materials because of the potentially beneficial differences in the reactions and hence the products generated.

CHAPTER THREE

3 Microwave Experimental Development and Design

"The aim of this chapter is to discuss the development of the microwave reactor, by:

- *identifying experimental variables*
- *establishing microwave type and design*
- *examining the reactor design and mode of temperature measurement*
- *determining the best method of product capture*

...and to determine the final design"

3.1 Introduction

After extensive investigation it was established that little work has been performed on investigating the microwave decomposition of plastics, with only one paper published on the microwave pyrolysis of mixed plastic wastes by Ludlow-Palafox and Chase (2001) and three papers on the microwave decomposition of plastic by Ito *et al.* (2006), Moriwaki *et al.* (2006b) and Osada and Yoshioka (2009). No work has been performed to investigate in-depth the microwave decomposition and pyrolysis of any one plastic type; hence, any understanding of the effect of individual decomposition/pyrolysis parameters has not been established in a reactor that would depict a possible industrial process. Nevertheless, numerous authors have investigated the microwave pyrolysis of materials including; tyres (Yatsun *et al.*, 2008), coal (Monsef-Mirzai *et al.*, 1995), sewage sludge (Menéndez *et al.*, 2002) and biomass (Krieger-Brockett, 1994), with approximately 290 papers published in the area. Subsequently, the methods utilised by these authors were used to assist in the development of a microwave reactor system for the pyrolysis of plastics.

For the purpose of the planned investigation it was necessary to build a reactor system able to both withstand the extreme conditions that are likely to occur in a microwave pyrolysis process and also to be used in such a fashion that experimental parameters can be investigated and parallels drawn with previous thermal pyrolysis experimentation.

The following chapter discusses the design considerations, technical challenges and dangers of developing such a system and the reasoning for the development of the final microwave reactor.

3.2 Experimental Parameters

Research surrounding the conventional thermal pyrolysis techniques of single plastics and mixed plastic wastes (as referred to in Section 2.4.7) has primarily focused on fluidised bed reactors (Kaminsky *et al.*, 2004, Williams and Williams, 1999), cycle-sphere reactors (Ludlow-Palafox and Chase, 2006), fixed bed reactors (Williams and Williams, 1998, Ballice, 2001), screw reactors (Serrano *et al.*, 2001, Day *et al.*, 1999) and rotary kilns (Kaminsky, 1992). The primary aim of these experiments was to achieve an understanding of resulting product distributions in relation to changes in experimental conditions and feedstock type.

The systematic investigation of microwave pyrolysis on a "single plastic" has not been undertaken. To date it has not been possible to draw conclusions of the effect of microwave parameters on petrochemical derived polymeric materials. Therefore, there is a lack of a fundamental knowledge of parameters controlling a microwave pyrolysis process. Hence, it was important to determine the variables that might affect the microwave pyrolysis process, particularly those which can be investigated experimentally. These have been established and listed as dependent and independent variables as listed in Table 3-1 and Table 3-2:

Table 3-1 Independent Variables (* indicates variable that does not lend itself easily to experimental variation)

Independent Variables	
Reactor	**Carrier Gas**
Dimensions (R_d)	Gas Density (ρ_G)
*Reactor Specific Heat Capacity (C_R)	Flow Rate (G_F)
*Reactor Thermal Conductivity (K_R)	*Gas Thermal Conductivity (K_G)
	*Gas Specific Heat Capacity (C_G)
Feedstock/Receptor	
Particle diameter (d_p)	**Microwave**
*Particle density (ρ_p)	Frequency (MW_{Hz})
*Particle Specific Heat Capacity (C_p)	Mode
*Particle Thermal Conductivity (K_p)	Chamber Dimensions
*Activation Energy (E)	Power (P_{MW})
*Preexponential Factor (A)	Duration (D_{MW})
Feedstock/Receptor Load (M_{init}/M_R)	

Table 3-2 Dependent Variables

Dependent Variables	
Heating Rate (H_R)	Composition of Solid (C_s)
Temperature (T)	Composition of Oil (C_O)
Conversion Rate (C_R)	Composition of Gas (C_G)
Solid Yield (M_s)	
Oil Yield (M_O)	
Gas Yield (M_G)	

Of the independent variables; specific heat capacities, thermal conductivities, activation energies, and the pre-exponential factors cannot be changed experimentally because these are material specific parameters, so require the addition of further chemical components. Of the remaining variables, reactor dimensions and material were maintained as a constant. Reactor development and design is discussed in section 3.3. Microwave variables are subject to limitation by design; these are discussed further in Section 3.3.

3.3 Reactor Development

In the design and development of the microwave reactor system it was important to take into consideration microwave parameters, the interaction of materials with microwaves, chemical interactions and the measurement of independent variables.

3.3.1 Microwave Parameters

The type and design of microwave equipment used within the investigation is a key consideration as it is directly responsible for the electromagnetic field frequency, mode, strength, spatial variation and operational flexibility (Stadler *et al.*, 2003, Thostenson and Chou, 1999). As such, it is important to examine the microwave factors which are likely to affect the pyrolysis process, making informed decisions on the best design for the application. Due to the complex nature of microwave heating factors such as; microwave frequency, microwave mode, reactor geometry, temperature variation, surrounding medium properties, dielectric properties and cavity geometry can all influence the distribution of electromagnetic waves and the resulting heating patterns.

3.3.1.1 Frequency

Two microwave frequencies are readily available and regulated for use within the public sphere, these being 0.915GHz (328 mm) and 2.45GHz (122 mm) (Bansal and Singh, 2012). However, of these

frequencies 0.915 GHz is not readily available on a laboratory scale, with minimum availability in magnetron power of 5 kW. Hence, almost all microwave chemistry is performed and microwave pyrolysis experimentation conducted at the 2.45 GHz frequency (frequency properties summarised in Table 3-3). Therefore, this was the chosen frequency for this investigation. The choice of frequency enabled comparisons to be drawn with previously published works such as Kaminsky *et al.* (1976) Ludlow-Palafox and Chase (2006) , Yatsun *et al.* (2008) and Lam *et al.* (2012), thus building on a small knowledge base whilst advancing the understanding of microwave-induced pyrolysis of single polymer types at this frequency.

Table 3-3 Properties of 2.45GHz electromagnetic wave (Hokuto Electronics Corporation, 2012)

Property	Unit
Frequency	2.45 GHz
Wavelength	122 mm
Photon Energy	~10^{-5} eV
Penetration Depth in 80°C Water	66 mm
Magnetron Electrical Conversion Efficiency	50 – 72%

The well developed sector utilising 2.45 GHz also enabled access to two types of power delivery into the microwave units themselves; Pulse Width Modulation (PWM) and Inverter technology. Pulse Width Modulation uses a technique of applying a set power, but cycling this on and off to achieve a lower sum power, this is best demonstrated in Figure 3-1 in which 390 watts is pulsed for 14 seconds in 22, resulting in an time averaged power of 250 watts.

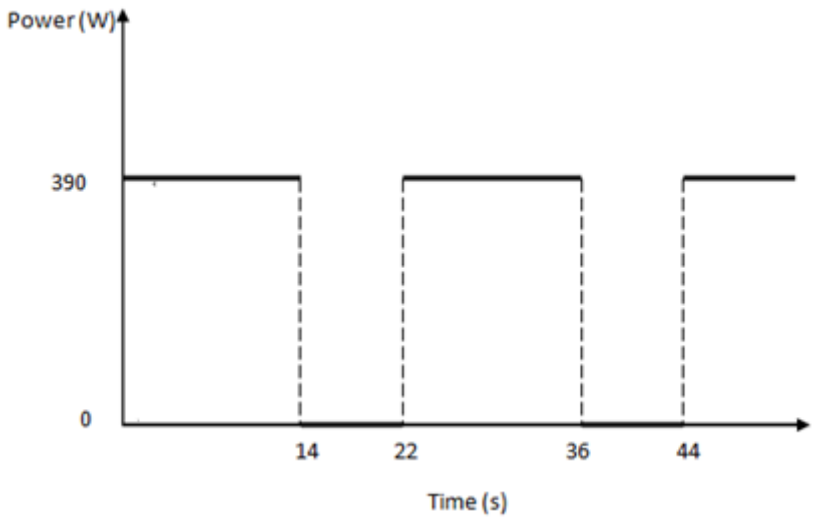


Figure 3-1 Pulse Width Modulation achieving a time averaged power application of 250W

Inverter technology enables a true stepping down of the power applied within the microwave oven allowing for the application of a constant power, this is shown in Figure 3-2.

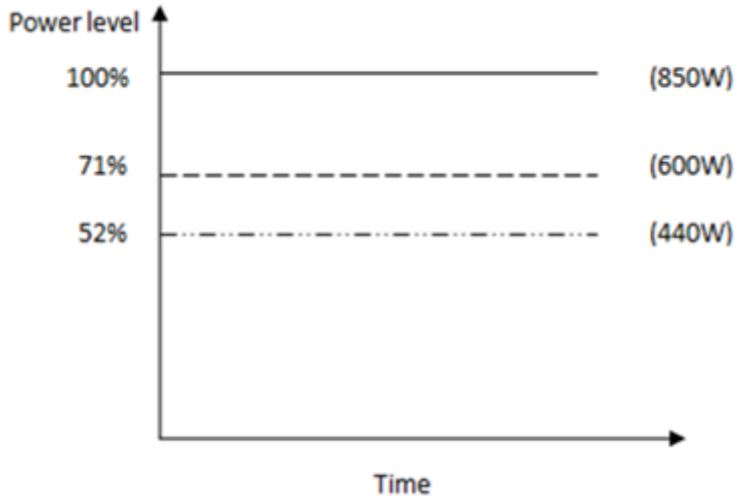


Figure 3-2 Constant power application by inverter technology

Pulse width modulation is undesirable in chemical applications as large variations in heating rate/temperature can be induced with constant cycling of microwave power. It was decided that inverter technology should be employed in the microwave pyrolysis process to eliminate the possibility that the constant cycling of the electromagnetic field during PWM, might introduce an added variable into the microwave pyrolysis process. This is justifiable by the evidence introduced by Galema (1997a), in which it was proposed that the reduction in the energy of activation may result from the storage of vibrational energy within molecules or through entropy effects. This has been further explored by Miklavc (2001) in which microwaves were used to increase rotational excitation and promote favourable collision geometry. Experiments were not conclusive but did point towards increases in wave amplitude resulting in increased reaction rates. If this is true then PWM eliminates variations in amplitude, eliminating the possibility of this effect.

3.3.1.2 Mode

Two categories of microwave oven currently exist; single mode and multi mode units (Will *et al.*, 2003, Thostenson and Chou, 1999). These are often used in very different ways and utilise different designs, as shown in Figure 3-3.

3.3.1.2.1 Single Mode

A single mode unit utilises a solution to Maxwell equations to create a resonant mode (Thostenson and Chou, 1999), with the wavelength of the frequency being utilised dictating the dimensions of the

microwave chamber, so the resonant mode can be established. The resultant microwave unit has a non-uniform, yet predictable electromagnetic field.

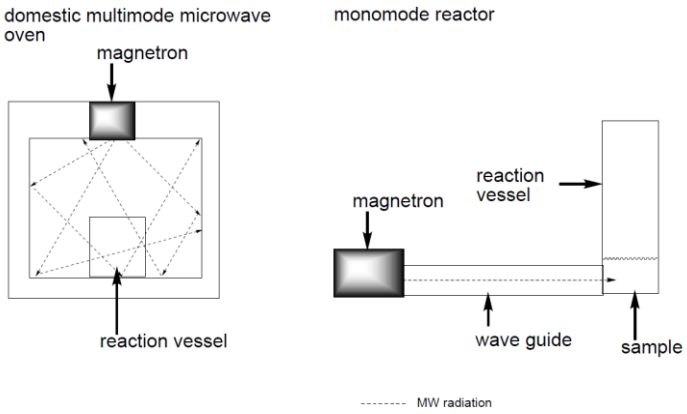


Figure 3-3 Schematic design of multimode and single mode microwave chambers (Kuhnert, 2002)

Within this field a nodal point exists focused on the centre of the sample reactor. This point in the wave is subsequently used to achieve optimum coupling between the microwave field and the material, generating a "hotspot" within the sample. This is extremely useful in laboratory scale investigations in which the specific action of microwaves and materials require investigating, with the added ability of seeing the dielectric properties of the material during processing (Robinson *et al.*, 2010, Thostenson and Chou, 1999).

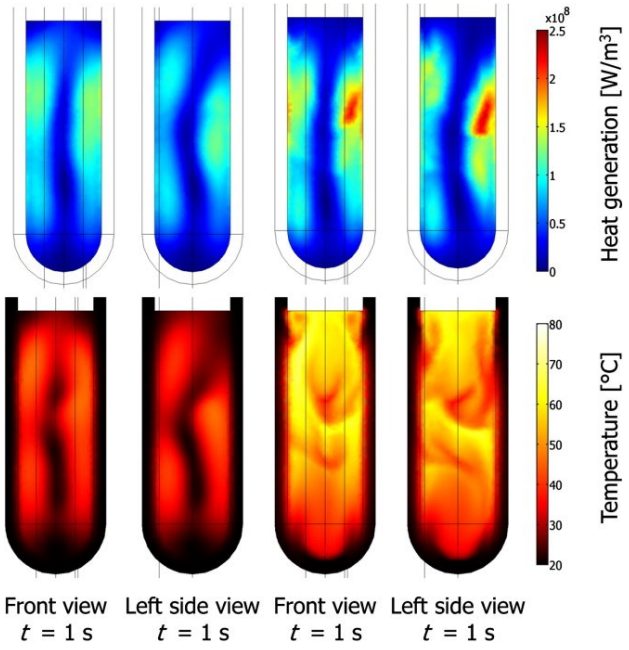


Figure 3-4 Thermal distribution of water within a single mode microwave cavity after 1 seconds microwave exposure: modelled (top) and measured (bottom) (Sturm *et al.*, 2012).

However, increasing evidence is arising from recent publications that single mode microwave cavities do not deliver a uniform field density once a material is introduced (Robinson *et al.*, 2010, Sturm *et al.*, 2012). This results in the attenuation of microwaves in the outer most regions of the microwave reactor and uneven heating ensuing. This has been best demonstrated by Sturm *et al.* (2012) in which he modelled the heating of water within a single mode microwave cavity (see Figure 3-4).

Nevertheless, when scaling a microwave process for industrial needs, the ideal single mode microwave field is of little use, as it is limited to the centimetre scale and if greater sizes are attempted problems occur with non-uniformity in fields (Robinson *et al.*, 2010, Thostenson and Chou, 1999).

3.3.1.2.2 Multimode

The multimode microwave utilises a cavity which is much larger in dimensions than one wavelength and so is able to support multiple resonant modes. With increasing size the number of possible resonant modes also increases. This is also accompanied by the formation of constructive and destructive interference by reflectance of cavity walls and conductive elements of the sample.

This results in the formation of multiple hot spots within the microwave cavity. The addition of materials/objects in this field can often cause a disturbance, resulting in an instantaneous cascade to differing field densities within the microwave cavity (as seen in Figure 3-5), this often results in localised overheating/hot spotting (Santos *et al.*, 2010).

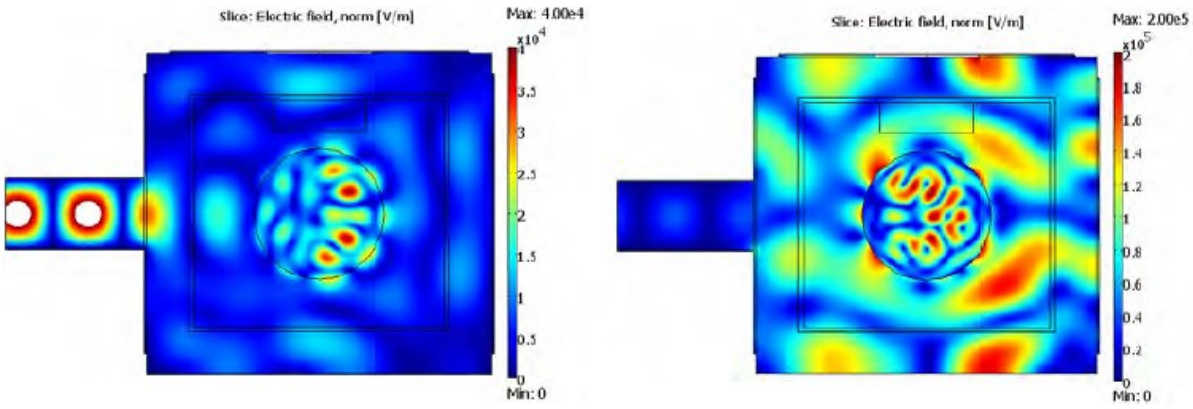


Figure 3-5 Changes in field distribution within a 2.45 GHz microwave oven with ε' = 6.25 (left) and ε' = 9.00 from Santos *et al.* (2010)

However, this can be combated by several methods:

- Increasing cavity size – by increasing the size of the cavity the number of resonant modes increase. Overlap of these modes consequently ensues and greater field uniformity can be achieved. Nevertheless, limitations of this method occur when attempting to achieve field uniformity as 100 times the wavelength of the operating frequency is required; at 2.45GHz this equates to approximately 12.20 metres (Kimrey and Janney, 1988, Thostenson and Chou, 1999).
- Sample movement – in a non-uniform electromagnetic field it is possible to achieve exposure uniformity over the total volume of the sample by moving the sample through the areas of high and low field density. This results in a time averaged uniformity.
- Mode Stirring – this method uses a device to disturb the waves travelling through the chamber, continuously redistributing the electromagnetic field. In essence this achieves the same as sample movement, by time averaged field uniformity.
- Multiple Microwave Sources – by adding multiple microwave sources the number of modes within a cavity can be increased indefinitely. As a consequence, field uniformity can be achieved within a microwave cavity of significantly decreased size.

Higher power densities are also possible within single mode cavities, However, for batch processes, larger volumes of material, samples of complicated shape or with spatial variation of dielectric properties; multimode microwaves prove to be superior and significantly more versatile. Multimode cavities also offer the capability of producing electric fields able to encompass significantly larger volumes but notwithstanding compromise in the field definition. Hence, they are favoured and routinely used throughout academic and industrial research to assess the suitability of microwave treatment for large scale applications. This is demonstrated across all facets of the research community with use in catalysis (Will *et al.*, 2003, Wan, 1993, Larhed *et al.*, 2002, Bren *et al.*, 2007), chemical synthesis (Stadler *et al.*, 2003, Kappe and Dallinger, 2006, Tu and Liu, 2000, Yan *et al.*, 1997), drying (Maskan, 2000, Drouzas and Schubert, 1996, Turner and Jolly, 1991) and pyrolysis (Salema and Ani, 2011, Menéndez *et al.*, 2002, Monsef-Mirzai *et al.*, 1995, Ludlow-Palafox and Chase, 2006, Zou *et al.*, 2007).

After careful consideration it was decided that a multimode microwave system would be used in the investigation. Further to this, recent investigations indicate that the single mode microwave process shows little in the way of advantages over a multimode process. Particularly when examining the possible yields and products of a microwave decomposition process, with the spatial variation in field density being just as unpredictable. This, in combination with smaller sample sizes associated with a single mode process means it is likely to yield a result less representative of a much larger process.

A Panasonic multimode microwave oven (Model No. NN-SD277S) using inverter technology was utilised within the investigation. The power output of the unit was verified using standard test IEC 705:1988 and the following equation utilised.

$$P = \frac{W_v . \Delta T . (4.1868)}{D}$$

Equation 3-1 Measurement of microwave power output by the IEC 705-88 method

Where:

P	=	Power (Watts)
W_v	=	Volume of water (millilitres)
ΔT	=	Temperature rise (degrees Celsius)
D	=	Microwave Duration (Seconds)

From this the power output of the microwave oven was determined to be on average within 2% of the stated nominal values of 250W, 440W, 600W and 850W.

3.3.2 Reaction Vessel Design

The reaction vessel design (shape/size/material) is an important consideration in any decomposition process. It must facilitate the change in experimental parameters whilst enabling the observation of results during the investigation without undergoing any change itself or partaking in any chemical reaction (Conner *et al.*, 2004). Thus, the microwave reactor was designed so that the dependent variables of temperature, heating rate, mass of solid/oil/gas and conversion rate could be directly measured or derived. In doing so the following design parameters needed to be examined:

- Temperature measurement
- Reactor material
- Reactor configuration

3.3.2.1 Temperature Measurement

The nature and effect of microwave irradiation is still relatively uncertain with the effect it has upon the decomposition process of materials still poorly understood. Until recently, this has largely been as a result of the limited ability to establish accurately the temperature within a microwave reactor, resulting in the inability to differentiate between purely thermal/kinetic effects and those that are a result of the interaction of microwaves and non-thermal effects.

The accurate measurement of temperature and subsequent heating rates is essential to establish reaction kinetics. At present, microwave decomposition reactions utilise three techniques in the measurement of temperature, these being; thermocouples, fibre optic thermometers or infrared pyrometers.

It is extensively discussed by Kappe (2013) that the use of such temperature measurement devices as mercury thermometers and thermocouples should never be used within a microwave cavity. The current preferred method of temperature measurement is the use of infrared pyrometer measuring the external surface temperature of a reactor at a pre-defined distance. This eliminates error due to changes in emissivity but are limited in that they cannot be used to determine accurately the temperature of a reaction mixture contained within due to thermal lag over the sample and the reactor itself. The most accurate way of measuring temperature is through use of a fibre optic temperature probes utilising the fibre optic cable with of a crystal mounted in contact with the sample. This enables the measurement of the precise temperature within a sample as it is in direct contact with it. However, these are of little use at higher temperature pyrolysis applications as they would normally have a maximum operational temperature range of 300°C. They are also limited in the fact that they are only able to monitor a single spot within the reaction mixture. For full discussion of temperature measurement within microwave chambers please refer to (Kappe, 2013).

3.3.2.1.1 Thermocouples

Thermocouples present a significant problem when utilised within a microwave chamber, due to their construction utilising metals. This leads to disturbances occurring in the localised electromagnetic field changing the local environment within the region of the thermocouple (Pert *et al.*, 2001, Durka *et al.*, 2010). The result is that the deposit of energy increases abruptly close to the tip of the thermocouple. Increased heating ensues, often leading to thermal runaway and increased thermal gradients (Pert *et al.*, 2001).

Further problems with using thermocouples include: direct heating of the thermocouple due to the dielectric properties of its insulating material or by induction of a current within the thermocouple itself. Induction of currents within the thermocouple can also lead to electrostatic discharge within the microwave chamber (Will *et al.*, 2003).

3.3.2.1.2 Fibre Optic

Fibre optic thermometry is the most common technique for the measurement of temperature within a microwave synthesis reactor and widely accepted as the best technique within synthetic chemistry (Pert *et al.*, 2001, Will *et al.*, 2003). The thermometer is able to be physically placed into the reactor without causing disturbances to the electromagnetic field, measuring directly the temperature from

within the sample. However, the reading gained from the fibre optic thermometer only reflects the immediate environment, hence; multiple readings are often required from different points within a reactor before an accurate temperature can be gained.

Nevertheless, the temperature able to be read by this technique is limited by the maximum operational temperature of 300^{o}C. This is due to the materials the fibre optic is made from; typically silica glass, and a plastic coating of PTFE or similar. In addition, it was noted by Herrero *et al.* (2007) that in some cases samples heated at higher rates could be incorrectly determined for their reaction temperatures due to lag in the thermometer of up to 13 seconds before a true temperature can be displayed. Due to these issues, fibre optic temperature probes cannot be utilised within a pyrolysis study in which temperatures are undoubtedly going to be in excess of 400^{o}C.

3.3.2.1.3 Infrared Pyrometer

As a consequence of these limitations, the final option of infrared pyrometers was utilised within this investigation. The method infers temperature of an object by measuring the portion of thermal (infrared) radiation emitted from a sample/object. The energy emitted from the materials surface is proportional to the temperature of the material, which is defined as the emissivity. As such, the temperature of a given material can be accurately measured.

It is often the case that infrared pyrometers are used as a non-invasive means of establishing the external surface temperature of a reaction vessel within a microwave field, based on the principle that the reactor represents the sample temperature due to a high degree of thermal conductivity between the sample and the reactor wall. For liquid samples this is would follow but solid samples rarely have high thermal conductivities and notoriously act as insulators. Hence, in microwave pyrolysis applications where the material (but not the reactor) is heated volumetrically, a situation can easily arise in which external reactor temperature does not accurately represent the internal temperature. However care is needed because they are limited in their use due to the probe only sensing the temperature at the surface of the sample. In samples of significant volume/depth the internal temperature can be significantly larger than that of the surface. However, if a sample is relatively thin the surface temperature will likely reflect the bulk temperature of the sample (Ito *et al.*, 2006, Moriwaki *et al.*, 2006b).

Nevertheless, it is important to acknowledge that the temperature measurement given by the infrared sensor will have an element of error within its reading due to the material property of emissivity. Emissivity is related to the radiation given off by a particular material. A material which perfectly absorbs all wavelengths from the electromagnetic spectrum is known as a black body. A black body is

also a perfect emitter. The ratio of a materials emissions to a perfect emitter is referred to as its emissivity.

Hence, when measuring the temperature of the sample undergoing pyrolysis we must understand its emissivity at the beginning of the pyrolysis run and at the end. As such, at the beginning of a run PVC will be present in its pure form and at the end we will be left with char. For PVC at 25^{o}C is 0.91(Calex UK, 2013). For carbon at 500^{o}C the emissivity is 0.79 (Calex UK, 2013) . As the final temperature of the experiment is an important value the emissivity of the infrared sensor was set to 0.79. Therefore at the beginning of an experiment the temperature will have an error of +14%, which diminishes as the PVC heats and undergoes pyrolysis converting to char.

3.3.2.2 Reactor Material

The material used in the construction of a microwave pyrolysis reaction vessel is extremely important. Firstly, it must not take part in any chemical reaction so must be chemically stable/inert. Secondly, it must be resistant to temperatures in excess of 800^{o}C. Finally, its interaction with the microwave field must be minimal. Only one readily available material is able to satisfy all of the above criteria, fused quartz. It is found to be largely un-reactive, when exposed to most acids and metals, with the exceptions being phosphoric and hydrofluoric acids. It is also slightly attacked by alkaline solutions and some basic oxides at elevated temperatures. It is also resistant to temperatures of up to 1200^{o}C at which point it begins to deform and its dielectric response is very low. Its key properties are summarised in Table 3-4. A further important property of fused quartz glass is the ability to mould and shape it into almost any design of reactor, which is important consideration for microwave reactor configuration.

Fused quartz has been extensively used in both thermal and microwave pyrolysis investigations by (Menéndez *et al.* (2002), Domínguez *et al.* (2007), Huang *et al.* (2008), hence its use within this investigation.

Table 3-4 Material and electrical properties of fused quartz (National-Scientific-Company, 2013)

Property	Typical Value
Thermal	
Coefficient of Thermal Expansion	5.5x10 -7 cm/cm . ^{o}C (20^{o}C-320^{o}C)
Thermal Conductivity	1.4 W/m . ^{o}C
Specific Heat	670 J/kg . ^{o}C
Softening Point	1683^{o}C
Annealing Point	1215 ^{o}C
Strain Point	1120 ^{o}C
Electrical	
Electrical Resistivity	7x10 7 ohm cm (350^{o}C)
Dielectric:	
Dielectric Properties	(20^{o}C and 1 MHz)
Constant	3.75
Strength	5x10 7 V/m
Loss Factor	Less than 4x10 -4
Dissipation Factor	Less than 1x10 -4

3.3.2.3 Reactor Configuration

The reaction vessel is an essential part of the microwave system design. The following parameters were deemed absolutely necessary within the design so that the accurate measurement of dependent variables could be achieved (as listed in Table 3-2), whilst maintaining constant those independent variables not being investigated. The criteria were as follows:

- Maintain vessel position within the microwave cavity
- Maintain an inert atmosphere and constant purge-gas flow-rate
- Enable continuous monitoring of sample surface temperature
- Promote the removal of gaseous reaction products from the reaction vessel to the condensing system
- Allow for measurement of all reaction vessel component weights
- Facilitate ease of solvent washing for collection of condensed oils on reactor components in a quantitative manner
- Enable ease of cleaning

With these in mind the design was made and constructed as shown in Figure 4-3.

Of greatest influence on the design was the optics of the infrared pyrometers available for use. Of the available units it was found that the CALEX, PyroUSB infrared pyrometer matched the requirement of the experimental setup, with the ability to sense temperatures between -40°C and 1000°C, a measurement accuracy of ± 1.0% of the measured temperature and a response time of 240ms. However, the optics of the instrument dictated the design of the IR viewing window, as line of sight could not be impeded by glass or inaccurate measurement would be gained. Also, the spot size of the IR pyrometer must be equal to or less than the size of the measurement window. Thus, the sight paths of the pyrometer were established (as shown in Figure 3-6) and the window designed around the one which gave optimal measurement as well as minimising the effect on other parameters.

The IR viewing window was a key component in the design of the microwave, as it facilitated the measurement of temperature and heating rates experienced in the reactor, giving the ability to ascertain thermal and non-thermal effects; a factor of upmost importance in a microwave pyrolysis investigation (Pert *et al.*, 2001, Robinson *et al.*, 2010). It also was designed so that its position within the microwave chamber remained constant and an inert purge gas could be applied to the reactor vessel.

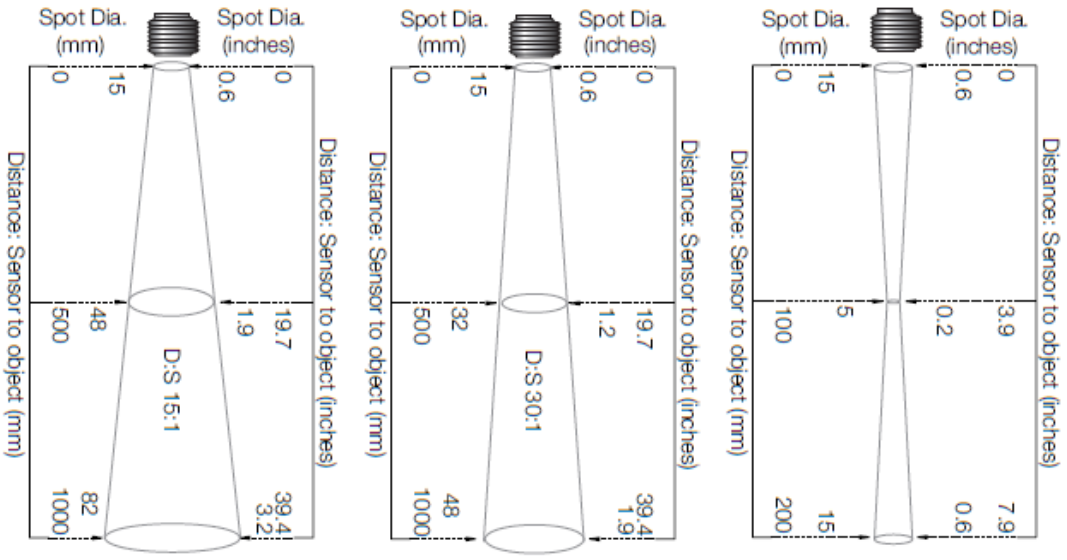


Figure 3-6 IR pyrometers optical sight paths for differing models (Calex PyroUSB model number 151 (left), 301 (centre) and CF (right)

It was decided that the Calex PyroUSB-CF would allow for optimal design of the reactor vessel, minimising the diameter of the window and consequently maximising the purge gas flow velocity through the unit (as shown in Figure 3-7). This aided in maintaining clear line of site by preventing the pyrolysis gases from migrating into the IR viewing window. The flow of gas also facilitated the

cooling of the IR Pyrometer during the pyrolysis process by maintaining a constant flow of N_2 over the lens of the unit.

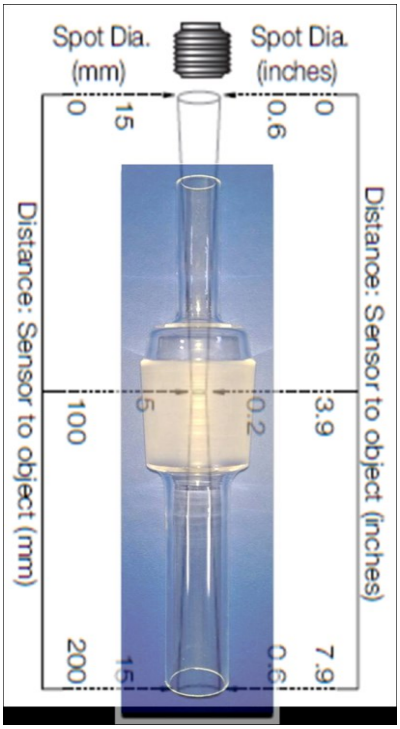


Figure 3-7 IR viewing window design accommodating sight path of Calex PyroUSB-CF (not to scale)

The top tube of the IR viewing window was then used in conjunction with a standard brass bulkhead fitting in the roof of the microwave chamber so that it could be slid through and locked into place. This meant that the position of the reactor system in the microwave chamber was maintained throughout all experimentation, whilst the Infrared pyrometer was not intruding the microwave field, monitoring passively. The brass fitting also provided the additional function of a microwave choke, stopping any microwave radiation from escaping the chamber.

The resultant quartz joining collar and bulb flask reactor were designed to enable an air tight seal to be achieved; this was done through the use of ground quartz-glass quickfit joints. It also enabled for pyrolysis gases to be carried out of the reactor to a condensing system. The resulting design is shown in Figure 3-8.

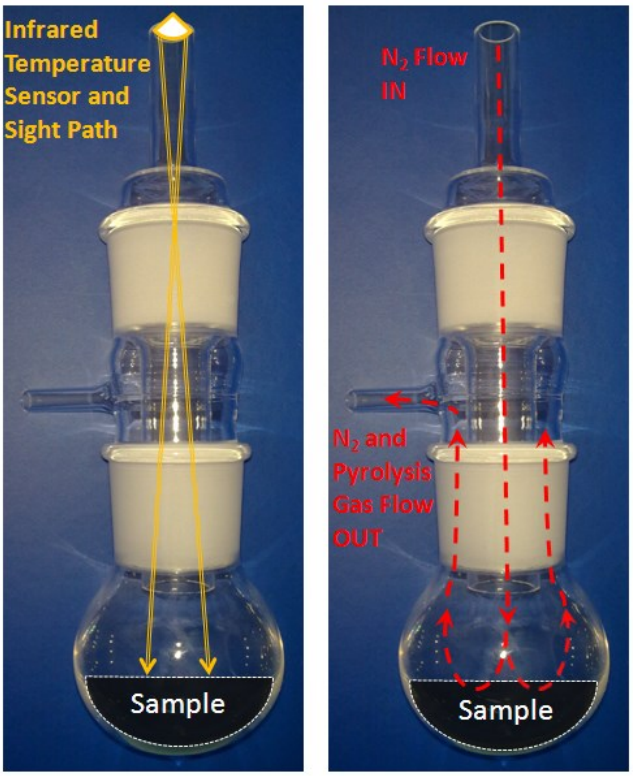


Figure 3-8 Final design of microwave reactor enabling measurement of temperature/heating rate by IR pyrometer, maintenance of an inert atmosphere by N_2 purge and evacuation of pyrolysis gases

This modular design also facilitated the accurate measurement of sample component weights and enabled effective cleaning after each run. This was essential, as any remaining pyrolysis material was likely to be amorphous char comprising aromatic hydrocarbons, this being extremely susceptible to microwave heating, with the possibility of localised temperatures surrounding the residue reaching 1277^{o}C when next exposed to microwave radiation (Rao *et al.*, 1999). These high temperatures would affect the results and may damage the quartz rector by inducing devitrification reactions.

3.4 Product Capture: Oil/Gas

Liquid products from the pyrolysis process needed to be condensed and collected for mass balance and further chemical analysis. This can be problematic due to the high volatility of a number of the components, even at low temperatures, making the design of effective condensation systems crucial in ascertaining accurate mass balances during a pyrolytic process. To achieve this, 5 systems were built and evaluated:

1. $Microwave\ reactor \xrightarrow[Product]{Gaseous\ Oil} Ether\ Condenser$
2. $Microwave\ reator \xrightarrow[Product]{Gaseous\ Oil} Ether\ condenser \rightarrow Liquid\ Nitrogen\ Cold\ Finger\ Trap$
3. $Microwave\ reator \xrightarrow[Product]{Gaseous\ Oil} LN_2\ Cold\ Finger\ Trap$
4. $Microwave\ reator \xrightarrow[Product]{Gaseous\ Oil} 2\ x\ LN_2\ Cold\ Finger\ Trap\ in\ series$
5. $Microwave\ reator \xrightarrow[Product]{Gaseous\ Oil} 3\ x\ LN_2\ Cold\ Finger\ Trap\ in\ series$

For each of the evaluation tests, ether condensers were operated at -10°C and liquid nitrogen traps (~-196°C), with 5 minutes equilibration time allowed before use. To test the system efficiency, 10g of water was placed into the microwave reactor (see Figure 3.8) and purged with nitrogen at a constant flow of 1 L/min. The system was then exposed to 850W microwave power for 5 minutes. The total mass of condensed water collected in the trap(s) was measured at the end of the experiment. The results of which were as follow:

Table 3-5 Water condensation yield by the differing condensation system arrangements tested

Condenser Configuration Method	Wt.% of Condensed Water	S.D. over 5 replicates
1	52.49	8.42
2	93.38	7.65
3	61.32	0.72
4	98.11	1.54
5	97.32	1.78

The results of this preliminary investigation indicated that a condensation system using two or more liquid nitrogen cold finger traps would result in approximately 98% recover of volatilised water with the least variation in result. The results also demonstrated that no more than two liquid nitrogen cold finger traps would be needed as extra traps resulted in an increased standard deviation across the result (The SD is 1.54 vs 1.78), most likely due to compounded measurement error. As such, a condensation system consisting of two liquid nitrogen cold finger traps in series was adopted for use throughout the investigation.

3.5 Conclusion

The design of the microwave pyrolysis system has predominately been driven by the need to control the variables not under investigation. This has been successful in the application of a microwave field with frequency, chamber dimensions, power and microwave duration being kept constant. However, due to the complexities of the interaction of microwaves within any given cavity, particularly when exposed to materials of changing dielectric properties, it is not possible to generate a microwave field with an even or predictable distribution. As such, it must be recognised that field density cannot be classified as an independent variable because it is influenced by a myriad of perturbing factors occurring within a microwave cavity at any given time. With this recognition, all other dependent variables are able to be measured and quantified.

.

CHAPTER FOUR

4 Experimental Methods and Analytical Techniques

"The aim of this chapter is to give an in depth explanation of:

- *the equipment and materials used*
- *the experimental procedures*
- *analytical techniques employed*
- *the calculations used in ascertaining mass balances and product analysis*

In order to understand the thermal and microwave degradation of plastic polymers"

4.1 Introduction

Initial investigations were performed to ascertain the model thermal degradation of the polymers undergoing investigation. This was completed using a combination of Thermal Gravimetric Analysis (TGA) and Pyrolysis Gas Chromatography/Mass Spectrometry, so that mass balances, thermal kinetics and product distributions could be determined.

Subsequently, for the investigation of the microwave degradation of polymers a custom design batch reactor system was constructed; enabling the control of microwave power, duration and carrier gas flow rate. The reactor system also enabled the direct recording of thermal profiles and mass balances, but furthermore the collection solid, liquid and gaseous fractions.

In order to study the effect of microwave degradation parameters, a systematic variation of microwave power, microwave duration, heating rate, sample load, microwave receptor load and polymer type was undertaken. Analysis of products was subsequently performed.

Solid fractions were subjected to nitrogen adsorption surface area analysis, surface imaging by Scanning Electron Microscopy (SEM) and chemical composition by Pyrolysis Gas Chromatography/Mass Spectrometry (Py-GC/MS), Carbon-Hydrogen-Nitrogen (CHN) Ratio analysis, Fourier Transform Infrared Spectroscopy (FT-IR) and Bomb Calorimetry. Oil fractions were subjected to analysis by Fourier Transform Infrared Spectroscopy (FT-IR), Gas Chromatography/Mass Spectrometry (GC/MS), Gas Chromatography – Flame Ionisation Detection (GC-FID) and Carbon-Hydrogen-Nitrogen (CHN) Ratio analysis.

4.2 Materials

Pure polymers samples were sourced from Sigma Aldrich (Poole, UK) During the course of the experimentation two polymer feedstock were used as follows (Table 4-1):

Table 4-1 Plastic Polymers

Polymer Type	Manufacturer	Product No.	Weight Average Molecular Weight (M_w)	Number Average Molecular Weight (M_n)
Poly (Vinyl chloride) (CAS:9002-86-2)	Sigma Aldrich	346764	~233,000	~99,000
Poly (Acrylonitrile-co-Butadiene-co-Styrene) (~40wt.%Acrlonitrile) (CAS:9003-56-9)	Sigma Aldrich	180882		

To aid the collection, preparation and analysis of solid, oil and gas products, a number of solvents and gases were used. These are detailed in Table 4-2 and Table 4-3:

Table 4-2 List of Solvents

Solvent Type	Manufacturer	Product No.	Purity (%.vol)
Acetone GPC (CAS:67-64-1)	Fisher Scientific	A/0650/PC21	99+%
Di-chloromethane (DCM) (HPLC Grade) (CAS:75-09-2)	Fisher Scientific	D/1856/17	99.8+%
n-Hexane (HPLC Grade) (CAS:110-54-3)	Fisher Scientific	H/0406/17	95%
Methanol (HPLC Grade) (CAS:67-56-1)	Fisher Scientific	M/4056/17	99.8%+

Table 4-3 List of Gases

Gas Type	Manufacturer	Purity (%.vol)
Argon	BOC Group	99.998+%
Helium	BOC Group	99.996+%
Nitrogen, Oxygen Free	BOC Group	99.998+%
Nitrogen, Liquid	BOC Group	99.999%

Carbon microwave receptor with a particle size of 150µm - 250µm was prepared in house by the methodology given in Section 4.3.2.2.

4.3 Microwave Batch Reactor

4.3.1 Experimental Equipment

For the purposes of the experimentation undertaken it was necessary for a microwave pyrolysis system to be designed and constructed.

The system was designed to incorporate a nitrogen purge gas with flow regulation, internal vessel temperature measurement by IR sensor, an adjustable multimode microwave oven, custom design reaction vessel and liquid nitrogen gas condensation system. These components are shown in Figure 4-1, Part C 1-5 respectively.

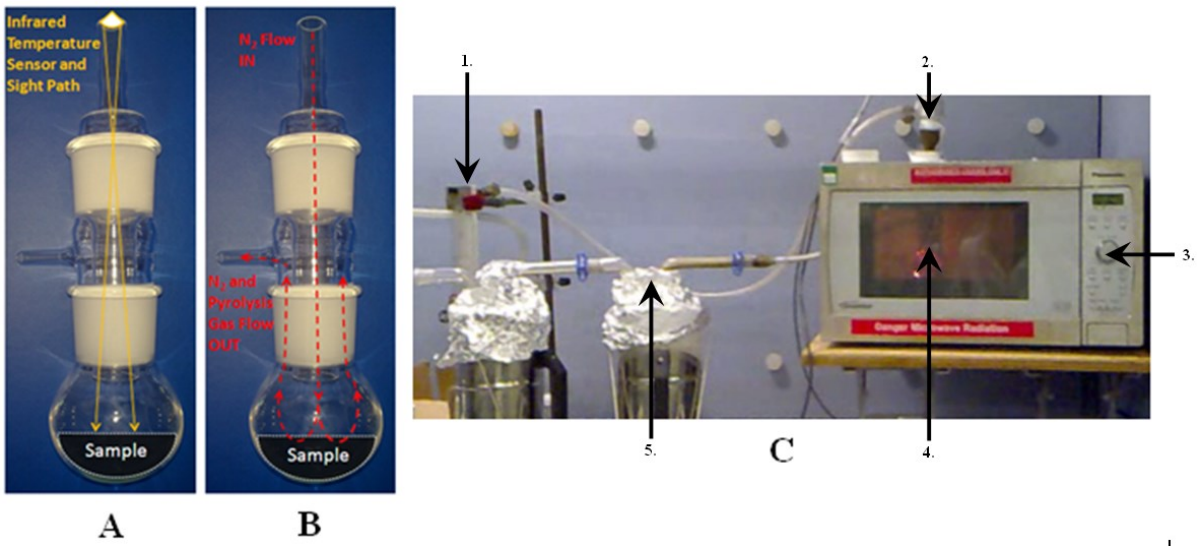


Figure 4-1 Microwave Reactor Design: A) Quartz Reactor with Infrared Sensor Sight Path, B) Quartz Reactor with Gas Flow, C) Microwave Reactor Final Setup

During each experimental run a nitrogen purge gas was passed through the apparatus creating an inert atmosphere for the microwave decomposition to occur. This was regulated via a Platton Nitrogen Gas Variable Flow meter, 0.1-1.2 l/min at 0.1 l/min intervals. This was connected to the Infrared Sensor's (Calex Pyro USB-CF) purge collar which had been adapted to fit the fused quartz IR sensor viewing window/dreschel head.

The custom designed quartz reaction vessel was fitted within a modified Panasonic multimode microwave oven (Model No. NN-SD277S). This enabled the continuous purge of the microwave reaction vessel with a set Nitrogen flow rate.

This configuration had a multifaceted operation; to maintain a clear line of site for the IR sensor, so that the sample undergoing decomposition (as shown in Figure 4-1, part A and B) could be monitored continuously throughout each experiment and thermal profiles recorded.

The resultant decomposition gases from each experiment were forced from the reaction chamber through a PTFE tube to the liquid nitrogen condensing system, where they were condensed and collected for further analysis.

4.3.2 Experimental Procedure

4.3.2.1 Polymer Sample Preparation

As received polymers from Sigma Aldrich were either in powder or pelletized form, with no particle size distribution provided. To ensure a consistency throughout all experimentation, it was decided to harmonise the particle size to between 45µm and 250µm, which meant that particle size reduction was required. This was achieved by the method of cryogenic milling.

This used a Retsch – CryoMill (Germany) (see Figure 4-2) with 50ml stainless steel grinding jar. Approximately 3.0g ± 0.2g of pelletized plastic wasplaced inside the grinding jar with a single stainless steel ball. The jar was placed within the CryoMill and reduced in temperature to -196^{o}C over a four minute period whilst oscillating at 5Hz. Once at -196^{o}C, the mill would oscillate for a period of 7 minutes at 23Hz. The mill was then allowed to return to room temperature and the sample removed. The milled plastic would be dried at 50^{o}C for 24hrs to remove any condensed moisture from the milling process.

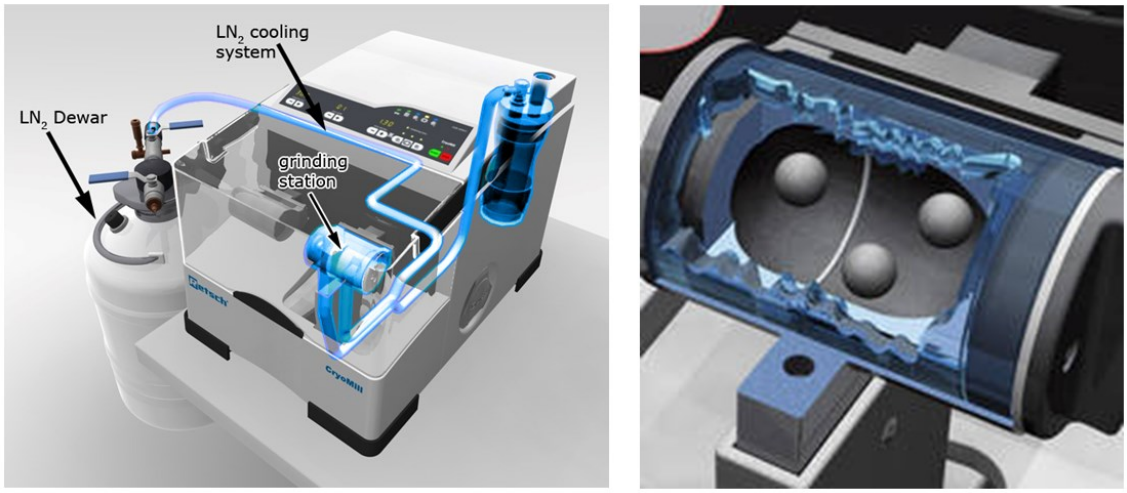


Figure 4-2 Retcsh Cryo-mill: Schematic of Cryo-mill (Left) and cutaway of grinding jar (right) (Retsch, 2012).

The milled-dried material was passed through 500µm, 250µm, 150µm and 45µm sieves as per ASTM D1921 (Standard Test Methods for Particle Size (Sieve Analysis) of Plastic Materials) Test Method B. Fractions would then be separated into particle size ranges of <500µm and >250µm or <250µm and >150µm or <150µm and >45µm. This milling and sieving process was repeated until sufficient material was gained to perform all experiments. The plastic was then stored in a sealed air tight container until required.

Materials received as a powder would be subjected to 24hrs drying at 50°C to maintain method consistency, then sieved according to ASTM D1921 - Test Method B and separated as described above.

4.3.2.2 Carbon Additive Preparation

In order to assist/initiate the microwave decomposition process in some of the tests, carbon char was used, due to its high loss factor. This was prepared in-house through the carbonisation of Coconut endocarp obtained from the *Cocos nucifera,* Malaysia. This was supplied pre-washed and chipped.

The dried material was sieved using 8mm and 4mm sieves. The fraction that was retained on the 4mm sieve was utilised. The separated material was dried for 2 days at 50°C to remove any excess moisture.

Following sample preparation, the carbonisation process was performed, using a Carbolite rotary furnace model HTR11/150 (Hope Valley, UK). For this 200.0g ± 0.5g of >4mm endocarp was loaded into the reaction vessel and installed within the furnace. A nitrogen purge of 500 ml/min was applied

to the reactor for the duration of the process. The sample was heated at 10°C/min to 835°C (to remove all volatile species), where it was held for one hour and then allowed to cool. A constant lateral rotation of 10 rpm and a nitrogen purge of 500 ml/min were applied to the reactor for the duration of the process.

Particle size reduction was then performed using a 'TEMA, Laboratory Disc Mill'. Fractions were then separated into particle size ranges of <500µm and >250µm <250µm and >150µm or <150µm >45µm. These were then stored in sealed laboratory sample bags. Before use, the prepared char was subjected to 24hrs drying at 110°C to remove any absorbed water.

4.3.2.3 Microwave Pyrolysis

At the beginning of each experiment the PTFE transfer tube, Quartz Infrared Viewing Window, Quartz Joining Collar, Quartz Bulb Flask and Cold Traps (as shown in Figure 4-3) were weighed individually to ascertain starting weights of each component; to enable the mass balances to be calculated at the end of the experiment.

A pre-defined mass of prepared polymer (Section 4.3.2.1) between 0.500g and 5.000g ± 0.01g would be weighed into the Quartz bulb reactor. A weight of carbon receptor of between 0.500g and 5.00g ± 0.01g (Section 4.3.2.2) would be added and the contents thoroughly mixed (by stirring) until an even distribution of plastic and carbon particles was achieved.

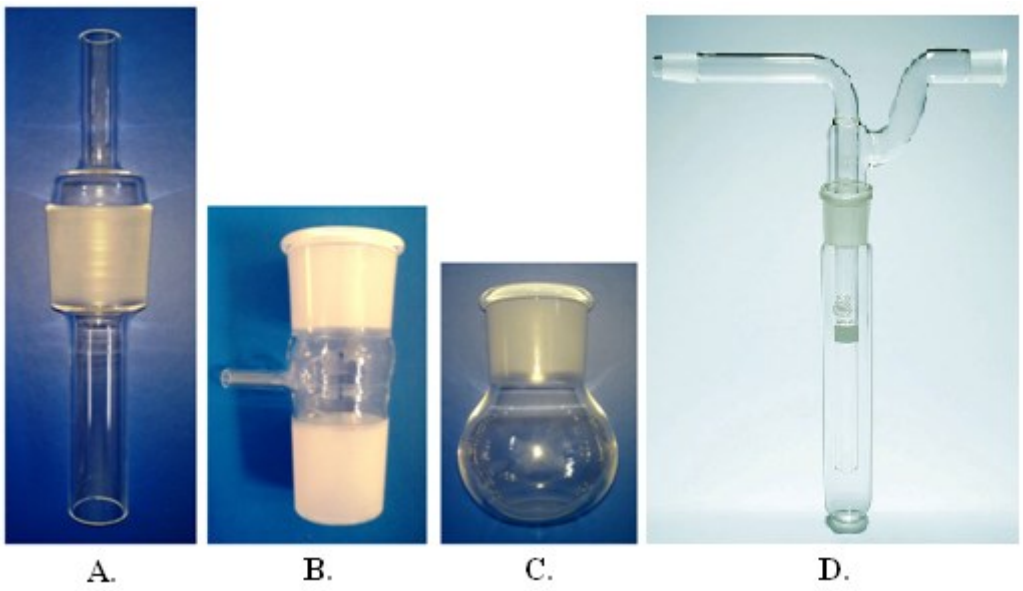


Figure 4-3 Microwave Pyrolysis Experiment Glassware: A.) Quartz IR Viewing Window, B.) Quartz Joining Collar, C.) Quartz Bulb Flask and D.) Quickfit Cold Trap

Subsequently, the reactor was assembled as shown in Figure 4-1, with IR sensor and liquid nitrogen cold traps attached. The system was then purged with Nitrogen gas at a rate of 1 L/min for 5 minutes, at to remove any oxygen from the system and allow sufficient time for the whole body of the cold traps temperature to cool and stabilise. The nitrogen purge would then be set to that required for the experiment (dependent upon experimental parameter conditions) and microwave power/duration. The experiment would then commence.

For the duration of the experiment the IR sensor would record the surface temperature of the sample at 1 second intervals.

On completion of the microwave run the reactor was allowed to cool to room temperature and the cold traps were removed from the liquid nitrogen dewars and allowed to warm to room temperature, whilst maintaining the nitrogen purge passed through them of oxidation of remaining residues and the risk of water vapour condensing within the traps.The Quartz bulb flask was weighed to determine the weight of plastic and carbon residue.

The Quartz IR Window and Joining Collar were washed 5 times with 50 ml of DCM and the liquid quantitatively transferred to a sealed glass flask. This process was also performed on the cold traps and PTFE transfer tube. The collected liquid was then passed through a pre weighed Büchner Funnel fitted with an FP4 Glass frit. This was subsequently rinsed 3 times with 50 ml of DCM to ensure no petrochemical residue remained within the frit. The filter was dried at 50^{o}C for 1 hrs to remove any solvent residue and then weighed to determine the solid residues retained on the filter.

The filtered solution of DCM and pyrolysis oil was quantitatively transferred to a pre-weighed 1 litre pear shaped evaporation flask. This was rotary evaporated (Buchi R23 Rotovap, Germany) at 40^{o}C for 1 hour at 1 atmosphere to remove all DCM. The flask was then weighed and the yield of oil calculated. The residue oil was transferred to sealed brown glass sample bottles and stored at 6^{o}C.

During the preparation of oils through separation via rotary evaporation the loss of volatile organic compounds with boiling points lower than that of dichloromethane (40^{o}C) will occur. However, due to the consistent method of using a set volume of dichloromethane to wash all condensing equipment and a set period of rotary evaporation of 1 hour at 40°C, the losses were considered to be consistent throughout all samples examined. It would be desirable to be able to examine the lower boiling point compounds, however, their separation from the di-chloromethane solvent would be extremely difficult requiring the crude chromatographic process or by performing multiple fractional distillation is to enhance the removal of dichloromethane from the low boiling point volatile organic

compounds. However, the likely losses during this process would render the results with such error that accurate weights of these compounds are unlikely to be derived. It is also most likely that a significant proportion of these compounds would be lost to the surrounding environment or into the vacuum system or if any such process were attempted.

4.3.3 Experimental Calculations

4.3.3.1 Mass Balances

During the microwave decomposition process the polymer is broken down into fragments. The recombination and secondary reactions these undergo result in the formation of solid, liquid and gaseous products. As such, the overall process mass balance was calculated as:

$$M_{init} = M_s + M_o + M_g$$

Equation 4-1 Mass Balance

Where M_{Init} = initial mass of polymer
M_s = mass of solid
M_o = mass of oil
M_g = mass of gas

The mass of solid was calculated from:

$$M_s = (RF_{Fl} - RF_{init}) + (JC_{Fl} - JC_{init}) + (VW_{Fl} - VW_{init}) + (TT_{Fl} - TT_{init}) + (FP_{Fl} - FP_{init}) + (M_R)$$

Equation 4-2 Solid Mass Calculation

Where M_s = Total Mass of Solid
RF_{init} = Reaction flask initial weight
RF_{Fl} = Reaction flask final weight
JC_{init} = Joining collar initial weight
JC_{Fl} = Joining collar final weight
VW_{Init} = Viewing window initial weight
VW_{Fl} = Viewing window final weight
TT_{Init} = Transfer tube initial weight
TT_{Fl} = Transfer tube final weight
FP_{Init} = Filter paper initial weight
M_R = Mass of receptor

FP_{Fl} = Filter Paper final weight

The mass of oil was calculated from:

$$M_o = EF_{Fl} - EF_{init}$$

Equation 4-3 Oil Mass Calculation

Where M_O = Total Mass of Oil

EF_{init} = Evaporator flask initial weight

EF_{Fl} = Evaporator flask final weight

The mass of gas was calculated by difference, where:

$$M_g = M_{init} - \sum(M_s + M_o)$$

Equation 4-4 Mass of Gases Calculated by Difference

Masses of each component were then represented as a fraction for comparative purposes by re-arrangement of the following equation.

$$Total\ \% = \left(\frac{M_S + M_o + M_g}{M_{Init}}\right) * 100$$

Equation 4-5 Mass Fractions

Where Total% = Total mass as a percentage

M_{Init} = initial mass of polymer

M_s = mass of solid

M_o = mass of oil

M_g = mass of gas

Calculated error from measured values was derived using the following equations.

For calculations requiring addition and subtraction e.g. x = a + b – c, then error equals

$$S_x = \sqrt{S_a^2 + S_b^2 + S_c^2}$$

Equation 4-6 Calculated Error (addition and subtraction)

Where S_x = Uncertainty in result

a,b,c = Are numbers used for calculation

x = Result of calculation

S_a,S_b,S_c = Uncertainty of numbers used for calculation

For calculations requiring multiplication and division e.g. x = a*b/c, then error equals

$$S_x = x.\sqrt{\left(\frac{S_a}{a}\right)+\left(\frac{S_b}{b}\right)+\left(\frac{S_c}{c}\right)}$$

Equation 4-7 Calculated Error (multiplication and division)

Where S_x = Uncertainty in result

a,b,c = Are numbers used for calculation

x = Result of calculation

4.4 Model Thermal Pyrolysis

The model thermal pyrolysis experimentation relied upon the use of Simultaneous Thermal Gravimetric Analysis (TGA/DSC) and Pyrolysis-Gas Chromatography/Mass Spectrometry (Py-GC/MS). These techniques were used to effectively examine the effect of heating rate and maximum temperature on the physical and kinetic properties of materials when undergoing thermal decomposition, extent of decomposition as well as product distribution by pyrolysis.

4.4.1 Thermal Gravimetric Analysis (TGA/DSC)

. Any process which causes a change in weight or energy within the sample can be investigated using these techniques. The combination of both mass loss and heat flow allows for the identification of endothermic and exothermic events in which mass is lost e.g. evaporation of a solvent or decomposition of a polymer structure, as well as identification of phase-change events as glass transitions, melting point, crystallisation etc.

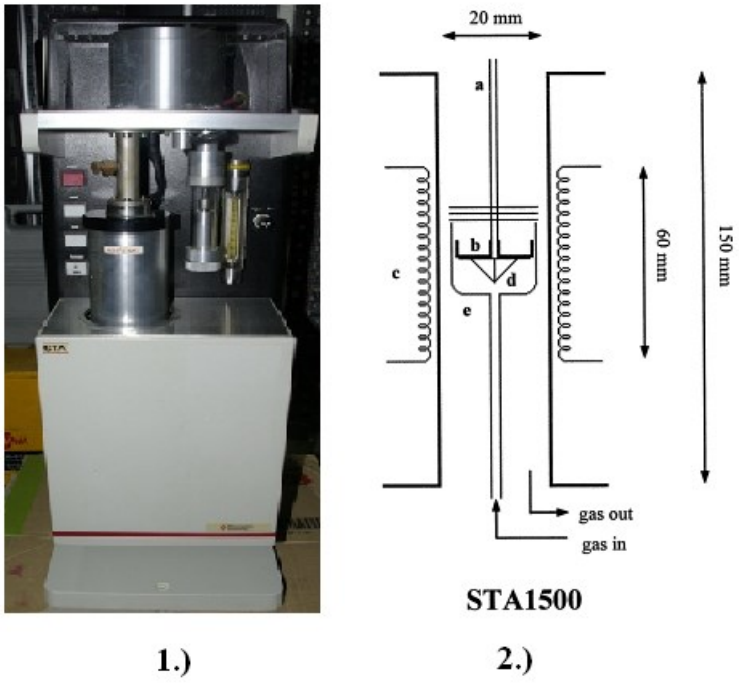


Figure 4-4 1.) Rheometric Scientific STA 1500 TGA/DTA and 2.) Schematic of Rheometric STA1500 furnace (Russell *et al.*, 1998), a. hangdown, b. crucible, c. Furnace winding, d. Sample thermocouple and e. Microenvironment cup

Approximately 20mg of sample was accurately weighed into an alumina crucible. This was placed on the STA hangdown for analysis. The experiments were performed under nitrogen at a continuous flow; 50ml/min to maintain an inert atmosphere. The samples were heated from 0-1000^{o}C at heating rates of 1, 10, 30 and 50^{o}C/min, weight (mg) and heat flow (mW) being recorded at a rate of 1 sample point per 1^{o}C. The resulting information was used to model the decomposition behaviour of polymers undergoing investigation.

4.4.2 Pyrolysis Gas Chromatography/Mass Spectrometry

The products of thermal pyrolysis are not only controlled by the parent material, but also the operating conditions used; heating rate, maximum temperature and residence time at this temperature. These, together with the material properties, influence the amount and nature of the volatiles produced during pyrolysis.

Pyrolysis - Gas Chromatography/Mass Spectrometry (Py-GC-MS) is an analytical method by which the degradation products of a material can be collected, examined and identified. The usefulness of the technique is based upon the application of thermal energy to produce volatile fragments from macromolecules which are subsequently capable of being analysed using GC/MS. This technique is of particular use in the separation of complex pyrolysis products and used alongside mass spectral

libraries, enabling the confident identification of organic compounds (Qian *et al.*, 1996). Nevertheless, the method is limited because high boiling point compounds are often unable to be detected due to incompatible chromatographic conditions (van der Peyl *et al.*, 1991)

Nevertheless, it is particularly suitable for examining the sample response to the pyrolysis conditions of heating rate, temperature, the presence of reactive gases and catalysts on a small, highly controllable scale. Thus, this method has been used to examine a number of these factors so that the effect of operating conditions can be identified.

Samples used in experimentation were prepared as described in Section 4.3.2.1. Py-GC-MS experimentation was carried out using similar methodology as Perng (2001), Jiang *et al.* (2010) and Zhao *et al.* (2012).

A CDS 5200 pyrolyser (see Figure 4-5) unit (see Figure 4-5) with cryo focusing ability, was coupled with a Perkin Elmer Clarus 500 GC and a Perkin Elmer Clarus 560MS Ei+ quadrapole mass spectrometer.



Figure 4-5 CDS 5200 Pyroprobe, pyrolysis unit

Samples of approximately 2mg ± 0.02mg were placed inside a quartz sample tube and then inserted into the pyroprobe's platinum filament (see Figure 4-6). The pyroprobe was calibrated by the manufacturer to ensure thermal accuracy. The sample pyroprobe was inserted into the reaction chamber which was then purged with helium at a rate of 15ml/min for 2 minutes so that an inert

atmosphere could be attained. Subsequently, the sample would be heated at the pre-determined rate and to a set temperature, with the evolved volatile products being carried via a heated transfer line (at 300^{o}C) to the injector of the GC. The gases were then held on the front of the injector which was kept at -150^{o}C throughout the pyrolysis of the sample. Upon completion of the pyrolysis the injector was heated to 300^{o}C, resulting in chemicals being trapped at -150^{o}C volatilising.

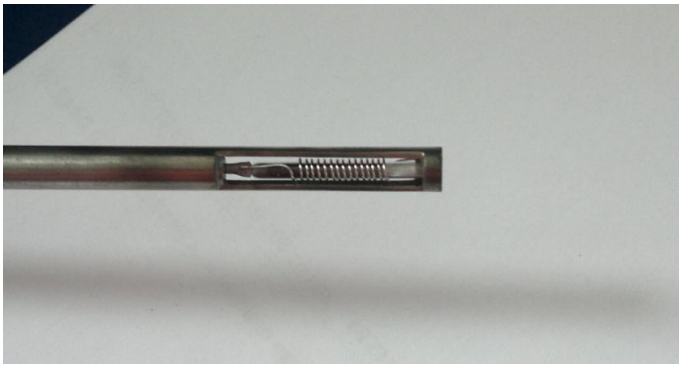


Figure 4-6 Pyrolysis units heated coil with quartz sample tube

The resulting gases were then passed into the fused silica capillary column; Supelco Petrocol DH (100m x 0.25mm) . The output from the GC was then transferred to the MS in which the mass spectra were recorded under electron impact ionisation energy of 70eV. The MS detector scanned from 4 – 502m/z; full details of MS method are given in Section 4.6.1. Data analysis was subsequently performed using Perkin Elmer Turbomass Ver. 5.3.0 software comparing results with the 'NIST Mass Spectral Data Library 2005' where reliable identification of the components was carried out.

The Py-GC-MS method was developed and tested using a polyethylene standard of 2mg ± 0.02mg. Extensive method development was required. The resulting chromatogram is shown in Figure 4-7.

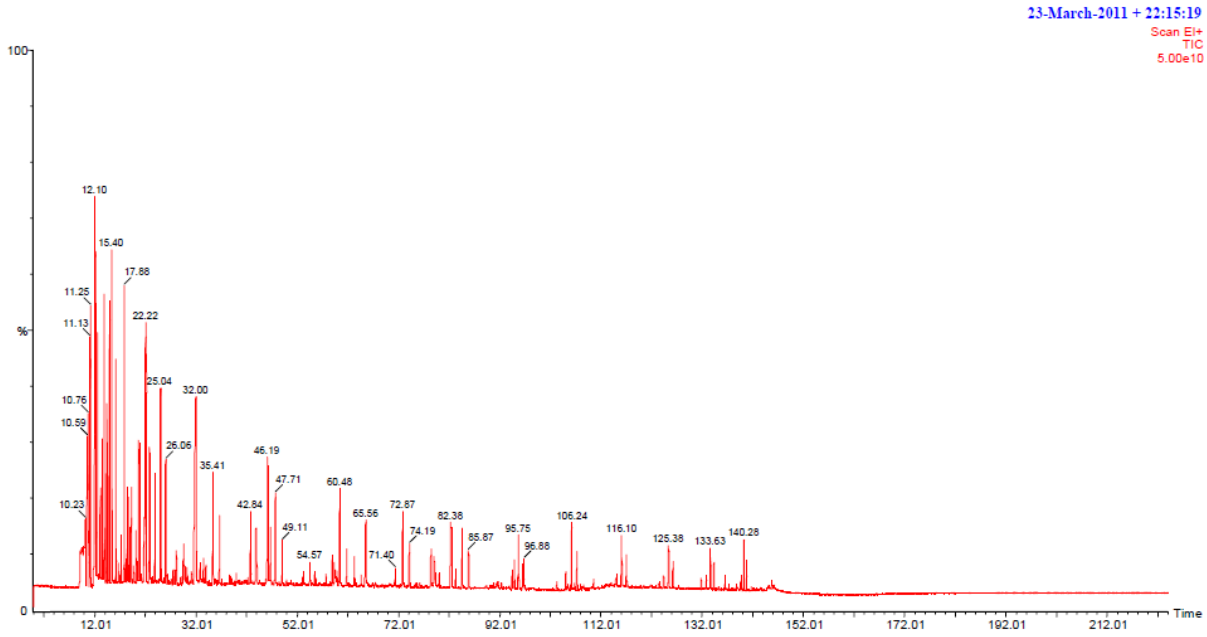


Figure 4-7 Py-GC/MS final polyethylene test method result

4.5 Char Analysis

The analysis of chars resulting from microwave decomposition experimentation was performed to determine and understand changes to the physical and chemical attributes resulting from the reaction with plastic decomposition products and as a result of interacting with the microwave field.

4.5.1 Thermal Gravimetric Analysis/Differential Scanning Calorimetry (TGA/DSC)

Thermal Gravimetric Analysis/Differential Scanning Calorimetry was performed to identify changes in the stability of the char and the extent of decomposition of the polymer. This was performed using the equipment and method described in section 4.4.1, with the single difference being analysis was performed at a heating rate of 10^{o}C/min. This method was used to examine chars post pyrolysis to detect the presence of any un-pyrolysed material or the presence of lower molecular weight hydrocarbons remaining on the char.

4.5.2 Carbon Hydrogen Nitrogen Analysis (CHN)

CHN analysis of dried and ground samples of particle size <500 µm was carried out by MEDAC Ltd, Surrey UK.

4.5.3 Scanning Electron Microscopy (SEM)

A JEOL-5610LV scanning electron microscope was employed for the examination of gold coated solid samples; microwave receptor and pyrolytic char. The method allowed for the examination of the samples surface from 150x to 10,000x magnification.

4.5.4 Fourier Transform Infrared Spectroscopy

The FTIR absorbance spectra of each sample was determined using a MAGNA 560 IR Spectrophotometer (Nicolet, USA). The FTIR was set to measure absorbance between 600nm and 4000cm^{-1}. The number of scans and scan resolution was set at 250 and 4cm^{-1} respectively. Before sample analysis was performed a background spectrum would be collected which was subsequently subtracted from the sample spectra.

For each char sample a small amount was taken, in the region of 0.10mg. This was then mixed by grinding with Potassium Bromide (Spectrosol, VWR International Ltd., Poole, UK) in a ratio of 1:100 w/w. Approximately, 150 mg of the mixture was taken and put under 10 metric tonnes pressure for 10 minutes, in a 10mm diameter die press. The disc created was analysed by the Spectrometer producing an infrared spectrum.

4.5.5 Pyrolysis-Gas Chromatography/Mass Spectrometry

py-GC/MS was utilised to examine the residual char from each pyrolysis process to determine if any un-pyrolysed material or the presence of lower molecular weight hydrocarbons remaining on the char. If residue was present this would have presented itself as signature peaks on GC chromatograms, however char was clean with no un-pyrolysed material remaining, with chromatograms repeatedly seen; as displayed in Appendix B.

4.6 Oil Analysis

4.6.1 Gas Chromatography/Mass Spectrometry (GC/MS)

Gas chromatography-mass spectroscopy (GC-MS) is extensively used in the examination of gas and liquid hydrocarbons, so that either or both qualitative and quantitative analysis is achieved (Gudzinowicz *et al.*, 1976, Hübschmann, 2001).

Samples were prepared by pipetting 1000µl of liquid sample (Section 4.3.2.3), into 3000µl of dichloromethane and allowed to dissolve. This solution was then transferred to a 2.5ml brown glass GC vial leaving ~1mm of head space, to minimise evaporation of compounds. This was then crimp sealed with a PTFE/Silicone septum.

For each analysis, 3µl of sample was injected on to the GC and analysed using a bespoke GC method developed in-house. For this a Pneumatic Split/ Splitless Packed Injector held at 300°C with a split ration of 1:20 was used, with an on column flow of 1ml/min. The column was initially held at 40°C for 4 minutes, then ramped at 1.3°C/min to 200°C, with no holding period, then ramped to 300°C at 2.7°C/min and isothermed at 300°C for 60 minutes.

For the duration of the run the MS utilised an Ei+ source using ionisation energy of 70eV with a scan span of 50-502Da, scan time of 0.49 seconds, cycle time of 0.39 seconds and an inter scan delay of 0.1 seconds. The source was held at 350°C for the duration of the analysis.

An adapted method by Ludlow-Palafox and Chase (2001) was used in the quantification of differing component types by the integration of total ion chromatograms (TiC). Classification by chain length and products type was then performed. The method does not rely upon quantification by calibration of the instrument, but due to total ion content percentage (TiC%) reflecting wt.% (approximately) composition analysis can be performed.

4.6.2 Gas Chromatography/Flame Ionisation Detection - Simulated Distillation (GC/FID-SimDis)

Simulated distillation is a chromatographic technique whereby the theoretical boiling point distribution of a liquid hydrocarbon mixture can be ascertained (Green *et al.*, 1964, Raia *et al.*, 2000). It is often used to support or replace physical distillation data. The method relies upon the separation of hydrocarbons by gas chromatography on a non-polar column, this ensuring that each component is separated dependent upon boiling point/volatility (Villalanti *et al.*, 2006). Each component is subsequently detected through the use of a Flame Ionisation Detector (FID).

An adapted version of the simulated distillation methodology based upon the principles and methods set out in Green *et al.* (1964), ASTM 2887 and Wang (2005) was employed in characterising the boiling point distributions of liquid hydrocarbons generated from the experimentation.

The GC/MS method developed in Section 4.6.1 was utilised in the simulated distillation methodology. A calibration mixture for the development of ASTM D2887 from Stanhope Seta (SIMDIS STVM P/N:

99906-0), containing n-alkanes from n-pentane (C_5) to *n*-tetratetracontane (C_{44}) was checked and characterised using the GC/MS method. Retention times were subsequently assigned to each component within the mixture. The column was subsequently attached to a flame ionisation detector and injection of the calibration mixture performed again. The mass fraction of each boiling point interval was calculated from the sum of the area of the peaks within that interval, assuming the area of each peak was proportional to its mass fraction (Tong and Karasek, 1984, Kpere-Diabo, 2009). Cumulative peak area was calculated and checked against the boiling point distribution of the standard as to confirm method validity.

4.6.3 Fourier Transform Infrared Spectroscopy

The FTIR spectra of each oil sample was obtained using the instrument and conditions described in section 4.5.4. The oil was mounted between two NaCl discs rather than being pressed as a KBr disc.

4.6.4 Carbon Hydrogen Nitrogen Ration Analysis

CHN analysis was performed on the liquid samples as described in Section 4.5.2.

The analysis was performed on 500mg of liquid sample as prepared in Section 4.3.2.3

4.6.5 Bomb Calorimetry

The calorific values of oil samples were determined using a Parr 6100 Oxygen Bomb Calorimeter with a Parr 1108 oxygen bomb. The samples were ignited at 25^{o}C in 99% pure oxygen at 3.03MPa (30 atm), supplied by BOC. Two ml of distilled water was added to the bomb using a syringe to act as a sequestering agent or absorbent.

Before determination of samples could be carried out, the bomb calorimeter was standardised against benzoic acid with a certified specific energy of combustion at standard bomb conditions of 26.454 MJ kg^{-1}.

4.7 Gas Compositional Analysis

Gas composition from pyrolysis experiments was not examined due to limitations of experimental equipment. This was largely due to the use of a liquid nitrogen condensing system, with such efficiency that nitrogen carrier gas was condensed. This resulted in an unknown volume of nitrogen gas condensed, hence if analysis were to be attempted the dilution of the sample would not be known. Further to this, it was not possible to control the thawing process of liquid nitrogen condensers. Hence, the gases produced had to be vented to atmosphere unimpeded, so that excessive pressure build up was avoided within the condensers, which may subsequently have result in vessel failure (explosion).

CHAPTER FIVE

5 Investigation of the Microwave Decomposition of Acrylonitrile-co-Butadiene-co-Styrene and Styrene

"The aim of this chapter is to examine, the underlying factors determining the thermal and microwave decomposition of ABS, by:

- *examining the thermal decomposition of ABS in relation to temperature and heating rate*
- *determine the thermal decomposition pyrolysis products in correlation to temperature*
- *examining the microwave decomposition process of pure ABS*
- *characterise and determine the behaviour of carbon additive when exposed to microwave radiation*
- *establish the effect of carbon additive on the microwave decomposition process*
- *determine the relationships between product yields and experimental variables of carbon additive, weight of ABS and microwave power*
- *determining the composition of oils and identify their correlation to key experimental variables*
- *compare product composition with that of the thermal process*

.... and draw conclusion on the overall microwave decomposition process"

5.1 Introduction

Acrylonitrile-co-Butadiene-co Styrene (ABS) is a thermosetting polymer comprised of poly(styrene-co- acrylonitrile) forming a continuous amorphous chain, dispersed with a second phase of butadiene copolymer (Arostegui *et al.*, 2006, Suzuki and Wilkie, 1995). The proportions of each component can be adjusted to suit its physical performance requirements. Acrylonitrile provides chemical and heat resistance whilst also increasing durability where as butadiene enhances impact strength and styrene promotes structural rigidity (Balart *et al.*, 2006); as such the compound is most commonly represented as in Figure 5-1.

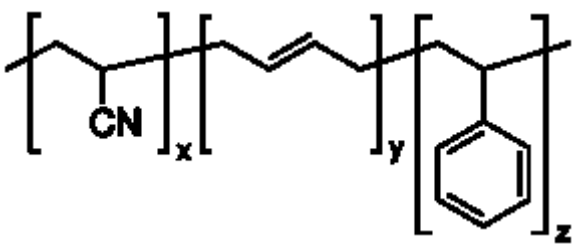


Figure 5-1 Generic Structure of Acrylonitrile-co-butadiene-co-styrene (x,y and z = integers) (Sigma-Aldrich, 2013)

As a consequence of these properties, ABS is used extensively for a myriad of engineering applications and represents one of the most abundant polymers used today. It is used extensively in the production of electrical equipment and the production of shaped composites for the automotive industry (Mantaux *et al.*, 2004). From manufacturing data it is estimated to make up 2wt.% of all plastics manufactured within the UK (Aguado, 1999, Gupta *et al.*, 1998), however little information is available on rates of recycling, as discussed in Section 2.3.

A number of techniques are currently employed in the recycling of ABS, the choice of which is very much dependent upon the stage of the lifecycle the composite from which it is taken. For example, during manufacture or for composites in which the quality can be ensured, primary/secondary recycling methods of grinding following direct reuse by injection moulding are employed (Bai *et al.*, 2007).

Primary/secondary recycling of ABS is limited to the number of times that the process can be repeated, due to the degradation of the poly(butadiene) component in the mixture after 5 cycles. This results in loss of material impact strength (Bai *et al.*, 2007). Thus, alternative methods of recycling/reuse of those sources of ABS, in which quality cannot be guaranteed, centre around tertiary recycling techniques involving polymer dissolution using solvent based processes (Arostegui *et al.*, 2006).

The products of such a process are often reformed to produce lesser grades of ABS composite. Further to this, the methods of conventional thermal and catalytic pyrolysis have also been used and predominantly result in the production of fuel fractions (Faravelli *et al.*, 2001, Vasile *et al.*, 2006), with reasonable success observed. Nevertheless, these methods currently suffer from the limitations as outlined in Section 1.1 and 2.4. Hence, the viability of the microwave assisted decomposition process has been explored for ABS polymer in the following chapter.

5.2 Conventional Thermal Decomposition of ABS

5.2.1 Thermal Gravimetric Analysis

The thermal decomposition behaviour of ABS was studied using the method described in section 4.4 using the TGA. The data produced is shown in Figure 5-2. It can be seen that ABS undergoes degradation in a single decomposition event in which almost 100wt.% loss is observed, with a nominal residual of less than 1wt.% remaining. This event takes place over the temperatures of 235^{o}C to 500^{o}C, in good agreement with those results observed by Suzuki and Wilkie (1995) and Balart *et al.* (2006).

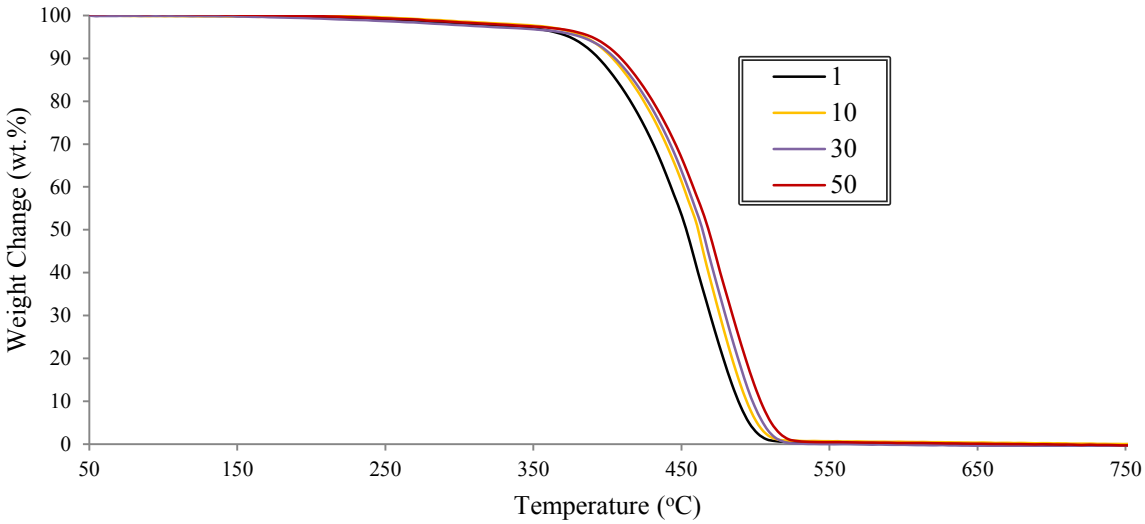


Figure 5-2 Thermal Degradation profiles of ABS under nitrogen atmosphere at 1, 10, 30 and 50°C/min

Nevertheless, upon examination of the DTG plots (see Figure 5-3) it becomes apparent that decomposition takes place over two distinct stages, the first of which occurs at 160 to 355°C and the second from 355 to 540°C. These temperatures are different from the observations of Fătu *et al.* (1989) and Shapi (1991), whereby the decomposition temperatures of ABS under investigation were at 180°C to 480°C and the second observed between 480°C and 620°C. A further third peak was determined by Yang *et al.* (2004). Nevertheless, these disparities can be explained by differences in the test parameters used during these investigations as well as differing component ratios/ABS composition.

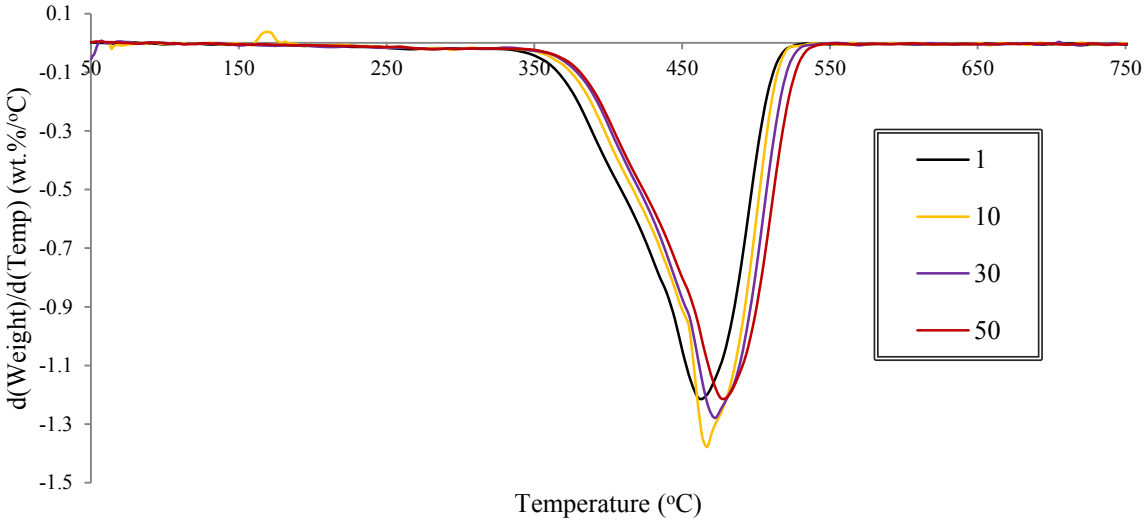


Figure 5-3 Differential Thermal Gravimetric Analysis of ABS at 1, 10, 30 and 50°C presented as wt.%/°C vs Temperature

During the current analysis at 10°C/min, the appearance of three differing gradients up to peak decomposition temperatures at 465°C are apparent indicating that the major decomposition event taking place is in reality three overlapping decompositions. This would appear to correspond with the progressive decomposition of ABS as outlined by (Suzuki and Wilkie, 1995) and later referred to by Yang *et al.* (2004) whereby it occurs dependent upon the constituents, with breakages occurring at the butadiene regions of the polymer then progressing to that of the styrene-co-acrylonitrile (SAN). It was also recognised that the decomposition products are affected when the content of butadiene increases with the ultimate result of increasing carbonaceous residue. However, this will not be considered in this investigation as a uniform ABS feedstock has been used.

Over the range of heating rates used in this investigation (1-50°C/min) it was found that little difference could be observed in the decomposition event temperatures, with only a minor shift of 15°C between the two decompositions observed. This is illustrated on the DTG plots (Figure 5-3), whereby the weight loss over this period for heating rates of 1 and 10°C/min is seen to peak at -1.21 (461°C) and -1.38wt.%/min (466°C), respectively. Upon increasing heating rates further, a minor shift occurs with peak decomposition occurring at 472°C and 476°C for 30 and 50°C/min experiments. No further increase/decrease of decomposition rate was observed. The shift in decomposition temperature is probably attributable to thermal lag within the system as previously observed during the decomposition of PVC in Figure 6-3.

The decomposition undertaken by ABS is a free-radical driven process, whereby end chain and random scissions take place simultaneously (di Cortemiglia *et al.*, 1985, Suzuki and Wilkie, 1995), so little further information can be gained from TGA, hence the examination of the decomposition process/products has been continued using the method of Py-GC/MS.

5.2.2 Py-GC/MS

The thermal decomposition of ABS was examined utilising Py-GC/MS, with samples exposed to final pyrolysis temperatures of 200, 300, 400, 500 and 600°C at a heating rate of 20°C/min. From this it was found that ABS did not release organic material detectable by the Py-GC/MS method employed until 500°C was achieved. At which point the polymer underwent complete degradation with no further decomposition observed, as evidenced by the lack of change in the GC/MS trace. To gain further understanding of the decomposition processes occurring, smaller pyrolysis temperature intervals are required over the region of decomposition (180 – 540°C).

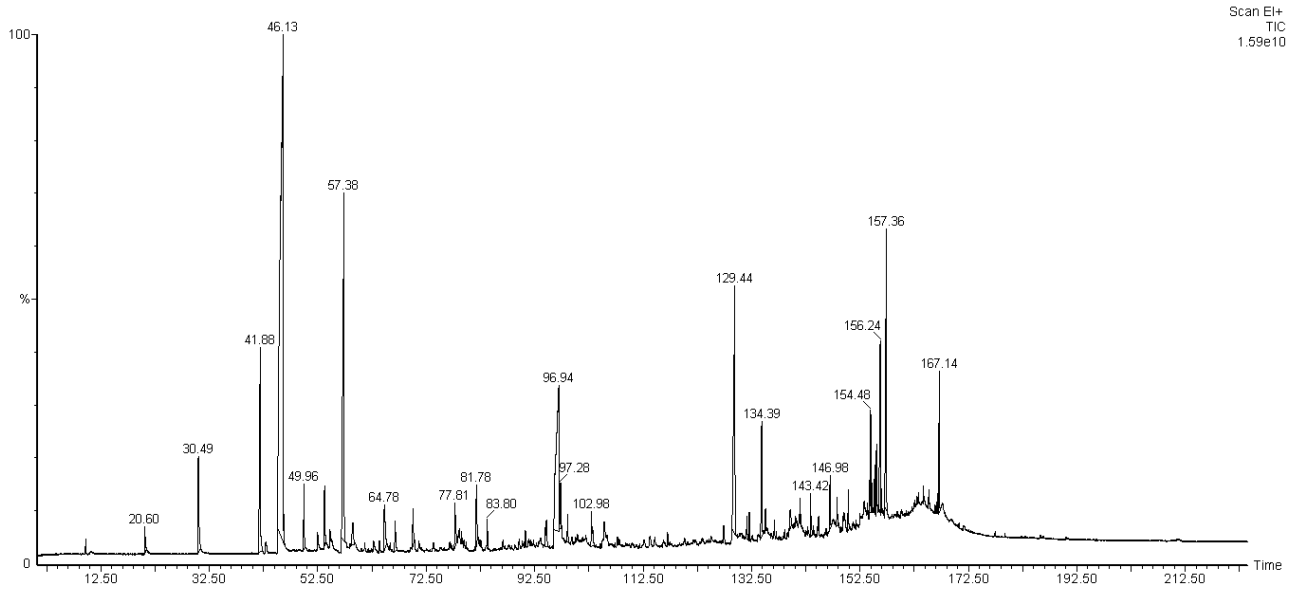


Figure 5-4 Py-GC/MS trace of ABS at when pyrolysed to 500°C at 20°C/min

Nevertheless, upon examining the GC/MS traces produced from final pyrolysis temperatures of 500°C or more (see Figure 5-4), it became apparent that the decomposition of ABS was consistent, with a number of significant constituents found within the products of decomposition. The most evident of these were found at peaks of 46.13, 57.38, 96.94, 129.44 and 157.36 Cm, corresponding to 34.03, 11.09, 9.29, 7.77 and 5.76 %TiC, representing a total of 67.94 %TiC of all components produced.

It is evident from these components that they are formed from a random chain scission process. There is evidence of 3-methyl-3-phenyl-azetidine comprising chain segments of a styrene and acrylonitrile monomer, with the acrylonitrile cyclising most likely as a result of hydrogen abstractions and hydrogen transfer mechanisms. In a similar fashion the formation of benzenebutanitrile is likely to have occurred from a fragmentation of the polymer chain into styrene radicals and the cleavage of the cyano side group from acrylonitrile to form cyano radicals. These may undergo radical condensation reactions to form the subsequent component. Nevertheless, results from Dong *et al.* (2001) in which thermal degradation of ABS with simultaneous with FT-IR analysis suggested that some nitrile groups in ABS were transformed in to double bonds through cyclisation reactions. It would appear that side chain cleavage reactions as well as cyclisation of the nitrile group exist within the system observed.

These were found to correspond to the components of styrene, 3-methyl-3-phenyl-azetidine, benzenebutanenitrile, 1,1'-(1,3-Propanediyl)bis-benzene and 1,5-Diphenylhex-3-ene, respectively. There structures are shown in Figure 5-5.

Table 5-1 Pyrolysis products from the Py-GC/MS of ABS at 500°C or greater under a heating rate of 20°C/min semi-quantified by Total Ion Count (TiC)

Retention Time (Cm)	Compound Name	Empirical Formula	%TiC
20.60	Benzene	C_6H_6	0.45
30.49	Toluene	C_7H_8	1.77
41.88	O-Xylene	C_8H_{10}	4.92
46.13	Styrene	C_8H_8	34.03
46.27	P-Xylene	C_8H_{10}	0.16
49.96	(1-Methylethyl)-benzene	C_9H_{12}	1.12
53.76	Propyl-benzene	C_9H_{12}	1.09
57.38	3-Methyl-3-phenyl-azetidine	$C_{10}H_{13}N$	11.09
64.78	1-Ethynyl-4-methyl-benzene	C_9H_8	1.18
66.80	DL-2-Benzylamino-1-propanol	$C_{10}H_{15}NO$	0.74
70.07	1-Ethenyl-3-ethyl-benzene	$C_{10}H_{12}$	0.79
77.81	1,2-Dihydro-naphthalene	$C_{10}H_{10}$	1.09
81.78	Naphthalene	$C_{10}H_8$	1.47
83.80	(Z)- 8-Methyl-2-undecene	$C_{12}H_{24}$	0.42
94.67	1-Cyclopenten-1-yl-benzene	$C_{11}H_{12}$	0.99
96.94	Benzenebutanenitrile	$C_{10}H_{11}N$	9.29
97.28	(1,3,5-Cycloheptatrien-7-yl)propanedinitrile	$C_{10}H_8N_2$	0.83
98.60	3-Cyclohexen-1-yl-benzene	$C_{12}H_{14}$	0.52
102.98	2-Ethenyl-naphthalene	$C_{12}H_{10}$	0.90
129.44	1,1'-(1,3-Propanediyl)bis-benzene	$C_{15}H_{16}$	7.77
131.63	1,1'-(1-Methyl-1,3-propanediyl)bis-benzene	$C_{16}H_{18}$	0.42
132.09	5-Methyl-3-undecene	$C_{12}H_{24}$	0.40
134.39	5-Phenyl-2-pentenal	$C_{11}H_{12}O$	2.42
135.08	1,2-Diphenylcyclopropane	$C_{15}H_{14}$	0.41
139.65	1-Octenyl-benzene	$C_{14}H_{20}$	0.55
141.48	1-(1-Propynyl)-cyclohexene	C_9H_{12}	0.31
143.42	(4-Bromobutyl)-benzene	$C_{10}H_{13}Br$	0.51
148.31	Eicosanoic acid	$C_{20}H_{40}O_2$	0.57
150.32	1-Chloro-tetradecane	$C_{14}H_{29}Cl$	0.50
154.27	Tetradecanenitrile	$C_{14}H_{27}N$	0.38
154.48	Benzadehyde o-benzyloxime	$C_{14}H_{13}NO$	1.63
154.73	(+-)-N-Benzyl-alpha-methyl-N-nitrosobenzylamine	$C_{15}H_{16}ON_2$	0.33
156.24	(1-Benzyl-2-o-tolyl-ethyl)-isonitrile	$C_{17}H_{17}N$	2.86
157.36	1,5-Diphenylhex-3-ene	$C_{18}H_{20}$	5.76
167.14	1-Benzyl-3,3-dimethyl-2-phenyl-azetidine	$C_{18}H_{21}N$	2.31

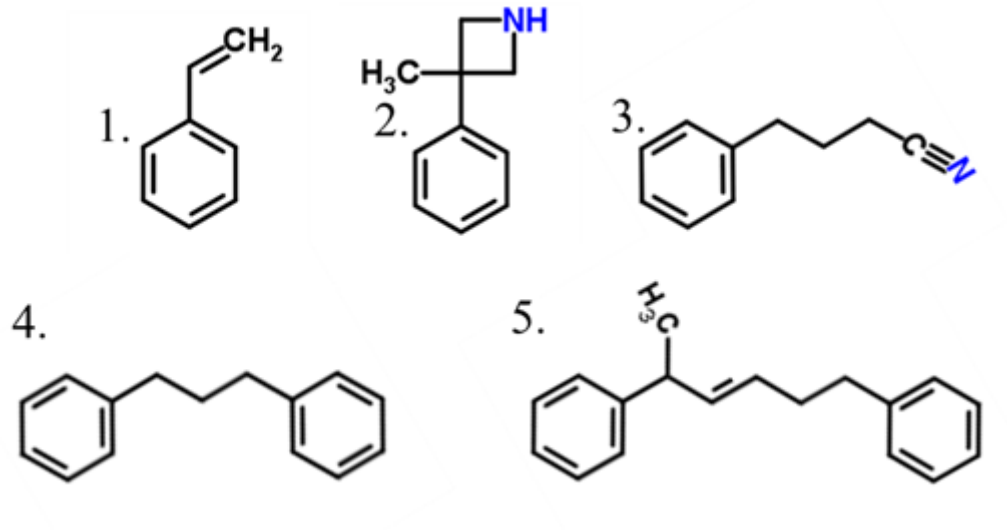


Figure 5-5 Major organic components structures, as formed during Py-GC/MS of ABS in excess of 500°C at 20°C/min: 1). Styrene, 2). 3-methyl-3-phenyl-azetidine, 3). benzenebutanitrile, 4). 1,1'-(propanediyl)bis-benzene and 5). 1,5-Diphenylhex-3-ene

When the products of thermal pyrolysis are grouped into their relevant species; as shown in Figure 5-6, it is found that the distribution of organics consists almost solely of branched aromatic structures, forming 94.65 %TiC, with a further 1.92 %TiC forming aromatic and polyaromatics. A small percentage of alkanes equating to 1.45 %TiC are also present in the form of carboxylic acids.

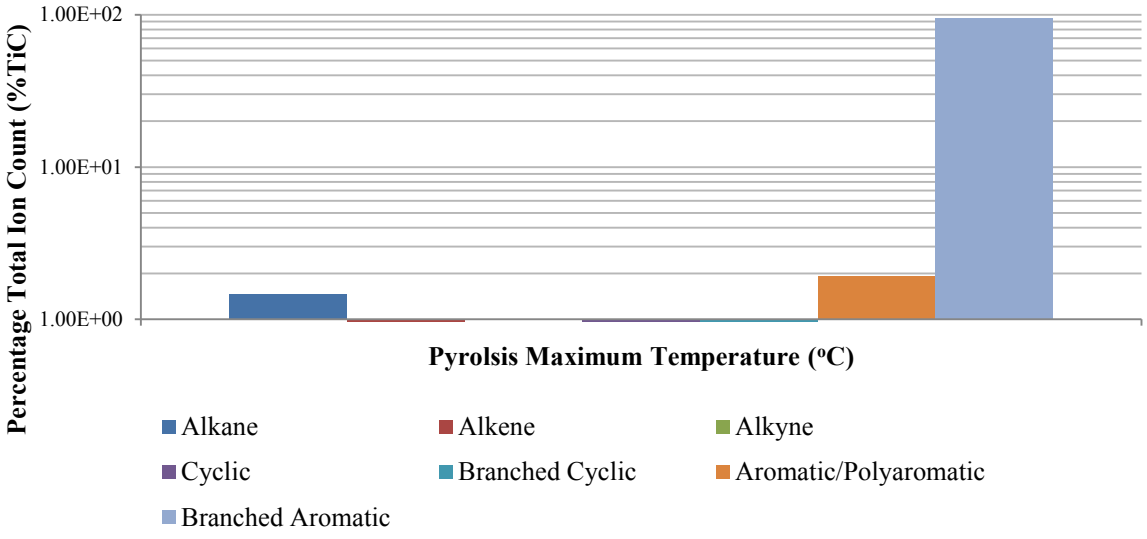


Figure 5-6 Speciated products of ABS pyrolysis at a maximum temperature of 600°C (by major organic group)

When this is examined in conjunction with carbon number distribution, as shown in Figure 5-7, it becomes apparent that the product distribution in the thermal decomposition process is narrow with 64 %TiC of compounds taking the form of C_8 or C_{10} hydrocarbons. These are largely branched aromatic structures. in the form of styrene or styrene with acrylonitrile-derived chains attached. The two remaining large groups at C_{15} and C_{18} (16 %TiC) correspond to dimers of styrene.

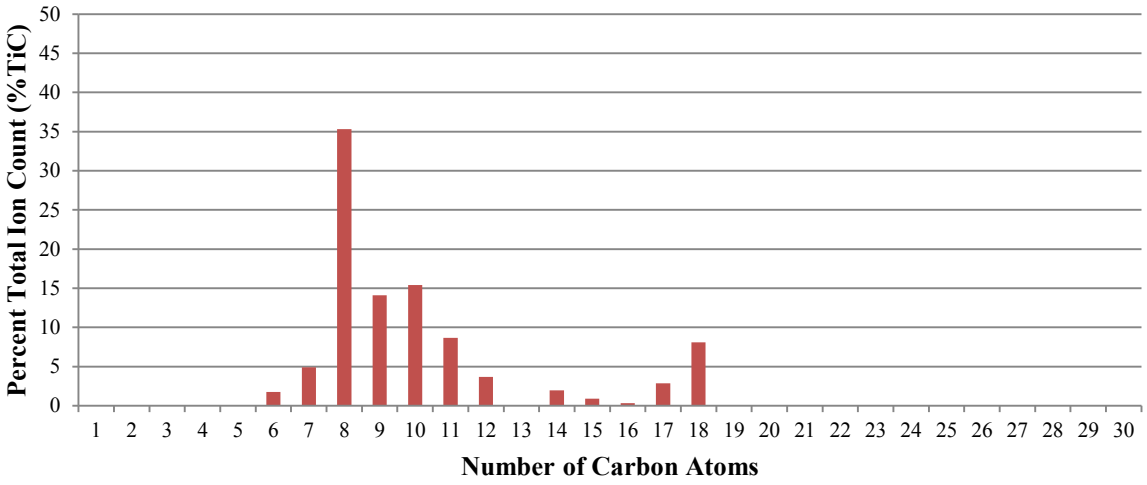


Figure 5-7 Semi quantification of product distribution by TiC of compounds produced from Py-GC/MS to 600°C at 20°C/min

5.3 Microwave Decomposition of ABS

With ABS containing considerable quantities of acrylonitrile monomer and the resulting large dipole moment from the CN bond, it would be reasonable to presume that the polymer would be microwave responsive. Nevertheless, the frequency/temperature relationship at which the dielectric response of ABS occurs has not been measured or determined in literature, with merely indications given from acrylonitrile-butadiene copolymer, with responses at the frequencies of 10 MHz at 25°C which shifts to 100 MHz at 80°C (Von Hippel, 1966, Bur, 1985). Further investigations by at Polli *et al.* (2009), demonstrated the microwave response of ABS to be similar to that of PVC when a frequency of 11GHz was applied (see Figure 5-8).

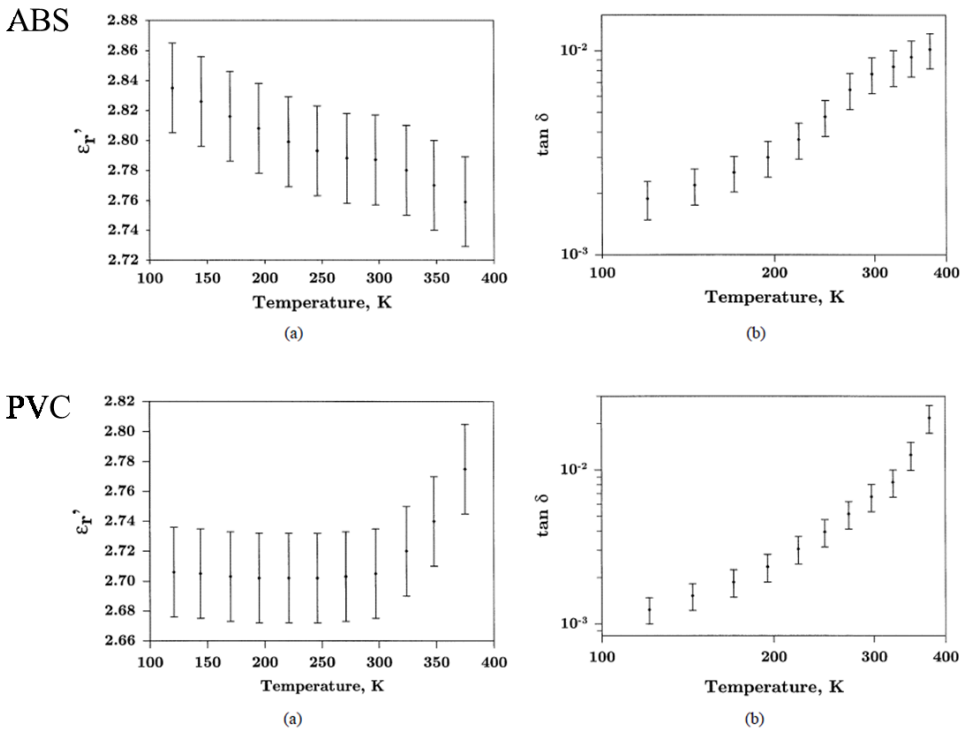


Figure 5-8 Measurements of (a) relative permittivity and (b) loss tangent for ABS and PVC at 11GHz for temperatures between 100 and 400°C (Polli *et al.*, 2009)

Yarlagadda and Chai (1998) investigated the dielectric properties of ABS over frequencies of 0.5-20GHz. The result of which showed that ABS displayed a high dielectric constant but low loss tangent at 2.45GHz (see Figure 5-9) compared to those frequencies in excess of ~8GHz; at ambient temperatures. This indicated that the polymer would not heat readily under the application of 2.45GHz microwave irradiation. Hence, it was necessary to evaluate the response of ABS to microwaves at this frequency. Initial testing was performed under microwave powers of 440, 600, and 850W for periods between 1 and 30 minutes on 5g ABS samples at 2.45GHz using the equipment previously described in Section 4.3.

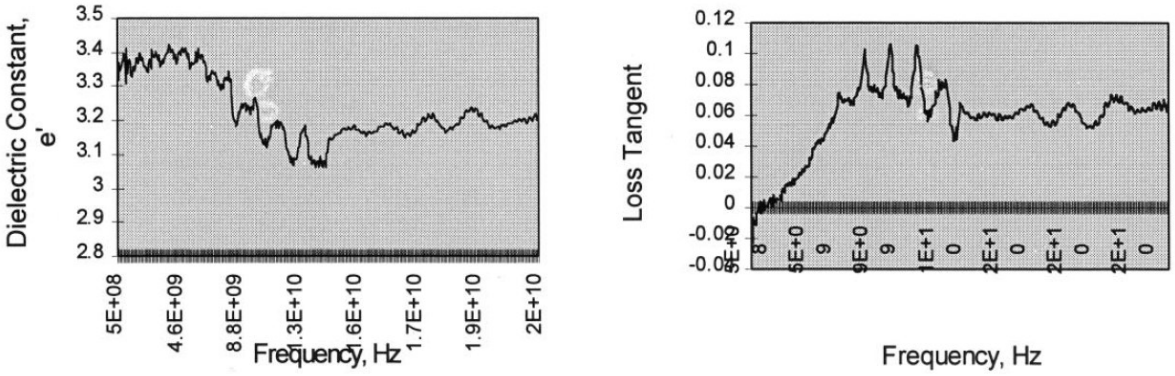


Figure 5-9 ABS dielectric properties as derived by Yarlagadda and Chai (1998) for frequencies of 0.5Ghz to 20GHz

The results of this testing, are presented in Figure 5-10. From this it was confirmed that ABS did not heat readily with samples demonstrating a heating rate no greater than 1.7°C/min across the microwave powers of 440, 600 and 850W. From these experiments, mass balances were also performed to determine if polymer decomposition has occurred during the microwave irradiation process; the results of which are presented in
Table 5-2.

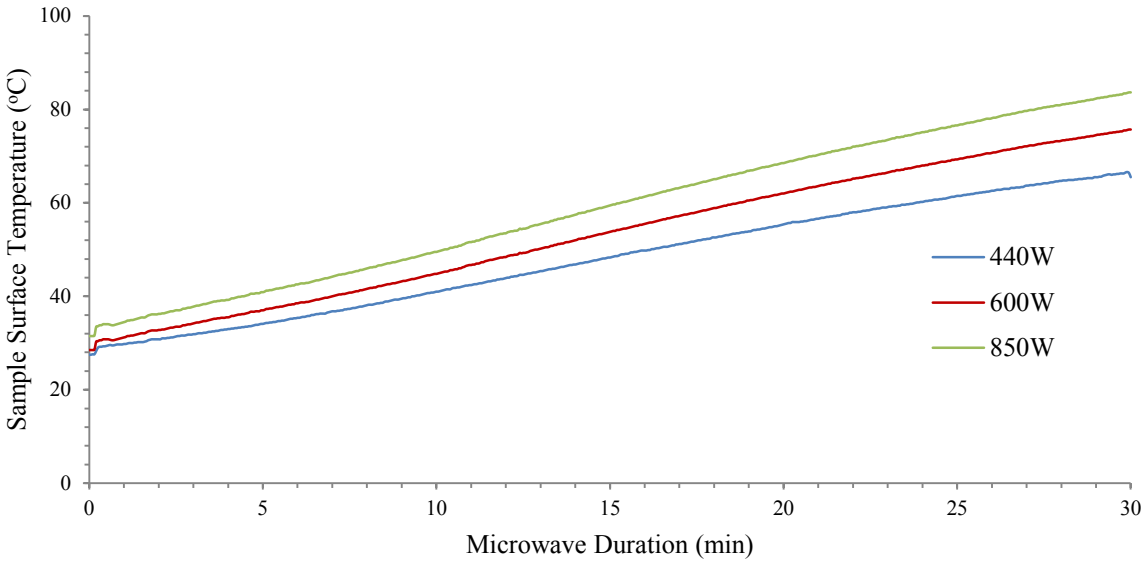


Figure 5-10 Mean temperature profile for 5g of ABS exposed to microwave powers of 440, 600 and 850W (standard deviation too low to be displayed)

Table 5-2 Mass loss from 5g of ABS exposed to microwave powers of 440, 600 and 850W

Microwave Power (W)	Microwave Duration (min)	Weight Loss (wt.%)	S.D. (n=3)
440W	10	0.25	0.05
	20	0.38	0.07
	30	0.58	0.11
600W	10	0.38	0.08
	20	0.47	0.09
	30	0.50	0.10
850W	10	0.45	0.09
	20	0.48	0.10
	30	0.45	0.09
	Mean	0.44 (n=27)	0.09 (n=27)

Thus, it was confirmed that ABS does not heat readily under the conditions utilised, which corroborated the work undertaken by Yarlagadda and Chai (1998) that irradiation at 2.45GHz is unlikely to result in substantial heating due to poor dielectric properties. A microwave receptor would be necessary to assist in the decomposition process. As such the microwave induced pyrolysis process was examined for ABS; results of which are presented in Section 5.4.

5.4 Microwave-receptor Induced Pyrolysis

The examination of the key parameters of microwave power, sample load and carbon absorbent were tested using the in house designed stationary phase microwave system described previously.

The first used a fixed weight of ABS (5g) with weights of 0, 0.5, 1.0, 2.0 and 3.0 grams of carbon receptor. The second method used a total weight of 5 grams and the ratio of carbon to ABS adjusted from 20% to 80% (w/w). For both these methodologies, the key parameter of microwave power was varied. The resultant yields of char, oil and gas were determined, with char/oil analysed by the methodologies outlined in Section 4.5 and 4.6.

5.4.1 Microwave Receptor

To ascertain the viability of the microwave process as a method of achieving full decomposition for maximum recovery of chemicals from the polymer, it was necessary to facilitate the decomposition of the residue. Hence, a carbon char was utilised as a microwave receptor to induce the decomposition process of the full polymer structure, similar to that used in Ludlow-Palafox and Chase (2001) and Menéndez *et al.* (2002). Before use this was characterised for its physical/chemical characteristics and its microwave response, so that a baseline of its performance could be established.

5.4.1.1 Chemical and Structural Characterisation

The carbon was produced as described in Section 4.3.2.2. . It was subsequently characterised to determine its physical and chemical properties prior to use described in Section 4.5.as described in Section 4.5.

Examination of the XRD diffractogram of the carbon receptor (Figure 5-11) shows two overlapping peaks. The first rises sharply to 24.32^{o} and then falls slowly on the high angle side. A crystalline reflection is then observed in the tail of the peak at 43.49^{o}. This is typical of a 2-dimensional lattice reflection, giving evidence that the carbon receptor consists of graphitic layers which are orientated independently of each other in space. This is in good agreement with those patterns produced in the works of Clark and Rhodes (1940), Houska and Warren (1954) and more recently, Ungár *et al.* (2002)

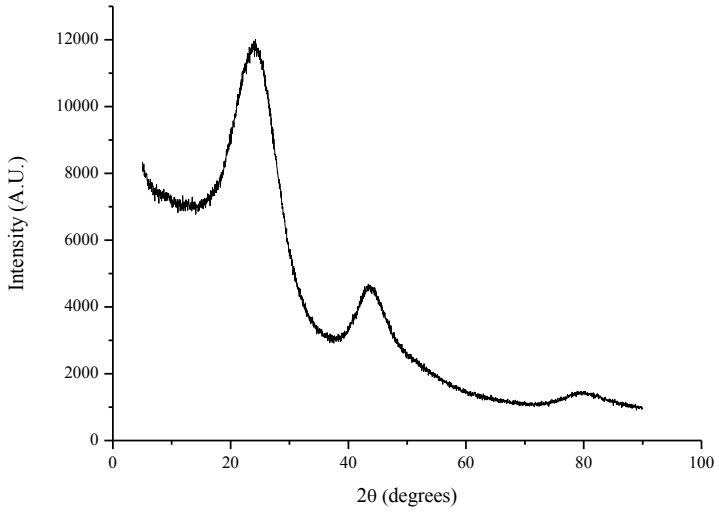


Figure 5-11 2Ɵ diffractogram of powdered carbon receptor (as produced in Section 4.3.2.2)

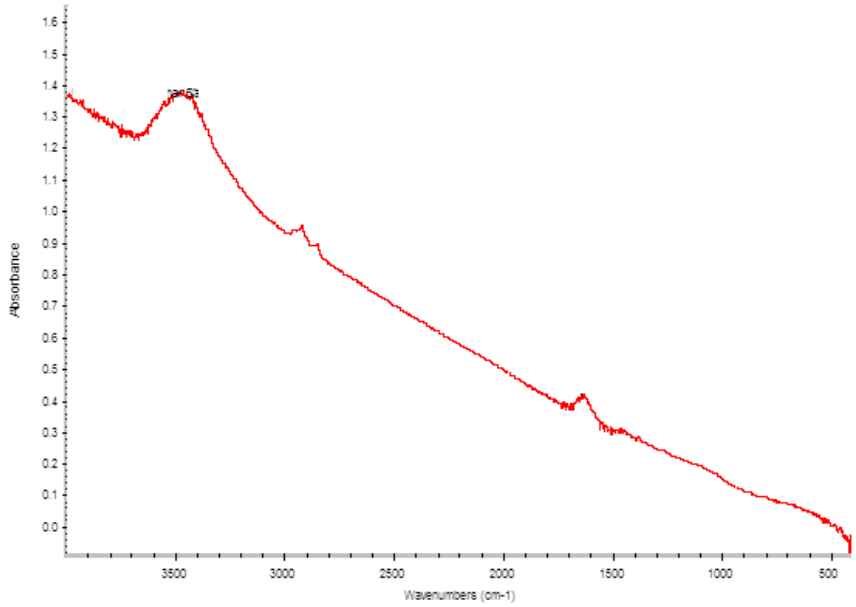


Figure 5-12 Typical FT-IR spectrum of chars produced from coconut husk.

The FT-IR spectrum of the carbonised coconut was limited in the intensity of the peaks that could be observed, due to the nature of char absorbing a significant proportion of the Infrared radiation. However, the presence of O-H stretching from traces of water, absorbed from the atmosphere were identified at peak 3439 cm^{-1}. The peaks seen at 1467 and 2932 cm^{-1} indicated C-H deformations and C-H stretching representing the presence of alkyl groups on the carbon. Aromatic rings are also indicated by the absorption between 1700-1500cm^{-1}.

The results of CHN analysis (see Table 5-3) support the findings from XRD and FT-IR analysis, with the elimination of hydrogen and nitrogen from the coconut and increasing proportions of carbon present. When studied in conjunction with Figure 5-11 and Figure 5-12 there is good evidence that the coconut underwent extensive carbonisation and development of graphitic structure, following the carbonisation mechanisms outlined by the processes discussed by Evans and Marsh (1971) and developed further by Lewis (1982).

Table 5-3 Carbon, Hydrogen and Nitrogen content of coconut and coconut char (n=3)

Element (wt.%)	Coconut	Coconut Char
Carbon	63.49 (σ 0.049)	92.64 (σ 0.035)
Hydrogen	6.76 (σ 0.132)	0.51 (σ 0.071)
Nitrogen	0.45 (σ 0.041)	0.48 (σ 0.000)

Upon examining the carbon under SEM it was seen that the structure consists of angular fragments, consistent with the process of manufacture (milling), with surface pores of between 10µm and 20µm in width. Within these significant deposition of debris is evident, most likely as a result of volatile organic matter undergoing carbonisation through secondary reactions as it escaped the porous structure of the original coconut (Achaw and Afrane, 2008).

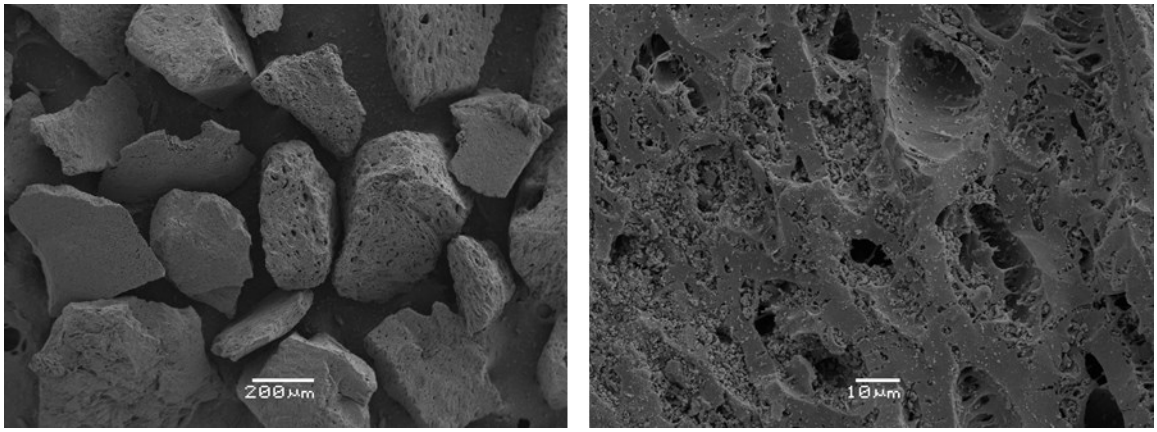


Figure 5-13 Micrographs of carbonised coconut of particle sizes between 500µm and 250µm (after size reduction) at 70x (left) and 1000x (right) magnification

Upon further examination using BET analysis it was found that the carbon exhibited a total surface area of 41.2m^2/g (σ 3.44, n=5), confirming that the char had very little porous structure and also in good agreement with those results gained by (Achaw and Afrane, 2008).

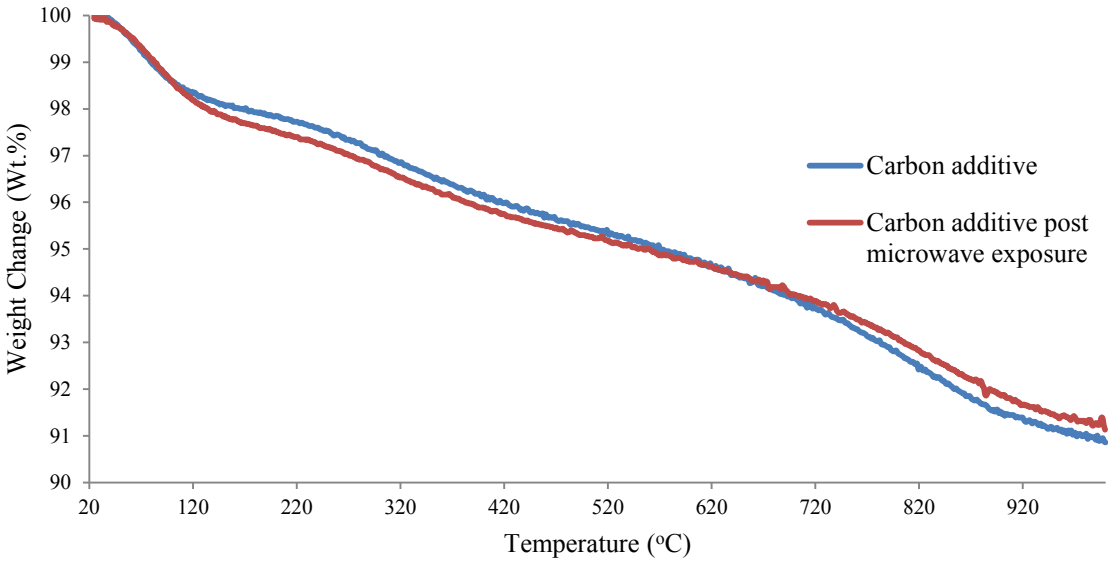


Figure 5-14 Thermal behaviour of carbon char when heated from 0-1000°C at 10°C/min under nitrogen atmosphere (TGA) for raw carbon additive and that which has been exposed to 850W microwave radiation for 10 minutes.

The carbon was also examined for its thermal stability between the temperatures of 0 and 1000°C (see Figure 5-14). It was found that the char exhibited a weight loss of 1.5wt.% by 100°C equating to absorbed moisture from the atmosphere. A further 5.7wt.% was lost from the char by 800°C and a further 1.8wt.% by 1000°C. This equated to a total loss of 7.5wt.% of the carbon mass between the temperatures of 20-1000°C. After exposure of the char to microwave radiation at 850W achieving temperatures of approximately 1000°C it was found that the characteristics of the char under thermal decomposition demonstrated minimal difference, with similar decomposition occurring across all temperature ranges.

5.4.1.2 Microwave Response

The microwave response of the carbon was examined by exposing weights of 0.5g, 1.0g, 2.0g and 3.0g to powers of 440W, 600W and 850W. Thermal profiles were subsequently recorded and heating rates/maximum temperatures ascertained; as shown in Figure 5-15.

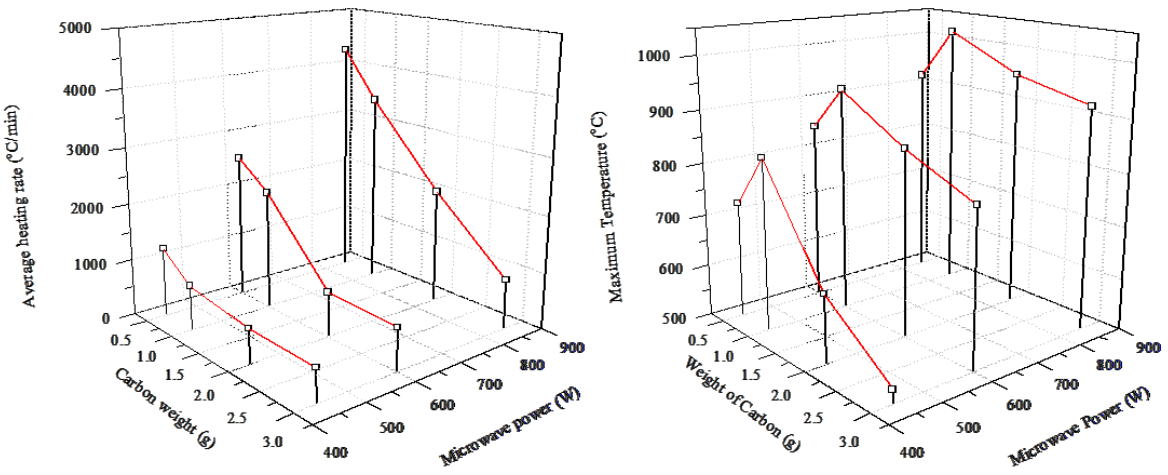


Figure 5-15 Average heating rates (left) and maximum temperatures (right) of 0.5g - 3.0g carbon when exposed to 440W, 600W and 850W microwave power

From these experiments it was determined that the rate and extent to which carbon heated is a function of microwave power and sample mass. This was evidenced by the observation that the minimum sample mass of 0.5g heated at the greatest rates over all microwave powers; achieving 1226°C/min, 2574°C/min and 4284°C/min at 440W, 600W and 850W respectively, although the heating rates decreased as the carbon mass increased. However, no relationship between power per unit mass of carbon and heating rate could be determined. As the heating rates observed were significant it was checked that they were theoretically possible and not as a result of surface heating of the carbon sample.

Table 5-4 Theoretical heating rates of differing masses of carbon at microwave powers of 440W, 600W and 850W (assuming no losses of energy)

	Possible Heating Rate (°C/min) at set Microwave Powers (Watts or J/s)		
Char Sample Mass (g)	440W	600W	850W
0.5	40,930.23	55,813.95	79,069.77
1.0	20,465.12	27,906.98	39,534.88
1.5	13,643.41	18,604.65	26,356.59
2.0	10,232.56	13,953.49	19,767.44
2.5	8,186.047	11,162.79	15,813.95
3.0	6,821.705	9,302.326	13,178.29
3.5	5,847.176	7,973.422	11,295.68
4.0	5,116.279	6,976.744	9,883.721
4.5	4,547.804	6,201.55	8,785.53

As such calculations were performed taking into account the specific heat capacity of bio char the applied power and the sample mass. The specific heat capacity of biocahr was determined from literature to be approximately 1.29 J/g/k (Dupont *et al.*, 2014). Therefore, if the application of power were 440W (J/s), 600W (J/s) or 850W (J/s) and all power absorbed the following heating rates could be achieved as presented in Table 5-4.

It was possible to determine an exponential relationship with microwave power per unit mass; with an $R^2 = 0.9718$ when plotted for an input power of 850W, but not at any other power. This indicated that the ratio of power to sample mass was not a limiting factor.

The maximum temperature achieved did not reflect the sample heating rate. However, an optimal mass did appear, with 1.0g carbon attaining maximum temperature across all microwave powers, with diminishing maximum observed either side. This indicated that the balance between thermal losses from the reactor and the power to mass ratio of carbon used, were critical factors in determining the maximum temperatures achieved.

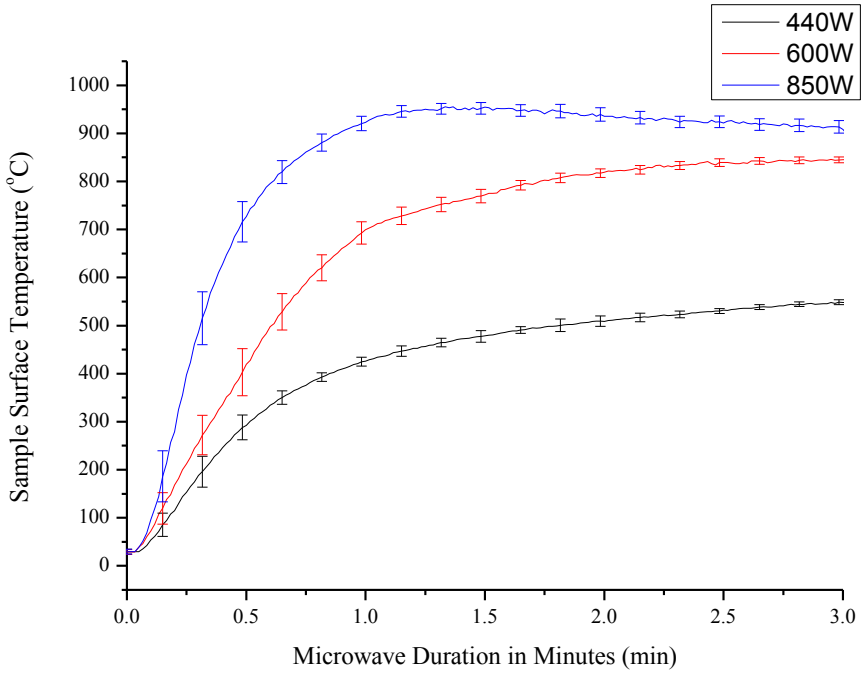


Figure 5-16 Thermal profiles of 3g carbon samples when exposed to microwave powers of 440W, 600W and 850W

Upon examination of the thermal profiles it was found that the carbon additive heated in a predictable fashion, with the heating rate demonstrating a gradual decline with increased temperature until a

plateau was formed. The plateau indicated the formation of a steady state condition in which the energy absorbed by the material was equal to the thermal losses from the reactor in the form of conduction, convection and radiation. The rate of energy loss resulting from thermal conductance is a sum total of each materials conductivity, and finally its derived heat transfer co-efficient which is the measure of energy lost per unit area (W/m^2). In this instance the heat transfer co-efficient of the carbon char and the quartz reactor are the factors of most influence. However, the surface area of the sample undergoing heating has a significant influence on the energy retained as when this increases the total energy lost increases. Convection is unlikely to have a significant effect on the losses from the reactor as the system has a forced flow of nitrogen over the sample internally and air externally. The final factor influence the losses will be radiation, in which radiation emitted from the sample will transmit energy away.

The losses from the sample then go to prevent further heating of the sample as losses from the boundary prevent the formation of localised hot spotting and the possible increase of sample dielectrics. This is discussed further in Sections 6.3.2.1 and 6.3.2.2.

The profiles also showed no step changes in heating rate, as demonstrated in samples of 3g carbon (see Figure 5-16). This was a good indication that that the dielectric properties of the carbon were constant or changed at an even rate over the temperature range examined. These results were consistent with those observed by Bradshaw *et al.* (1998) and Fang and Lai (1996) in which the microwave heating of activated carbons demonstrated similar trends in heating profiles.

From this it was expected that the high dielectric of carbon was such that the heating rates and maxima achieved when combined with plastics would demonstrate a similar relationship to that of the pure carbon compound.

5.4.1.3 Carbon Catalytic Activity

The catalytic activity of carbon was checked through the method of py-GC/MS and TGA. This was performed by producing mixtures of the carbon additive and the plastics of PVC or ABS. These were then subjected to thermal gravimetric analysis to 1000° C at a heating rate of 10^{o}C/min and the mass loss for each polymer derived. This was performed on ratios of 10wt% to 90wt%, 30wt.% to 70wt.%, 50wt.% to 50wt.%, 70wt.% to 30wt.% and 90wt.% to 10wt.%, carbon to polymer respectively. From this it is possible to see the respective profiles of mass loss and the overall extent mass loss. This gave evidence that the carbon char did not act as a catalyst during thermal pyrolysis conditions. It was found that the profiles and residual mass of polymer were not affected by the proportions of char.

Testing by py-GC/MS was performed in a similar manner with the same ratios of carbon to polymer. The chromatograms produced were integrated and the proportions of each chemical were calculated with respect to each other. From this could be seen that no change in chemical distribution had occurred. The combination of the TGA and PYGCMS results gained the confidence that no catalytic activity was occurring with the carbon char when conventional thermal pyrolysis was undertaken. However, this was not necessarily reflective of what might occur under microwave conditions as the carbon may release electrons from the surface due to the excitation of free electrons across the graphitic structure contained within the char. This could not be measured or compensated for and was considered as a possible mechanism for any differing results observed in later work.

5.4.2 Thermal Profiles

When thermal profiles were examined for fixed carbon mass and power ratio experiments (see Figure 5-17 and Figure 5-18) it was found that all experiments were able to achieve pyrolysis temperatures in excess of 450^{o}C. Nevertheless, the manner in which this temperature was achieved varied dependent upon the mass of carbon utilised and the microwave irradiation power.

Thermal profiles were found to take the form of two distinct types:

1. an initial phase of heating to temperatures of approximately 150-160^{o}C, followed by a sudden phase of rapid heating, ultimately resulting in a temperature plateau
2. a single phase of rapid heating from the point of microwave irradiation, resulting in a temperature plateau

A Type 1 thermal profile was found to occur when low masses of carbon receptor or lower microwave irradiation powers were utilised. This would appear to indicate that:

- ABS requires a critical temperature to be achieved (150^{o}C) at which point the dielectric of the material changes and the mass of the sample undergoes rapid self-heating and decomposition.
- Low masses of carbon receptor are unable to convert sufficient quantities of energy to induce surrounding ABS to undergo a dielectric change; with heat energy dissipating throughout the sample.

The process demonstrated similarities to those occurring in PVC (discussed later in Section 6.4.1.1), whereby the dielectric changes and heating accelerates. The temperature at which the dielectric change occurs corresponds to the initial degradation seen in the thermal decomposition of ABS (see

Figure 5-3). This would suggest that the point at which the first bonds break within the polymer structure initiates a "cascade" of heating and subsequent polymer fragmentation reactions. This provides greater evidence that the formation of radical species in a microwave field results in those species undergoing microwave heating.

With this in mind it is also possible that Type 2 thermal profiles exist through high electromagnetic field strengths inducing the movement of π-electrons in the graphitic sheets found within the carbon receptor. These electrons may subsequently be able to achieve sufficient energy to jump from the carbon into the surrounding atmosphere or materials, resulting in their ionisation; radical heating most probably ensues.

Nevertheless, it was found that over the experiments performed that the point at which the sharp heating event occurred was accompanied by the complete decomposition of the sample. This was clearly evident by the instantaneous evolution of white gaseous products in to the liquid nitrogen condensing system. This was followed by the evolution of much darker brown/black gaseous products, at which point the temperature of the system stabilised and no further evolution of products was observed

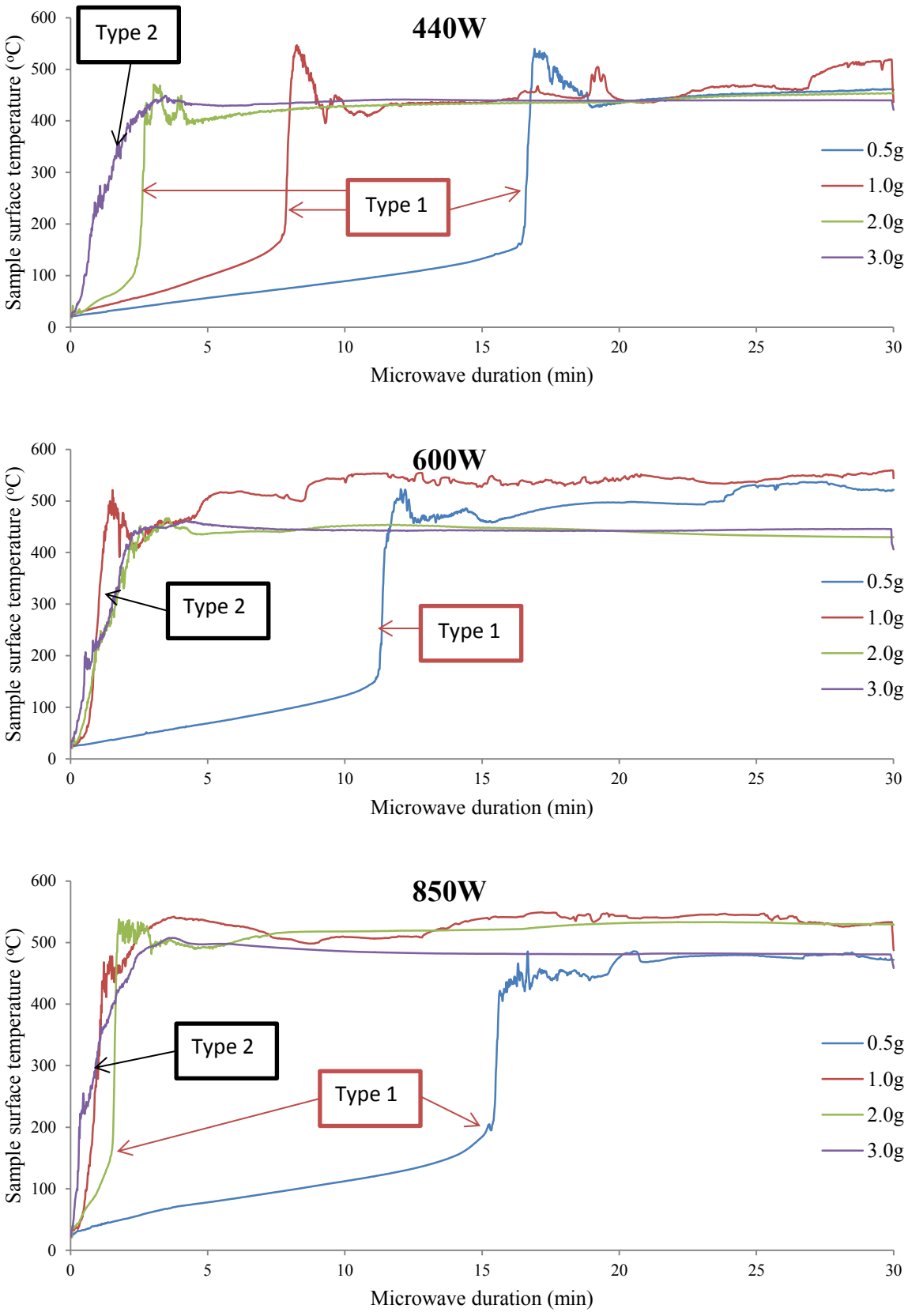


Figure 5-17 Thermal profiles for 5g ABS with either 0.5, 1.0, 2.0 and 3.0g carbon receptor exposed to microwave irradiation at 440W, 600W and 850W

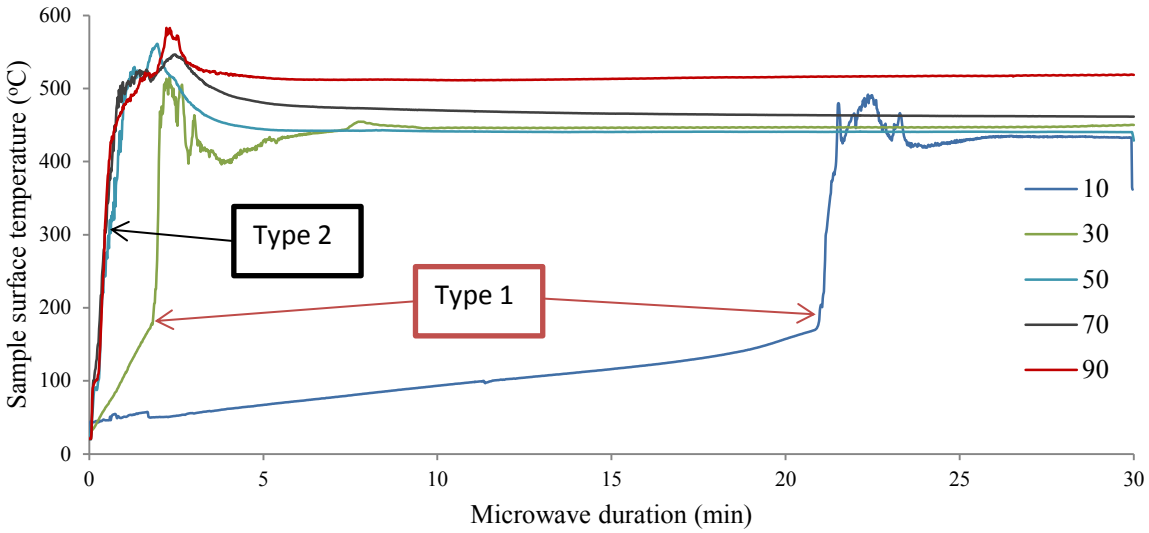


Figure 5-18 Thermal profiles for 5 g samples ABS/carbon receptor with 10, 30, 50, 70 and 90wt% carbon receptor exposed to microwave irradiation at 850W

5.4.3 Product Yield

The percentage yields of oil and gas from both fixed weight and ratio experiments are shown in Figure 5-19 and Figure 5-20. It is apparent from fixed carbon weight experiments that considerable variation in oil and gas yield are achievable, producing between 25-54wt.% and 45-74wt.%, oil and gas respectively. Char yield was consistent and not observed to exceed 2wt.% - indicating that the ABS was essentially, fully decomposed during the pyrolysis process. Chars from the microwave pyrolysis process were subsequently subjected to TGA to confirm the extent of pyrolysis and the residues thermal stability. This was able to be of sufficient information to conclude that the solid residual of almost all ABS experiments was thermally stable up to temperatures in excess of 800°C. This indicated that the residue formed was largely polyaromatic in structure, following the normal rules of thermal decomposition in which the growth of polyaromatic structure occurs as temperatures increase and the elimination of heteroatoms and organic chain fragments persists. Further testing was performed using py-GC/MS to ascertain if any lighter organic residues were retained on char. The results gained displayed no such species. A selection of these results are displayed in Appendix B. Maximum values of oil were achieved when 440W and 1g of carbon were utilised, resulting in 54.3wt% oil. When using at weight of carbon either side of this peak value, the oil yield was observed to lie between 38.6 and 45.6wt.% oil. In comparison to oil yields achieved at 600W and 850W, 440W produced greater oil yields across all masses of carbon used. This is most likely due to consistently slower heating rates at 440W resulting in significantly less gasification of the oils produced.

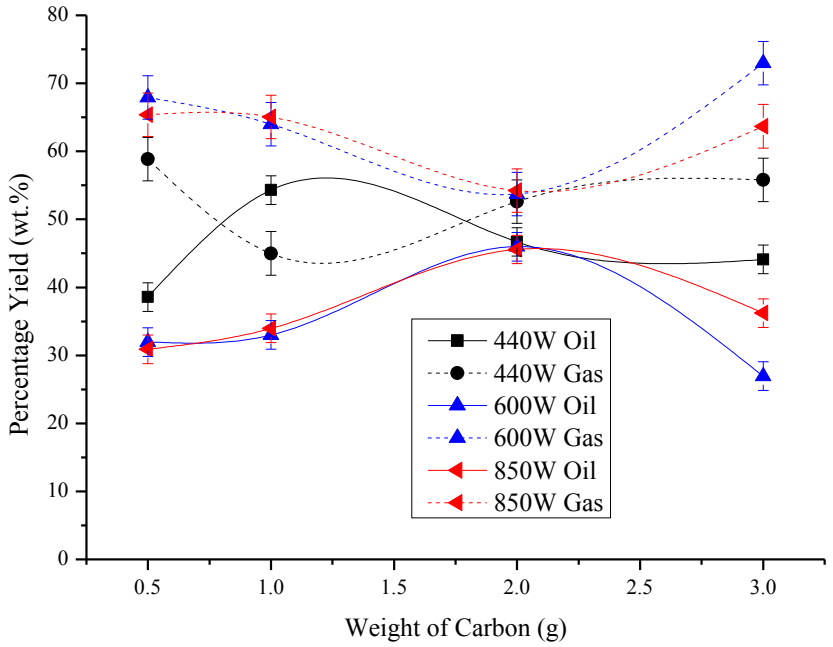


Figure 5-19 Char, oil and gas yields for 0g-3g carbon, PVC samples exposed to 440W, 600W and 850W

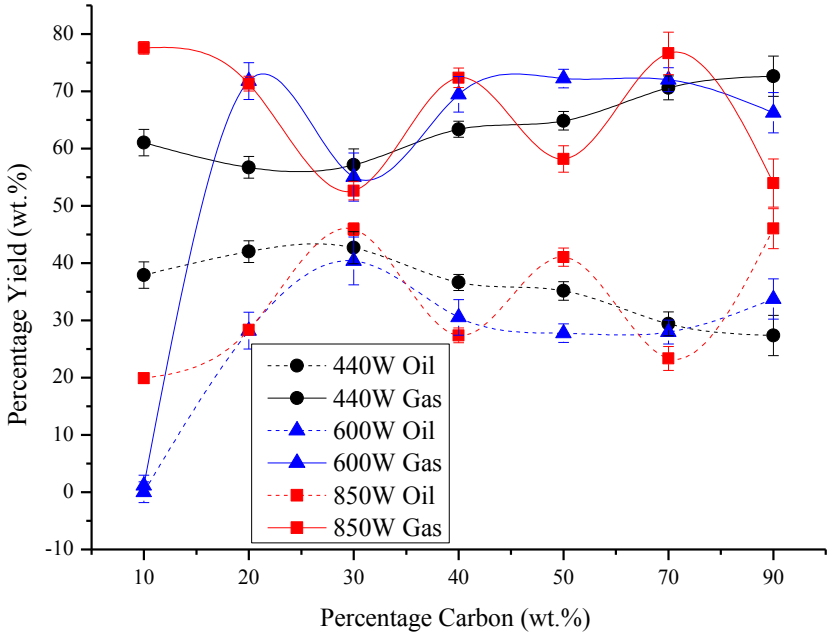


Figure 5-20 ABS oil and gas yields for pyrolysis over the microwave powers of 440W, 600W and 850W for 10wt.% to 90wt.% carbon receptor of a total 5g mass

However, for fixed mass experiments utilising 600W and 850W a similar trend in oil yields was observed, with less than 2.1wt.% difference in yields when 0.5g to 2.0g of carbon were used. This was of significant interest because the thermal profiles for these experiments displayed marked differences in the time at which decomposition was initiated. For 3.0g experiments the thermal profiles displayed significant similarities (see Figure 5-17), although significant differences in oil yield were observed, with 26.9wt.% and 36.2wt.% achieved for 600W and 850W respectively. This observation suggests that microwave power density plays a significant role in the decomposition process.

Upon examination of oil and gas yields produced during ratio experiments (see Figure 5-20) it was observed that significantly less oil was made than during fixed mass tests. This was reflected in the oil yields of between 20 and 46wt.% over the course of all experiments. Conversely, much greater gas yields were able to be attained with yields between 53 to 78wt%. Again, this is a trend which is not unexpected, given the much higher heating rates achievable with higher carbon loading. Nevertheless, no relationship in oil yield could be discerned with respect to carbon percentage.

After comprehensive data analysis was performed (akin to that performed in Section 6.4.1.3) no relationship between heating rate and oil yield could be found for either fixed carbon and ratio experiments. However, after comparing maximum achieved temperatures with oil and gas yields (see Figure 5-21) a statistically significant trend could be identified, with oil yields falling significantly with increased maximum temperature; from ~70 wt.% oil at 415°C to ~24 wt.% at 550°C . The inverse was observed for gas yields, which increased from ~28 wt.% at 415°C to ~77 wt.% at 515°C.

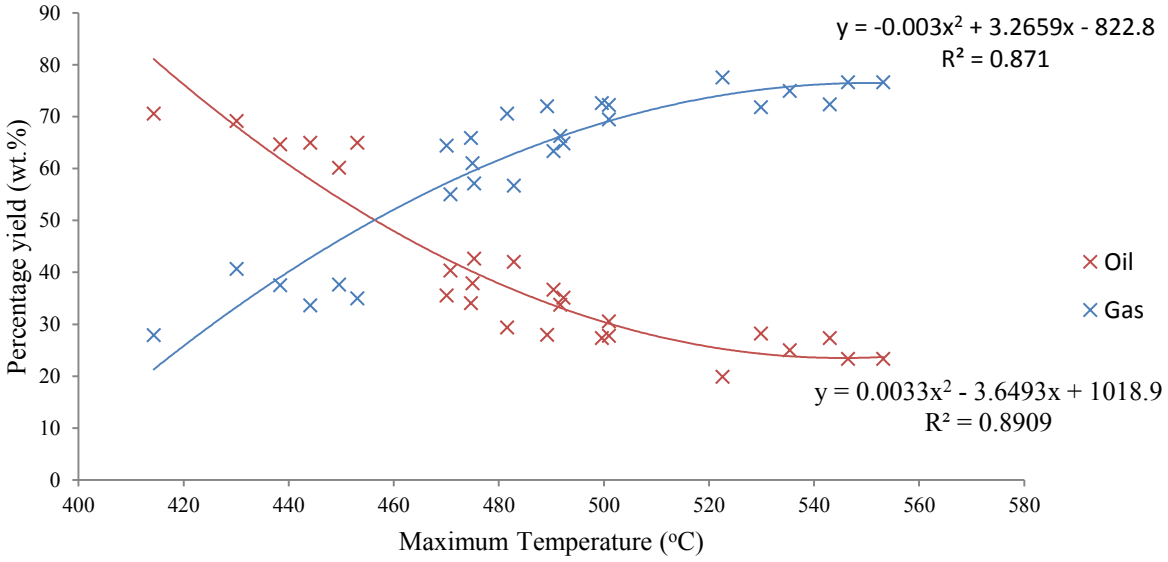


Figure 5-21 Relationship between maximum temperature and oil/gas yield, as derived from both fixed mass and ratio experiments

As such, the parameter that controlled the maximum achieved temperature must determine the yields of oil and gas. This could not be identified.

As previously suggested, the parameter which probably has the greatest effect in determining the heating of the sample; the dielectric property of the carbon, ABS and decomposition products all change significantly throughout the experiment. Hence, the system heating rate and maximum temperature are a result of the decomposition process and the path it follows. However, the decomposition process is also linked to the temperature of each of the components previously mentioned. This interdependency suggests that the measurement of temperature and thus heating rate is not sufficient to understand the interdependency of the factors governing the products of the process.

Nevertheless, these results demonstrate a clear relationship between temperature and resulting pyrolysis/gasification reactions. The carbon influences the heating rate along with the dielectric loss factor of the plastic and so the ensuing decomposition reaction.

5.4.4 Product Composition

Despite extensive analysis of the collected data, the only variable that correlated with the oil composition was the maximum temperature achieved during the pyrolysis process.

The relationship with increasing maximum temperature and product composition becomes clearer upon examining Figure 5-22, Figure 5-23 and Figure 5-24. At lower maximum temperatures (in the region of 425 ± 25^{o}C) it is seen that products largely take the form of C_8, C_{10}, and C_{12} hydrocarbons. From these three groups, 39.51 %TiC is represented by Styrene. This is a 5 %TiC greater recovery than by that of the model thermal pyrolysis method (see Figure 5-7 and Table 5-1). This provides good evidence that monomer recovery is distinctly possible from the microwave process. However, the proportion of components in the C_8 group is almost identical, with a maximum of 42.5 %TiC attainable, attributable to the key contribution of Ethyl-benzene. This would indicate that the cleavage of styrene from the polymer structure is a consistent process, with a small propensity for the addition of hydrogen to the ethylene side group, to form ethyl-benzene.

The remainder of the products that form a significant proportion of the oil (see Table 5-6) are largely branched aromatic structures, some of which have a nitrogenous side chain. The latter indicating the fragmentation of the original polymer chain, resulting in styrene-butadiene and styrene-acrylonitrile derivatives. Nevertheless, a small proportion of monomer fragmentation has also occurred.

Significant changes in the carbon atom distribution occur as the maximum temperature increases (see Figure 5-23), with the disappearance of C_8 hydrocarbons in their entirety and a shift towards greater carbon number compounds. This is shown by substantial increases of C_{10}, C_{11}, C_{13} and C_{14} hydrocarbons. This gives strong evidence that increased decomposition of the polymer has occurred, with monomers undergoing cracking and secondary reactions. This is further evidenced by increases in gas yield and the greater propensity to form naphthalene based polyaromatic hydrocarbons; as seen in Table 5-7. With further increases in the maximum temperature towards 550°C, the distribution of carbon numbers (see Figure 5-24) changes vastly, with the disappearance of almost all hydrocarbons from C_7 to C_9 and substantial increases in C_{14} and C_{16}. The C_{14} and C_{16} groups comprise largely of 1-Octenyl-benzene and 1-(Phenylmethylene)-1H-indene.

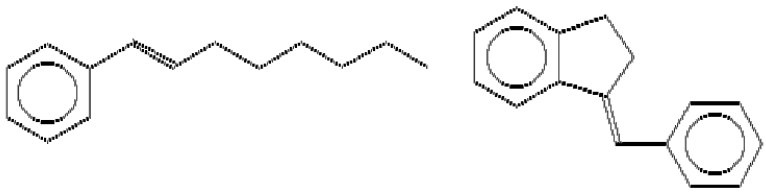


Table 5-5 1-Octenyl-benzene (left) and 1-(Phenylmethylene)-1H-indene

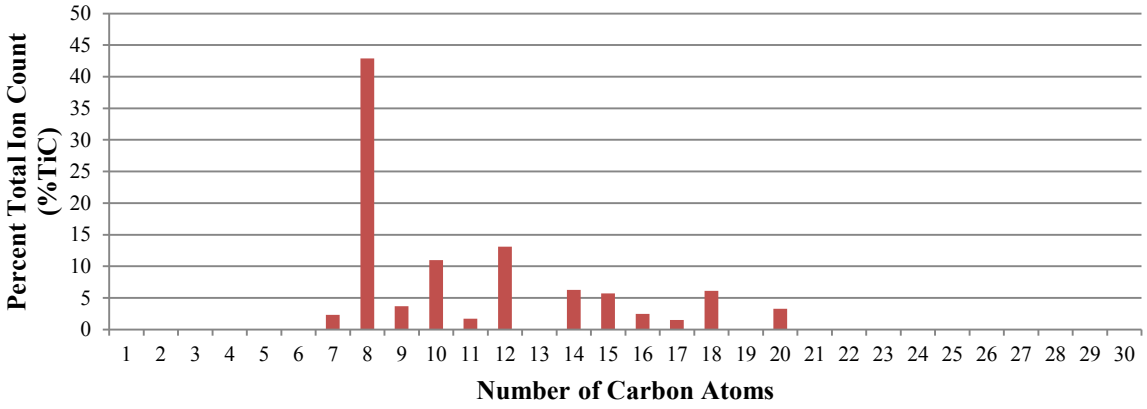


Figure 5-22 Semi quantification of product distribution by TiC of compounds produced in a microwave process achieving 414°C

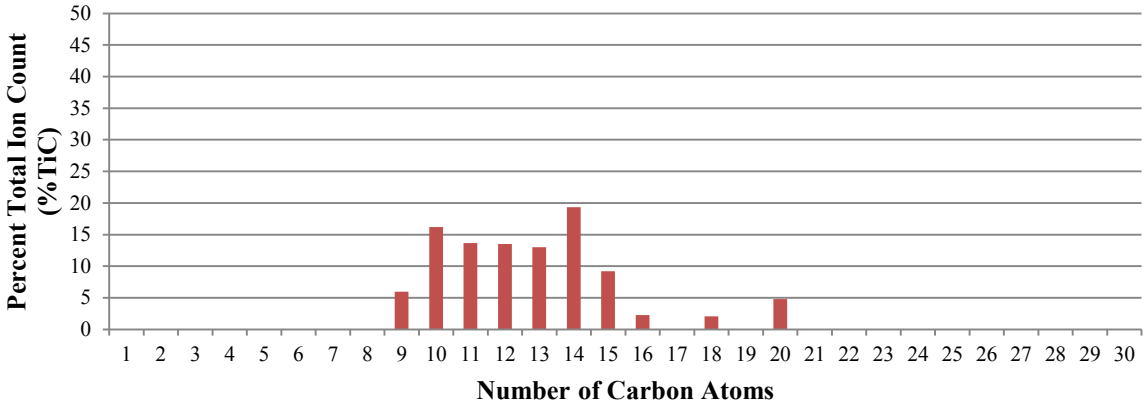


Figure 5-23 Semi quantification of product distribution by TiC of compounds produced in a microwave process achieving 490°C

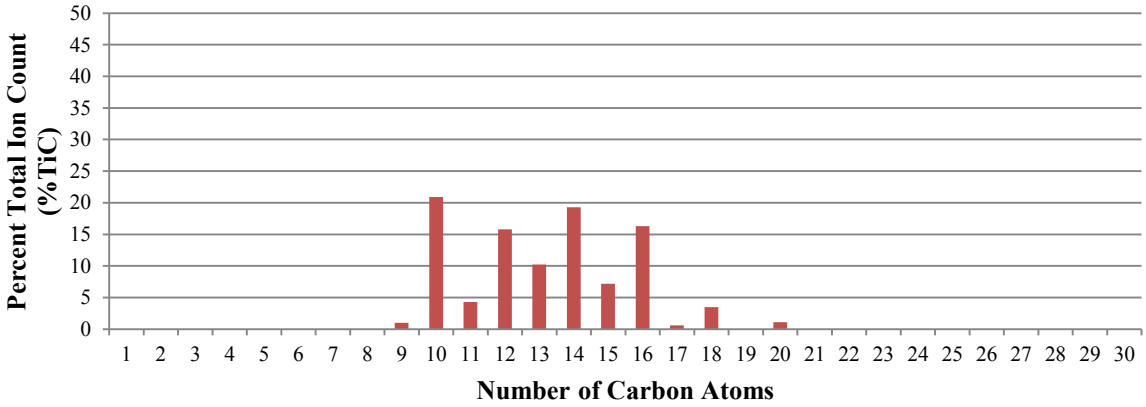


Figure 5-24 Semi quantification of product distribution by TiC of compounds produced in a microwave process achieving 553°C

Table 5-6 Top ten products during the microwave decomposition of ABS attaining a maximum temperature of 414°C

Retention Time (Cm)	Compound Name	Empirical Formula	Percentage TiC (%TiC)
45.94	Styrene	C_8H_8	39.51
56.903	3-Methyl-3-phenyl-azetidine	$C_{10}H_{13}N$	6.33
81.794	Naphthalene	$C_{10}H_8$	5.39
96.285	Benzenebutanenitrile	$C_{10}H_{11}N$	4.67
157.005	1,5-Diphenylhex-3-ene	$C_{18}H_{20}$	3.80
128.838	1,1'-(1,3-Propanediyl)-benzene	$C_{15}H_{16}$	3.76
64.606	1-Ethynyl-4-methyl-benzene	C_9H_8	3.71
102.804	2-Ethenyl-naphthalene	$C_{12}H_{10}$	3.52
41.464	Ethylbenzene	C_8H_{10}	3.39
30.182	Toluene	C_7H_8	2.31

Table 5-7 Top ten products produced during the microwave decomposition of ABS attaining a maximum temperature of 490°C

Retention Time (Cm)	Compound Name	Empirical Formula	%TiC
96.048	Benzocycloheptatriene	$C_{11}H_{10}$	9.65
102.967	2-Ethenyl-naphthalene	$C_{12}H_{10}$	9.39
56.78	3-Methyl-3-phenyl-azetidine	$C_{10}H_{13}N$	6.81
138.829	Phenanthrene	$C_{14}H_{10}$	5.96
64.598	1-Ethynyl-4-methyl- benzene	C_9H_8	5.95
104.724	1-(2-Propenyl)- naphthalene	$C_{13}H_{12}$	5.40
128.846	1,1'-(1,3-Propanediyl) benzene	$C_{15}H_{16}$	4.18
77.578	1,2-Dihydro-naphthalene	$C_{10}H_{10}$	4.03
94.357	1-Cyclopenten-1-yl-benzene	$C_{11}H_{12}$	4.03
139.564	1-Octenyl-benzene	$C_{14}H_{20}$	3.67

Table 5-8 Top ten products produced during the microwave decomposition of ABS attaining a maximum temperature of 553°C

Retention Time (Cm)	Compound Name	Empirical Formula	%TiC
82.382	1-Methylene-1h-indene	$C_{10}H_8$	11.72
139.384	1-Octenyl-benzene	$C_{14}H_{20}$	8.61
103.351	Biphenyl	$C_{12}H_{10}$	8.24
156.285	2,3-Dihydrofluoranthene	$C_{16}H_{12}$	5.71
96.367	Benzenebutanenitrile	$C_{10}H_{11}N$	5.66
149.415	1-(Phenylmethylene)-1h-indene	$C_{16}H_{12}$	4.53
94.61	1-Ethylidene-1H-indene	$C_{11}H_{10}$	4.28
146.899	6H-Cyclobuta[jk]phenanthrene	$C_{15}H_{10}$	4.14
123.496	Fluorene	$C_{13}H_{10}$	3.56
110.581	Biphenylene	$C_{12}H_8$	3.42

The lack of consistency in the pyrolysis products, demonstrate that components are formed through the radical condensation mechanism, with 1-Octenyl-benzene most likely produced through the condensation of styrene and aliphatic radicals. The occurrence of 1-(Phenylmethylene)-1H-indene indicates a similar process but with the condensation of multiple styrene radicals and aliphatic components.

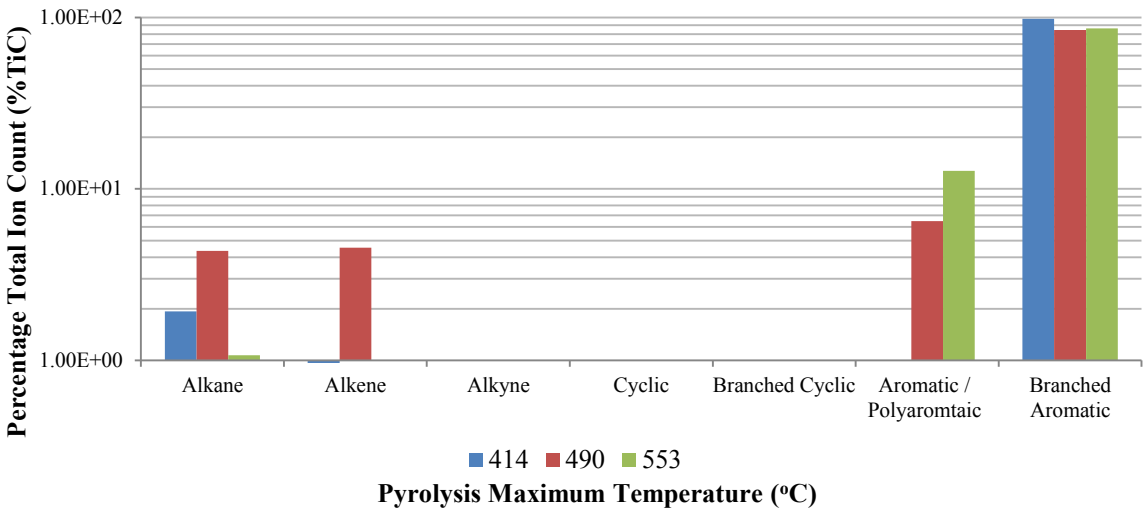


Figure 5-25 Speciated products of ABS microwave pyrolysis at a maximum temperatures of 414, 490 and 553°C (by major organic group)

The grouped product distributions (see Figure 5-25) reinforce the argument that a shift from systematic cleavage of monomers, to a random chain cleavage and secondary reaction based mechanism. This is evidenced by the occurrence of aromatic species at 490°C, with 6.48 %TiC, increasing with temperature to 12.72 %TiC by 553°C and the disappearance alkanes and alkenes with increased temperature. Alongside this, the increase of gaseous non condensable products gives further evidence to the significant fragmentation/cracking of monomer units

5.5 Conclusions

It was found that the microwave decomposition of ABS could not be achieved without the assistance of a carbon additive.

- With carbon added it was observed that the initial decomposition of the plastic occurred at 150-160°C. At which point the dielectric of the material apparently changes and the plastic undergoes sudden and complete decomposition.
- The amount of carbon receptor used in the process was found to be critical in the time required to reach the point at which the decomposition occurred but, had little/no influence on the heating rates achieved during the phase of decomposition.
- The implied creation of radical species during the decomposition assisted in the further decomposition of the plastic, as a result of their charge imbalance and subsequent increased dielectric properties.

- Microwave power was significant in discerning the yield of char, oil and gas, with a critical power threshold required to be overcome to achieve greater yields of gas.
- Lower microwave power favoured the formation of oil.
- Char formation was found to be consistent, with no greater than 2wt.% formed under all experimental conditionsOil composition was found to change with maximum temperature.
- Lower temperature pyrolysis favoured cleavage of monomer units, allowing for the recovery of oil containing substantially greater levels of styrene than that of a similar thermal process; 39.5 %TiC as compared to 34.5%TiC respectively. This indicated a favourable reaction pathway to exist under microwave conditions.
- Maximum temperatures toward 550^{o}C pushed oil distributions to heavier fractions and for C_7 to C_9 components to disappear, indicating that the degradation mechanisms shifted towards significant cracking and radical condensation reactions.

The microwave decomposition of ABS has demonstrated significant advantages over that of a thermal process, with the possibility of substantial recovery of monomer units. However, it also allowed for the adjustment of power to push the process towards the production of gaseous compounds, demonstrating the versatility of the microwave process. This shows significant promise for a commercial system with the potential to recover substantial volumes of relatively pure compound mixtures.

CHAPTER SIX

6 Microwave Decomposition of Poly Vinyl Chloride

"The aim of this chapter is to examine, the underlying factors determining the thermal and microwave decomposition of PVC, by:

- *examining the thermal decomposition of PVC in relation to temperature and heating rate*
- *determine the thermal decomposition pyrolysis products in correlation to temperature*
- *examining the microwave decomposition process of pure PVC*
- *determine the effect of microwave power and sample load on the decomposition of pure PVC*
- *establish the effect of carbon additive on the microwave decomposition process*
- *determine the relationships between product yields and experimental variables of carbon additive, weight of PVC and microwave power*
- *determining the composition of oils and identify their correlation to key experimental variables*
- *compare product composition with that of the thermal process*

.... and draw conclusion on the overall microwave decomposition process"

6.1 Introduction

Poly Vinyl Chloride (PVC) is used extensively throughout our homes and industry. Behind polyethylene and polypropylene, PVC represents the third largest plastic produced in Europe, with an estimated 5.57 Mtonne manufactured on an annual basis (APME, 2011). Of this between 30 – 50% of this ends up in the waste stream within 1 year of manufacture (Tukker, 1996). The remaining material is often used for relatively long life applications, such as in the construction industry or the production of furniture and fittings (Shent *et al.*, 1999), posing a longer term issue surrounding their end of life disposal.

Very little PVC waste is recycled, as only a small proportion consists of purely PVC. Almost all PVC products comprise the polymer and additives; with each blend uniquely formulated to the application for which it is required. If post-consumer PVC is attempted the resulting material is often of an inferior quality which can only be utilised in products which do not require strict material requirements; ultimately 'down-cycling' PVC. With current recycling techniques, it is estimated that a maximum of 18wt.% PVC can be recycled, with the remaining proportion being placed in landfill or diverted for incineration (European Commision, 2000). Hence, it can be seen that waste PVC poses a significant problem.

Within landfill, PVC acts as a largely inert substance, taking centuries to undergo any form of decomposition/degradation, hence is not classed as posing a threat of contamination to ground gas or groundwater (Mersiowsky *et al.*, 1999, Mersiowsky *et al.*, 2001), with little change occurring to the polymer mix as a result of harsh chemical conditions or microbial attack. With the introduction of the Landfill Directive (1999/31/EC) and the Packaging and Packaging Waste Directive (94/62/EC) considerable volumes of PVC are being diverted away from landfill to incineration, posing, what some might consider, to be a much greater risk to the environment due to the potential production of chlorinated combustion by-products (see figure 6.1).

The incineration of plastic is common place, with it forming a significant contribution to the energy during the incineration process (Mattila *et al.*, 1992), often facilitating the positive energy balance within Energy from Waste (EfW) plants. However, if these plastics are poorly mixed in incinerator feeds, the result is often localised depletion of oxygen during the combustion process and the resulting formation of Products of Incomplete Combustion (PICs)(Tsang, 1990).

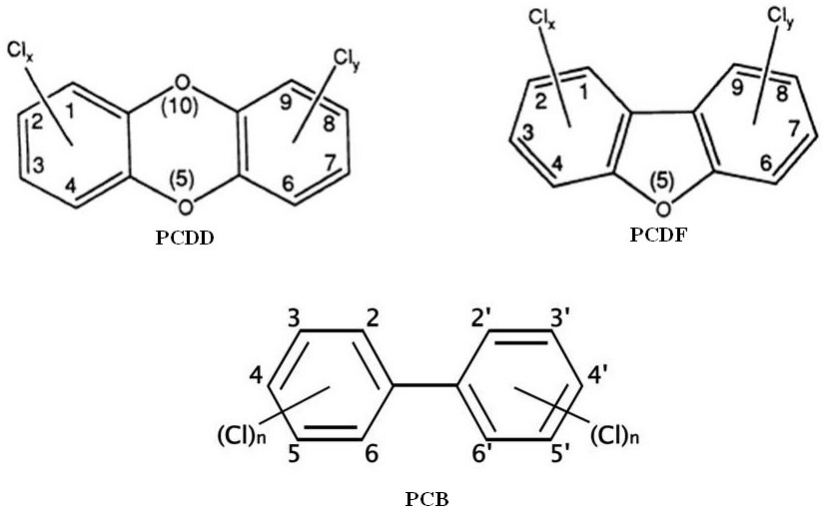


Figure 6-1 Polychlorinated dibenzodioxin (PCDD), Polychlorinated dibenzofurans (PCDF) and Polychlorinated biphenyl (PCB)

Whilst plastics often form PICs during incineration, PVC poses a significantly greater dilemma, with the release of not only PICs but the liberation of chlorine in the form of hydrochloric acid (Uchida *et al.*, 1983). This combination has been held responsible for significant corrosion occurring within incinerators as well as the formation of chlorinated organic compounds such as Polychlorinated dibenzodioxins (PCDDs) (Aurell, 1977, Giugliano *et al.*, 1989, Wagner and Green, 1993), Polychlorinated dibenzofurans (PCDFs) (Aurell, 1977, Christmann *et al.*, 1989) and polychlorinated biphenyl (PCBs) (Ballschmiter *et al.*, 1987, Sakai *et al.*, 1993). These have all been attributed to significant toxicological effects, including soft tissue cancers/neurological damage in humans and

environmental damage to plants and death in animals (Muto and Takizawa, 1992, Buekens and Cen, 2011).

However, PCDDs, PDCFs and PCBs are almost undetectable in gas emissions of well-regulated incineration process, with emissions at the point of leaving the furnace to enter the flue at 3-10ng/m^3(Buekens and Cen, 2011). Those dioxins that are present become concentrated in solid residues, such as fly ash and flue gas cleaning products (Lundin and Marklund, 2008). This results in a much smaller volume of waste, but is classified as being toxic to humans and the environment (Ivan Diaz-Loya *et al.*, 2012) posing a significant problem for final disposal.

Applying pyrolysis as a treatment option offers an alternative route to not only recovering energy but chemical value from PVC (Kantarelis *et al.*, 2009). The process can be considered to be a form of chemical recycling with the cracking of the polymer to recover smaller molecules of similar or related chemical structure (as described in section 2.4.7.1).

During a pyrolysis process, chlorine is released from the PVC polymer structure between the temperatures of 220^{o}C and 400^{o}C (Bockhorn *et al.*, 1999b), ultimately resulting in the production of chlorinated hydrocarbons. These contaminate other gaseous and liquid hydrocarbon products rendering them useless for many applications as well as producing potentially harmful products of PCDDs, PCDFs, and PCBs (Miranda *et al.*, 2001a).

Nevertheless, the application of microwaves in the decomposition and pyrolysis of PVC does pose an interesting and potentially viable route for recycling PVC. This is as a result of the enhanced interaction of PVC and microwaves. The polymer is dielectrically active due to the chlorine being present, allowing it to heat. The chlorine then preferential dissociates from the polymer backbone before decomposition of the main organic components, with the residual hydrocarbon matrix remaining with a low dielectric potential, unable to heat any further (Moriwaki *et al.*, 2006b, Osada and Yoshioka, 2009).

This behaviour poses great potential in the pyrolysis of PVC, providing a potential pathway for both the recovery of HCl and the residual de-hydrochlorinated char. However, no research work has been reported on this route. As such, this chapter sets out to provide a comprehensive investigation into this potentially exciting route for the recovery of valuable products from PVC. This will be undertaken by

6.2 Conventional Thermal Decomposition of Polyvinylchloride

In order to determine the specific effects/differences that a microwave pyrolysis process has on the decomposition of PVC, it was necessary to form a comprehensive understanding of the conventional thermal degradation behaviour of the polymer. Thus, the effects of degradation temperature and heating rate (Miranda *et al.*, 2010) on the extent of decomposition and the products formed were studied. To achieving this, the experimental techniques of Thermal Gravimetric Analysis/Differential Scanning Calorimetry and Pyrolysis Gas Chromatography/Mass Spectrometry were employed; as previously discussed in Section 4.4.

6.2.1 Thermal Gravimetric Analysis

PVC samples were exposed to heating rates of 1, 10, 30 and 50°C/min. The resulting decomposition was examined and events determined/calculated by the method of extrapolated onset analysis from the Thermal Gravimentric (TG) plot. This method involved the extrapolation of two linear regions and determining the point of intersection, as per the method given in Ozawa (1993).

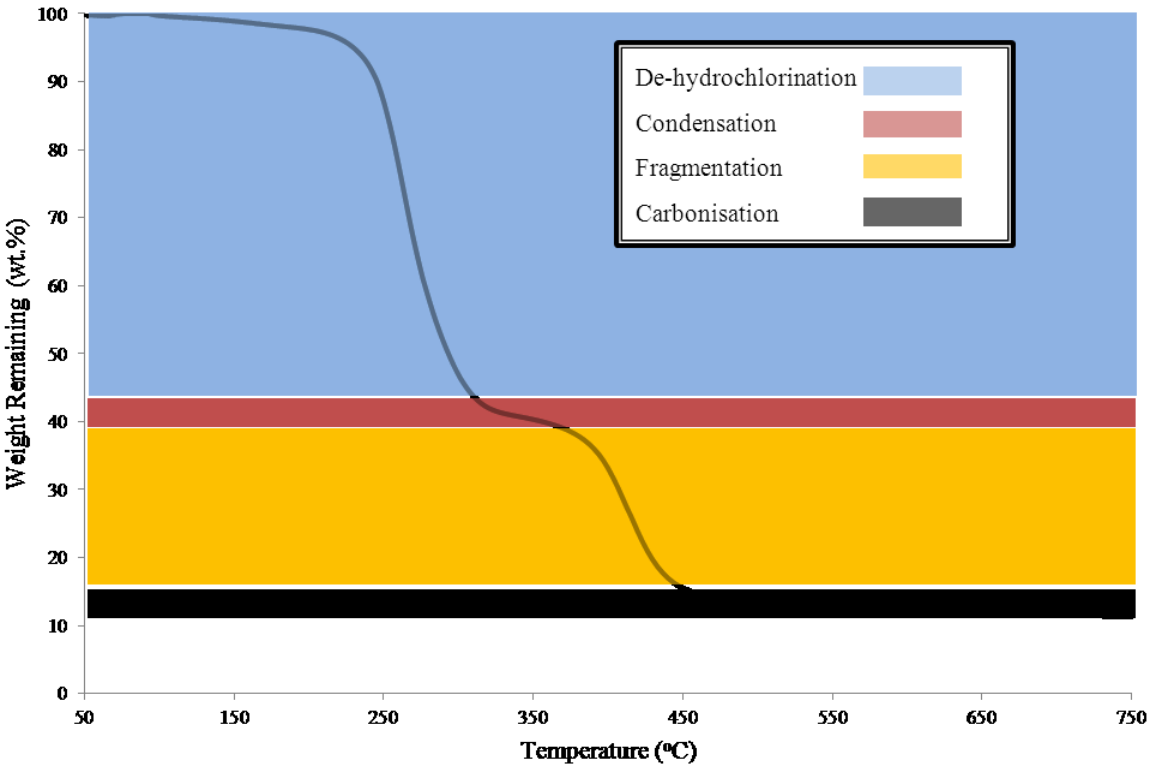


Figure 6-2 Generalised model of PVC decomposition from Thermal Gravimetric Analysis (TGA) under nitrogen purge gas at 10°C/min from 0-1000°C

The thermal degradation of PVC can generally be described in the phases presented in Figure 6-2, whereby the polymer undergoes de-hydrochlorination, condensation of the residual polymer structure, fragmentation of the condensed polymer and aromatisation of residue (Marongiu *et al.*, 2003).

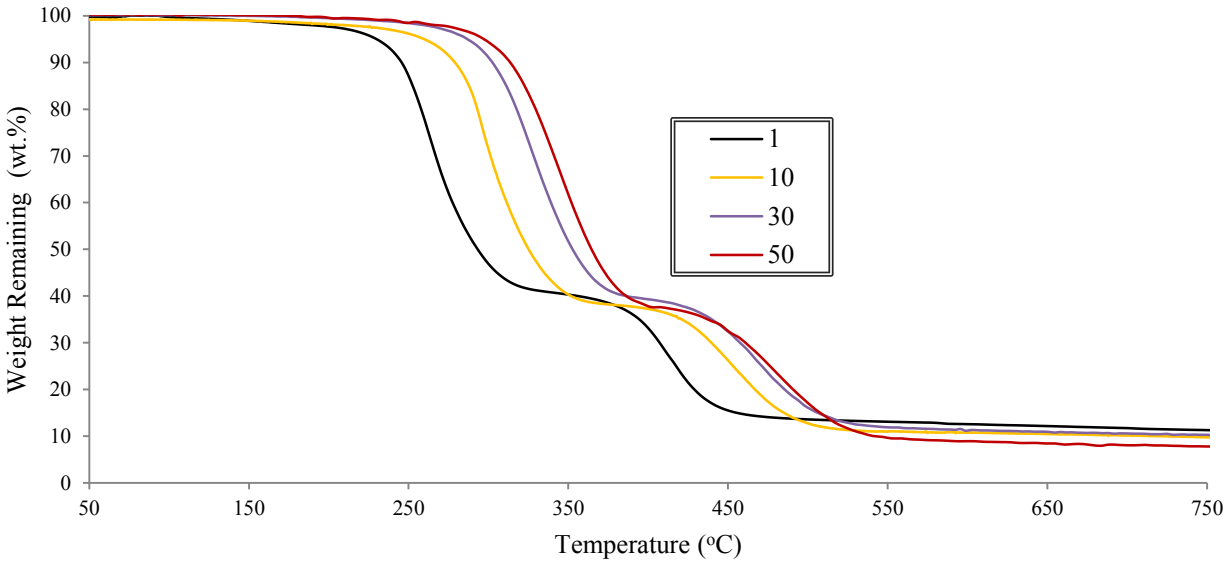


Figure 6-3 Thermal Degradation profiles of PVC under nitrogen atmosphere at 1, 10, 30 and 50°C/min

The first stage of PVC decomposition occurs between the temperatures of 239°C and 379°C over the heating rates investigated (see Table 6-1). It can be seen clearly that the first decomposition step represents the greatest weight loss, with between 57.86wt.% and 61.60wt.% at heating rates of 1°C/min and 50°C/min respectively (see Figure 6-3). Rates between these temperatures do not give losses outside of this range.

The 57wt.% lost corresponds with the molecular weight fraction of HCl being cleaved from the polymer backbone. The further loss in weight (up to 61.60wt.%) is likely to correspond to the formation of aromatic species such as benzene, naphthalene and phenanthrene (Marongiu *et al.*, 2003, Bockhorn *et al.*, 1999b, Troitskii *et al.*, 1973).

The proposed mechanism forming these aromatic species is as a result of the cleavage of either C–C (D^o:602±21 KJ/mol (Darwent, 1970)), C–H (D^o:473±4.0 KJ/mol (Darwent, 1970)), or C–Cl (D^o:338.1 KJ/mol(Darwent, 1970)) bonds; with the weakest bond C–Cl the most likely candidate for cleavage to occur. The product of the initial cleavage is the highly reactive chlorine radical and reference radical (see Equation 6-1).

$$-(CH_2 - CHCl) - \xrightarrow{yields} -(CH_2\ \ ^{\bullet}CH) -\ \ + Cl^{\bullet}$$

Equation 6-1 Radical formation resulting from cleavage of C-Cl bonds on the PVC polymer; as proposed byBockhorn et al. (1999b) and Marongiu et al. (2003).

The subsequent abstraction of hydrogen from the PVC polymer by chlorine radicals and successive β-scissions of Cl can give rise to the formation of a polyene structure (see Equation 6-2).

$$Cl^{\bullet} +\ \ -(CH_2 - CHCl) - \xrightarrow{yields} -(CH^{\bullet} - CHCl) -\ \ + HCl$$

$$-(\ CH^{\bullet} - CHCl) - \xrightarrow{yields} -(CH = CH) - + Cl^{\bullet}$$

Equation 6-2 Radical Chain Propagation step for de-hydrochlorination as per Montaudo and Puglisi (1991) and Marongiu et al. (2003)

Table 6-1 Effect of heating rate on 1st stage of PVC decomposition with decomposition start/finish temperatures, total mass loss, temperature of peak mass loss and mass loss rate

Sample Heating Rate (°C/min)	Start Temp (°C)	End Temp (°C)	Mass Loss (wt.%)	Temp of Peak Loss Rate (°C)	Loss Rate (wt.%/°C)
1	238.95	310.91	57.86	263.19	1.214
10	275.40	331.45	60.13	299.78	1.268
20	286.95	351.40	58.51	314.60	1.133
30	293.00	363.22	58.83	326.73	0.959
40	299.44	371.56	58.07	335.22	0.879
50	302.05	378.50	61.60	344.66	0.899

Table 6-2 Effect of heating rate on the 2nd stage of PVC decomposition with start/finish temperatures, total mass loss, temperature of peak mass loss and mass loss rate

Sample Heating Rate (°C/min)	Start Temp (°C)	End Temp (°C)	Mass Loss (wt.%)	Temp of Peak Loss Rate (°C)	Loss Rate (wt.%/°C)
1	389.98	441.64	23.91	412.40	0.575
10	421.13	490.33	25.31	450.07	0.387
20	428.30	500.44	24.86	461.87	0.439
30	437.09	507.88	24.97	467.58	0.417
40	436.69	520.42	24.59	475.48	0.401
50	438.58	525.37	27.58	481.54	0.388

Due to the prevailing reaction forming C to C double bonds, the overall de-hydrochlorination process is endothermic requiring $\Delta_R H = 72KJ\ mol^{-1}$ (Bockhorn *et al.*, 1999b). The formation of benzene is a good indicator of an endothermic process, hence a cessation/reduction in its production during the pyrolysis process would demonstrate a shift towards an exothermic reaction pathway(Bockhorn *et al.*, 1999b).

In summation, the process by which the de-hydrochlorination occurs appears to be dominated by the growth of the polyene structure, by an ion pairing route between Cl and its neighbouring H. However, the generation of free radicals during the process produces labile defects on the polymer chain which often result in cyclisation occurring or crosslinking between polymer chains, terminating polyene growth and producing aromatic species.

It can be observed from Figure 6-3 and the derived thermal decomposition points from Table 6-1 and Table 6-2, that a higher heating rate shifted the weight loss curve rightward to a higher temperature range resulting in a disparity of 63^{o}C between 1^{o}C/min and 50^{o}C/min over the de-hydrochlorination stage. This is also reflected in the second stage of the decomposition (fragmentation) whereby a difference of 48^{o}C is observed. A constant weight of PVC was reached across the range of heating rates by 550^{o}C.

Upon examining Figure 6-4 and Figure 6-5 it becomes apparent that the decomposition of PVC follows the expected pattern of increased peak weight loss per unit time. With this, the initial onset of degradation is consistent across the heating rates of 10-40^{o}C/min when the 1wt.% loss rule (Cullis and Hirschler, 1983, Hirschler, 1986) is applied.

However, when extrapolated onset analysis is used significant differences are observed (see Table 6-1 and Table 6-2). These results suggest that the degradation of PVC under dynamic thermal conditions above 10^{o}C/min begin at ~200^{o}C, which is in good agreement with (Marongiu *et al.*, 2003, Miranda *et al.*, 1999).

During the de-hydrochlorination step, lower heating rates favour the greatest rate of decomposition, with a maximum rate of 1.27%/^{o}C occurring at 10^{o}C/min. This relationship persists during the fragmentation stage of the decomposition, whereby a gradual decline in decomposition per unit temperature occurred with increasing heating rate; the greatest decomposition rate of 0.575wt.%/^{o}C at 1^{o}C/min to 0.388wt.%/^{o}C occurring at 50^{o}C/min.

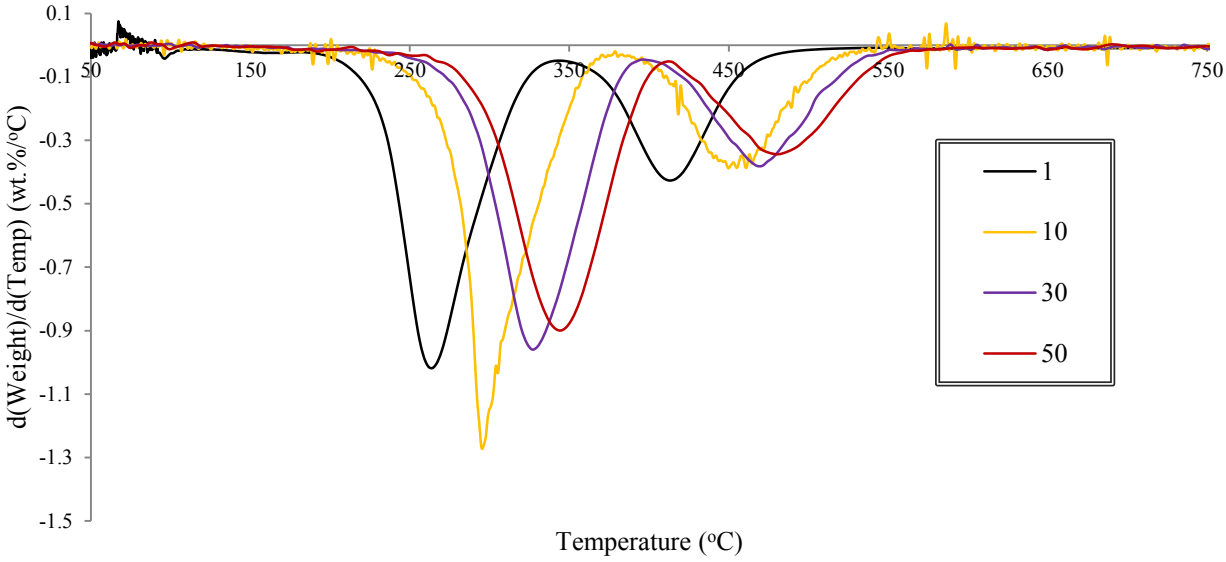


Figure 6-4 Differential Thermal Gravimetric Analysis of PVC at 1, 10, 30 and 50°C presented as wt.%/°C vs Temperature

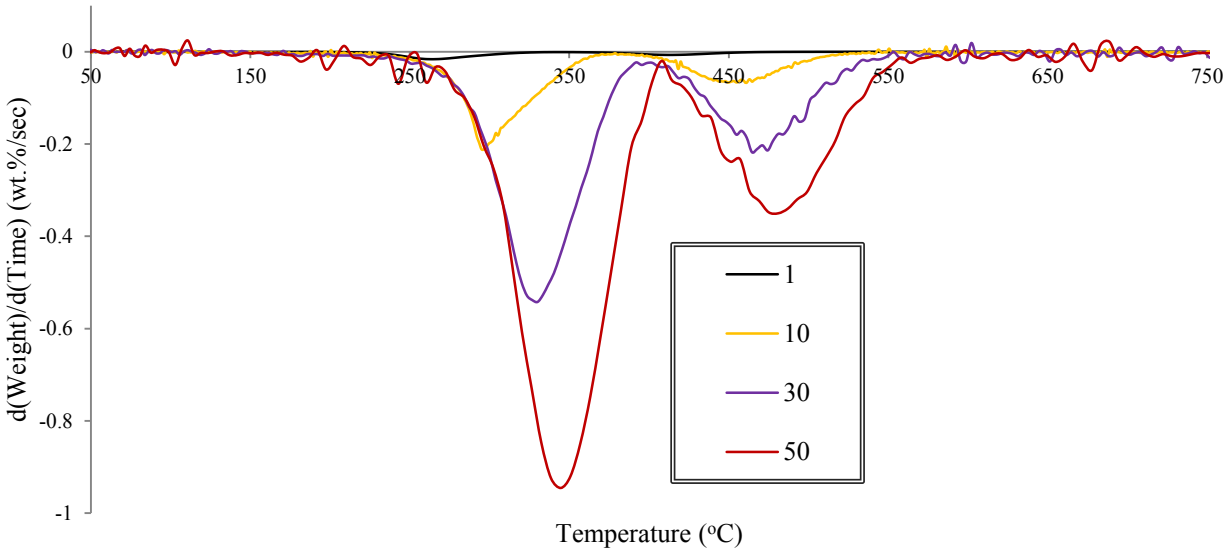


Figure 6-5 Differential Thermal Gravimetric Analysis of PVC at 1, 10, 30 and 50°C presented as wt.%/sec vs Temperature

Nevertheless, it is apparent that as heating rate increased, peak decomposition rates shifted to higher temperatures whilst the decomposition was spread over a greater temperature range. There was a ~50°C shift in the first-stage end temperature. This indicated that the observed differences in the decomposition peak and the thermal response are most likely attributable to thermal lag within the instrument or low thermal conductivity across the sample. Further, the effects seen with heating rate

in relation to mass loss per unit temperature (see Figure 6-4), may also be due to the promotion of reaction pathways which exhibit increased degradation rates with the peak rate of decomposition occurring at 10°C/min. This trend has also been observed by Wu *et al.* (1994), Marcilla and Beltrán (1995), Bockhorn *et al.* (1999b) and Miranda *et al.* (1999).

During both stages of the decomposition, 10°C/min heating rates showed significant variation from the trend. Both of the highest rates of weight loss per unit temperature occurred during de-hydrochlorination and the lowest during fragmentation. Behnisch and Zimmermann (1988) proposed that the degradation rate was influenced by concentration gradients of HCl within the PVC samples, with differing concentrations of HCl resulting in preferential catalysis of allylic chlorides or tertiary chloride at low and high concentrations respectively (Behnisch and Zimmermann, 1988, Marcilla and Beltrán, 1995, Marongiu *et al.*, 2003, Miranda *et al.*, 1999, Montaudo and Puglisi, 1991, Starnes Jr, 2002).

Changes observed in char formation have been attributed to changes in the activation energies arising from competitive reactions of intermediates forming volatiles and char (Miranda *et al.*, 2001b, Jiménez *et al.*, 1993). The overall trend shows a gradual decline in char formation with increasing heating rate. Wu *et al.* (1994) proposed that this could to be attributed to differences in the activation energy of char formation being 52.0 kcal mol^{-1}, lower than that of the activation energy of devolatilisation of 63.8 kcal mol^{-1}, hence higher heating rates push the reaction towards formation of volatile species. This is an extensively reported effect during biomass pyrolysis, where almost total gasification of the feedstock is achieved using very high heating rates.

6.2.2 Py-GC/MS

Pyrolysis component analysis via Py-GC/MS has been utilised to investigate the decomposition products of PVC under dynamic heating. This provided a baseline analysis of the products of pyrolysis from the PVC utilised in this investigation, over a range of temperatures, so that thermal and microwave degradation mechanisms could be compared and contrasted.

The information gained from TGA (figure 6.3?) provided a clear range of temperatures that required investigation to determine the products generated within each stage of decomposition (de-hydrochlorination and fragmentation). Thus, PVC was subjected to tests at 200, 300, 400 and 500°C; the temperature range over which the greatest loss of mass observed. A final run was conducted at 800°C to establish the pyrolysis products formed from the rearrangment of the remaining char. All of these experiments were performed at a midrange heating rate of 20°C/min. The organic products formed during this testing are presented in Table 6-3 and Table 6-4 -.

From the products identified in Table 6-3 and Table 6-4 - it can be seen that at a final pyrolysis temperature of 200^{o}C – 300^{o}C, the organic species produced are plentiful, with the formation of aromatic, branched aromatic and polyaromatic hydrocarbons. This is clear evidence that the initial dehydrochlorination phase of PVC decomposition also involves the decomposition of the organic structure. Of the species present during this phase; benzene, toluene, xylene, styrene, ethenylmethylbenzene, 2-Methylnaphthalene, biphenyl and phenanthrene are most prevalent (see Figure 6-7), representing 85.37%TiC then 50.04%TiC at 200^{o}C and 300^{o}C respectively.

Table 6-3 Pyrolysis products from the Py-GC/MS of PVC at 200, 300, 400, 500 and 800°C under a heating rate of 20°C/min semi-quantified by Total Ion Count (TiC)

Retention Time (Cm)	Compound Name	Empirical Formula	200°C %TiC*	200°C TiC/mg**	300°C %TiC	300°C TiC/mg	400°C %TiC	400°C TiC/mg	500°C %TiC	500°C TiC/mg	800°C %TiC	800°C TiC/mg
10.177	Ethylene	C_2H_4	-	-	19.73	6.0899×10^8	18.04	9.6977×10^8	16.12	8.6325×10^8	10.49	4.2068×10^8
14.229	(Z)-3-Penten-1-yne	C_5H_6	2.86	7.2495×10^7	1.46	4.4935×10^7	1.77	9.4947×10^7	2.52	1.3475×10^8	0.38	1.5432×10^7
15.38	Cyclopentene	C_5H_8	-	-	-	-	0.51	2.7537×10^7	0.54	2.8809×10^7	-	-
17.276	Tetrahydro-5,6-2H-pyran-2-one	$C_5H_8O_2$	-	-	-	-	0.25	1.3515×10^7	0.26	1.3933×10^7	0.30	1.2016×10^7
21.532	Benzene	C_6H_6	41.06	1.0422×10^9	32.48	1.0026×10^9	27.05	1.4542×10^9	25.62	1.3714×10^9	26.92	1.0799×10^9
22.324	3-Methyl-3-penten-1-yne	C_6H_8	0.43	1.0906×10^7	-	-	0.62	3.3329×10^7	0.38	2.0156×10^7	-	-
23.737	7-Azabicyclo[4,2,0]octan-8-one	$C_7H_{11}NO$	-	-	-	-	0.23	1.2573×10^7	0.18	9.7783E+06	-	-
24.84	2,3,3-Trimethyl-cyclobutanone	$C_7H_{12}0$	-	-	-	-	0.24	1.3168×10^7	0.21	1.1306×10^7	8.27	3.3187×10^8
31.767	Toluene	C_7H_8	11.02	2.7977×10^8	8.35	2.5769×10^8	9.29	4.9963×10^8	9.19	4.9220×10^8	-	-
32.715	3-(2-Propenyl)-cyclopentene	C_8H_{12}	-	-	-	-	-	-	0.40	2.1263×10^7	-	-
43.245	Ethylbenzene	C_8H_{10}	1.57	3.9884×10^7	1.12	3.4619×10^7	1.51	8.1030×10^7	1.54	8.2544×10^7	1.34	5.3774×10^7
44.323	O-Xylene	C_8H_{10}	2.94	7.4617×10^7	-	-	2.67	1.4336×10^8	0.95	5.0655×10^7	0.93	3.7242×10^7
46.667	Styrene	C_8H_8	2.87	7.2794×10^7	2.31	7.1443×10^7	1.99	1.0710×10^8	2.51	1.3443×10^8	2.11	8.4656×10^7
47.321	P-Xylene	C_8H_{10}	-	-	1.36	4.2029×10^7	-	-	1.57	8.4116×10^7	1.46	5.8619×10^7
53.995	1-Ethenyl-3-methyl-benzene	C_9H_{12}	2.06	5.2364×10^7	0.42	1.2821×10^7	1.47	7.9122×10^7	0.67	3.5943×10^7	0.47	1.9033×10^7
55.473	Propyl-benzene	C_9H_{12}	-	-	-	-	1.21	6.5218×10^7	0.70	3.7627×10^7	0.44	1.7803×10^7
59.958	β-Ethenyl-benzeneethanol	$C_{10}H_{12}O$	-	-	-	-	0.44	2.3547×10^7	0.37	1.9873×10^7	-	-
64.337	Indane	C_9H_{10}	-	-	0.71	2.1935×10^7	0.89	4.7990×10^7	1.86	9.9340×10^7	1.48	5.9477×10^7
66.551	1-Ethynyl-4-methyl-benzene	C_9H_8	5.18	1.3138×10^8	3.95	1.2179×10^8	2.97	1.5957×10^8	3.72	1.9920×10^8	4.40	1.7633×10^8
72.244	4-Ethenyl-1,2-dimethyl-benzene	$C_{10}H_{12}$	-	-	-	-	1.01	5.4118×10^7	-	-	-	-
79.637	2-Methylindene	$C_{10}H_{10}$	1.59	4.0285×10^7	5.34	1.6479×10^8	1.01	5.4316×10^7	1.55	8.3060×10^7	1.35	5.4088×10^7
80.225	1,4-Dihydronaphthalene	$C_{10}H_{10}$	0.98	2.4803×10^7	-	-	2.45	1.3184×10^8	0.25	1.3399×10^7	1.01	4.0669×10^7
80.454	1-Methyl-4-(1-propynyl)-benzene	$C_{10}H_{10}$	-	-	-	-	0.24	1.3089×10^7	0.25	1.3399×10^7	0.23	9.3261×10^6
83.795	Naphthalene	$C_{10}H_8$	-	-	7.80	2.4072×10^8	7.17	3.8550×10^8	7.69	4.1180×10^8	7.04	2.8252×10^8
93.631	1,3-Dimethyl-1H-indene	$C_{11}H_{12}$	-	-	-	-	0.30	1.6000×10^7	-	-	0.43	1.7247×10^7
96.35	2-Methyl-naphthalene	$C_{11}H_{10}$	12.00	3.0443×10^8	4.24	1.3098×10^8	2.38	1.2782×10^8	2.48	1.3265×10^8	2.44	9.7863×10^7
98.066	3-Methyl-naphthalene	$C_{11}H_{10}$	2.41	6.1071×10^7	-	-	1.90	1.0197×10^8	2.11	1.1297×10^8	2.07	8.2971×10^7

***Percentage TiC of organic compounds**
****TiC of organic compound per weight original sample in mg**
*****Continued on next page*****

Table 6-4 -3 Pyrolysis products from the Py-GC/MS of PVC at 200, 300, 400, 500 and 800°C under a heating rate of 20°C/min semi-quantified by Total Ion Count (TiC)

Retention		Empirical	200°C		300°C		400°C		500°C		800°C	
Time (Cm)	Compound Name	Formula	%TiC	TiC/mg	%TiC	TiC/mg	%TiC	TiC/mg	%TiC	TiC/mg	%TiC	TiC/mg
104.748	Biphenyl	$C_{12}H_{10}$	2.17	5.5006 X 10^7	1.78	5.4921 X 10^7	1.78	9.5645 X 10^7	1.86	9.9653 X 10^7	1.73	6.9504 X 10^7
106.725	2-Ethyl-naphthalene	$C_{12}H_{12}$	-	-	-	-	0.40	2.1695 X 10^7	2.56	1.3697 X 10^8	0.27	1.0849 X 10^7
106.995	1-(2-Propenyl)-naphthalene	$C_{13}H_{12}$	0.72	1.8167 X 10^7	0.58	1.7799 X 10^7	1.02	5.4604 X 10^7	1.95	1.0464 X 10^8	0.61	2.4347 X 10^7
107.542	(Z)-3-Tetradecene	$C_{14}H_{28}$	0.67	1.6883 X 10^7	-	-	0.26	1.4170 X 10^7	1.04	5.5781 X 10^7	0.22	8.8163 X 10^6
109.388	1,3-Dimethyl-naphthalene	$C_{12}H_{12}$	-	-	-	-	1.11	5.9439 X 10^7	0.31	1.6788 X 10^7	0.28	1.1398 X 10^7
109.789	1,1-Diphenyl-2-propanol	$C_{15}H_{16}O$	-	-	-	-	1.17	6.3058 X 10^7	0.36	1.9134 X 10^7	0.38	1.5092 X 10^7
110.091	2-Ethenyl-naphthalene	$C_{12}H_{10}$	-	-	-	-	-	-	0.37	2.0052 X 10^7	0.26	1.0391 X 10^7
114.657	1-Chloro-tetradecane	$C_{14}H_{29}Cl$	0.44	1.1187 X 10^7	1.32	4.0845 X 10^7	0.26	1.3733 X 10^7	-	-	-	-
115.392	Naphtho[2,1-b]furan	$C_{12}H_8O$	-	-	-	-	-	-	-	-	-	-
116.324	1-(2-Propenyl)-naphthalene	$C_{13}H_{12}$	-	-	-	-	-	-	0.30	1.6045 X 10^7	0.29	1.1595 X 10^7
124.95	Fluorene	$C_{13}H_{10}$	1.53	3.8825 X 10^7	1.35	4.1769 X 10^7	1.06	5.7172 X 10^7	1.51	8.0921 X 10^7	1.51	6.0575 X 10^7
126.862	2,4A-Dihydro-fluorene	$C_{13}H_{12}$	1.27	3.2226 X 10^7	0.90	2.7683 X 10^7	0.68	3.6823 X 10^7	0.50	2.7013 X 10^7	0.66	2.6620 X 10^7
128.683	1H-Phenalene	$C_{13}H_{10}$	-	-	-	-	0.19	1.0033 X 10^7	0.39	2.1139 X 10^7	0.37	1.4868 X 10^7
134.9	(E)-Stilbene	$C_{14}H_{12}$	0.48	1.2207 X 10^7	0.40	1.2306 X 10^7	0.37	2.0055 X 10^7	0.49	2.6451 X 10^7	0.36	1.4240 X 10^7
135.178	4-Methyl-9H-fluorene	$C_{14}H_{12}$	-	-	-	-	0.29	1.5844 X 10^7	0.33	1.7537 X 10^7	0.34	1.3548 X 10^7
140.144	Phenanthrene	$C_{14}H_{10}$	2.09	5.3114 X 10^7	1.83	5.6632 X 10^7	1.54	8.3066 X 10^7	1.63	8.7122 X 10^7	1.64	6.5946 X 10^7
140.741	Anthracene	$C_{14}H_{10}$	0.40	1.0210 X 10^7	-	-	0.31	1.6840 X 10^7	0.43	2.3044 X 10^7	0.40	1.5914 X 10^7
144.359	1-(Phenylmethylene)-1H-indene	$C_{16}H_{12}$	0.77	1.9610 X 10^7	0.36	1.0978 X 10^7	0.63	3.3626 X 10^7	0.28	1.4790 X 10^7	0.31	1.2544 X 10^7
146.81	8,9-Dihydrocyclopenta[DEF]phenanthrene	$C_{15}H_{12}$	2.03	5.1507 X 10^7	1.41	4.3537 X 10^7	1.09	5.8708 X 10^7	0.46	2.4709 X 10^7	0.24	9.7007 X 10^6
147.128	1-Methyl-anthracene	$C_{15}H_{12}$	-	-	-	-	-	-	0.28	1.4742 X 10^7	0.36	1.4397 X 10^7
148.117	2-Methyl-anthracene	$C_{15}H_{12}$	-	-	-	-	-	-	0.23	1.2374 X 10^7	0.47	1.8775 X 10^7
150.29	2-Phenylnaphthalene	$C_{16}H_{12}$	-	-	0.45	1.3864 X 10^7	-	-	0.38	2.0222 X 10^7	0.36	1.4597 X 10^7
160.697	7H-Benzo[c]fluorine	$C_{17}H_{12}$	0.47	1.2045 X 10^7	0.37	1.1297 X 10^7	0.22	1.1831 X 10^7	0.31	1.6338 X 10^7	0.32	1.2770 X 10^7
162.298	Benzanthrene	$C_{17}H_{12}$	-	-	-	-	-	-	-	-	2.62	1.0528 X 10^8
168.106	1-Heneicosyl-formate	$C_{22}H_{44}O_2$	-	-	-	-	-	-	-	-	0.90	3.5984 X 10^7
178.595	16-Heptadecenal	$C_{17}H_{32}O$	-	-	-	-	-	-	-	-	1.16	4.6524 X 10^7
191.616	1,19-Eicosadiene	$C_{20}H_{38}$	-	-	-	-	-	-	-	-	6.55	2.6283 X 10^8
192.58	9-Hexacosene	$C_{26}H_{52}$	-	-	-	-	-	-	-	-	1.33	5.3438 X 10^7
208.428	17-Pentatriacontene	$C_{35}H_{70}$	-	-	-	-	-	-	-	-	2.00	8.0129 X 10^7

***Percentage TiC of organic compounds**
****TiC of organic compound per weight original sample in mg**

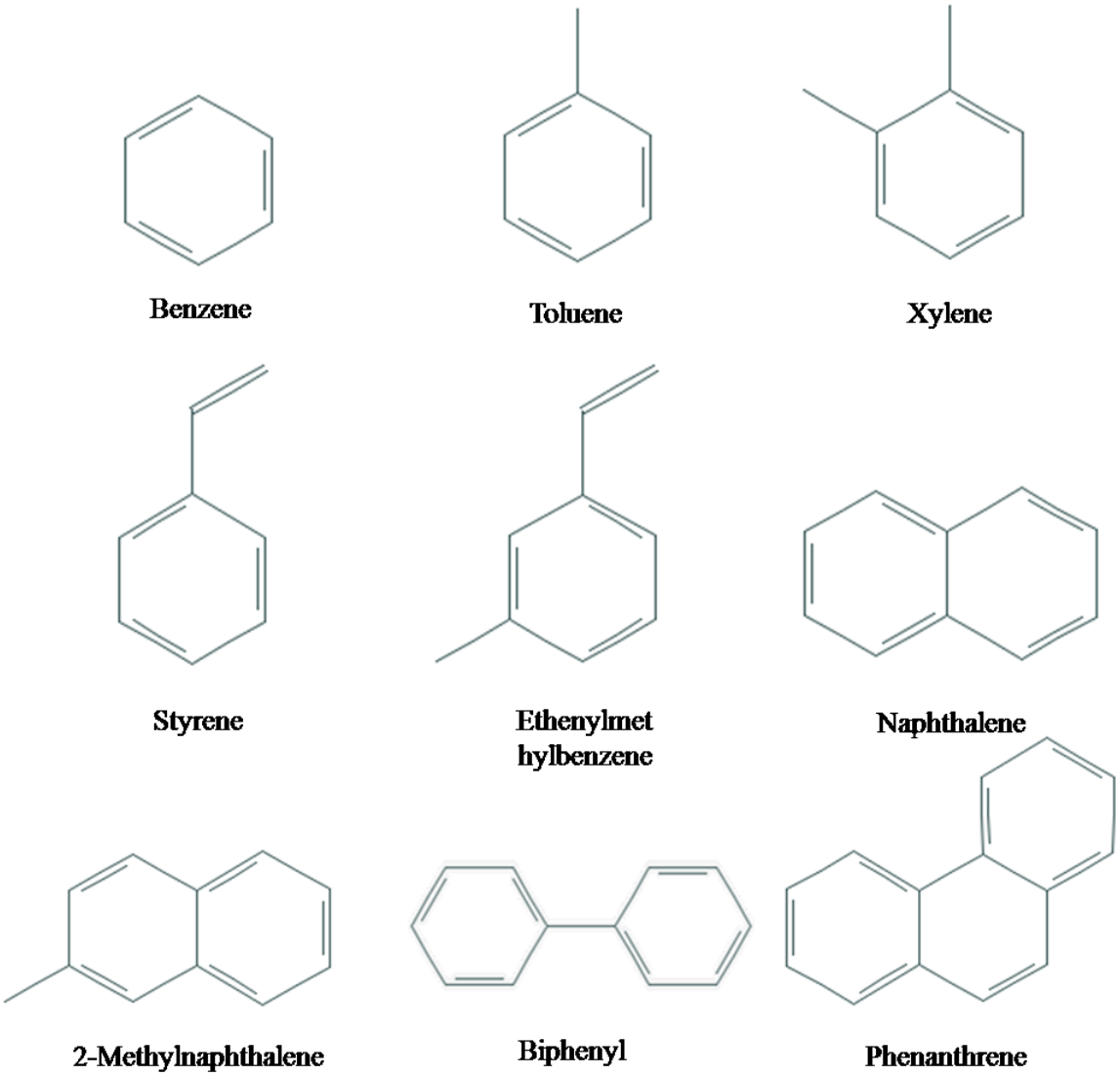


Figure 6-6 Common aromatic species produced during the decomposition of PVC by Py-GCMS

When examined in terms of TiC/mg, the aforementioned organic structures show little change in the quantities found, except for the branched alkyl aromatic structures of ethylbenzene, ethenylmethylbenzene and methylnaphthalene, which reduced by 43.67%, 75.52%, 56.98% of TiC/mg respectively.

Whilst these structures are reducing in their proportions, a number of significant new peaks appear; these being ethylene, indane, naphthalene and 2-phenylnaphthalene. The change in proportion of aromatic and branched aromatic species can be observed further in Figure 6-7.

As a percentage of total TiC signal between pyrolysis runs at 200°C and 300°C, shifts occur, with reductions in aromatic species coinciding with the increased occurrence of alkene species. The presence of these compounds indicates that the cleaving of branches is occurring between these temperatures or the process of intermolecular hydrogen transfer. The resulting condensed organic structures are formed.

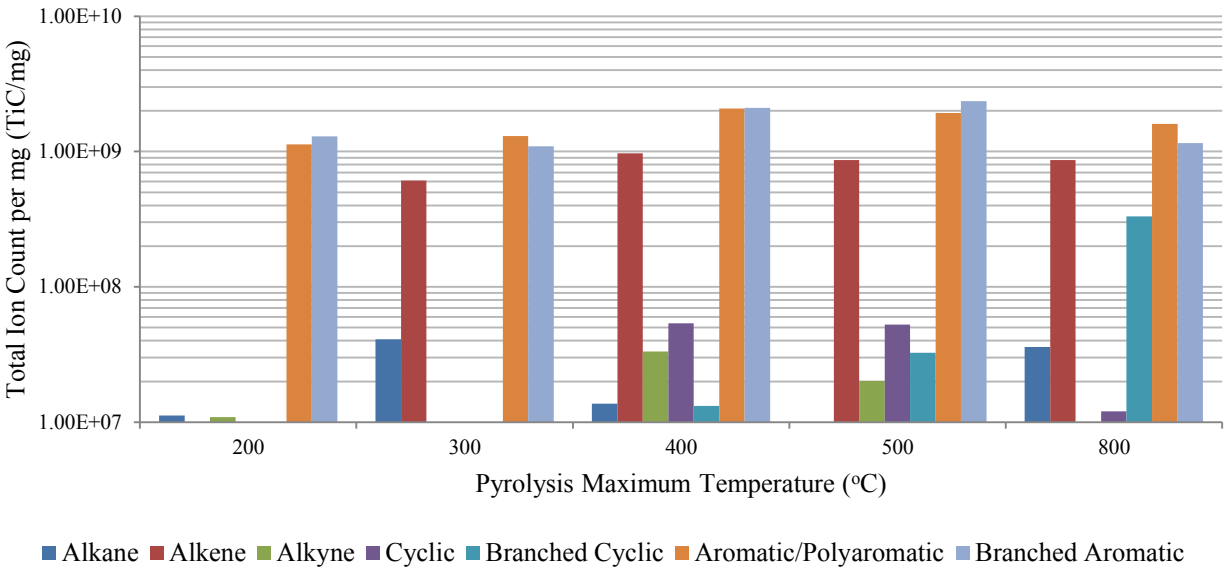


Figure 6-7 Speciated products of PVC pyrolysis at differing maximum temperatures of 200, 300, 400, 500 and 800°C (by major organic group)

Benzene represents the most abundant species across all pyrolysis temperatures with ~41.0%TiC at 200°C, 32.5%TiC at 300°C, which continues to decline until a minimum is reached of ~26.0%TiC at 500°C. This decline does not represent a decrease in the quantity or proportion of benzene produced; as shown by the increasing TiC/mg benzene with temperature. Rather a decrease in the proportion of the total TiC of the chromatogram is observed, which occurs due to the remaining poly-ene structure undergoing further decomposition in the fragmentation stage of PVCs breakdown.

The dominance of benzene formation during the initial stages of pyrolysis (200°C – 300°C) has been examined by multiple authors, suggesting a number of possible routes for its production. The mechanisms proposed by Stromberg *et al.* (1959), Troitskii *et al.* (1973) Hirschler (1986), Montaudo and Puglisi (1991), McNeill *et al.* (1995), Bockhorn *et al.* (1999b), Starnes Jr (2002), Marongiu *et al.* (2003) and Moriwaki *et al.* (2006b) are all in agreement. The possible routes of benzene formation may occur during the de-hydrochlorination process, via the mechanisms of Diels Alder cyclisation, radical condensation and de-alkylation. The exact stepwise mechanism by which the reaction takes

place is under dispute and appears to be very much dependent upon the conditions by which the degradation takes place.

As the pyrolysis temperature approaches 400^{o}C, the condensation phase of the decomposition occurs. This coincides with a maximum production of ethylene and benzene in TiC/mg, indicating the end of the dehydrochlorination phase of the reaction and a shift from the endothermic to exothermic phase of the decomposition.

Between 400^{o}C and 500^{o}C, an increase in the branched aromatic and cyclic structures (see Figure 6-7) are observed; these being 3-(2-propenyl)-cyclopentene, methyl-naphthalene, ethyl-naphthalene, 1-(2-propenyl)-naphthalene, methyl-anthracene, 8,9-dihydrocyclopenta[DEF]phenanthrene (see Table 6-3, Table 6-4 -). This distribution of molecular moieties is likely to reflect the fact that the chemistry of the system is being dominated by radical species resulting in the number of labial defects on the poly-ene chain increasing and intermolecular cyclisation mechanisms (Marongiu *et al.*, 2003, Bockhorn *et al.*, 1999b).

With Figure 6-8 (see next page) it becomes clear that the increase in branched cyclic and aromatic hydrocarbons coincide with an increase in $C_8 - C_9$ and $C_{11} - C_{16}$ hydrocarbons but with a marked decrease in the number of C_2, C_6 and C_{10} hydrocarbons. This indicates that an increasing propensity exists for the lighter alkyaromatic molecules to undergo condensation reactions to form PAHs and PAH intermediary species, as also identified by Marongiu *et al.* (2003).

It is evident from the Py-GCMS (see Figure 6-8) results and those presented by Lattimer and Kroenke (1980)and Marongiu *et al.* (2003) that it is reasonable to conclude that benzene and naphthalene are produced almost entirely through intra-molecular cyclisation reactions, with the less abundant products of biphenyl, fluorine, anthracene, phenanthrene and benzanthrene following the same pathway (Lattimer and Kroenke, 1982, Marongiu *et al.*, 2003).

In the formation of styrene and indane, multiple authors have proposed that both the processes of intra-molecular cyclisation and inter-molecular hydrogen transfer between chains is most probable (Lattimer and Kroenke, 1982, Lattimer *et al.*, 1983, McNeill *et al.*, 1995, Montaudo and Puglisi, 1991). Toluene, xylene, methylnaphthalene and most other alkyl/branched aromatic structures are thought to form through multiple inter-molecular transfer of hydrogen between residual polyene chains (Lattimer and Kroenke, 1980, Lattimer and Kroenke, 1982, Marcilla and Beltrán, 1995, Marongiu *et al.*, 2003, McNeill *et al.*, 1995).

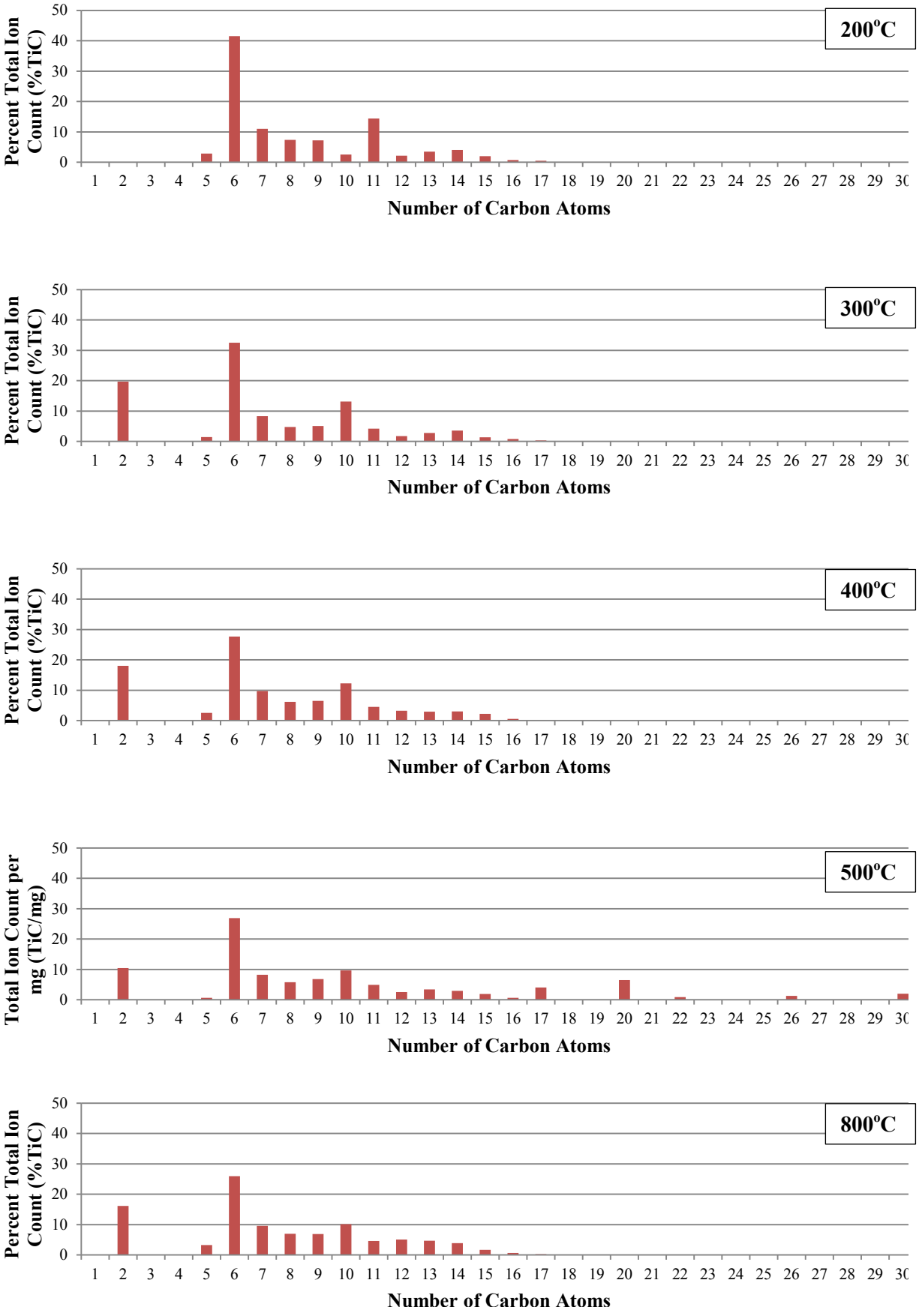


Figure 6-8 Semi quantification of product distribution by TiC of Py-GC/MS at 200, 300, 400, 500 and 800°C under a heating rate of 20°C/min

6.3 Microwave Decomposition

6.3.1 Introduction

The localised polarity of PVC has been well established by Moriwaki *et al.* (2006a) and Ito *et al.* (2006), with the electrical imbalance induced by the carbon to chlorine bond forming a dipole. Relative to other plastics, PVC has a high loss angle and dielectric (Moriwaki *et al.*, 2006b, Moriwaki *et al.*, 2006a, Ito *et al.*, 2006), allowing it to heat readily under microwave conditions. This is best explained by Equation 6-3, whereby the energy absorbed by the polymer can be estimated at a given temperature if certain factors are known.

$$P = kfE^2\varepsilon \tan\delta = 0.55fE^2\varepsilon \tan\delta \,.\, (10^{-10}) \quad (\mathrm{W/m^3})$$

Equation 6-3 Microwave power absorption

Where:

P = Microwave power absorbed ($\mathrm{W/m^3}$)

f = Microwave frequency (Hz)

E = Electromagnetic field strength ($\mathrm{S/cm^3}$)

ε' = relative permittivity

tan δ = loss angle

k = a constant ($= 2\pi\varepsilon_0 = 2\pi \times 8.85 \times 10^{-12}$)

The parameters in equation (see Equation 6-3), f and k were not able to be altered with the experimental equipment used. Only the electromagnetic field strength, relative permittivity and loss angle were changed. Of these parameters, the relative permittivity and loss angle are both material/temperature dependent; as shown in Figure 6-9, whereby Moriwaki *et al.* (2006a) confirmed the change in tan δ for PVC occurring between 20°C and 200°C from 0.013 to 0.038 respectively.

Over this temperature range, the link with tan δ proves to demonstrate a relationship which is unpredictable by mathematical techniques. Nevertheless, it is possible to see the behaviour of the PVC polymer used with step changes in tan δ seen at 120°C to 140°C.

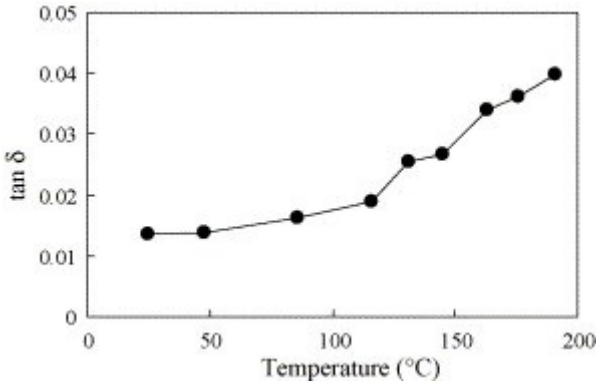


Figure 6-9 Change in tan δ of PVC with temperature (Moriwaki *et al.*, 2006a)

From the data gathered by Moriwaki *et al.* (2006a) and Ito *et al.* (2006) a basic knowledge has been established with respect to the interaction of 2.45GHz microwaves with PVC. Nevertheless, this knowledge is limited to single mode microwave systems and decomposition temperatures of less than 300°C. Hence, it has been necessary to design experiments to examine the key parameters of microwave power, duration and sample load on greater weights of powdered PVC to temperatures much higher than those previously examined.

6.3.2 Microwave Power

Microwave heating of pure PVC polymer was investigated initially using the apparatus shown in Figure 4-1 on sample weights of 5.00g ± 0.01g, which were subjected to irradiation at 440W, 600W and 850W for various durations between 0 and 30 minutes. The temperature of the sample was recorded every second throughout the experiments to ascertain thermal profiles and the resultant mass loss.

The thermal profiles from these tests are shown in Figure 6-10, Figure 6-11 and Figure 6-12 with the error represented as the standard deviation over 5 replicates. During the decomposition, PVC demonstrated three distinct stages of heating when exposed to a microwave field. In the first stage, a gradual increase in temperature occurs; in the second stage, rapid heating occurs and the third stage were sample cooling is observed. This profile is consistent with experimental data collected by Moriwaki *et al.* (2006a) and Ito *et al.* (2006). However, distinct differences appear at the points of inflection from the first to second stage of heating, indicating that a variation in tan δ is occurring. The first stage of heating is seen to span from 30°C (experimental starting temperature) until the points of inflection: 92.5°C (σ 1.69, n=5), 78.8°C (σ 1.00, n=5) and 100.1°C (σ 1.66, n=5) at 440W, 600W and 850W respectively.

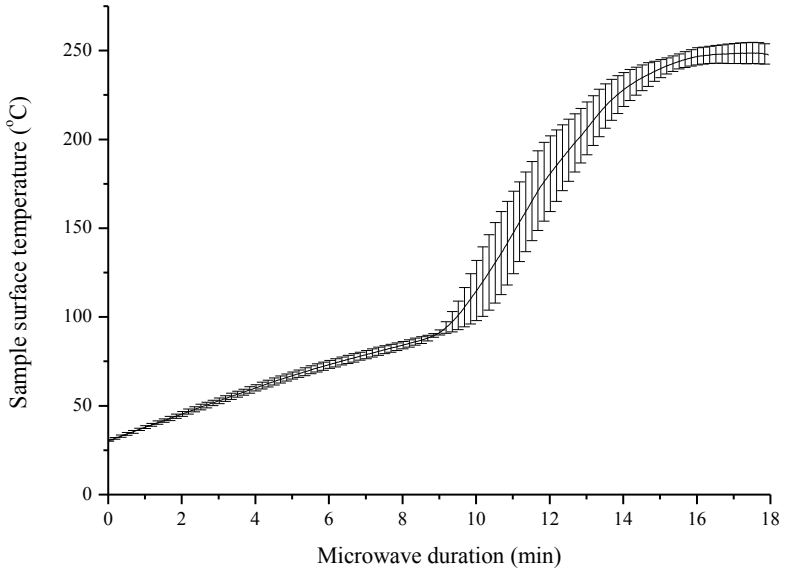


Figure 6-10 Mean temperature profile for 5g ± 0.01g of PVC exposed to microwave powers of 440W with standard deviation shown (n=5)

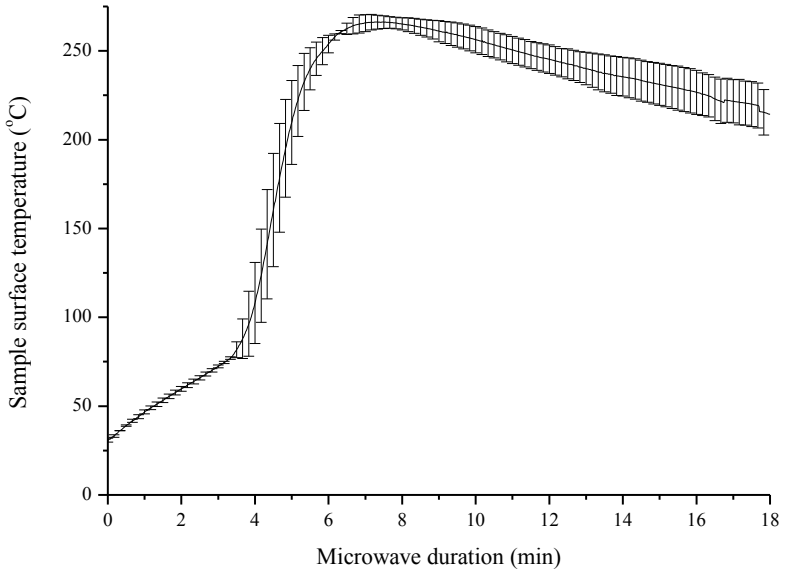


Figure 6-11 Mean temperature profile for 5g ± 0.01g of PVC exposed to microwave powers of 600W with standard deviation shown (n=5)

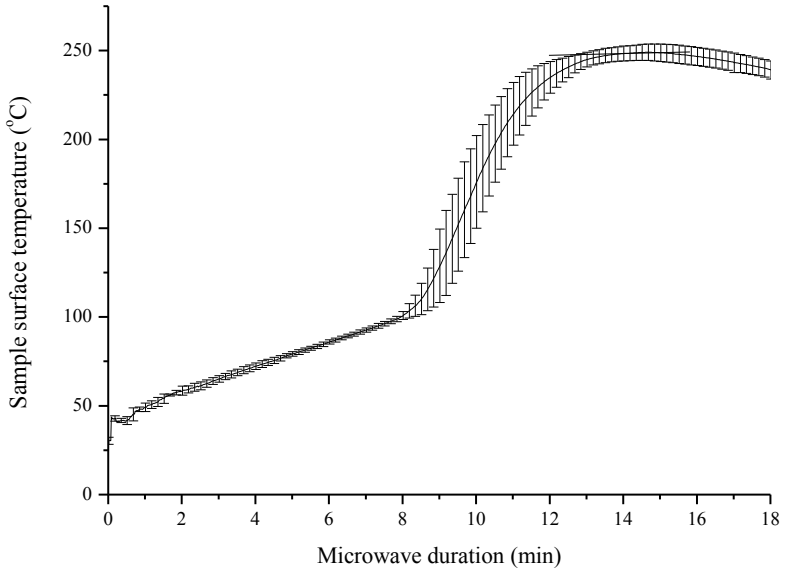


Figure 6-12 Mean temperature profile for 5g ± 0.01g of PVC exposed to microwave power of 850W with standard deviation shown (n=5)

The resultant heating rates of 6.59°C/min, 13.09°C/min and 7.05°C/min at 440W, 600W and 850W were calculated from the thermal profiles by linear fit analysis. These results indicate that the point at which inflection occurs is not constant with temperature but reliant upon the power applied. This has also been observed by Moriwaki *et al.* (2006a) and Ahmed and Siores (2001) whereby PVC and ceramics, respectively, display significant variance in the temperature at which heating rate inflection occurs. Hence the effect observed is not limited to PVC itself. However, neither author has discussed the reasoning for this occurrence.

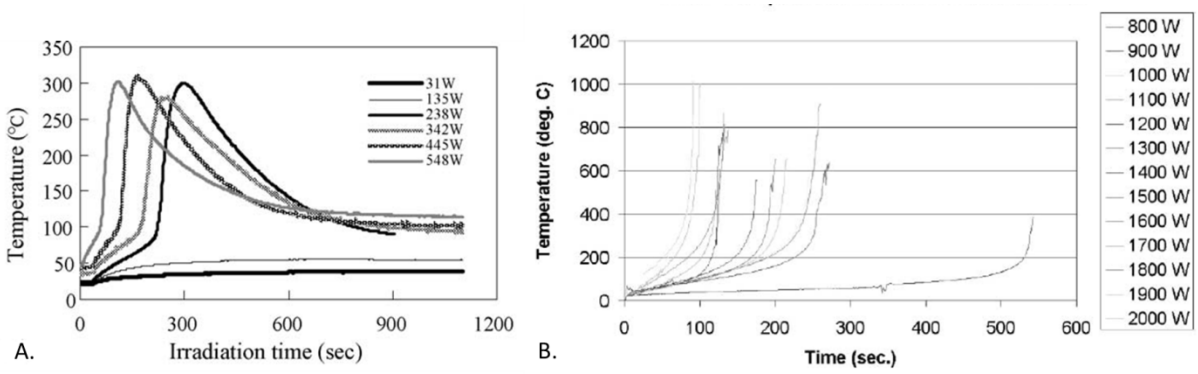


Figure 6-13 Variation in thermal runaway initiation point as demonstrated by (A.) PVC (Moriwaki *et al.*, 2006a) in which runaway initiates at temperatures between 84°C and 105°C and (B.) Ceramics (Ahmed and Siores, 2001)

Nevertheless, upon inflection, substantial changes in heating rate are observed. These correlate to significant changes in the dielectric loss, attributable to the glass transition temperature of PVC at 82°C (Ito *et al.*, 2006). This sudden and rapid rise in heating rate is also known as thermal runaway (Ito *et al.*, 2006, Moriwaki *et al.*, 2006a).

6.3.2.1 Thermal Runaway

The occurrence of thermal runaway is demonstrated clearly from the notable differences in the d(Temp)/d(time) for each of the heating profiles, with maximum heating rates of 35.45°C/min (σ 13.48), 112.62°C/min (σ 16.85), and 48.65°C/min (σ 16.79) (see Figure 6-14) for the respective powers of 440W, 600W and 850W. Average heating rates of 26.04°C/min (σ 8.17), 71.16°C/min (σ 8.60) and 45.75°C/min (σ 7.73) were observed for the respective powers of 440W, 600W and 850W. Over this period of heating, significant increases in relative standard deviations are observed.

Nevertheless, this increase in RSD is consistent across all powers and is most likely due to the mechanism of decomposition, resulting in uneven distribution of heat (otherwise known as hot spotting) coinciding with the occurrence of thermal runaway.

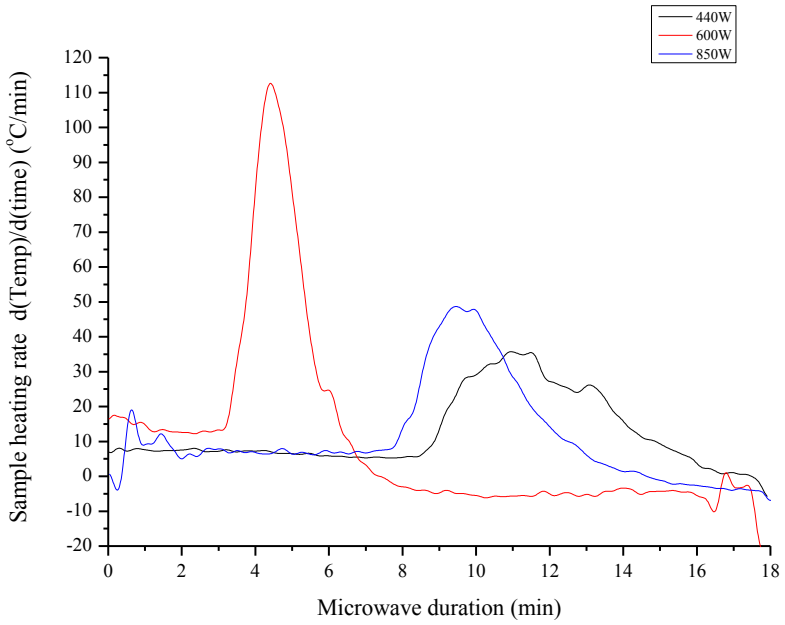


Figure 6-14 Heating rates for 5g ± 0.01g of PVC exposed to microwave powers if 440W, 600W and 850W over 18 minutes

The observed correlation of thermal runaway and sample temperature was recognised and modelled by Kriegsmann (1992), Pincombe and Smyth (1991) and Marchant and Pincombe (1994) using

perturbation methodologies. The derived correlation of sample temperature with applied power could be described by the typical S- shaped profile shown in Figure 6-15.

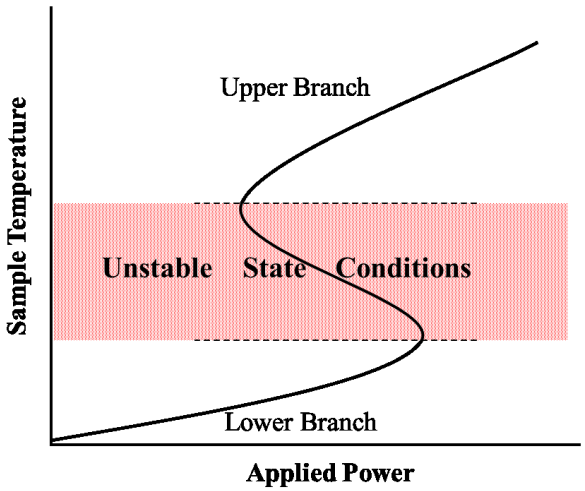


Figure 6-15 S- shaped model of thermal runaway as a function of power and temperature profile (Hill and Marchant, 1996)

The S-shaped form of the relationship between applied microwave power with sample temperature is a result of multi-valued changes in the dielectric response within the sample. The upper and lower branches of the curve are attributable to steady state conditions in which the energy losses from the sample and the energy input become equal and a steady temperature is formed. However, if a critical temperature is reached, a miniscule increase in power will result in the temperature of the sample entering a phase in which the dielectric of the sample changes significantly, jumping to the higher branch of the curve.

Conversely, if the temperature of the sample on the higher branch of the curve decreases to a critical point, a change in dielectric will arise and the thermal runaway of the sample will decline and so the temperature drops back to the lower branch of the curve. This is an important factor within this experimentation. The effect of the sample temperature being on the higher or lower branch of the curve determines the point at which PVC will begin its decomposition (Hill and Marchant, 1996).

Visual examination of the pattern of decomposition for 440W, 600W and 850W experiments (see Figure 6-16) clearly shows that decomposition initiates at a single point in the left side of the reactor flask, with the subsequent progression across the sample with increased microwave duration. This confirms the presence of a nodal point and hence a hot spot, resulting in thermal runaway within the microwave chamber at all microwave powers.

In Figure 6-16 the photographs were taken as individual samples of polyvinylchloride would be microwaved for a set duration. For instance 2 minutes for the first sample before minutes for the second sample 6 minutes for the third sample etc. After each microwave duration a photo would be taken of the sample and the resultant progression of sample decomposition was observed.

From further examination of Figure 6-16, it becomes apparent that the high heating rates demonstrated in Figure 6-14 with 600W power correlate to the high rate of progression of the decomposition reaction. The colouration of the sample to a dark brown/black (indicating the occurrence of de-hydrochlorination) occurs over a 6 minute period rather than 14 minutes that of 440W and 850W.

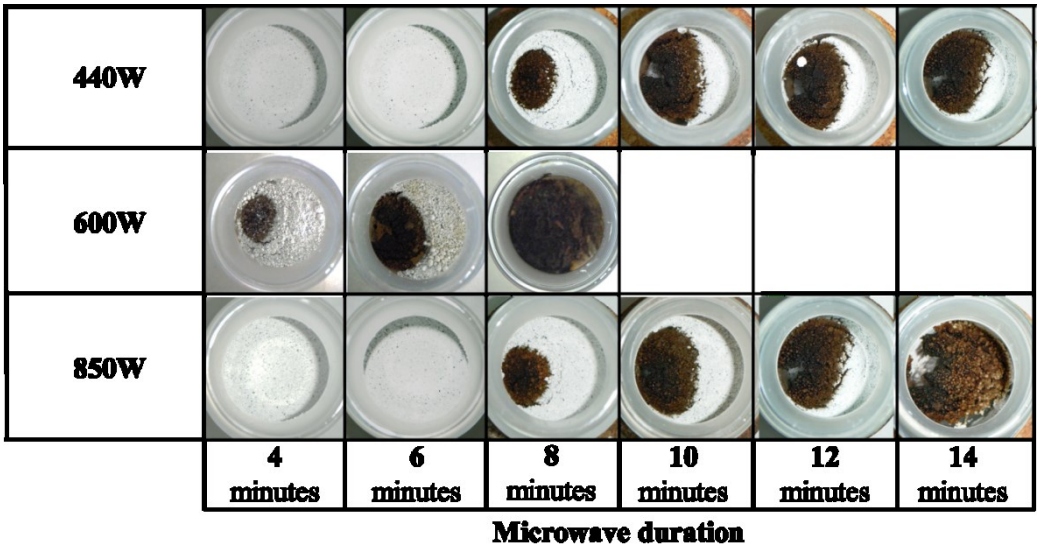


Figure 6-16 The progressive decomposition of 5g ± 0.01g of PVC when exposed to powers of 440W, 600W and 850W

Upon inspecting Figure 6-17 and Figure 6-19 A-C, it becomes apparent that decomposition takes place over 1 main peak with subsequent less pronounced decompositions thereafter. The first main peak has the greatest rate of decomposition; being 4.29 wt.%/min, 6.73 wt.%/min and 5.25 wt.%/min resulting in maximum temperatures of 248.27^{o}C (σ 2.29), 266.23^{o}C (σ 1.40), and 249.03^{o}C (σ 1.923) at 440W, 600W and 850W respectively. When the heating rates of this event are plotted against peak decomposition rates a clear relationship is observed (see Figure 6-19D). This is indicative of larger portions of the sample entering the stage of thermal runaway due to enhanced conversion of microwave energy to heat.

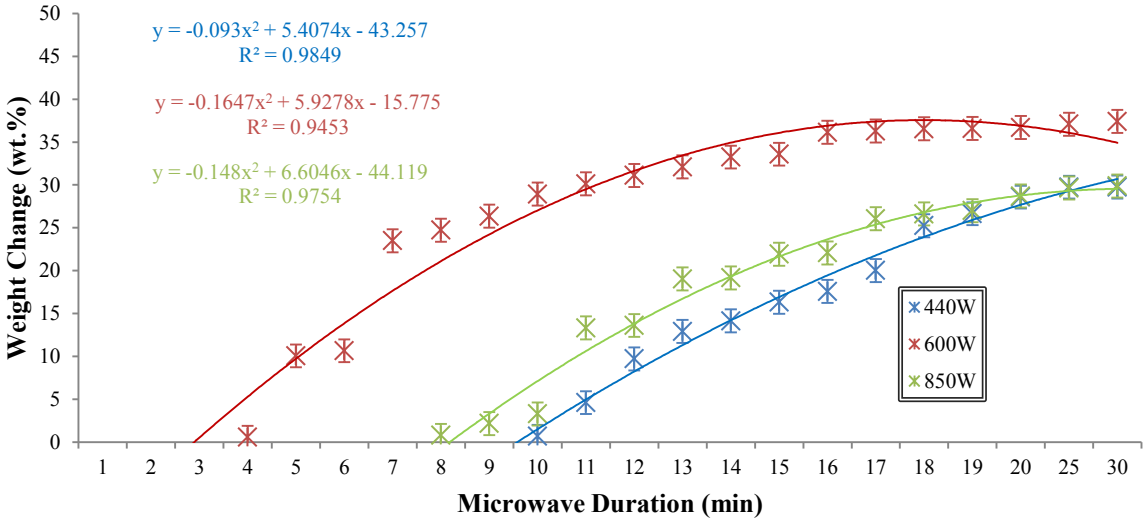


Figure 6-17 Percentage weight loss of 5g ± 0.01g of PVC on microwave irradiation over increasing duration

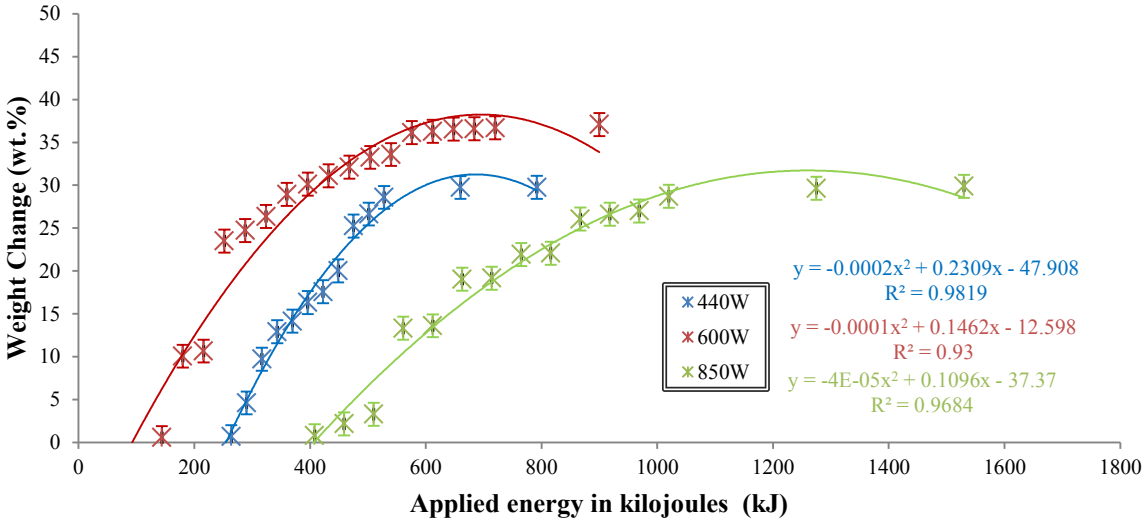


Figure 6-18 Percentage weight loss for 5g ± 0.01g of PVC vs. total applied energy in kilojoules

From Figure 6-18 the importance of the application of power in the decomposition process is demonstrated, with 600W applied power showing the greatest influence over the initial stages of decomposition until a sample loss of approximately 35wt.% has occurred. The same pattern is also observed for 440W applied power. Upon the application of 850W, the efficiency of energy conversion to mass loss declines significantly, with declining weight loss per unit energy applied and as a consequence substantially greater energy requirements to achieve the same levels of decomposition.

During the calculation of energy efficiency in PVCs' decomposition assumptions were made that the total energy input it into the system was absorbed by the sample and that the sample did not lose any

of this energy to the surrounding environment. This meant that the applied energy absorbed is representative of the energy required for this system to achieve the losses in mass and the specific power inputs. As such, the actual energy required per unit mass loss is less than the figures reported, however it is not possible to determine with any degree of accuracy the thermal losses from the reactor during the decomposition process or the power absorbed and/or lost to the microwave chamber.

It is also important to understand the proportions of chlorine lost from PVC when undergoing the microwave decomposition process, as it is reported by Moriwaki *et al.* (2006b) that this phase of decomposition consists solely of the de-hydrochlorination of PVC. To confirm the weight of chlorine released from polyvinylchloride during the microwave decomposition, 9 microwave runs were performed in which the off gas from the decomposition was passed through two dreschel bottles containing RO water. The hydrochloric acid gas readily dissolves into the water creating a solution which could then be titrated to determine the total loss of chlorine from the polymer. The titration was performed using 0.1 mol/l sodium hydroxide solution and a pH probe. When the titrated solution reached a pH of 7.00 the titration was complete. From this the mass of chlorine could be derived. The results of this are shown in table 6.5.

Table 6-5 Proportion of HCl in mass lost during the initial decomposition of PVC under the microwave powers of 440W, 600W and 850W

Microwave Power (W)	Microwave Duration (min)	PVC mass loss (g)	Mass of HCl as derived from titration (g)	Proportion of HCl of mass lost (%)
440	10	0.03	0.00	0.0
440	15	0.82	0.68	82.9
440	20	1.43	1.24	86.7
600	10	1.46	1.29	88.3
600	15	1.66	1.51	90.9
600	20	1.80	1.58	87.7
850	10	0.10	0.06	60.0
850	15	1.09	0.95	87.1
850	20	1.43	1.27	88.8

The results of this clearly show that the mass lost during the microwave decomposition of PVC at temperatures less than 260^{o}C largely does consist of HCl with on average 84.05wt.% of mass lost being this.

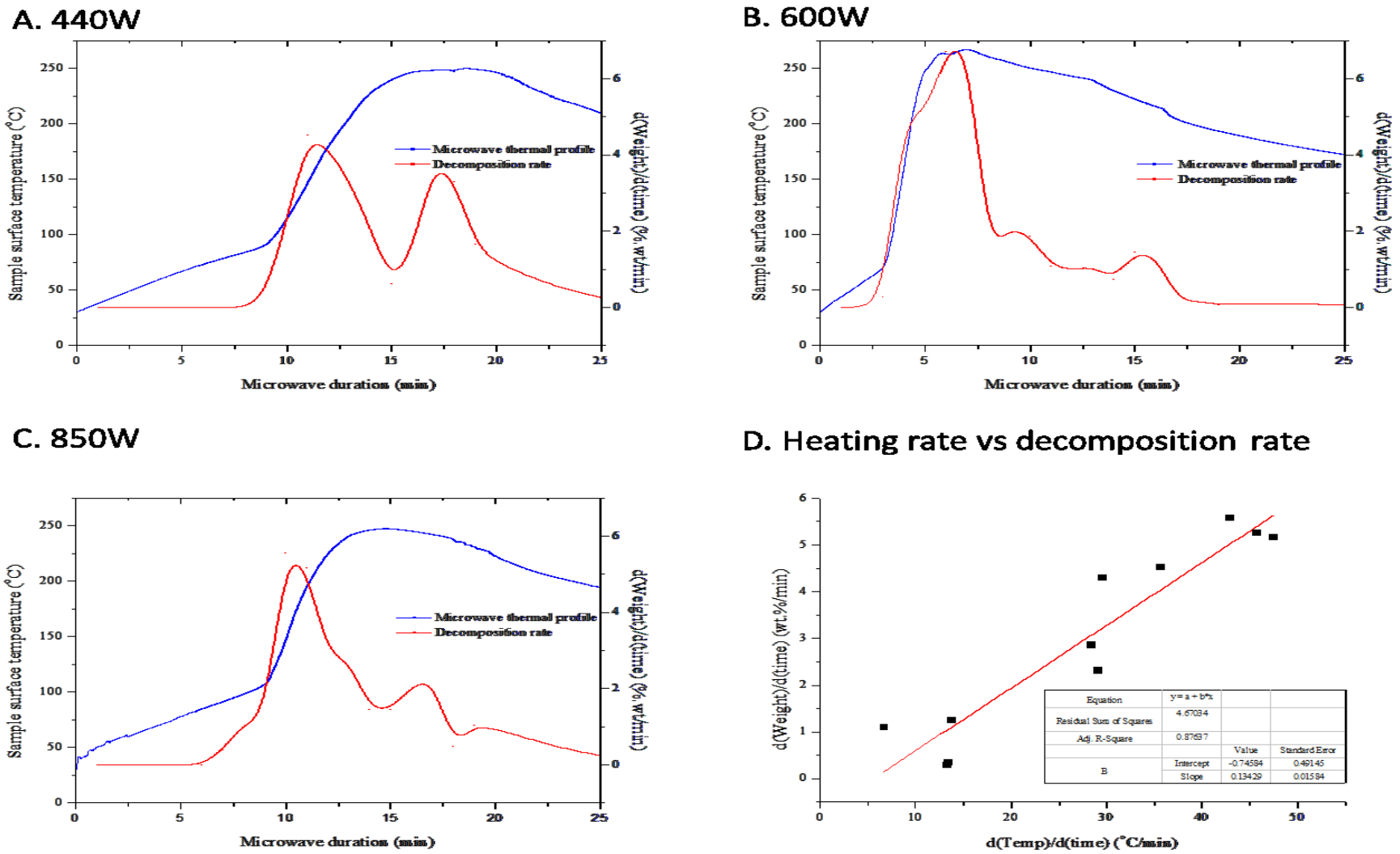


Figure 6-19 A-C: Microwave thermal profiles and decomposition rates of 5g ± 0.01g of PVC for (A.) 440W, (B.) 600W, and (C.) 850W. D: Heating rates as derived from the inflection from the first stage of heating to 200°C vs. decomposition rate from 5g ± 0.01g of PVC at powers of 440W, 600W and 850W

6.3.2.2 Power/Heating Anomalies

The non-linear behaviour temperature with increasing microwave power within the region of thermal runaway indicates that there is no simple relationship. The application of 600W power resulted in the greatest rate of heating, mass loss and hence shortest decomposition time (compared with 440W and 850W). This is rather counter-intuitive; the expectations would be that the heating rate of the sample would be proportional to the energy input on the system (more power = higher heating rate). This demonstrates a clear difference in the mode of absorption of microwave energy by PVC, compared to that of conventional thermal heating.

A similar result has also been observed in Figure 6-20, whereby Moriwaki *et al.* (2006a), exposed PVC to incident microwave powers ranging 218W to 551W. The lowest power (218W) demonstrating the greatest heating rate after the first stage ceased. This was not recognised by the authors and no theory/reason given for the result.

A similar result was observed by Moriwaki *et al.* (2006a), who exposed PVC to incident microwave powers ranging 218W to 551W (Figure 6-20). The lowest power (218W) demonstrating the greatest heating rate after the first stage ceased. This was not recognised or commented upon by the authors and no theory/reason given for the result.

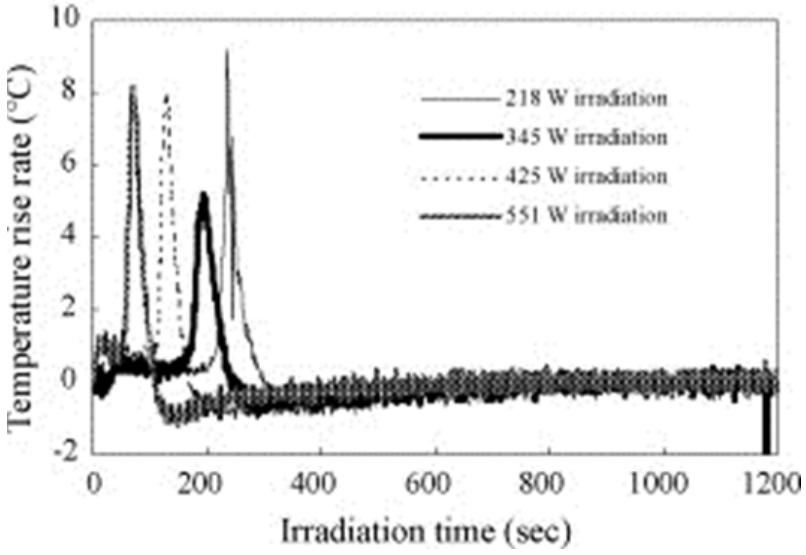


Figure 6-20 Heating rates of PVC samples of 1.25g ± 0.25g at differing microwave powers, from Moriwaki *et al.* (2006a)

The cause of this effect (thermal runaway) has been attributed to the formation of nodal points within the cavity, yet, this does not explain fully the observed pattern. The energy wave has not changed frequency, merely amplitude; hence a nodal point within the microwave chamber should occur at all powers (as was illustrated in Figure 6-16) subject to a proportion of the wave being absorbed with

each pass. This indicates that the non-linear heating effect seen is a function of the microwave power, ergo wave amplitude, which corresponds to changing wave phase angle.

One similar anomaly is observed in ferrite materials, known as "spin wave" excitation. This is the process by which electron spins show a propensity to align themselves as a result of exchange forces. A secondary function of this abnormality is that the aligned electrons demonstrate an increased susceptibility to move as a single unit when a signal field is applied (Suhl, 1956, Schlomann *et al.*, 1963, Tawansi *et al.*, 1998).

A number of organic polymers are known to exhibit magnetic properties resulting from the π-conjugated polymer backbone and R-side chain containing an unpaired electron; as illustrated in Figure 6-21. When PVC is undergoing microwave irradiation the likelihood that this electron spin wave excitation configuration will occur is high, due to the polymer backbone possessing π-conjugation and the high likelihood of vinyl radical formation.

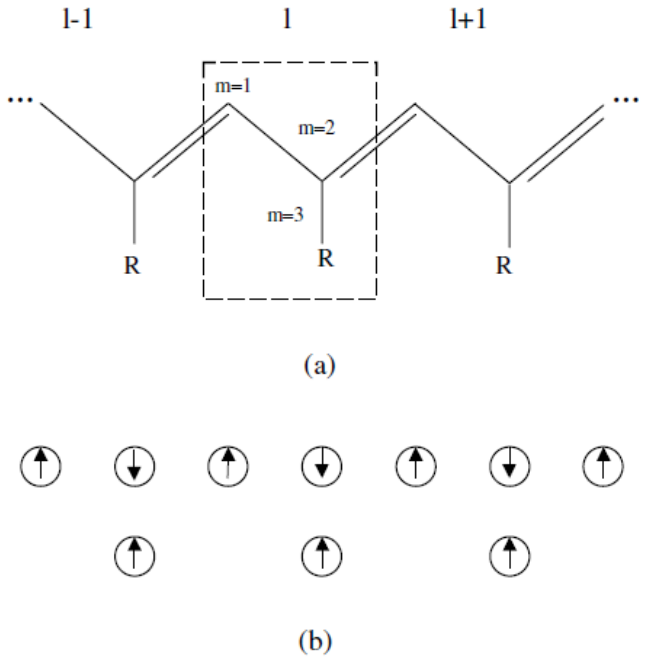


Figure 6-21 The (a) simplified structure of a one dimensional organic polymer ferromagnet and (b) arrangement of spin as illustrated by Zhao and Yao (2000)

This would contribute to the heating of the polymer because the power input exceeds the rate at which it can be lost through relaxation, hence we have the situation arising that the "spin wave" amplitudes increase beyond their thermal values (see Figure 6-22) (Schlomann *et al.*, 1960) causing additional heating. It is also observed that wave amplitude is a critical effect in this process, with amplitudes below or exceeding a threshold value resulting in decoupling of the "spin wave" (Kiselev *et al.*,

2003). As such, it is distinctly possible that wave amplitude might have a beneficial effect on the microwave heating process of certain polymers (i.e. as observed with 600W in Figure 6-19).

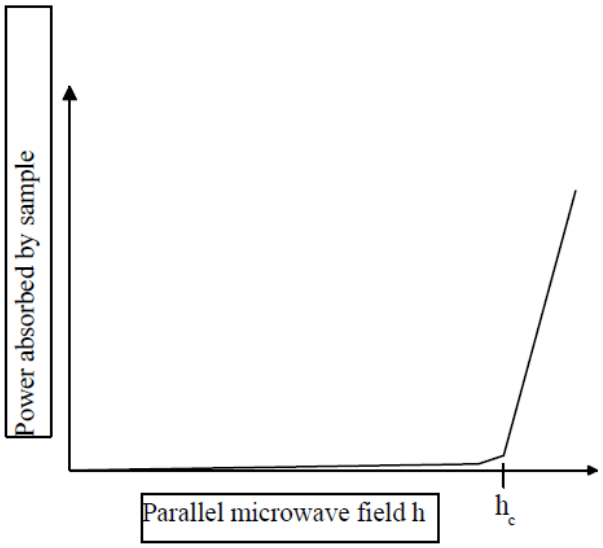


Figure 6-22 Microwave power absorption with respect to increasing microwave field strength showing critical threshold behaviour (h_c) (Sparks, 1965)

A further influence upon the microwave heating process is the Maxwell-Wagner effect. It relates to the interfacial boundary between two materials with differing dielectric properties (in this instance PVC and nitrogen gas), whereby charged particles are able to move in a delimited region; π-electrons in carbon materials (Zlotorzynski, 1995, Saad *et al.*, 1999). When the charge carriers are no longer able to move through the PVC matrix or couple to the changes of phase in the electric field, accumulation of charge will occur inthe non-conductive nitrogen filled voids. Subsequently the energy is dissipated at the material interface in the form of heat (Zlotorzynski, 1995, Steeman *et al.*, 1994, Saad *et al.*, 1999).

It has also been proposed by a number of authors that the storage of microwave energy might occur as vibrational energy of the molecule or by the alignment of molecules (Galema, 1997b, Strauss and Trainor, 1995, Marand *et al.*, 1992).

It is fair to conclude from these two factors alone that the interaction of microwaves with solid matter is a complex process. Further mechanisms which can also come into effect include: electronic polarisation, atomic polarisation, ionic conduction and dipole polarisation. Thus, without detailed modelling of the magnitude and influence of the parameters involved, it is not simply possible to

predict the exact reaction a sample might exhibit when placed in a microwave field. Hence, further investigation is required to verify the proposed heating mechanisms and thus validate this hypothesis.

6.3.3 Optimal Sample Mass

The effect of increased sample mass on the microwave heating/decomposition behaviour was investigated through performing experiments utilising 10g ± 0.01 and 15g ± 0.01 of PVC exposed to the same microwave experimental conditions as the 5g samples, the results of which are presented below.

Inspection of the heating profiles for the 10g samples (Figure 6-23) showed that all powers displayed similar heating profiles, otherwise not seen in 5g samples. Nevertheless the order in which each sample reached initial inflection was consistent with the previous results: 600W heated first, followed by 850 W and 440W.

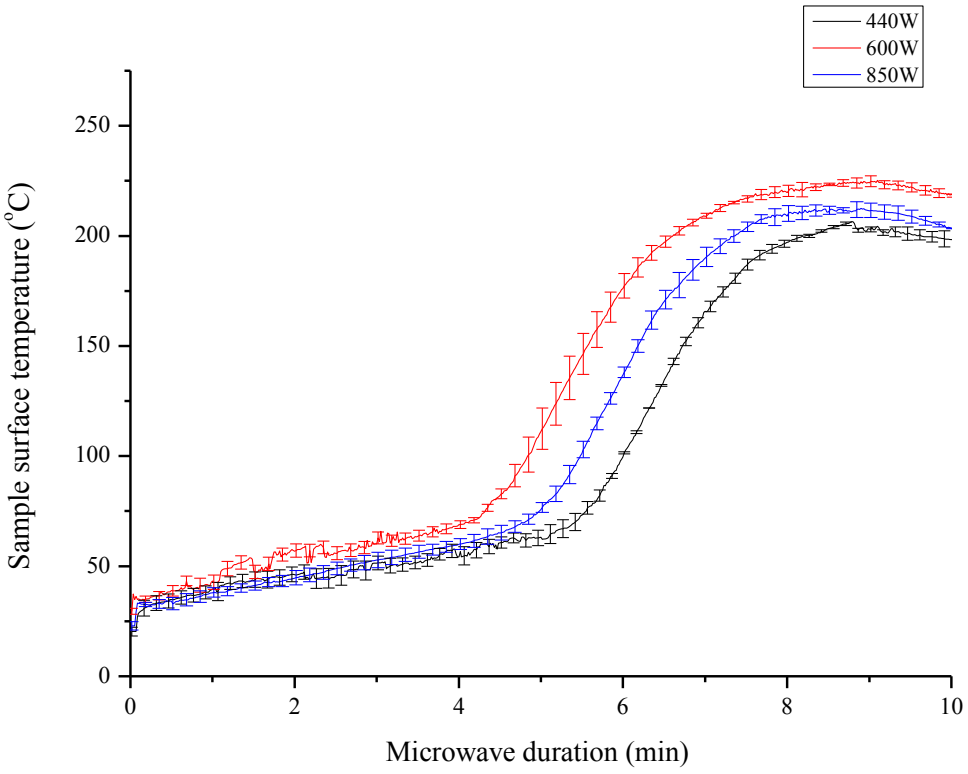


Figure 6-23 Temperature profile for 10g ± 0.01g of PVC exposed to microwave powers of 440W, 600W and 850W over 10 minutes

The temperature of the 1st inflection (corresponding to the dehydrochlorination reaction) was consistent across all samples, this being ~72°C with a delay in reaching this temperature of 38s between each profile. The temperature and durations required were significantly less than those seen

for 5g thermal profiles (see section 6.3.2). The reduction in 1st inflection point temperature posed an interesting dilemma. However, upon inspection of the progression of sample decomposition, this could be explained through the mode of microwave heating and the presence of inverted temperature profiles. These resulted in the true temperature of the sample being shielded from the IR detection by the cooler surface material. Similar observations were made by Pert *et al.* (2001). This clearly demonstrates the limitations of temperature measurement by IR pyrometer (please see section 3.3.2.1 for further discussion).

Nevertheless, as microwave duration increases, the thermal gradient across the sample decreases due to thermal conduction and the temperature at the surface becomes closer to that in the centre; as illustrated in Figure 6-24. The thermal gradient and hot spotting in the PVC during the microwave pyrolysis process was evident when each sample was investigated by gently exposing the core of sample using a spatula. During this process it was found that the de-hydrochlorination propagated from a central point, evidenced by the initial formation of a pea sized area of decomposed PVC. When samples were exposed to longer durations of microwaves it could be observed that the decomposed mass grew from this single point. This is consistent with the formation of a hot spot.

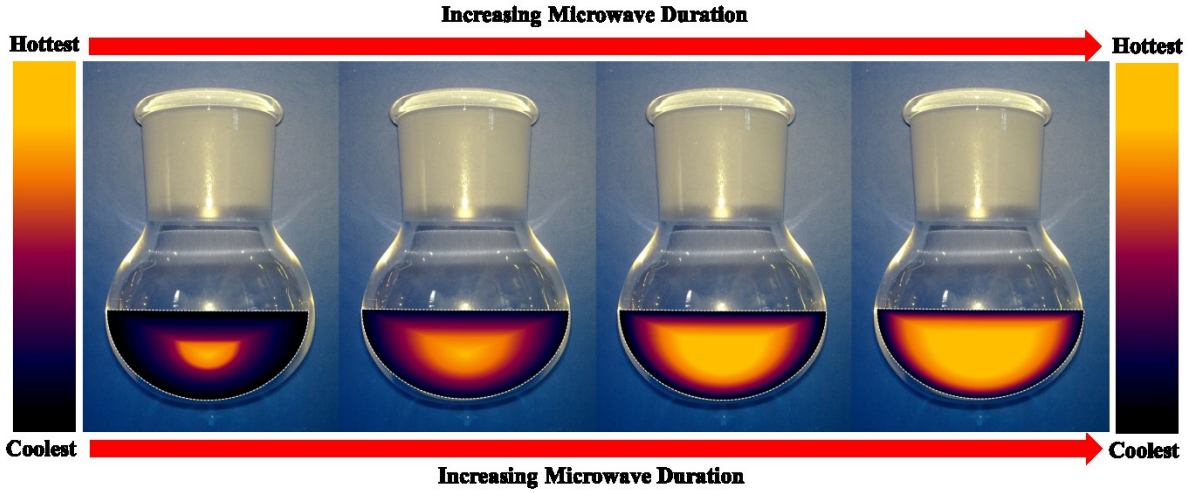


Figure 6-24 Decreasing thermal gradient across PVC sample with increased microwave duration

Upon reaching the first inflection, all samples were then heated to temperatures in excess of 200°C but demonstrated a marked decrease in overall temperature by approximately 40 ± 3°C, in comparison to those seen in the 5g experiments. Nevertheless, during the thermal runaway phase, average sample heating rates were seen to increase by approximately 20°C and 8°C over those for the 5g experiments with applied powers of 440W and 850W respectively. The increase in average heating rate over these

two powers also correlates to an increase in the extent and rate of sample decomposition (as shown in Figure 6-26).

.

This would suggest that with increased sample mass, the propagation of decomposition by the mechanism of thermal runaway is greater, most likely due to the lower proportion of thermal losses through conduction to the reactor wall and from the sample surface. This means that more of the sample reaches the critical temperature when tan δ increases sufficiently so that more microwave energy is absorbed for heating. Consequently, the PVC can then reach the upper branch of the s-shaped model of thermal runaway discussed previously and illustrated by Figure 6-15.

The temperature profiles of 15g samples (Figure 6-25) demonstrate the same profile as 5 and 10g experiments but with the distinct reduction in maximum temperature for powers of 440W and 600W.

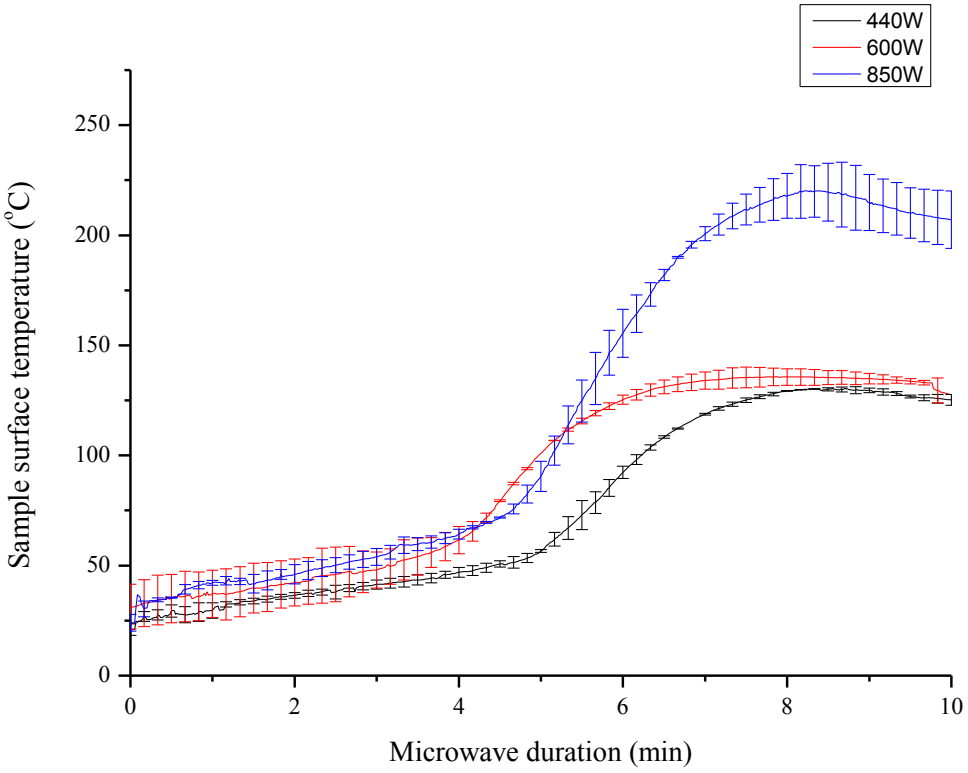


Figure 6-25 Temperature profile for 15g ± 0.01g of PVC exposed to microwave powers of 440W, 600W and 850W over 10 minutes

This is not consistent with the previous two sample masses and is probably indicative of one (or more) of three scenarios existing:

- The sample mass is absorbing more microwave energy so the energy available per gram of PVC in thermal runaway is insufficient to enable higher temperature to be achieved.

And/or

- The volume of sample is sufficient to cause thermal insulation of the interior and as a result of the low thermal conductivity of the PVC the overlying material does not enter thermal runaway with the bulk of the mass.

And/or

- The mass of sample is undergoing progressive thermal runaway as seen in Figure 6-16, resulting in the dissipation of energy converted to heat throughout the whole sample: being insufficient to elevate temperatures to those previously observed.

Further experimentation is required to prove which of these scenarios are occurring .

Nevertheless, in relation to the applied power, the order in which thermal runaway is entered is maintained with 600W showing the greatest propensity for initiation to occur. The reduction in the temperature and time of the 1st inflection is also observed for 15g experiments over that of 5g and 10g, providing evidence to support the hypothesis that the increased sample volume is sufficient to insulate the internal sample mass from conductive losses, enabling it to enter into the phase of thermal runaway at a much earlier point in the irradiation process.

Table 6-6 Summary heating rates and points of inflection as derived from 10g ± 0.01g thermal profiles (Figure 6-23)

	440W	600W	850W
Heating rate to 1st inflection (°C/min)	5.504	8.234	7.609
1st Inflection			
Duration (min)	5:28 (σ 0:13)	4:12 (σ 0:17)	4:52 (σ 0:06)
Temperature (°C)	72.13 (σ 2.828)	72.13 (σ 1.533)	71.26 (σ 2.263)
2nd Inflection			
Duration (min)	8:20 (σ 0:08)	7:25 (σ 0:11)	7:40 (σ 0:06)
Temperature (°C)	200.73 (σ 0.742)	215.73 (σ 0.577)	205.97 (σ 1.979)
Heating Rate from 1st to 2nd inflection (°C/min)	46.87	50.07	52.72
Maximum Temperature (°C)	206.4 (σ 0.848)	225.2 (σ 2.152)	212.5 (σ 3.406)

In conjunction with the pattern of peak decomposition recognised in Figure 6-19 and the reduction in the time required for all powers to reach the 2nd point of inflection (see Table 6-6 and Table 6-7) it is possible to conclude that the rate of decomposition is greatest for 600W experiments, closely followed by 850W and 440W. The relationship of microwave power, microwave duration and mass loss is shown in Figure 6-26. It becomes apparent that across all sample masses tested, 600W shows the greatest extent of decomposition, achieving a maximum of 37wt.%, 45.8 wt.% and 49.9 wt.% loss for 5g, 10g and 15g experiments respectively.

Table 6-7 Summary heating rates and points of inflection as derived from 15g ± 0.01g thermal profiles (Figure 6-25)

	440W	600W	850W
Heating rate to 1st inflection (°C/min)	5.376	5.536	7.112
1st Inflection			
Duration (min)	4:50 (σ 0:05)	3:59 (σ 0:22)	4:28 (σ 0:04)
Temperature (°C)	53.49 (σ 2.051)	60.65 (σ 4.450)	72.607 (σ 0.283)
2nd Inflection			
Duration (min)	7:11 (σ 0:04)	5:57 (σ 0:07)	7:13 (σ 0:12)
Temperature (°C)	130.654 (σ 0.778)	124.58 (σ 2.050)	204.54 (σ 4.738)
Heating Rate from 1st to 2nd inflection (°C/min)	34.95	40.44	60.96
Maximum Temperature (°C)	130.7 (σ 0.070)	135.9 (σ 3.606)	220.8 (σ 11.737)

The powers of 440W and 850W show equal extents of mass loss across all experimental masses with 29.7 wt.%, 43.8wt.% and 48.7wt% for 440W and 29.8 wt.%, 43.47 wt.% and 47.2 wt.% for 850W over 5g, 10g and 15g experiments respectively. This signifies that the decomposition is very much influenced by the incident wave amplitude, giving support to the hypotheses proposed in section 6.3.2.2. Nevertheless further work is required to confirm this. The results also demonstrate that greater levels of decomposition can be achieved with increased sample mass, with an absolute maximum of 49.9 wt.% lost on the scale examined in this study.

The pattern of decomposition presented in Figure 6-26 indicates that above a critical sample mass; the rate and extent of decomposition becomes uniform irrespective of power; so long as the sample is able to be heated beyond the critical temperature of 82°C, whereby the increase in tan δ is achieved and can be maintained on the upper branch of Figure 6-15.

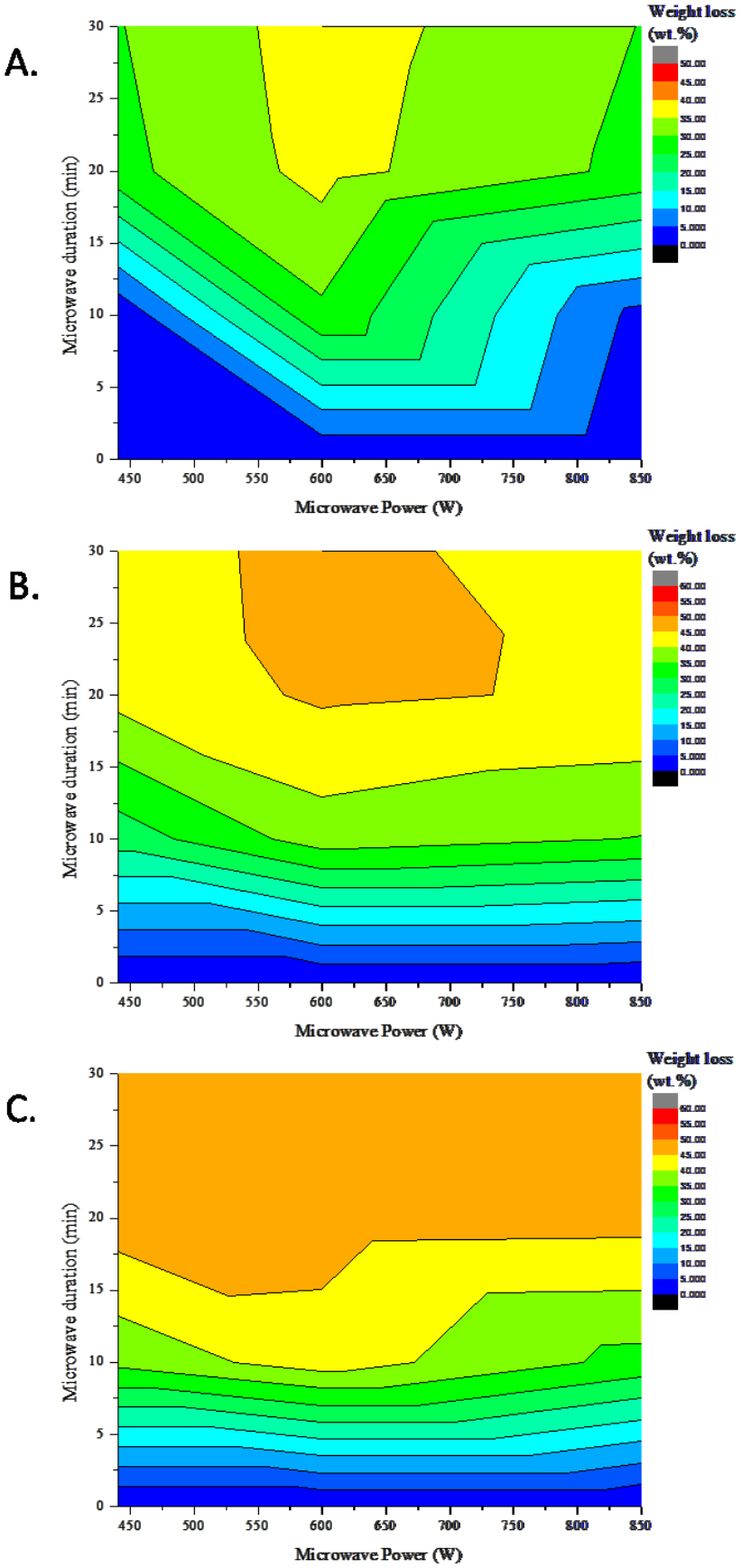


Figure 6-26 Percentage weight loss for samples of A.) 5g, B.) 10 g and C.) 15g of PVC when exposed to increasing microwave power and duration for microwave experiments as shown in Figure 4-1 (Trend given to aid the eye**)**

The energy required per gram of decomposed material is presented in Figure 6-27, Figure 6-28 and Figure 6-29. The results show that with increased sample mass, greater decomposition efficiency is achieved across all microwave powers. Nevertheless, the application of 600W power demonstrates the greatest decomposition extent and efficiency for the masses used, further supporting the mechanism of spin-wave heating proposed earlier.

However, at a sample weight of 10g the efficiency difference between 440W and 600W power application narrowed, with 600W demonstrating approximately 25kJ/g greater efficiency than 440W at 37.5 wt.% loss. This difference was seen to narrow further when a sample mass of 15g was utilised, with negligible differences observed in both the extent and efficiency of decomposition; peak

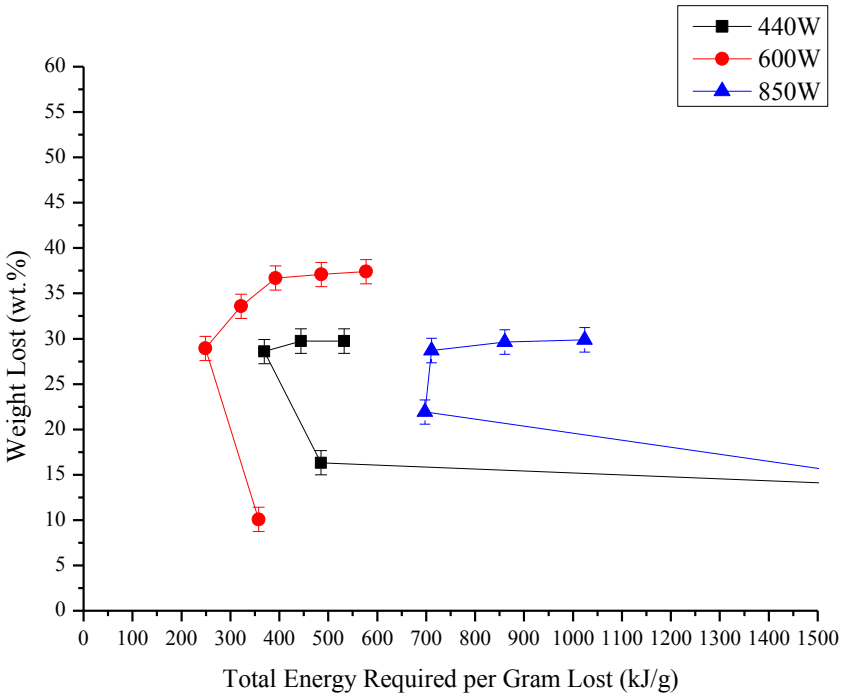


Figure 6-27 Total energy required per gram of weight lost vs. percentage weight loss for microwave experiments utilising 5g PVC at 440W, 600W and 850W

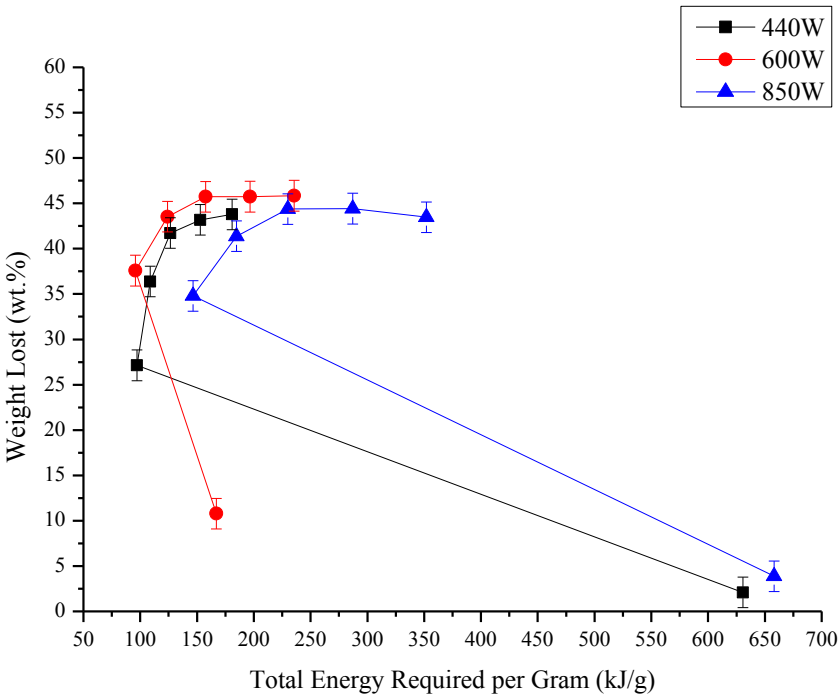


Figure 6-28 Total energy required per gram of weight lost vs. percentage weight loss for microwave experiments utilising 10g PVC at 440W, 600W and 850W

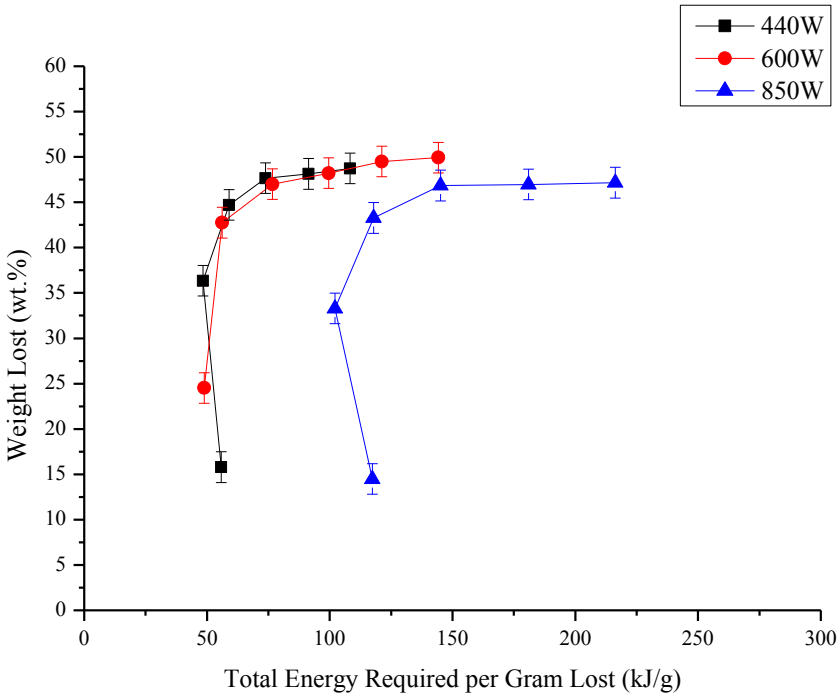


Figure 6-29 Total energy required per gram of weight lost vs. percentage weight loss for microwave experiments utilising 15g PVC at 440W, 600W and 850W

efficiency of approximately 48.5kJ/g was observed at 36 wt.% loss. This equates to 607.08 kJ/mol which in comparison to the ideal dehydrochlorination E_a of 124.0 – 276.4 kJ/mol (Jiménez *et al.*, 1993) equates to 2-6 times greater energy required.

As previously mentioned the energy balance does not take into account losses of microwave energy to the microwave chamber or from the reactor to the surrounding environment and carrier gas. As such, the energies calculated are a conservative measurement of the energy required to decompose the polyvinylchloride. Hence, in reality less energy will be required to decompose the sample. This has significant implications as it would indicate that the microwave process has a potentially high degree of efficiency.

At an applied power of 850W the efficiency of decomposition remained significantly less than the two lower power settings, but did however demonstrate the same pattern of increasing decomposition efficiency with greater samples weight.

To verify the pattern of results observed, a number of experiments were performed utilising the 'Milestone Rotosynth' microwave system. The Rotosynth microwave has a number of differences over that of the custom made stationary system. Key difference are: the utilisation of a mode stirrer to maintain an even field distribution throughout the microwave cavity; a rotating test tube shaped glass reactor; larger forced air cooled cavity. The Rotosynth system was modified so that a nitrogen purge and LN_2 condensing system could be fitted as in previous experimentation. It must be noted that due to the limitations of the temperature measurement system fitted to the device it was not possible to ascertain accurately the internal temperature of the reactor. PVC samples of 5g, 10g and 15g were systematically exposed to microwaves at 300 W intervals to 1200W and durations between 5 and 30 minutes at 5 minute intervals. The resultant patterns of decomposition and energy requirements were determined and are shown in Figure 6-30, Figure 6-31, Figure 6-32 and Figure 6-33.

Upon examining Figure 6-30 it is apparent that with increasing sample mass greater decomposition is achievable across the powers of 600W, 900W and 1200W. However, at 300W, less than 0.5wt.% decomposition is observed across all sample masses. For experiments utilising 5g samples it is apparent that less than 0.5wt.% decomposition is achievable between the powers of 300W-900W, with only 1200W demonstrating any decomposition after 10 minutes exposure, with a maximum of 37.01wt.% lost at 30 minutes. This shows significantly less decomposition than that achievable for 5g samples in the stationary system (as shown previously shown in Figure 6-26).

Increasing the sample mass to 10g showed that decomposition was achievable with a maximum of 35.6wt.%, 39.8wt.% and 48.0wt.% at 600W, 900W and 1200W respectively. When Figure 6-32 is examined in conjunction with Figure 6-30 (B), it becomes apparent that the energy required per %.wt lost between 15-35wt.% is significantly less at 600W than that of 900W and 1200W. At 34 ± 0.5 wt.% the energy required per gram lost merges at 323 ± 7 kJ/g for 600W and 1200W, with 900W requiring a further 100 ±7 kJ/g. This demonstrates the perpetuation of the anomaly observed at 600W in the microwave custom batch reactor, with the greatest efficiency for the transfer of energy from the microwave in conjunction with the greatest levels of decomposition.

Nevertheless, the Rotosynth microwave system shows lower levels of decomposition and energy efficiency than that of the microwave custom batch reactor for 10g samples, with it requiring approximately an additional 221 kJ/g at 600W and 35wt.% loss. It is most likely that this is as of a result of greater thermal losses from the reactor system (air-forced sample cooling) hindering the decomposition process. This hypothesis is supported by Moriwaki *et al.* (2006a), whereby he also observed that the maximum temperature achieved by a sample appeared to be a function of the applied power, energy absorbed by the sample and heat loss from the reactor, in the forms of conduction and convection.

When studying the sample weight of 15g, the maximum rate and extent of decomposition was observed (see Figure 6-34). The rate of decomposition was reflective of the rate of energy input, with 600W, 900W and 1200W showing peak decomposition rates of 3.01wt.%/min, 5.03wt.%/min and 6.57wt.%/min respectively and maximum decomposition of 46.6wt.%, 46.3wt.% and 53.6wt.% achieved for the respective powers of 600W, 900W and 1200W.

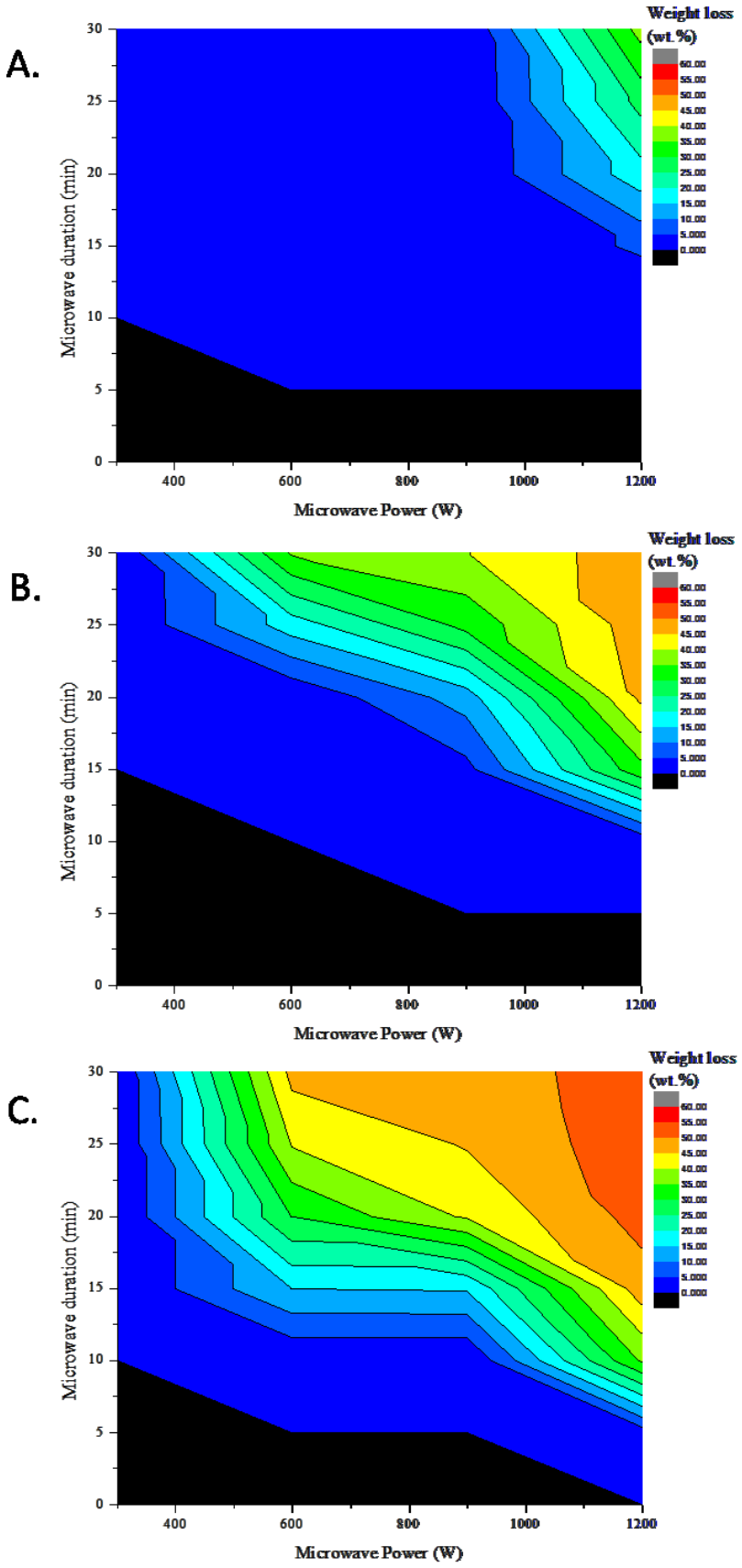


Figure 6-30 Percentage weight loss for samples of A.) 5g, B.) 10 g and C.) 15g of PVC when exposed to increasing microwave power and duration for microwave Milestone Rotosynth based experiments (Trend given to aid the eye**)**

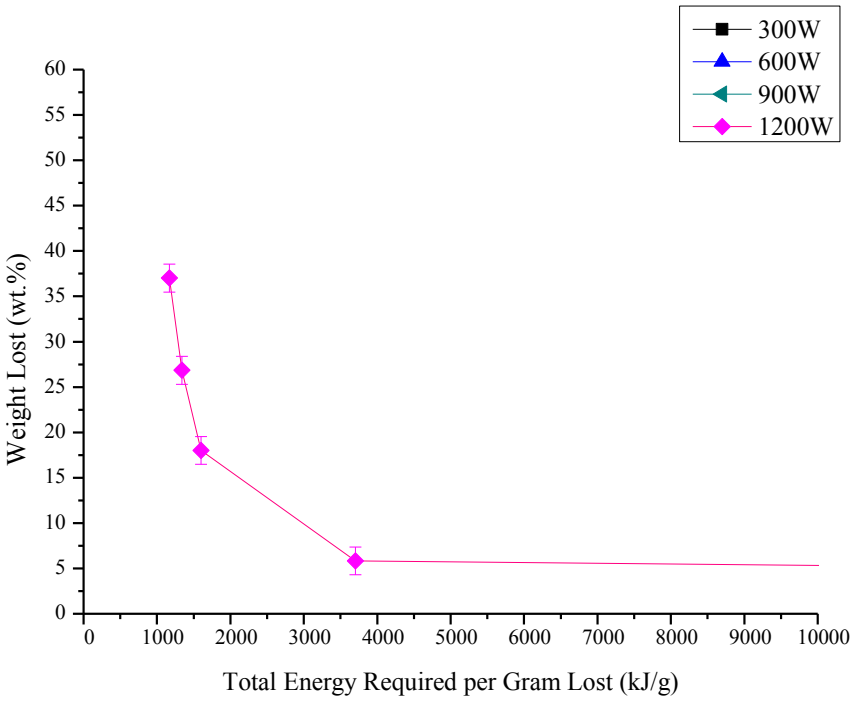


Figure 6-31 Total energy required per gram of weight lost vs. percentage weight loss for microwave experiments utilising 5g PVC at 300W 600W, 900W and 1200W for microwave Milestone Rotorsynth based experiments

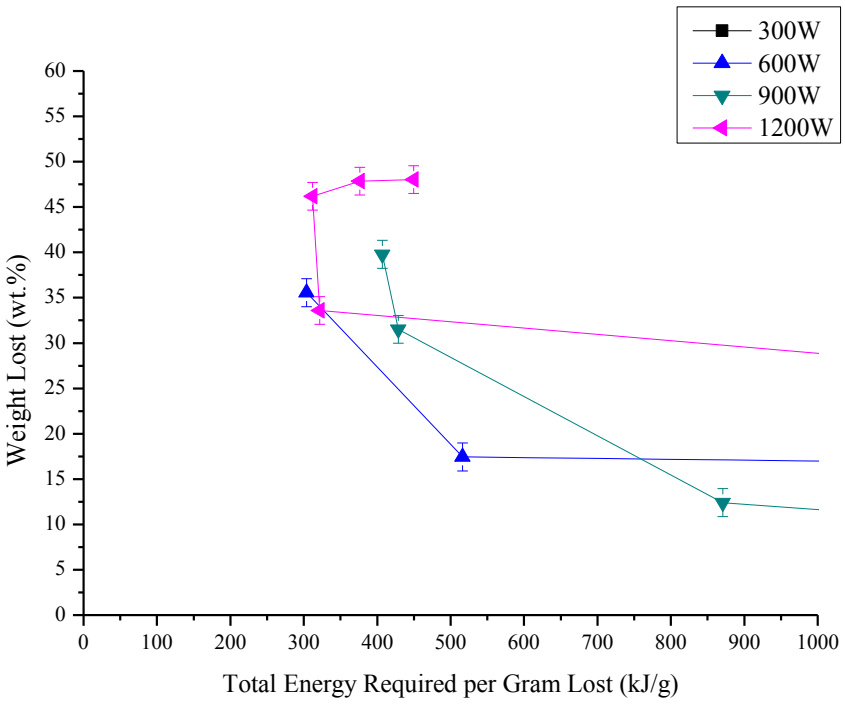


Figure 6-32 Total energy required per gram of weight lost vs. percentage weight loss for microwave experiments utilising 10g of PVC at 300W 600W, 900W and 1200W for microwave Milestone Rotorsynth based experiments

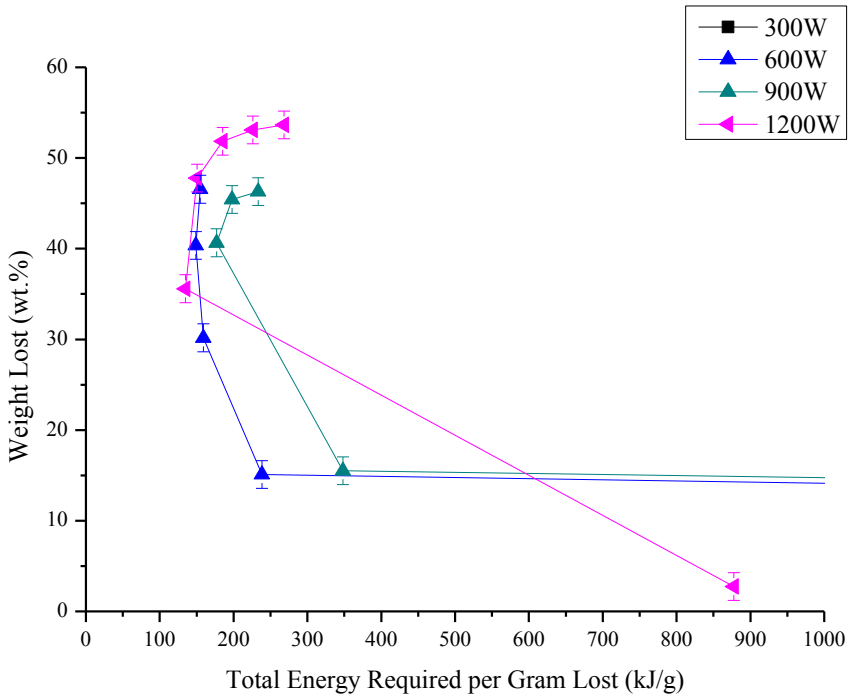


Figure 6-33 Total energy required per gram of weight lost vs. percentage weight loss for microwave experiments utilising 15g PVC at 300W 600W, 900W and 1200W for microwave Milestone Rotorsynth based experiments

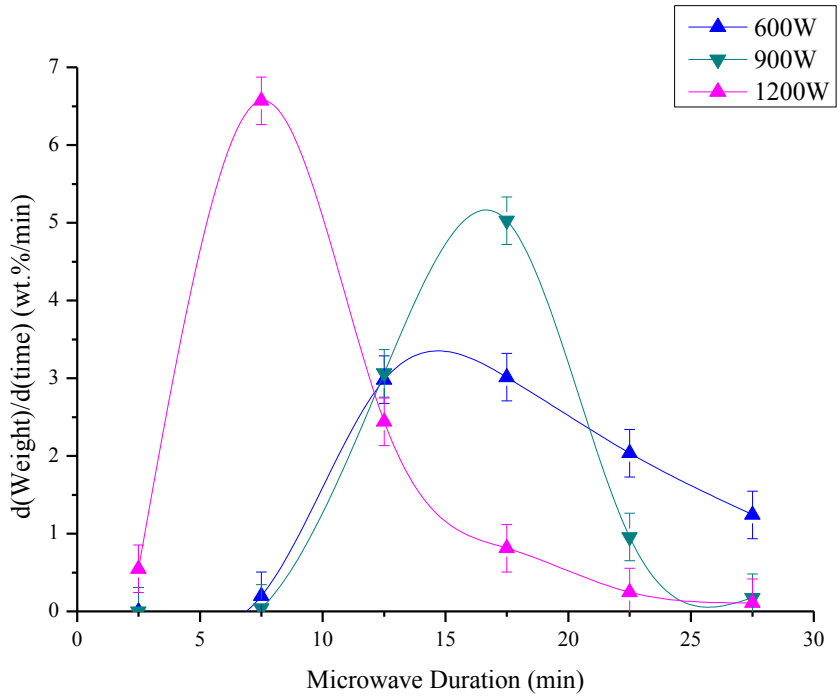


Figure 6-34 Decomposition rate for 15g samples exposed to 600W, 900W and 1200W utilising the Milestone Rotosynth microwave reactor system

The extent of decomposition observed was not reflective of the decomposition rate, with 600W demonstrating lower rates of decomposition over an extended period of time. compared with that of 900W and 1200W. This ultimately resulted in a greater extent of decomposition than that seen at 900W. It was also apparent that the decomposition process for 600W applied power had not ceased by the end of the test periods, whereas no further losses were observed for 900W and 1200W beyond 25 min duration.

From Figure 6-33 it can be seen that at 600W and 1200W, the Rotosynth achieved its highest energy efficiency for the decomposition of the PVC, when 145kJ/g electrical energy was consumed per gram of material decomposed. However, this is 97kJ/g higher than that of the microwave custom batch reactor . Nevertheless, the trend observed in the increasing extent of decomposition with greater sample mass is consistent with that seen in earlier experimentation. It is important to note that the enhanced extent of decomposition and energy efficiency noted for 600W applied power is repeated over the two microwave systems. This gives increased support to the hypothesis that optimal wave amplitudes exist in the coupling of PVC to microwaves at 2.45GHz and 600W applied power.

6.3.4 Decomposition Residue Analysis

During the initial microwave decomposition process, it was noted that an organic residue was collected in the liquid nitrogen condensers but this was not of a measurable quantity as it fell within the region of measurement error; masses less than 0.063g. Nevertheless, over repeated runs the residue was collected and analysed by GC/MS to determine the nature of the compounds formed during this stage; a representative chromatogram is presented in Figure 6-35.

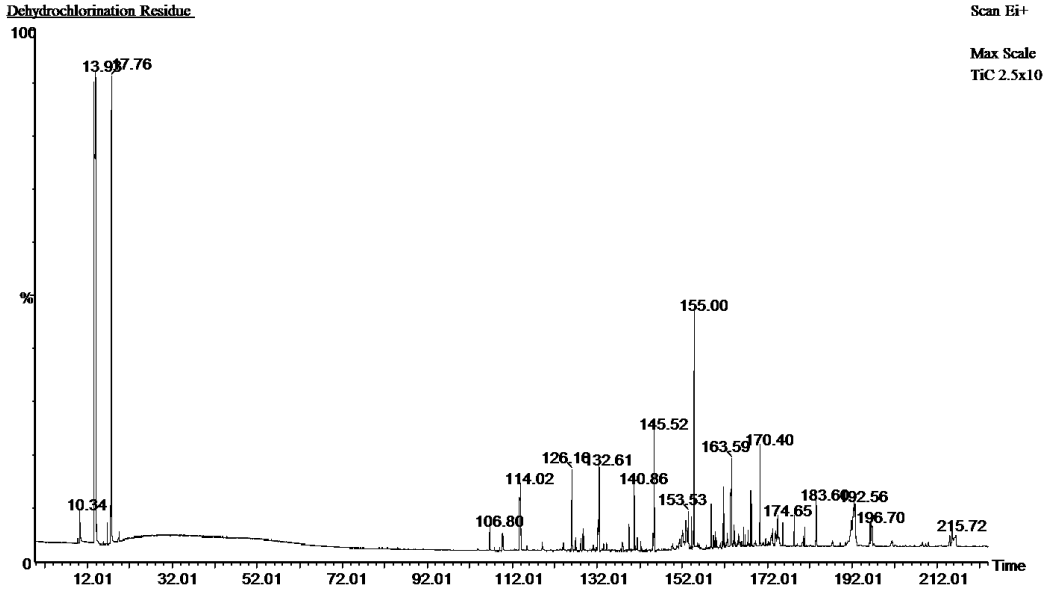


Figure 6-35 Liquid decomposition residue formed during the microwave decomposition of PVC analysed by GC/MS

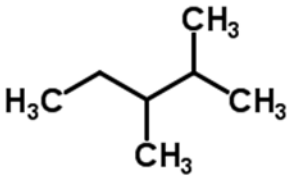
From the analysis it was found that the residue comprised primarily alkanes and alkenes. It also contained to a substantially lesser extent aromatic species; please see

Table 6-8 and Figure 6-37. These results demonstrate a significantly different composition to that observed during the thermal degradation of PVC at 200°C and 300°C, whereby aromatic and branched aromatic species made up the most significant proportion of the organic residue. The 10 most abundant compounds found in the residue (determined by %TiC) are shown in Figure 6-36, in which 46.05 %TiC was represented by three compounds: 2,3-Dimethyl-pentane(25.06%); Oxalic acid, octadecyl propyl ester (11.24%) and 1-Chloro-octadecane(9.75%).

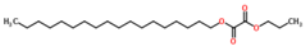
Table 6-8 Decomposition products formed during the exposure of PVC to microwave radiation

Retention Time (Cm)	Compound Name	Empirical Formula	%TiC	TiC/µl
16.68	2,2,3-Trimethyl-hexane	C_9H_{20}	0.53	7.60×10^7
17.76	2,3-Dimethyl-pentane	C_7H_{16}	25.06	3.62×10^9
109.78	(Z)-3-Tetradecene	$C_{14}H_{28}$	0.56	8.12×10^7
114.02	(Z)-5-Decen-1-ol	$C_{10}H_{20}O$	5.39	7.78×10^8
126.16	1-Chloro-dodecane	$C_{12}H_{25}Cl$	3.91	5.66×10^8
128.73	(Z)-6-Pentadecen-1-ol	$C_{15}H_{30}O$	0.74	1.07×10^8
128.95	6-Dodecenol	$C_{12}H_{24}O$	0.71	1.03×10^8
132.61	1-Chloro-tetradecane	$C_{14}H_{29}Cl$	5.08	7.33×10^8
139.54	Phenanthrene	$C_{14}H_{10}$	0.92	1.33×10^8
140.86	2-(Hexadecyloxy)-ethanol	$C_{18}H_{38}O_2$	1.92	2.77×10^8
141.43	(E)-5-Eicosene	$C_{20}H_{40}$	0.35	5.11×10^7
145.19	(E)-3-Octadecene	$C_{18}H_{36}$	0.93	1.34×10^8
145.52	1-Chloro-hexadecane	$C_{16}H_{33}Cl$	4.33	6.26×10^8
154.29	BIS(2-(2-Chloroethoxy)ethyl)ether	$C_8H_{16}O_3Cl_2$	1.16	1.68×10^8
154.62	Cyclohexadecane	$C_{16}H_{32}$	0.53	7.66×10^7
154.99	1-Chloro-octadecane	$C_{18}H_{37}$	9.75	1.41×10^9
158.87	(Z)-3-Hexadecene	$C_{16}H_{32}$	1.62	2.35×10^8
159.42	Eicosane	$C_{20}H_{42}$	0.27	3.99×10^7
159.92	Methyl-cyclodecane	$C_{11}H_{22}$	0.57	8.23×10^7
161.84	BIS(2-Methylpropyl) ester hexanedioic acid	$C_{14}H_{26}O_4$	1.29	1.87×10^8
162.73	Diisooctyl adipate	$C_{22}H_{42}O_4$	0.83	1.20×10^8
163.59	Pentanedioic acid, 2-methyl-, bis(1-methylpropyl) ester	$C_{14}H_{26}O_4$	2.11	3.05×10^8
166.45	11-Tricosene	$C_{23}H_{46}$	0.86	1.19×10^8
168.53	Adipic acid, di(oct-4-yl ester)	$C_{22}H_{42}O_4$	0.98	1.43×10^8
170.40	Decyl octyl adipate	$C_{24}H_{46}O_4$	3.19	4.61×10^8
173.38	Oxalic acid, pentadecyl propyl ester	$C_{20}H_{38}O_4$	3.82	5.53×10^8
174.65	Cyclohexanecarboxylic acid, pentadecyl ester	$C_{22}H_{42}O_4$	2.35	3.39×10^8
178.43	Cyclohexanecarboxylic acid, heptadecyl ester	$C_{24}H_{46}O_2$	3.04	4.39×10^8
180.86	Hexanedioic acid, dioctyl ester	$C_{22}H_{42}O_4$	0.64	9.25×10^7
183.60	Hexanedioic acid, mono(2-ethylhexyl)ester	$C_{14}H_{26}O_4$	5.31	7.68×10^8
192.56	Oxalic acid, octadecyl propyl ester	$C_{23}H_{44}O_4$	11.24	1.62×10^9

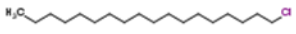
***Percentage TiC of organic compunds**
****TiCorganic compound per µl**



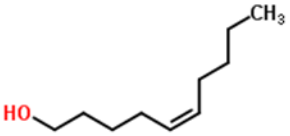
2,3-Dimethyl-pentane
(25.06%TiC)



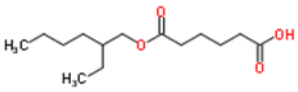
Oxalic acid, octadecyl p**ropyl** ester (11.24%TiC)



1-Chloro-octadecane
(9.75%TiC)



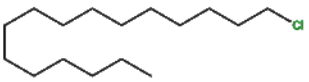
(Z)-5-Decen-1-ol
(5.39%TiC)



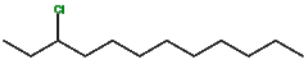
Hexanedioic acid, mono(2-ethylhexyl)ester (5.31%TiC)



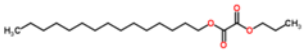
1-Chloro-tetradecane
(5.08%TiC)



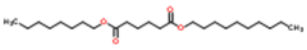
1-Chloro-hexadecane
(4.33%TiC)



1-Chloro-dodecane
(3.91%TiC)



Oxalic acid, pentadecyl **propyl ester (3.82%TiC)**



Decyl octyl adipate
(3.19%TiC)

Figure 6-36 Top ten compounds found in PVC decomposition residue by %TiC

The presence of these compounds has not been observed in the previous thermal degradation experiments reported in Section 6.2.2: Table 6-3 and Table 6-4 -, nor in the work of McNeill *et al.* (1995), Bockhorn *et al.* (1998), Starnes Jr (2002) and Marongiu *et al.* (2003).

The effects of increased residence time upon evolved products within the reactor system would most likely result in the prevalence of secondary reactions and subsequent char formation (Aznar *et al.*, 2006). This may account for the absence of lighter volatile aromatic species (see Table 6-8). In the Py-GC/MS performed, the products produced are able to escape the reaction conditions rapidly; hence lighter product distributions are seen in comparison to the microwave decomposition process.

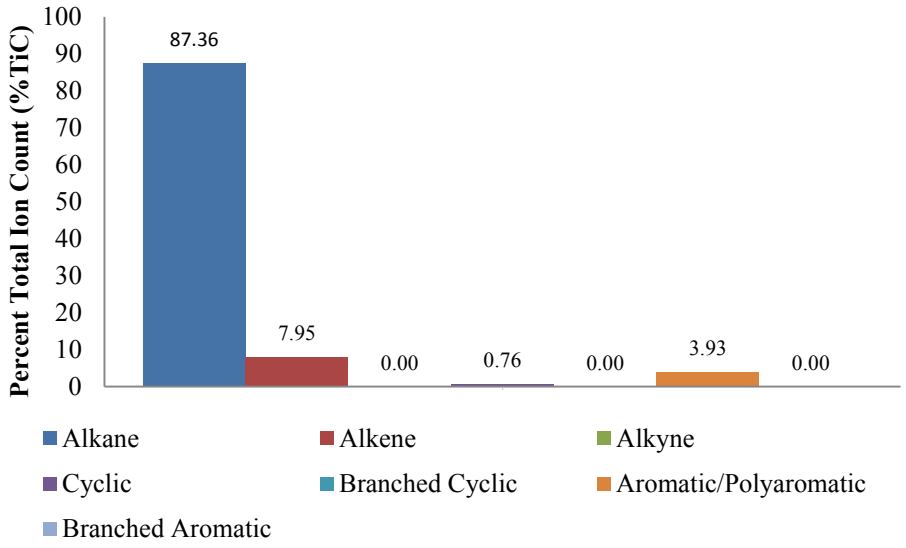


Figure 6-37 Cumulative speciated liquid decomposition products (by %TiC) from the microwave decomposition of PVC

The formation of alkanes and alkenes as alcohols, carboxylic acids, esters and adipates is considered to be indicative of features of the system under study.

Firstly, a significant presence of oxygen exists within the reactor system. This is most certainly attributable to the carboxylation of the original polymer as part of the stabilisation process during its manufacture. Secondly, the PVC is undergoing thermal decomposition (carbonisation/flash pyrolysis) with the elimination of heteroatoms, hydrogen and the de-alkylation of aromatic species via a free radical mechanism. These products subsequently react in their radical forms and the formation of the products observed occurs. This is similar to those mechanisms proposed in the pyrolysis of pitch by Lewis (1987).

It is also possible that this is an indication that the reaction pathway followed during the microwave decomposition of PVC is substantially different to that of the thermal process, with the possible suppression of the Diels Alder cyclisation pathway. However, no supporting evidence for this is seen in the work of Moriwaki *et al.* (2006b) and Ito *et al.* (2006) as the collection and characterisation of decomposition residue was not attempted by the authors.

6.3.5 Conclusions

During the microwave irradiation of PVC, knowledge the processes have been explored and knowledge of the mechanisms involved expanded and interpreted

It has been found that it is possible to induce heating of the polymer to in excess of 250^{o}C if a critical temperature of approximately 80^{o}C is achieved. At this point the dielectric properties of the material change; as previously observed by Ito *et al.* (2006) and Moriwaki *et al.* (2006a). During this period of heating the dehydrochlorination of PVC occurs. Nevertheless, this research undertaken has found significant trends which are otherwise yet unidentified, but indicate a spin wave interaction of the polymer and the microwave field.

It was noted that the heating of PVC is predictable, with a high degree of reproducibility in heating rates and extents of dehydrochlorination. However, the sample heating is not uniform, with the progressive heating and dehydrochlorination occurring from a hot spot within the sample, most likely formed due to a nodal point in the microwave field. Nevertheless, despite this the sample is found to follow the model of microwave heating as initially identified by Kriegsmann (1992) and presented as the S-shaped model of thermal runaway by Hill and Marchant (1996).

It was further identified that the proportion of sample entering in to thermal runaway dictated the rate at which the sample heated and the ensuing maxima in temperature and extent of decomposition. This process did not follow the expected pattern of increased power input resulting in accelerated heating, but rather that a correlation between wave amplitude/wave front angle at 600W, induced a greater response within PVC; not otherwise seen in other materials.

It was not possible to deduce the exact mechanism behind such an anomaly but it is conceivable that such mechanisms as organic spinwave interactions, Maxwell Wagner interfacial boundary effect or possible physical alignments of structures within the PVC resulted in the build-up of potential energy, similar to that of Wigner energy. Nevertheless, the anomaly was observed to persist across differing types of microwave equipment and over various sample loads implying that it was a real effect and not an artefact of the test equipment used for the majority of the experimentation.

It was also identified that increased sample mass resulted in greater extents of decomposition on the scale tested. Increasing levels of decomposition occurred as the surface area to volume ratio decreased and also the self-catalysing effect of HCl gas assisted in the dehydrochlorination mechanism.

At a critical mass of PVC, it was further found that the effects observed correlating to wave angle bore little relationship to the extent of dehydrochlorination but did give increased energy efficiency, with 600W applied power displaying the greatest efficiency in dehydrochlorination of PVC over all experiments.

During the microwave dehydrochlorination process it was also observed that organic compounds were produced consisting mainly of alkanes and alkenes, indicating the elimination of chain fragments or aromatic side groups produced during the charring of the polymer structure. This indicated a clear difference to that of a thermal decomposition process, as the distinct lack of aromatic and branched aromatic species implied the suppression of the Diels Alder reaction pathway, or that the crosslinking between polymer chains occurred to such an extent or rate as to hinder the escape of aromatic species. However, the presence of other organic residues indicated the earlier mechanism to occur.

It was also recognised during this phase of the investigation that the limitations of IR temperature measurement were such that an accurate representation of samples temperature within aliquots of more than 5g could not be ascertained.

Finally, it was found that during the microwave dehydrochlorination process it was possible to attain 95.85% removal of chlorine, with a residual 2.37wt.% found within the polymer residue of experiments performed for 15g sample masses at 1200W, equating to an energy required of 149kJ/g HCl removed.

6.4 Microwave Induced Pyrolysis

It was evident from the direct exposure of PVC to microwave radiation that the partial decomposition of the polymer backbone and dehydrochlorination is achievable(see Section 6.3). Nevertheless, a residual hydrocarbon mass equating to approximately 40wt.% of the original polymer remains, with potentially high chemical value locked within. Hence the next step was to investigate the mechanism of carbon assisted microwave pyrolysis.

6.4.1 Carbon Assisted Microwave Pyrolysis of PVC

Examination of the key parameters of microwave power, sample load and carbon absorbent were tested using the in house designed stationary phase microwave system. This was performed by using two methods. Examination of the key parameters of microwave power, sample load and carbon additive were tested using the in-house designed stationary phase microwave system. This was performed using two approaches, similar to those applied to ABS. The first used a fixed mass of PVC (5g) with various masses of carbon receptor being added: 0, 0.5, 1.0, 2.0 and 3.0 grams. The second method used a fixed reaction mass of 5 grams and the ratio of carbon to PVC adjusted from 20% to 80% w/w. For both of these methodologies the key parameter of microwave power was varied. The resultant yields of char, oil and gas were determined, with char/oil analysed by the methods outlined in Section 4.5 and 4.6. The results of the investigations are presented further in this chapter.

6.4.1.1 Thermal Profiles

The 5g samples of PVC with carbon receptor added, were exposed to microwave energy over a 30 minute period. Upon examination of the thermal profiles, it could be seen that they followed a specific pattern regardless of microwave power or carbon load. A typical profile is presented in Figure 6-38.

Initially the sample would undergo heating until approximately 70^{o}C was achieved, at which point it would display a thermal runaway event. The point at which this occurred was derived from the 1st inflection point. The sample would then heat rapidly to a maximum temperature before dropping-back and stabilising. From experimental observations it could be seen that the point at which the temperature fell and stabilised correlated to no further expulsion of visible gases from the reactor. The observed peak temperature behaviour was also seen by Cha *et al.* (1993) and later supported by Monsef-Mirzai *et al.* (1995), who theorised that the peak in temperature was a result of char becoming a better microwave receptor as de-volatilisation occurred at higher temperatures. Nevertheless, this would not account for the subsequent reduction in temperature.

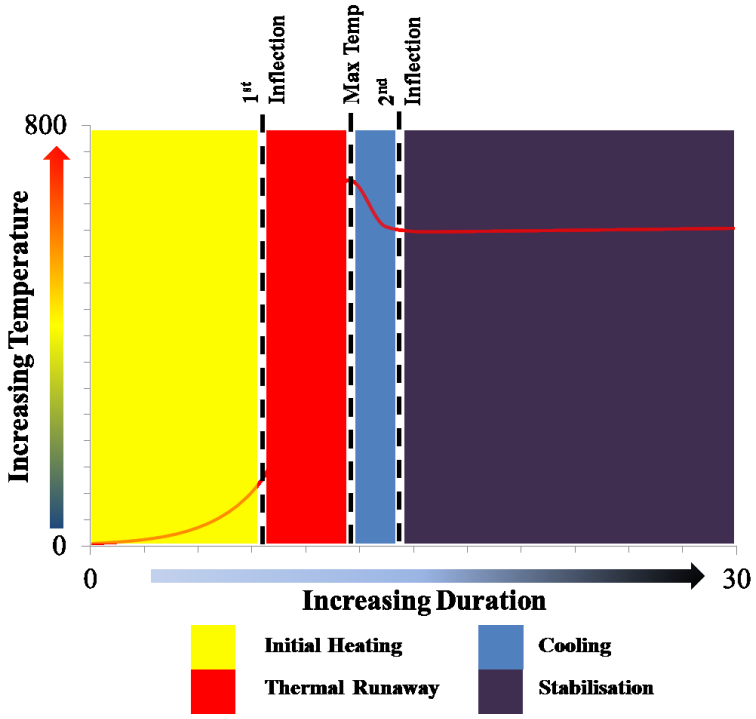


Figure 6-38 Simplified typical thermal profile of PVC during microwave induced pyrolysis run

The discrepancy between the stabilised and the maximum temperature was thought to be as a result of exothermic reactions occurring during the decomposition process, or as a consequence of dielectrically active decomposition products present within the reactor. These would most likely take the form of anions, cations, and free radical products. It could also be possible that the volatile products of pyrolysis naturally have a dipole moment. This theory is supported by Jesch and McLaughlin (1984), Gasner *et al.* (1986) and Bilali *et al.* (2005). The anomaly in peak temperature has also been observed in multiple recent works e.g. Zhao *et al.* (2010) and Zuo *et al.* (2011), but no recognition or explanation has been provided.

From the thermal profiles and the derived heating rates, it was established that intermediary times/temperatures would not be able to be investigated in experiments undertaken. This is because almost all the tests that achieved pyrolysis exhibited average heating rates from the 1st point of inflection to the maximum temperature which were in excess of 90°C/min (see Figure 6-39 and Figure 6-40). These rates of heating were such that accurately ceasing the reaction at a given temperature was virtually impossible.

6.4.1.2 Average Heating Rate

Upon examining the results from the studies using different carbon weights, applied power and heating rate (Figure 6-39 and Figure 6-40), it was apparent that the heating rate and carbon additive relationship was non-linear. Peak heating rates varied for each power applied with differing carbon loads. The greatest rates occurring for 0.5g at 600W and 2.0g at 850W.

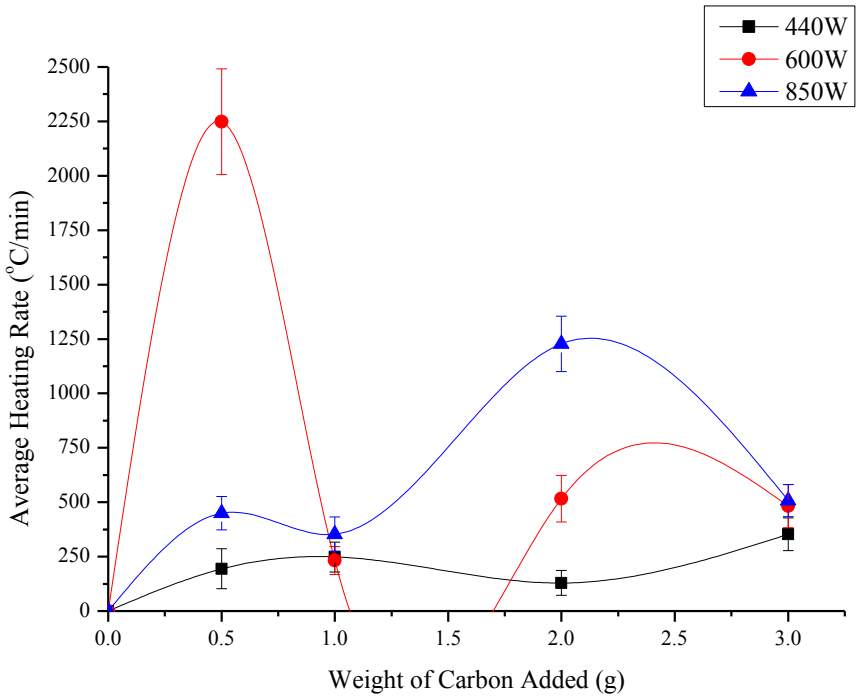


Figure 6-39 Average heating rates during the thermal runaway phase of PVC pyrolysis over the microwave powers of 440W, 600W and 850W for masses of carbon receptor from 0g to 3g

It was expected that the results would show with increasing mass of carbon, a Gaussian distribution of heating rates would result. This would be a consequence of a balance being struck between the weight of carbon in the system and its propensity to absorb microwaves (related to its di-electric loss factor), the weight of PVC to be heated and the rate at which energy was lost from the reactor (through product evaporation, radiation of heat energy into the cavity and by gas-flow cooling).

However, the results demonstrated a very different trend. These showed the development of a sinusoidal-like pattern for both the fixed and ratio carbon receptor results (see Figure 6-39 and Figure 6-40). This was demonstrated most clearly when each power level was examined from 440W to 600W with the progressive formation of greatly fluctuating heating rates shown in Figure 6-40. The pattern of fluctuation is similar in the ratio of carbon receptor results with the position of the troughs and peaks appearing at 40wt.% and 50wt.% respectively.

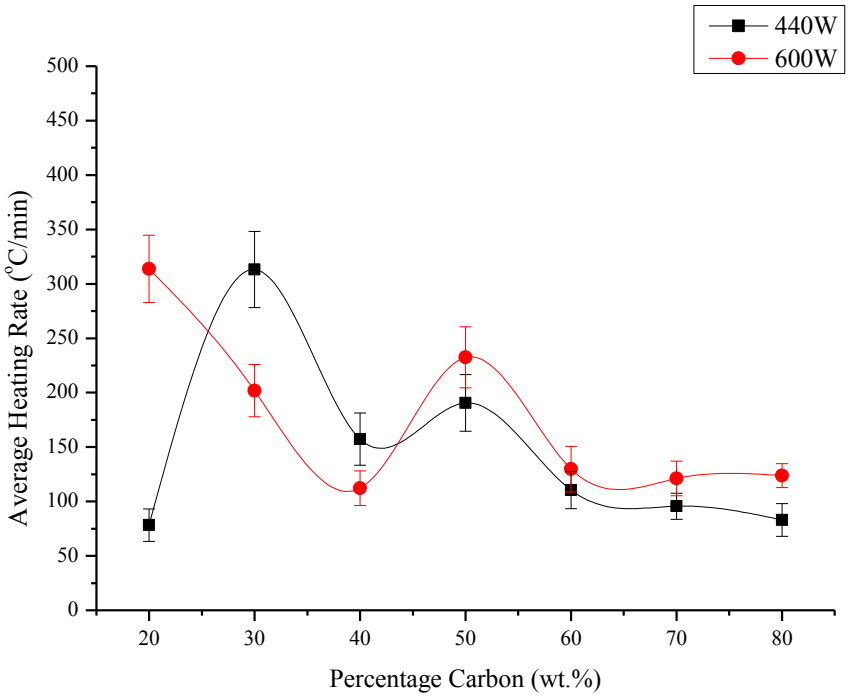


Figure 6-40 Average heating rates during the thermal runaway phase of PVC pyrolysis over the microwave powers of 440W and 600W for 20wt.% to 80wt.% carbon receptor of a total 5g mass

These results strongly suggest that microwaves do not interact with the carbon (microwave absorbent) or the PVC in a linear fashion. This is most probably due to changes in the di-electric properties of both the carbon and the plastic occurring during the decomposition stages. Despite the lack of linearity, there is a repeatability to the effects observed, suggesting that this heating result can be predicted.

Nevertheless, when Figure 6-39 and Figure 6-40 are analysed it appears that the two sets of experiments do not display any similarities in the average heating rate when the equivalent weight of microwave receptor is used; as clearly shown in Figure 6-41. The fixed-mass carbon experiments displayed significantly greater heating rates to the equivalent carbon receptor masses of 1.0g, 2.0g and 3.0g (20, 40 and 60wt.% respectively), for experiments utilising 600W power input and 2.0g and 3.0g of carbon receptor.

This difference cannot be easily explained for with few explanations possible, apart from that of the dispersion of carbon receptor is different for the equivalent carbon masses.

However, experiments cannot be designed to simulate this as they would require increasing the total mass contained within the reactor, introducing another variable into the investigation. This must be attributed to the nature of a microwave process, being sensitive to such variation in parameters.

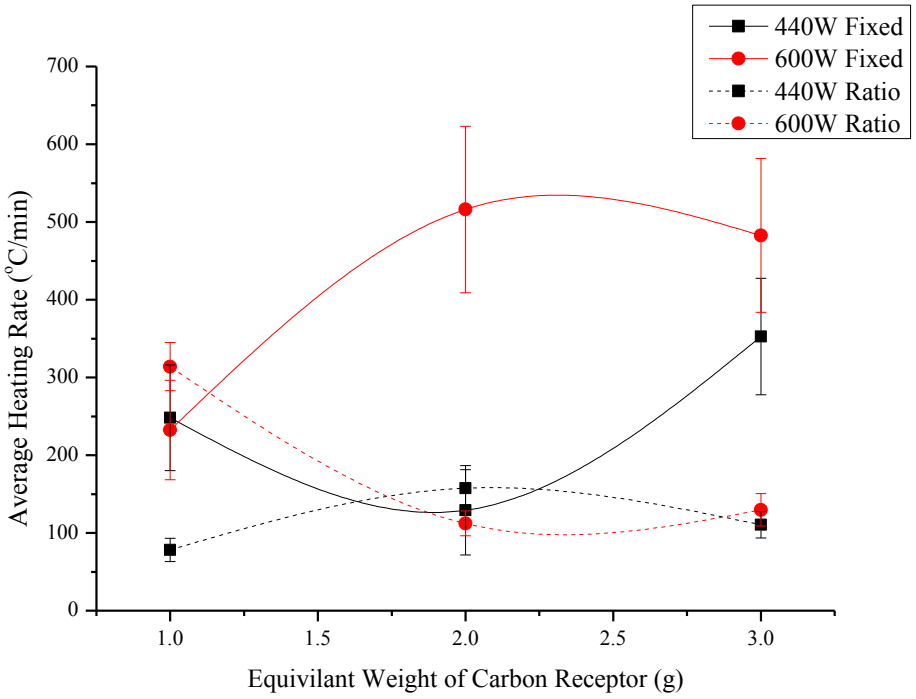


Figure 6-41 Comparison of equivalent carbon masses average heating rates for fixed and percentage ratio results.

The thermal profiles observed in the microwave study of PVC & carbon mixtures were distinctly different to those of pure carbon microwaved at the same powers (see Figure 5-16). This was most likely due to the influence of PVC decomposition on the thermal profile, with endothermic/exothermic reactions, thermal conduction mechanisms and the creation of microwave responsive species, determining the overall thermal profile seen. This was evident from Figure 5-15.

Hence, the average heating rate across the whole of the thermal runaway period was unlikely to reflect the complex nature of the competing processes occurring. Hence, it was decided that it was necessary to examine product yields and heating rates from differing regions of the thermal profile to better identify and understand the mechanisms undertaken.

6.4.1.3 Product Yields

The yields of char, oil and gas from the microwave decompositions undergone are shown in Figure 6-42 and Figure 6-43. From these results it is apparent that a microwave assisted decomposition process can result in significantly enhanced oil and gas yields, with approximately 72wt.% and 67wt.% respectively achievable under certain reaction conditions.

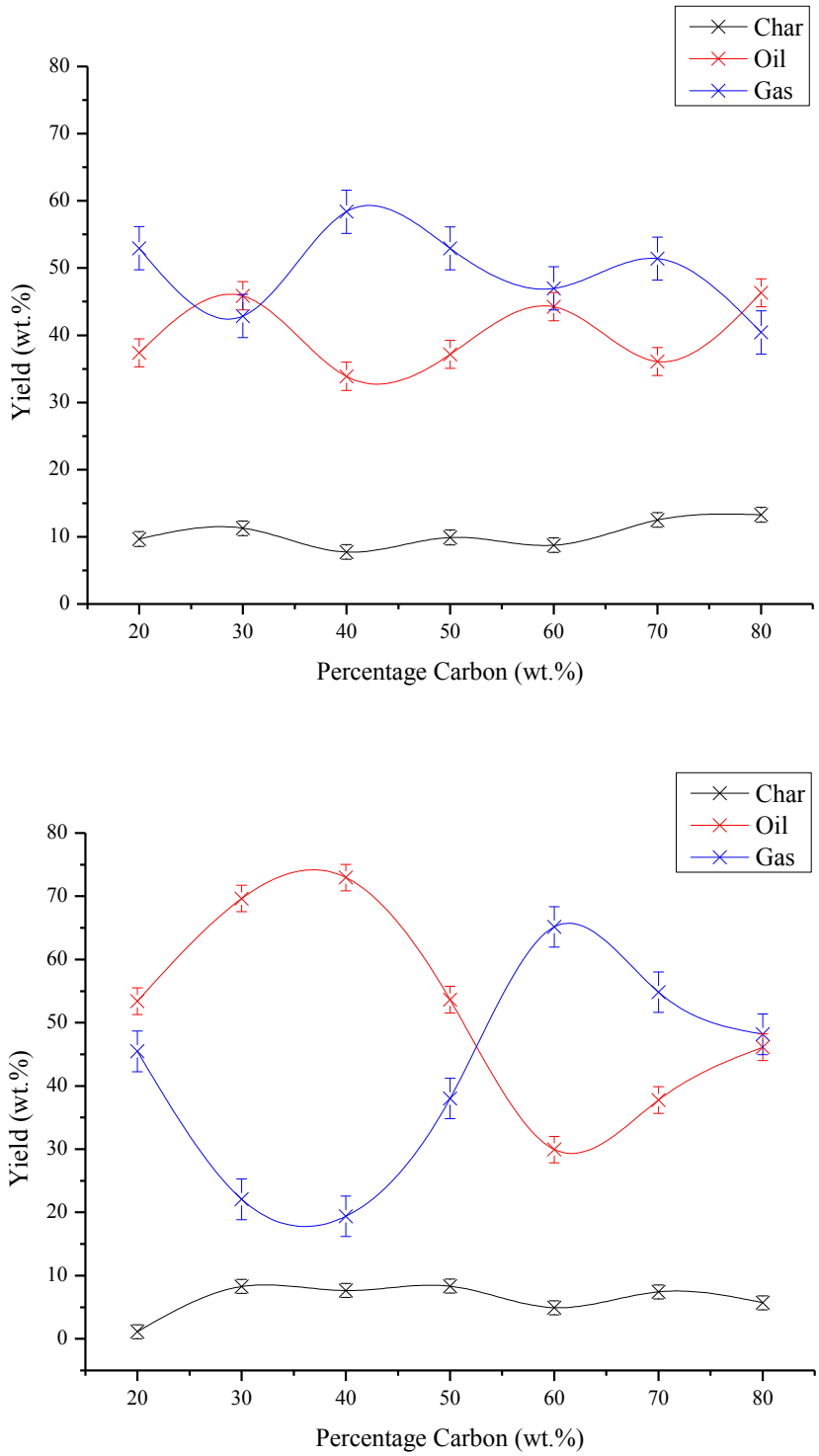


Figure 6-42 Char, oil and gas yields for pyrolysis over the microwave powers of 440W and 600W for 20wt.% to 80wt.% carbon receptor of a total 5g mass

The consequence of this effect is that significant reductions in char yields occur, especially in comparison to that of the conventional thermal pyrolysis process shown previously in Figure 6-3. This is most probably due to the increased temperatures occurring in the local environment around the additive carbon particles, resulting in flash-pyrolysis conditions occurring. Under flash-pyrolysis, the high heating rate and temperatures achieved will favour the formation of lower molecular weight molecules, which are less likely to carbonise, so greater levels of PVC decomposition will be observed and less char formed.

Nevertheless, across each power series no relationship between carbon weight and any component yield is immediately apparent. This is true in both ratio and fixed-mass experiments of carbon receptor.

It was necessary to examine these results in greater depth to try and determine possible relationships between the maximum temperatures and heating rates recorded during various phases of the thermal profile. Hence, the yields were compared with heating rates derived from the following phases of the thermal profile:

- 0 to 100, 0 to 200, 0 to 300, 0 to 400, 0 to 500, 0 to 600 and 0 to 700 degrees Celsius.
- 100 to 200, 200 to 300, 300 to 400, 400 to 500, 500 to 600 and 600 to 700 degrees Celsius
- 100 to 300, 100 to 400, 100 to 500, 100 to 600 and 100 to 700 degrees Celsius
- 200 to 400, 200 to 500, 200 to 600, 200 to 700 degrees Celsius
- 300 to 400, 300 to 500, 300 to 600, 300 to 700 degrees Celsius
- 400 to 600, 400 to 700 degrees Celsius
- 500 to 700 degrees Celsius

These results will be considered in the following sections (6.4.1.4 – 6.4.1.6)

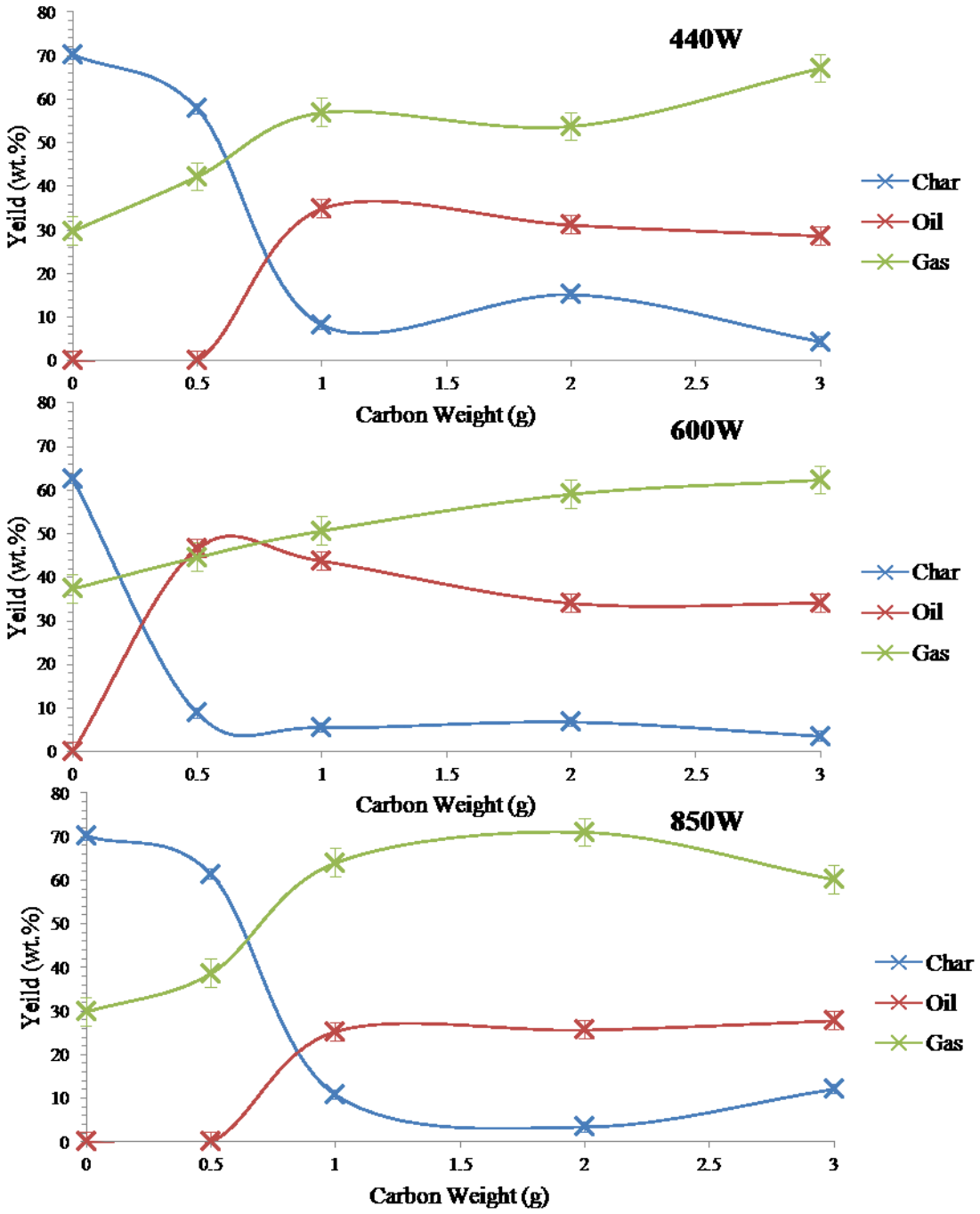


Figure 6-43 Char, oil and gas yields for 0g-3g carbon, PVC samples exposed to 440W, 600W and 850W

6.4.1.4 Char yield

The resulting char formed during the decomposition process demonstrated no clear correlation to the weight of carbon receptor added or any derived heating rates.

When char yield was plotted against gas yield, it could be observed that a relationship developed. It was apparent that during the dehydrochlorination phase a linear correlation existed, probably due to the fact that only char and gas were formed, removing the complication of extensive side reactions or formation of dielectrically responsive molecules.

Nevertheless, during the phase of decomposition above 400°C the continuation of the relationship prevailed (see Figure 6-44), with diminishing char with increasing gas yield. However, the results appeared power specific with the smallest char yield at 600W, followed by 440W and 850W, with diminishing yields with greater production of gas. This resulted in minimum char yields at 600W and 850W of approximately 3.50wt%. This is significantly less than those observed during thermal pyrolysis with a difference on average of approximately 7.00wt.%.

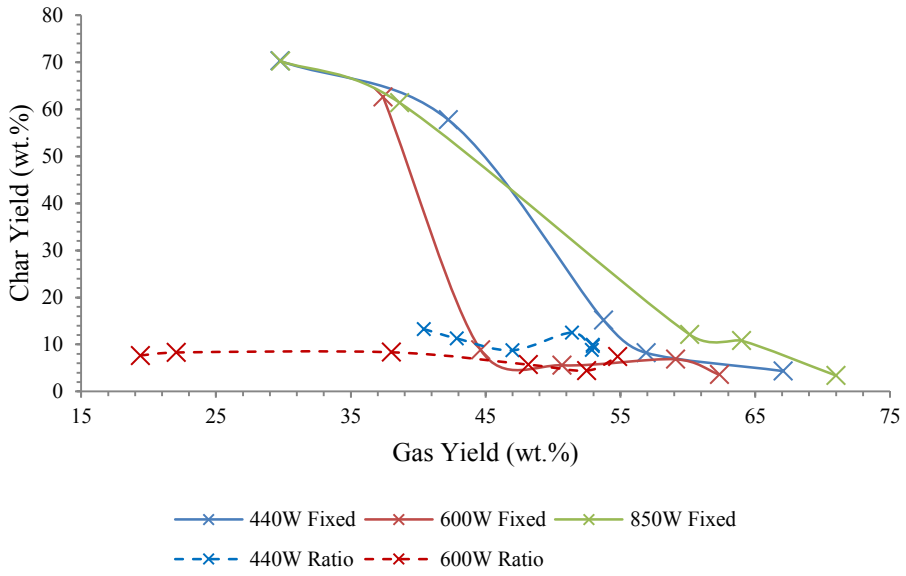


Figure 6-44 Gas yield vs char yield for both fixed carbon receptor masses and ratios, for 440W, 600W and 850W where applicable

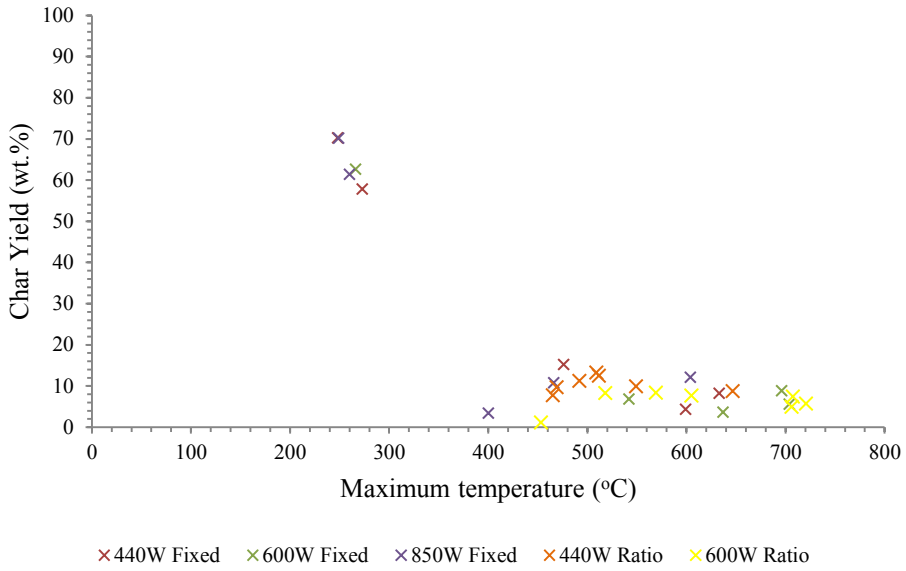


Figure 6-45 Char yield vs maximum temperature yield for both fixed carbon receptor weights and ratios, for 440W, 600W and 850W where applicable

This might be an indication that the decomposition mechanisms occurring during the microwave pyrolysis are different to those of a thermal pyrolysis process. However, this is not conclusive as comparable heating rates cannot be achieved in the thermal experiments undertaken, nor could be found in the literature.

From Figure 6-45 it is apparent that a trend exists between the maximum pyrolysis temperature and char yield during the dehydrochlorination phase upto 400°C, as previously indicated in Section 6.3.2. This does not persist at temperatures in excess of 400°C. Hence, it is reasonable to assume that the factor influencing gas yield is also most likely going to be that which effects char yield to the greatest extent.

6.4.1.5 Oil Yield

It can be seen from Figure 6-46 that oil yield is reflective of the maximum temperature achieved during each pyrolysis run. At temperatures less than approximately 400°C no oil is formed, which is in agreement with those results observed for thermal decomposition and shown in Figure 6-3.

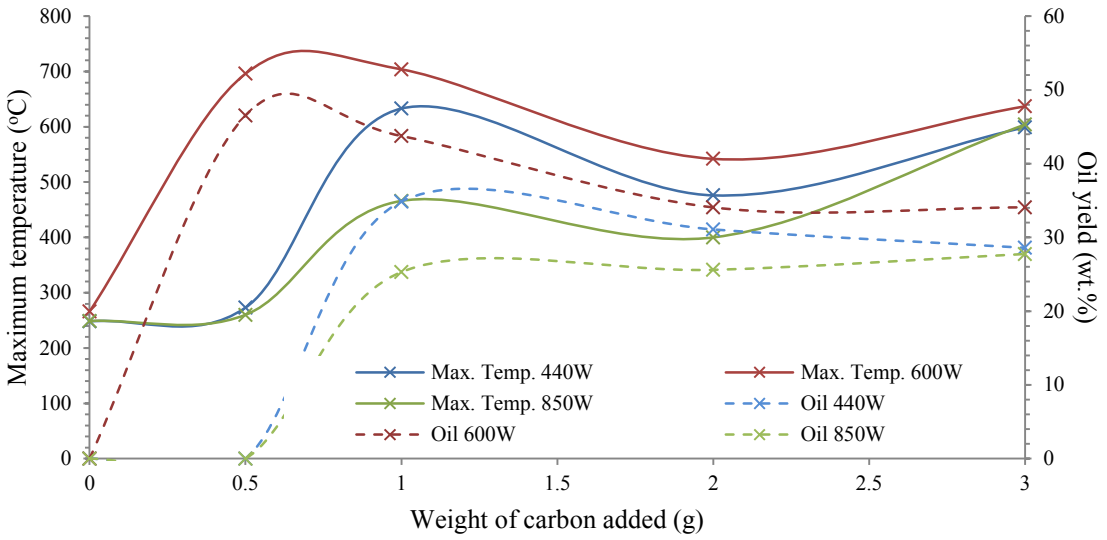


Figure 6-46 Oil yields and maximum achieved temperatures vs. weights of carbon between 0 to 3g carbon additive at 440W, 600W, and 850W.

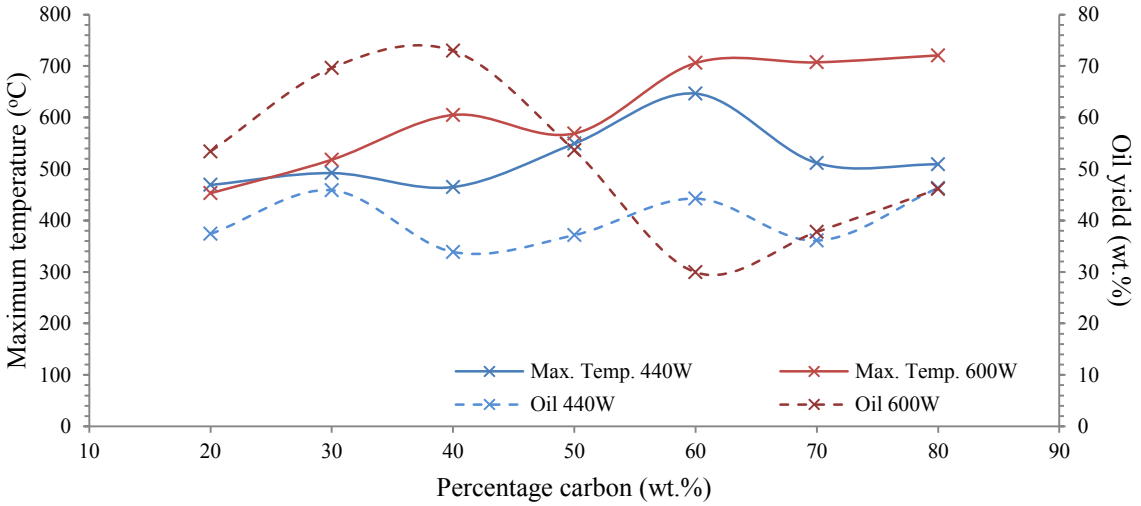


Figure 6-47 Oil yields and maximum achieved temperatures vs. percentage weights for pyrolysis over the microwave powers of 440W and 600W for 20wt.% to 80wt.% carbon receptor of a total 5g mass

The maximum temperatures achieved were achieved for experiments with differing carbon receptor weights at 600W applied power. This indicated that the interaction between PVC and the microwave amplitude (as discussed in Section 6.3.2.2) is persisting through the pyrolysis phase of the decomposition, aiding in the heating of the sample. This has been shown to be a specific effect of PVC decomposition, given that when carbon was microwaved alone at 600W, it did not display

preferential heating, rather following an incremental increase in temperature with microwave power (see Figure 5-16).

This relationship was largely reflected in the oil yield, with decreasing carbon content resulting in increased oil yields for fixed mass experiments at 440W and 600W (Figure 6-46). However, this was not seen for a microwave power of 850W, with oil yield showing no correlation with carbon mass. The breakdown in the relationship is also observed for experiments in which percentage weights of carbon are used (Figure 6-47), with oil yield purely reflecting the maximum temperature in 440W experiments and for 600W between 20wt.% and 40wt.% carbon receptor. The correlation between maximum achieved temperature and oil yield breaks down, with maximum temperatures greater than 700°C resulting in greatly diminished oil yields of approximately 30wt.% to 47wt.%. This reinforces the highly complex nature of the interaction between PVC, the carbon receptor and microwaves.

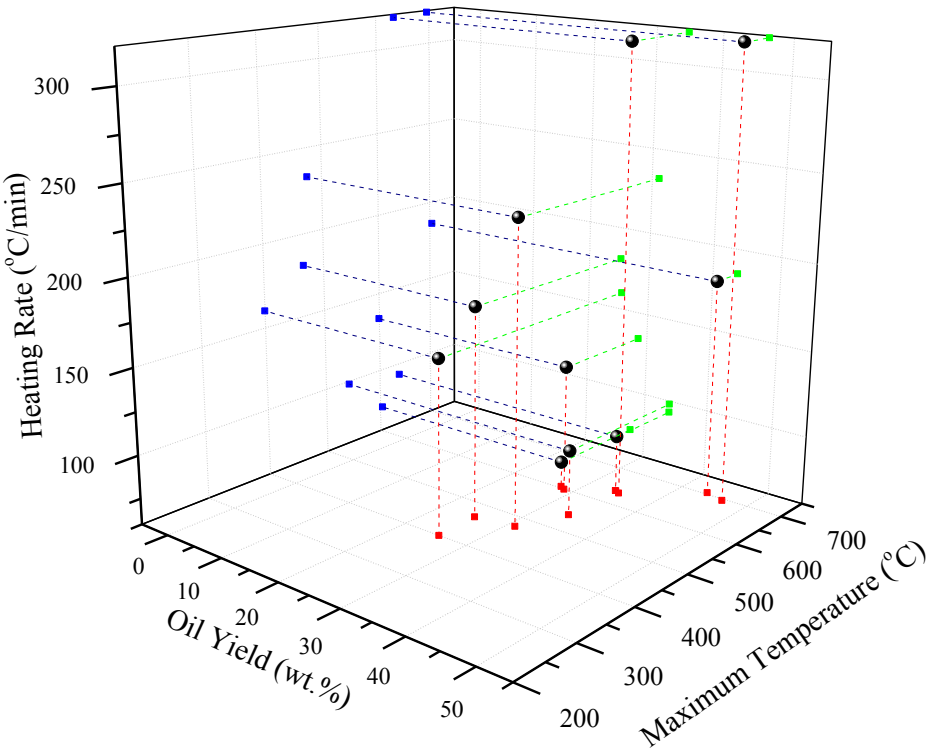


Figure 6-48 The relationship between oil yield, maximum temperature and heating rate from 390°C to 480°C for experiments utilising 0-3g carbon additive at 440W, 600W, and 850W (Red = Max. Temp. vs Oil Yield, Blue = Max. Temp. vs Heating Rate, Green = Oil Yield vs Heating Rate, Black = x,y,z co-ordinate)

From thermal decomposition work it was expected that oil yield would correlate to the heating rates over the fragmentation phase of PVC decomposition. This being temperatures between approximately 390°C and 480°C. The results of this are displayed in Figure 6-48. No such

relationship was observed, with neither heating rate vs. maximum temperature or oil yield vs. heating rate demonstrating correlation, with only a maximum temperature and oil yield showing a relationship.

Nevertheless, upon examining the results of maximum temperature, heating rate from 1st inflection to 250°C and oil yield (see Figure 6-49), the relationships and the processes underpinning oil production became apparent, with correlations appearing between oil yield, maximum temperature and heating rate.

The influence of temperature range and its control of oil yield is perplexing as it does not correspond to any given thermal degradation event, but rather lies within a range of temperatures over which PVC would normally undergo de-hydrochlorination and stabilisation to a polyene structure. This may be evidence of the differing mechanism of decomposition of PVC when undergoing microwave pyrolysis, suggested above. Alternatively, it may be an indication that the sample surface temperatures may be significantly cooler than internal temperatures. This temperature difference may be attributable to poor thermal conductivity from the centre of the sample to the outside (causing a thermal gradient) or a result of conductive cooling to the carrier gas flowing over the sample exterior surface. Nevertheless, irrespective of these effects and observations and based upon the data shown in Figure 6-49, it is fair to conclude that in order to achieve higher temperatures, lower heating rates are required. This is most clearly shown where samples achieved 700°C and a heating rate of approximately 50°C/min is required. This suggests that higher heating rates cause the fragmentation of the polymer structure and short chain hydrocarbons to be produced, following the accepted trend of increased heating rate favouring low molecular weight molecules and gas formation (Ahmed and Gupta, 2009).

These volatilised compounds are formed at a sufficiently high a rate that they are expelled from the reactor before secondary reactions can occur, preventing the formation of heavier molecules via the processes of free radical condensation (Encinar and González, 2008). At lower heating rates, fragmentation of the residual char occurs and radical species are able to form in sufficient densities and for long-enough residence times that secondary reactions can occur favouring the production of oil (Wang *et al.*, 2007).

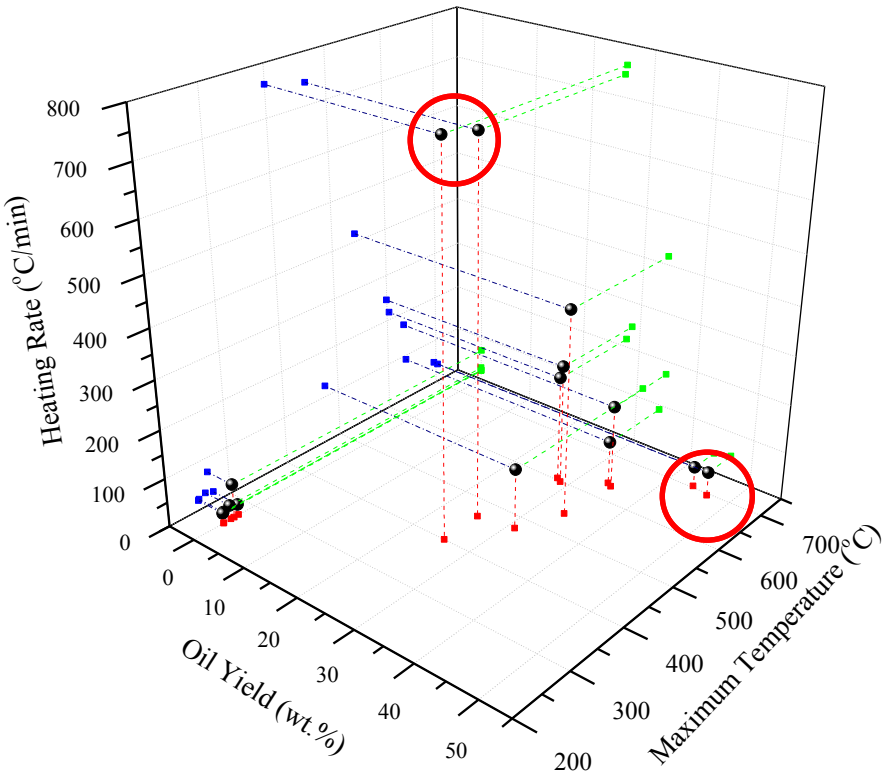


Figure 6-49 The relationship between oil yield, maximum temperature and heating rate from 1st inflection to 250°Cfor experiments utilising 0-3g carbon additive at 440W, 600W, and 850W (Red = Max. Temp. vs Oil Yield, Blue = Max. Temp. vs Heating Rate, Green = Oil Yield vs Heating Rate, Black = x,y,z co-ordinate)

During this process it is also likely that the free radical species will interact with the microwave field and subsequent molecular motions might be induced, enhancing heating effects. This motion/heating might induce certain reaction pathways to be favoured (Kubrakova, 2002); hence, certain microwave powers may further favour the production of oil or gas.

As a result of the increased secondary reactions the incorporation of chlorine into hydrocarbon species must occur, as any oil yield greater than 43wt.% of starting sample mass must contain chlorine (PVC containing 57wt.% Cl).

The relationship between oil yield and heating rate (shown in Figure 6-49), indicates that oil yield is seen to obey a power law relationship, ($88.153x^{-0.195}$ (R^2=0.855), where x = heating rate) for those yields of greater than 25wt.%. When oil yield is examined as a function of maximum temperature it is found to follow a 2nd order polynomial (Oil = $0.0005x^2$ - 0.4526x + 132.86 (R^2=0.954), where x = maximum temperature) between 400°C and 710°C. When maximum temperature is examined as a function of heating rate for those temperatures greater than 400°C and less than 710°C, it was found that a linear relationship exists (-0.3551x + 694.82 (R^2=0.955), x = heating rate). From this it can be concluded that oil yield is a combined function of heating rate and maximum temperature.

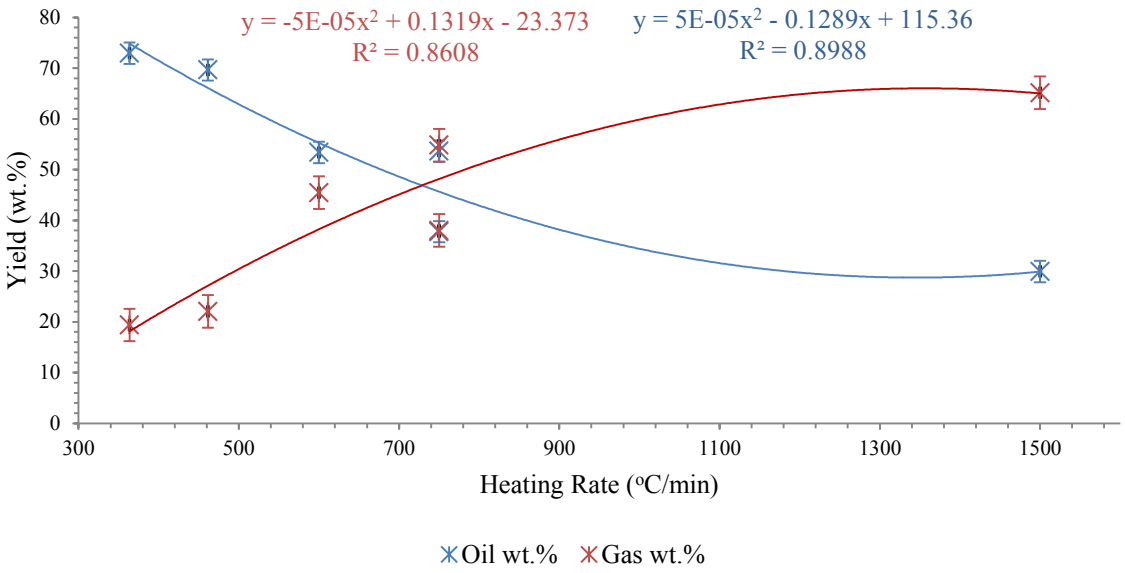


Figure 6-50 Yields of oil and gas vs. heating rates from 1st inflection to 250°C for pyrolysis over the microwave powers of 600W for 20wt.% to 80wt.% carbon receptor of a total 5g mass

Upon examining Figure 6-50, it is seen that the relationship between heating rate and oil yield persist, demonstrating that the relationship transcends differing experimental setup. It can also be seen that the yield of gas follows an equally similar trend to that of oil, indicating that a balance between the mechanisms of oil and gas formation are controlled predominantly by heating rate during the dehydrochlorination phase of PVC decomposition; this is discussed further in section 6.4.1.6.

The relationship between heating rate and product yield is very complex. This is because the maximum temperature and heating rate are functions of the dielectric response of both the carbon and PVC. It stands to reason that they themselves are a function of the mechanism of oil formation. Hence, in a microwave pyrolysis process it is not completely possible to say with great certainty which is the dependent factor in the process. This has significant implications for an industrial process. For maximum temperature and heating rate to be controlled, proportions of a dielectrically responsive additive must be such that the pyrolysis decomposition mechanisms have little influence over the temperatures achieved.

6.4.1.6 Gas Yield

Upon examination of Figure 6-51, it is found that for fixed carbon receptor experiments, at 440W the production of gas is seen to increase from 29.74wt.% at 0.0g to 42.23wt.% at 0.5 g carbon receptor. This then progressively increased to 67.08wt.% by 3.0g receptor.

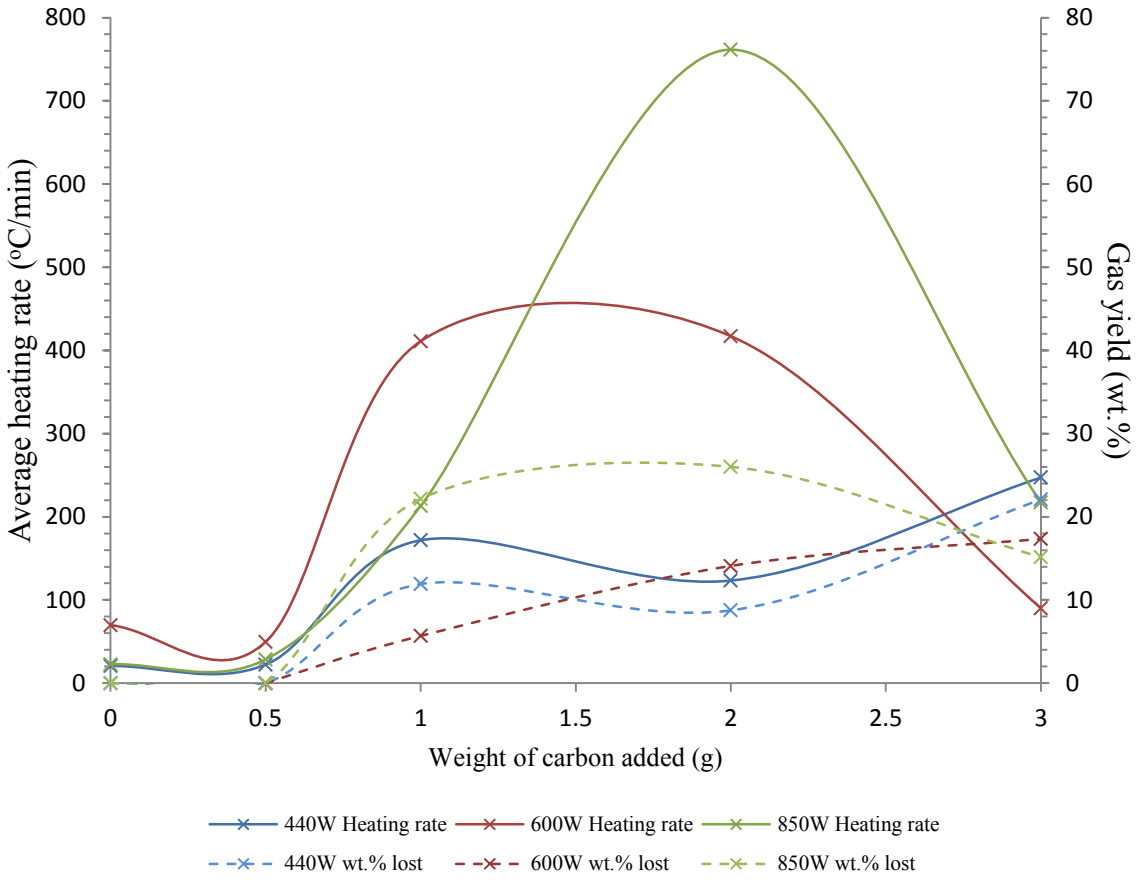


Figure 6-51 Gas yields and heating rates between 1st inflection and 250°C vs. Mass of carbon additive (0-3g) at 440W, 600W, and 850W.

When 600W power is applied a similar pattern is observed with increasing mass of gas being generated with addition of increasing carbon receptor. This increases from 37.40wt.% at 0.0g to 62.34wt.% for 3.0g carbon receptor. This pattern is not seen to persist at 850W power with heating rate peaking at 2.0g carbon receptor.

This would suggest that the role of the carbon additive is critical in the gas production process. A further complicating factor, which is a common feature of microwave pyrolysis systems, are the existence of plasmas. These were prevalent during all experimentation in which carbon was used as a microwave absorber. The effect of the plasma may be to crack volatile oils in to simple base molecules. The plasmas were observed to take the form of electrical arc discharges and quasi-spherical plasmas, as shown in Figure 6-52 .

These have also been observed by Tang and Huang (2005), Menéndez *et al.* (2011) and Salema and Ani (2012). They have theorised that a consequence of the plasma formation is a shift from oil to gas production during the pyrolysis process, with the breakdown of carbonaceous structure to form gaseous hydrocarbon fractions as free electrons and ions which can disrupt bonds.



Figure 6-52 Arc discharge and quasi spherical plasmas, formed during the microwave pyrolysis process of PVC

Upon examining Figure 6-50 and Figure 6-53 it appears that a good relationship exists between heating rate and gas yield, with increasing heating rates resulting in increased gas yield. However, it would appear that the relationship is specific to each experimental configuration.

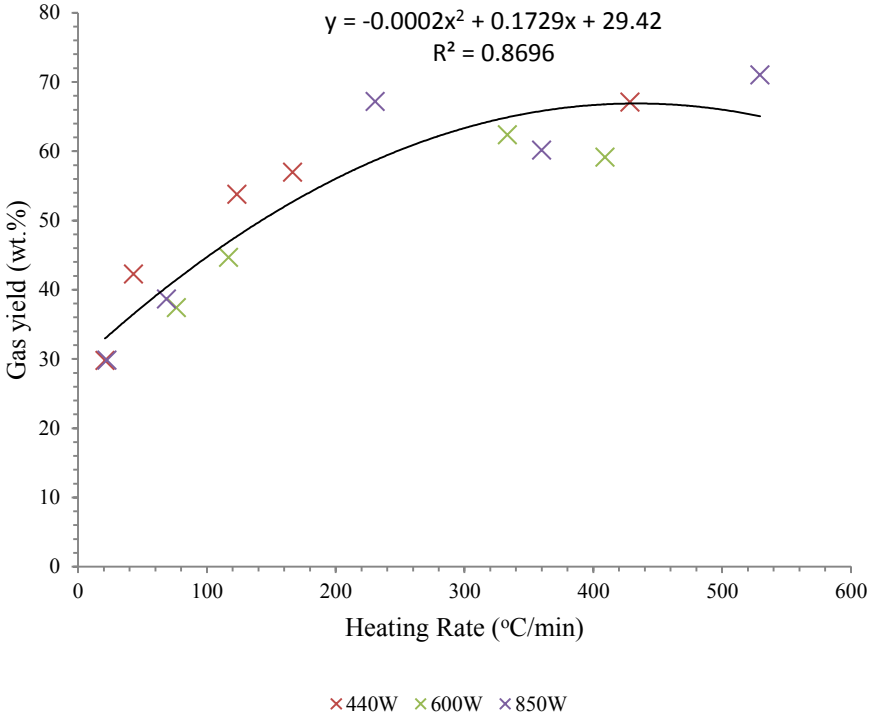


Figure 6-53 Heating rate vs. gas yield of 5g PVC containing between 0 to 3g carbon additive at 440W, 600W, and 850W.

6.4.2 Product Analysis

6.4.2.1 Solid Residue

Upon analysis of the solid residue by thermal gravimetric analysis, it was found that sample prepared using higher heating rates (>176.47°C/min) for 440W experiments resulted in greater thermal stability of the final residue, with minimal weight loss up to temperatures of 600°C (<2.5wt.%).

However, for heating rates less than this it was found that further decomposition of the residue occurred, with approximately 20wt.% loss by 600°C (see Figure 6-54). At lower heating rates the decomposition profile displayed the characteristic two stage weight loss associated with residual PVC, with only partial dehydrochlorintaion having occurred. This indicated that the pyrolysis process did not achieve sufficient temperature across the volume of the sample, to facilitate complete decomposition of PVC. Nevertheless, the recorded maximum temperatures for lower heating rates were significantly greater than those seen for higher rates. This could be a good indication that localised hot spotting in the field of the IR vision occurred, giving the false impression that the total volume of sample was at a uniform temperature. Nevertheless, the decomposition observed for 440W experiments demonstrated no greater thermal instability of chars than that of the raw carbon as was seen in Figure 5-14. This indicated that the residual post pyrolysis material seen on the surface of carbons was significantly carbonised, displaying similar thermal stability to that of the carbon char itself. Thus, full pyrolysis of the PVC had been achieved.

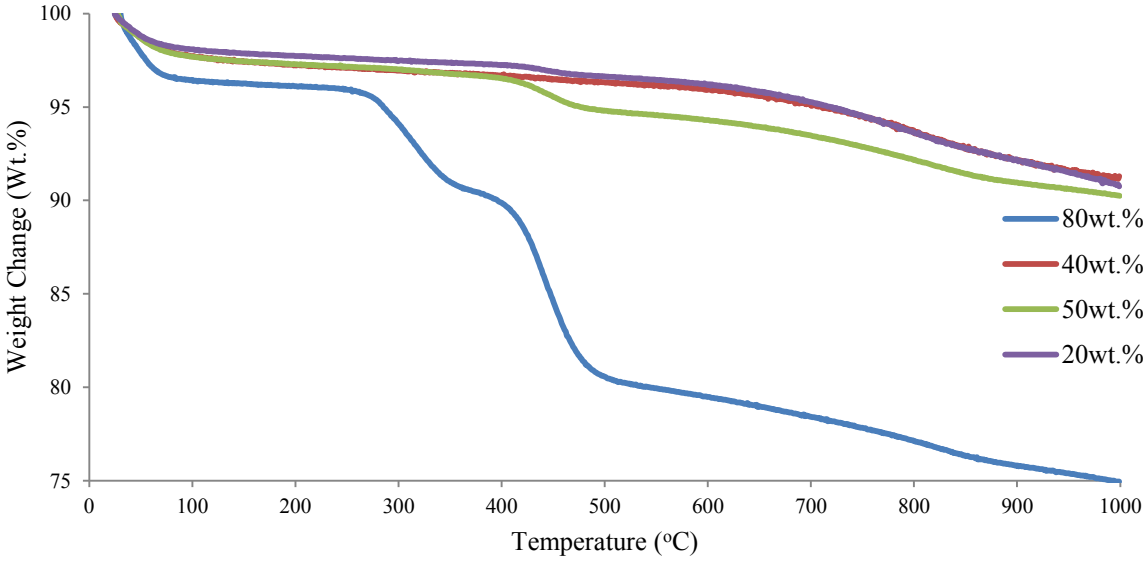


Figure 6-54 Thermal gravimetric analysis of char residues from microwave pyrolysis experiments at 440W for the ratios of 80, 40, 50, 20wt.% carbon with resulting heating rates of 43.48, 176.47, 181.82 and 352.94°C, respectively

When the chars from 440W, 20wt.% carbon experiments were examined, the presence of un-pyrolysed material was confirmed. This can be seen in Figure 6-55, whereby the char surface and pores are blocked with material, seen as molten residues over the surface of many of the particles. This is most evident in Figure 6-55, under 1000x magnification, whereby no pore structure is evident, indicating the complete covering of carbon particles by PVC residue.

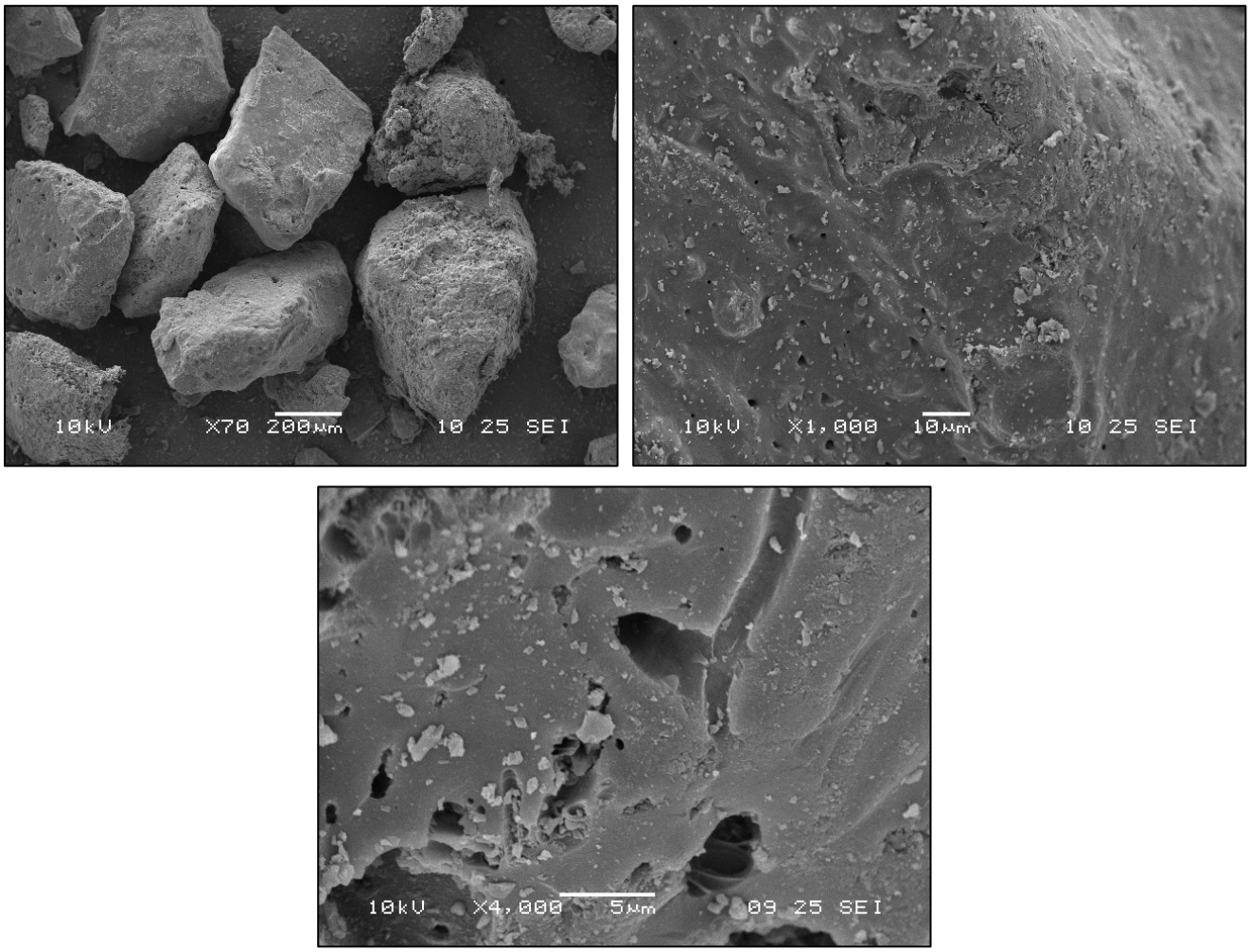


Figure 6-55 Residual chars form PVC pyrolysis for 80wt.% carbon at 440W under SEM. Top (left): 70x, Top (right): 1000x and Bottom (centre): 4000x magnification

At the higher microwave power of 600W it was found that a significant level of decomposition had occurred across all ratios of carbon added. This resulted in a higher degree of thermal stability of the residual char with less than 3.5wt.% loss up to temperatures of 700^{o}C. This indicated that the stability of the carbon additive itself had increased, suggesting that the char additive had actually undergone further carbonisation. This in itself might account for increased yields of gas and apparent lower yields of char. However, it was not possible to quantify this given the very small differences in weight recorded.

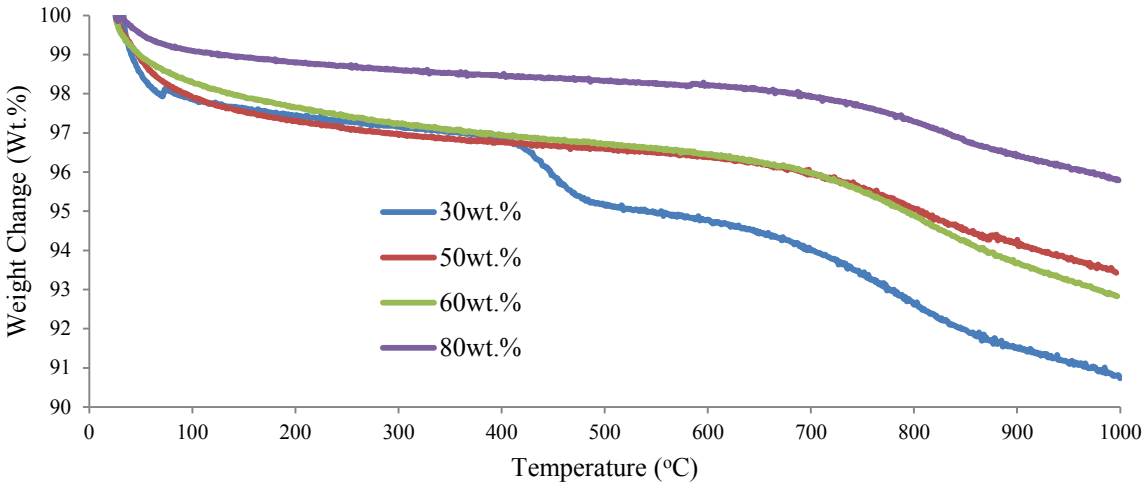


Figure 6-56 Thermal gravimetric of char residues from microwave pyrolysis experiments at 600W for the ratios of 30, 50, 60, 80wt.% carbon with resulting heating rates of 236.84, 720.00, 782.61 and >1000.00°C, respectively

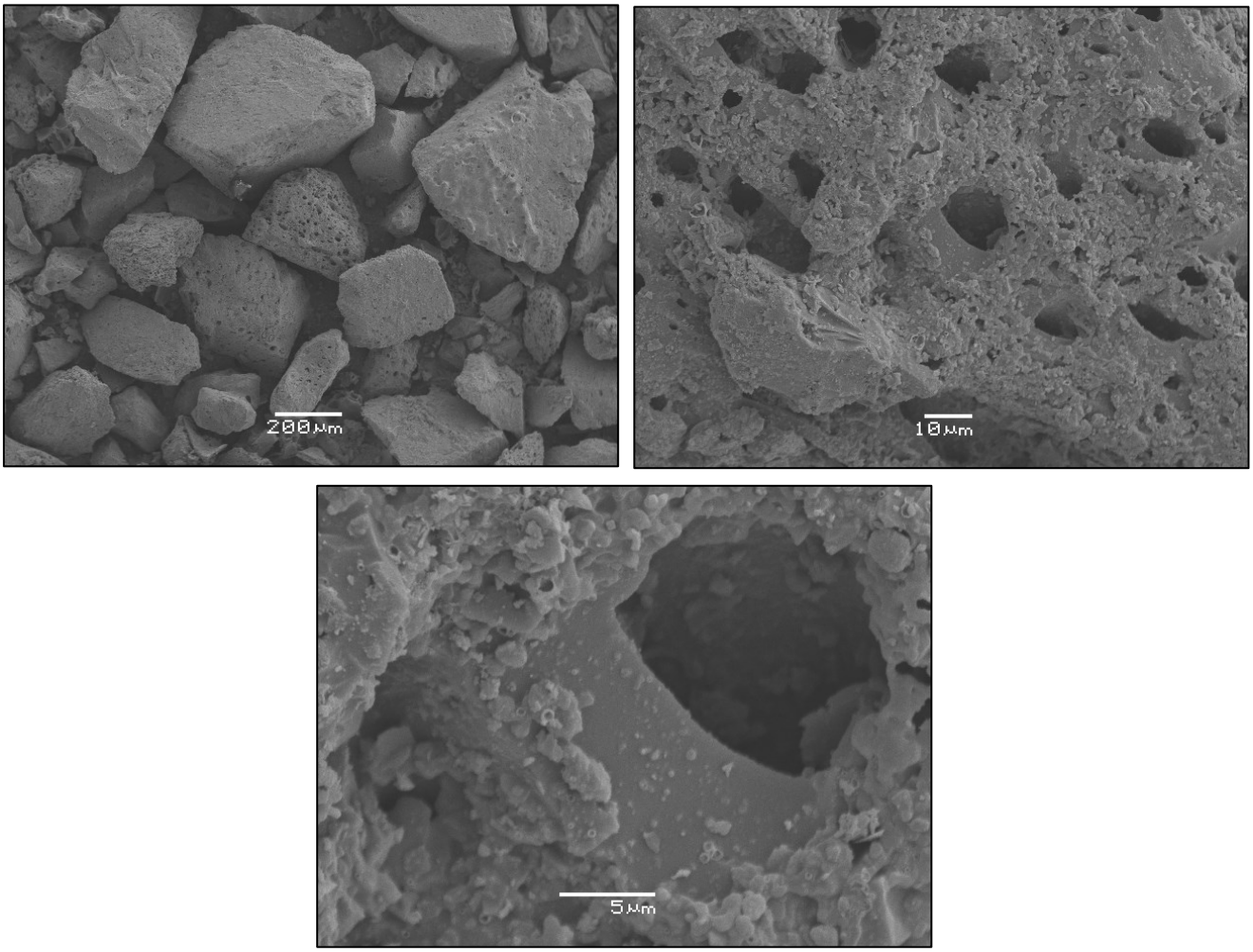


Figure 6-57 Residual chars form PVC pyrolysis for 80wt.% carbon at 600W under SEM. Top (left): 70x, Top (right): 1000x and Bottom (centre): 4000x magnification

During the 600W experiments it was noted that for the lowest heating rate, residual polymer could be observed, evidenced by the step weight loss in Figure 6-54 at 420°C for 30wt.% carbon experiments. This resulted in a loss of approximately 6.0wt.% by 700°C. This is significantly less than the losses observed for 440W experiments, indicating that greater levels of decomposition were achievable with increased applied power and greater temperatures being attained. This is also reflected by the increased yields of oil and gas, as seen in Figure 6-42.

Greater levels of decomposition can also be observed under SEM, with the surface of the carbon receptor particles showing visibly less residue on the surface of the material and clearer pore structure (see Figure 6-57, 1000x and 4000x magnification). This is most evident upon inspection of carbon particles from 80wt.%, 600W experiments, in which the thermal stability of the char is greatest, with no more than 4.2wt.% lost from the sample by 1000°C. This also demonstrated a significantly greater thermal stability than the carbon additive before microwave exposure.

The presence of deposits within the pore structure of the char demonstrates the possible ingress of oil/gas and subsequent char formation. This would indicate that within these structures a high degree of secondary reactions occurs, resulting in longer chain carbon species and the production of polyaromatic species.

6.4.2.2 Oil

Analysis was performed on all the oils produced, utilising a combination of gas chromatography and mass spectrometry to derive product compositions and boiling point distributions (the methods of which were described previously in sections 4.6.1 and 4.6.2).

6.4.2.2.1 Carbon Number Distribution

Carbon number distributions are presented for the oils produced at microwave powers of 440W and 600W in Figure 6-58 and Figure 6-59 , respectively. It is evident from these distributions that a wide range of products are generated with C_6 - C_{24} hydrocarbons, with differing distributions occurring dependent on experimental conditions.

Upon further examination it became clear that a correlation existed between carbon numbers and heating rates, during the dehydrochlorination phase (80-250°C) of the decomposition process, as previously observed in Section 6.4.1.5.

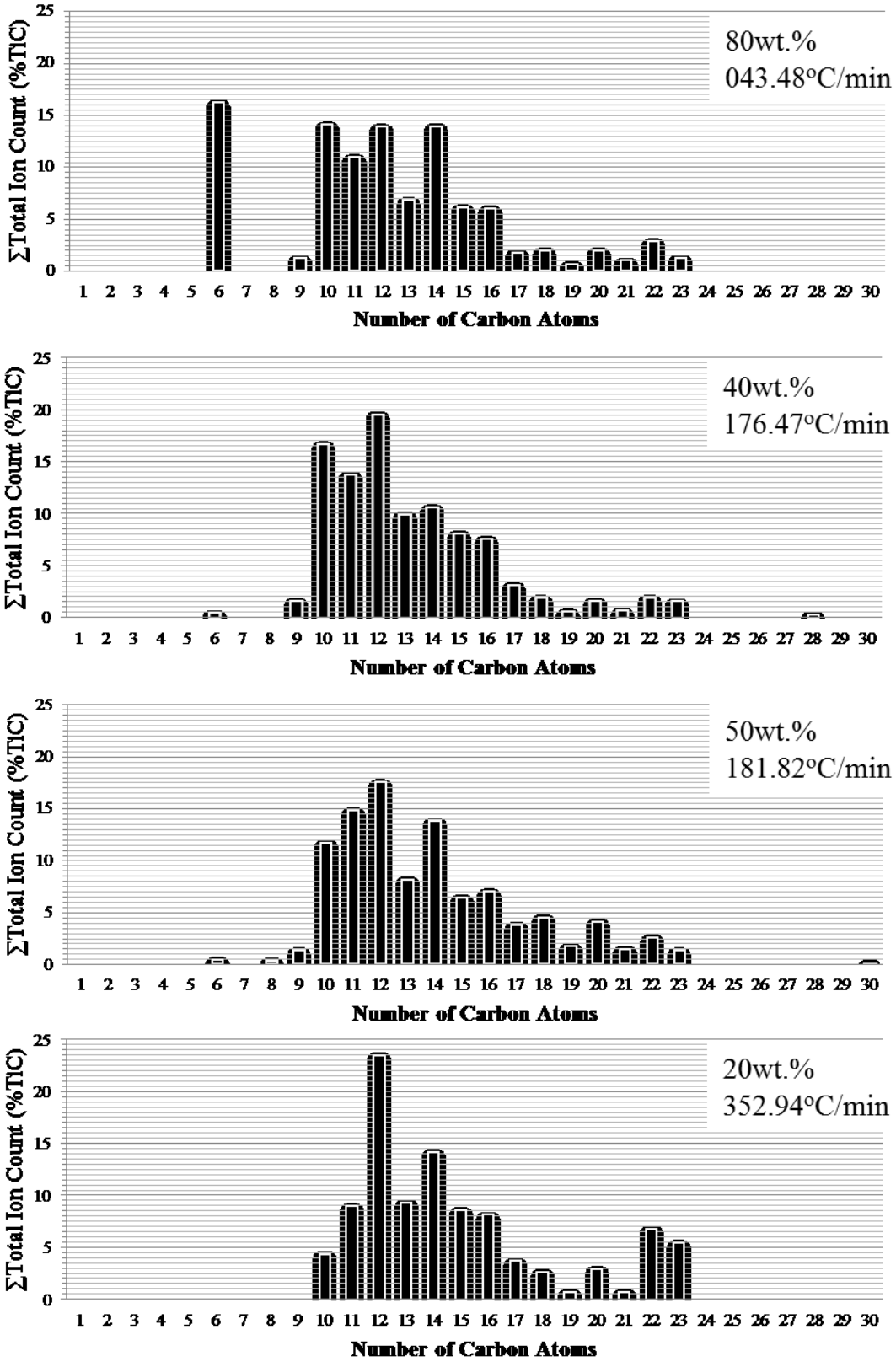


Figure 6-58 Semi quantification of product distribution by TiC of oil produced from 440 W carbon ratio experiments, ordered by heating rates as derived from 1st inflection to 250°C (lowest to highest)

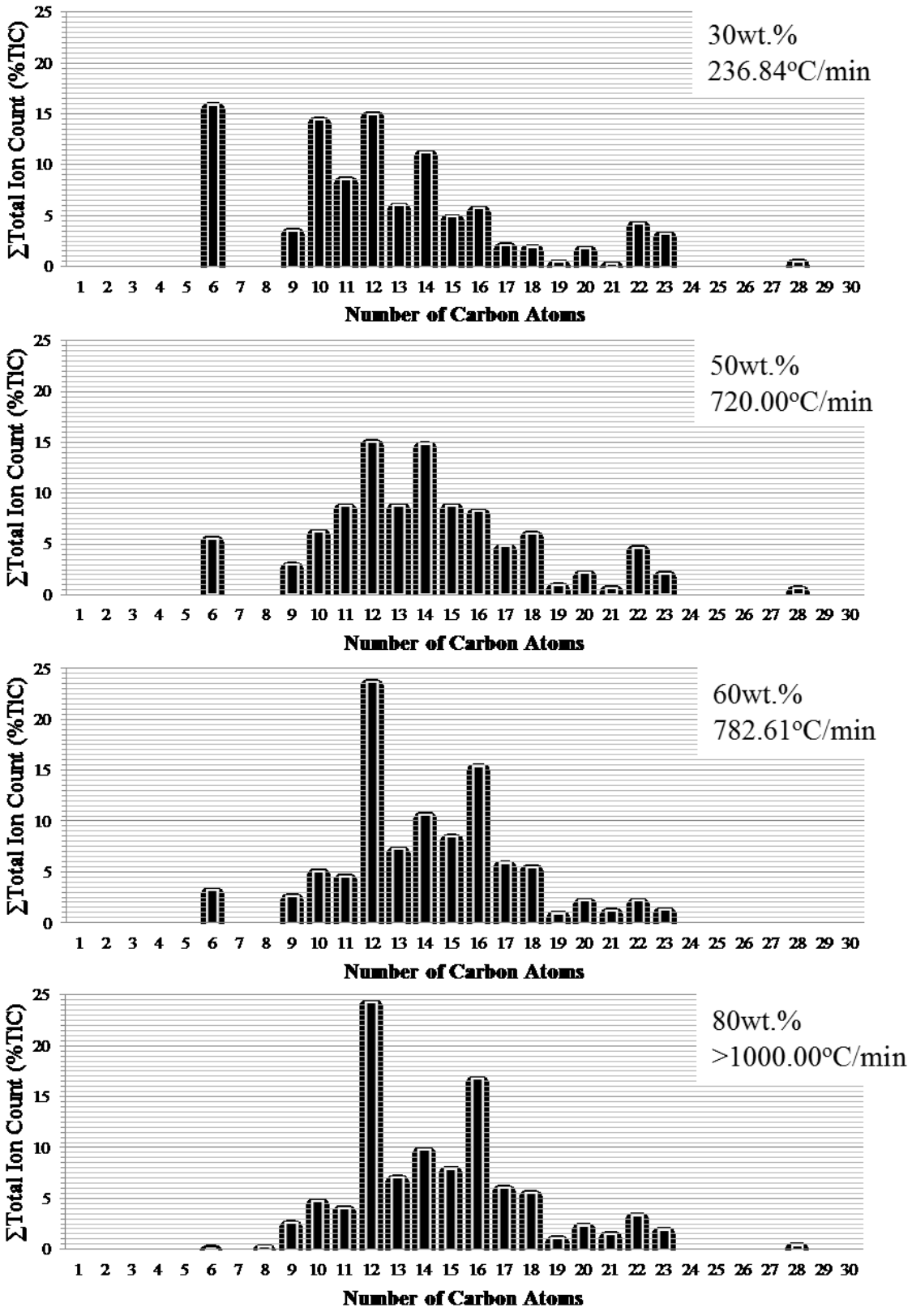


Figure 6-59 Semi quantification of product distribution by TiC of oil produced from 600 W ratio experiments, ordered by heating rates as derived from 1st inflection to 250°C (lowest to highest)

Hence, the carbon number distributions demonstrate that with increasing heating rate, along with decreasing maximum temperature, a shift in oil distribution from shorter chain to longer chain hydrocarbons occurs. This is presented for 440W experiments with the elimination of hydrocarbons from C_6 - C_9 and the development of hydrocarbons from C_{12} onwards (figure 6-58). The dominant products formed at lower heating rates/ higher temperatures were those of C_6, C_{10}, C_{11}, C_{12} and C_{14} hydrocarbons, of which Benzene, Azulene, Benzocycloheptatriene, (E)-3-Dodecene/Biphenyl and 3-Tetradecene are the most abundant for each carbon number respectively.

When the heating rate increases, C_{12} and C_{14} hydrocarbons predominate with the production of 3-Dodecene and (Z)-3-Tetradecene at the lighter end of the distribution. There is also a specific development of C_{22} and C_{23} hydrocarbons consisting of 11-Tricosene and 2-Benzoyl-3-phenyl-spiro(cyclopropane-1,7'-bicyclo[4.1.0]heptane) at heating rates of approximately 350^{o}C/min. Upon examination of the 600W experiments, the pattern observed was similar to that of 440W. However, changes in carbon number distribution varied greatly to those of 440W experiments at similar heating rates.

The same pattern of diminishing proportions of C_6 and C_{10} hydrocarbons are observed with increased heating rates, along with a significant reduction in the proportion of $C_7 – C_9$ and C_{11}. The C_{12} and C_{16} hydrocarbons exhibited a marked increase in their abundance with increased heating rate. These two peaks in particular were linked to significant increases of (E)-3-Dodecene and 1-Chloro-hexedecane respectively. The few compounds indicated as containing chlorine indicated that little of the chlorine from the original polymer remains, being driven off during the pyrolysis reaction. This is not unsurprising as the pyrolysis process always heated from low to high temperature, passing through the temperature range at which chlorine was evolved from PVCs structure (~250^{o}C).

It should be noted that proportion of C_{22} and C_{23} hydrocarbons produced at 600W was observed to diminish compared to 440W. However, this is most likely attributable to the greatly increased heating rates and temperatures achieved in comparison with 440W experiments. The notable lack of chlorinated species found within oils from low heating rates, suggested that chlorine is incorporated into heavier hydrocarbon species not analysable by the GC method employed, indicating that they are bound within hydrocarbons of boiling points greater than 550^{o}C or the char residue.

The increased gas production with higher heating rates, as demonstrated in Figure 6-53, along with the changes observed in the carbon number distributions, provides good evidence of the likelihood of vapour phase cracking of hydrocarbon species resulting in the production of light gases. The increased reaction rate resulting from a higher heating rate does give rise to greater production of primary

gaseous products (Ludlow-Palafox and Chase, 2001). This has also been observed by Fletcher *et al.* (1990) during the pyrolysis of coal.

The changes in product yield and composition are of considerable interest, given that the heating rates achievable in the microwave process are much greater than by conventional thermal means. This results in significant product changes, without the requirement for the addition of catalysts or major modification to the pyrolysis reactor. This is in good agreement with the speculated advantages of a microwave pyrolysis process as outlined by Miura *et al.* (2004).

6.4.2.2.2 Boiling Point Distribution

Comparison of the carbon number distributions (Figure 6-58 and Figure 6-59) with the boiling point distributions (Figure 6-60 and Figure 6-61) shows the difference in oils produced between the two microwave powers becoming increasingly apparent.

At 440W (see Figure 6-60) it can be seen that oil boiling-point distributions were largely similar, with 25wt.% of the oil formed falling within the range of 175°C to 225°C, 50wt.% between 300°C to 350°C and 75wt.% between 360°C to 480°C. Across the range of carbon ratios used it was seen that increasing heating rate pushed the distribution of boiling points to lower temperatures, further supporting the argument that increased heating rate produced lighter, shorter chain products. This is most evident when comparing the results of 43.48°C/min and 352.94°C/min, whereby the boiling point range varied significantly between 200°C and 350°C.

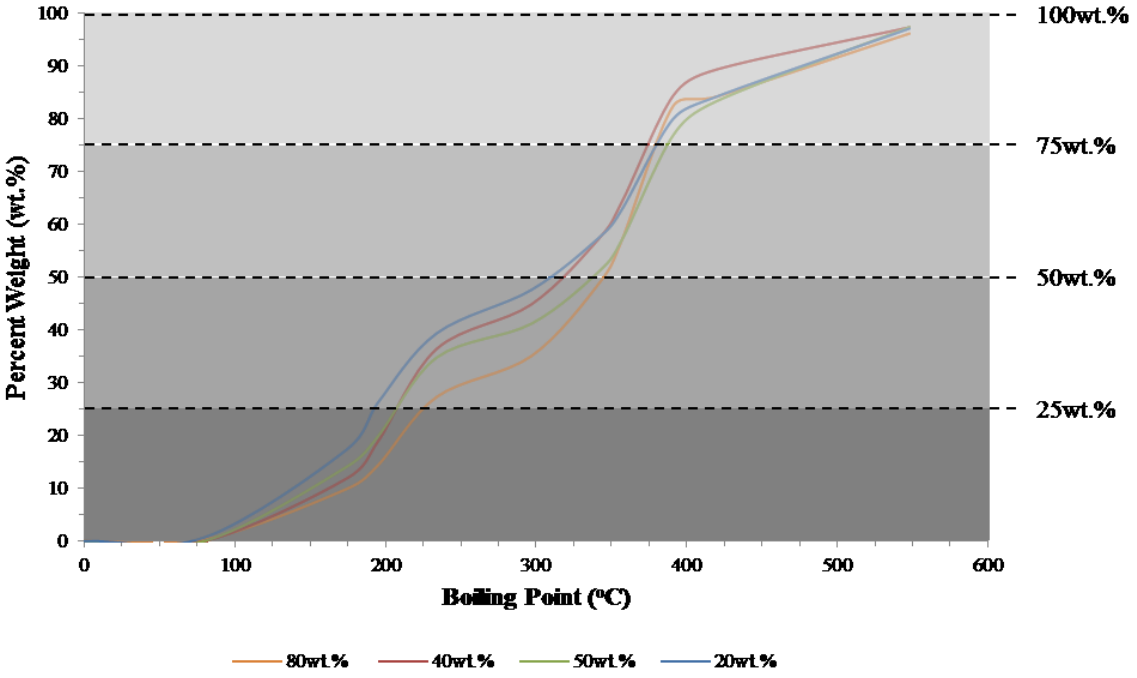


Figure 6-60 Boiling point distribution of oils derived from the 440W carbon ratio experiments with derived heating rates of 43.48, 176.47, 181.82, 352.94°C/min from 1st inflection to 250°C for 80, 40, 50 and 20wt.% carbon, respectively

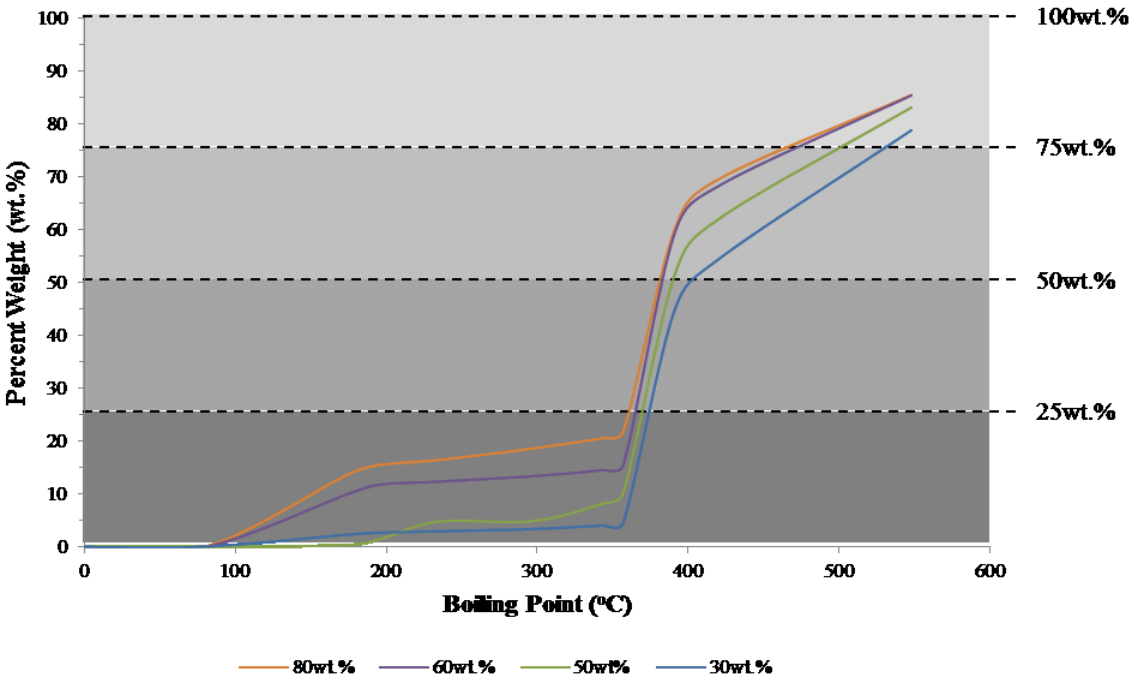


Figure 6-61 Boiling point distribution of oils derived from the 600W carbon ratio experiments with derived heating rates of 236.84, 720.00, 782.61, >1000°C/min from 1st inflection to 250°C for 80, 60, 50 and 30wt.% carbon, respectively

However, when inspecting the boiling point distributions formed from 600W ratio experiments (see Figure 6-61) a significant change occurs, with diminishing proportions of oil with boiling points below 350°C. Over this 350°C the proportions of oil vary significantly between the heating rates of 236.84°C/min and >1000°C/min, with decreasing proportions of oil found with increasing heating rate. A recurring feature of this study.

6.4.2.2.3 Product Speciation

Characterisation by FTIR was used to establish the groups present within PVC derived oils. Symmetrical and asymmetrical C-H stretching vibrations are observed at 2970 and 2880cm^{-1} together with the presence of di/trimethyl signatures at 1365cm^{-1}, indicate the presence of alkane components. This was further supported by the presence of methylene rocking at 736cm^{-1}.

Further signatures of aromatic C-H stretching at 3016cm^{-1} and aromatic C-H out of plane bending were observed at 1216 to 705cm^{-1} along with aromatic combination bands at 1759 to 1726cm^{-1}, these may also correspond to the presence of Alkyl carbonate or carboyxylic acid groups. The strong

signature at 1736cm^{-1} also indicated the possibility of aliphatic chloro compounds. The presence of signatures at 1260 and 890cm^{-1} also suggested the presence of expoxy and oxane rings. Skeletal vibrations in aromatic rings are expected at 1500-1450cm^{-1} but also increase the likelihood of overlapping peaks.

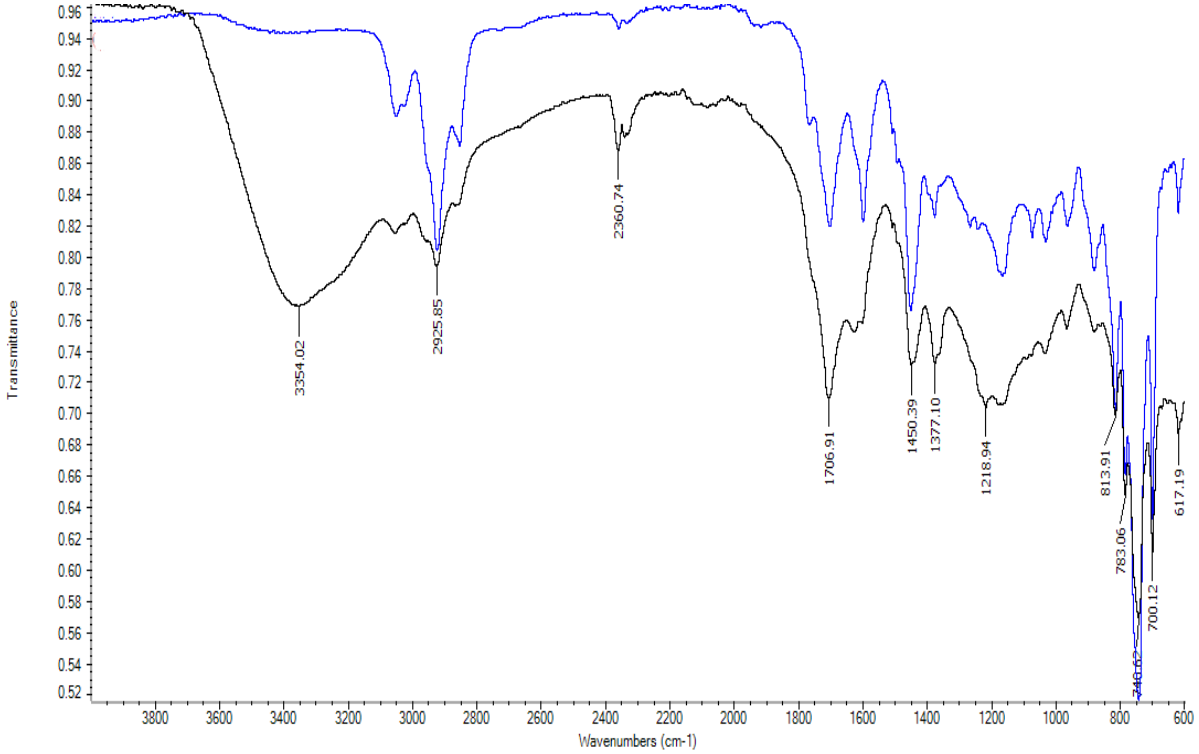


Figure 6-62 Typical FTIR spectrum of PVC oils from 440W (blue) and 600W (black) ratio experiments

Between the two spectra for 440W and 600W, noticeable differences arise, with more intense peaks arising at 3016, 1737, 1365, 1264, 1216, and 736cm^{-1} for 440W, all indicating the increased aromatic structure of the oils.

The aggregate groups of organic species was derived from GC-MS results in which the identified individual compound was manually examined and assigned its grouping. For example, if benzene or hexane were indicated from the GCMS identification against the NIST 2005 spectral database, then benzene would be grouped as an aromatic species with no branching (has no side chains present in the aromatic ring), and hexane would be grouped as an alkane. This was performed for each individual GC-MS chromatogram and is presented in Figure 6-63 and Figure 6-64 as formation of organic groupings with respect to the derived heating rate observed during each individual experiment.

From examination of speciated product distributions by GC-MS (as shown in Figure 6-63 and Figure 6-64), it is evident oils consist largely of branched aromatic structures (approximately 43 – 67 %TiC) and aromatic/polyaromatic species (approximately 7 – 26%TiC).

For experiments performed at 440W it was found that overall, the cyclic, branched cyclic and alkyne structures were consistently seen in all oils produced during microwave experiments, with little or no variation observed across all heating rates. Nevertheless, substantial variation in alkanes, alkenes, aromatic/polyaromatic and branched aromatic structures occurred.

At a heating rate of approximately 50^{o}C/min a high proportion of alkenes (19.4%TiC) were found in oils. This subsequently decreased to 8.1%TiC with increasing heating rate to 113^{o}C/min. During this period of increased heating rate the proportion of branched aromatic structures was observed to increase by almost 11%TiC.

This is logical, as lower heating rates are seen to result in higher maximum temperatures being observed, which consequently favour greater decomposition to oil, rather than gas formation. Hence, oil is likely to be composed of aromatic/polyaromatic species as the propensity for heavier molecular weight species formation (and ultimately charring) increases, due to the successive dehydrogenation reactions increasing the stability of aromatic/polyaromatic species (Marongiu *et al.*, 2003). Alongside this, the increase in alkenes and decrease in branched aromatic structures is also probable due to successive cyclo-addition reactions of alkylaromatic radicals alongside the successive elimination of side groups from aromatic structures.

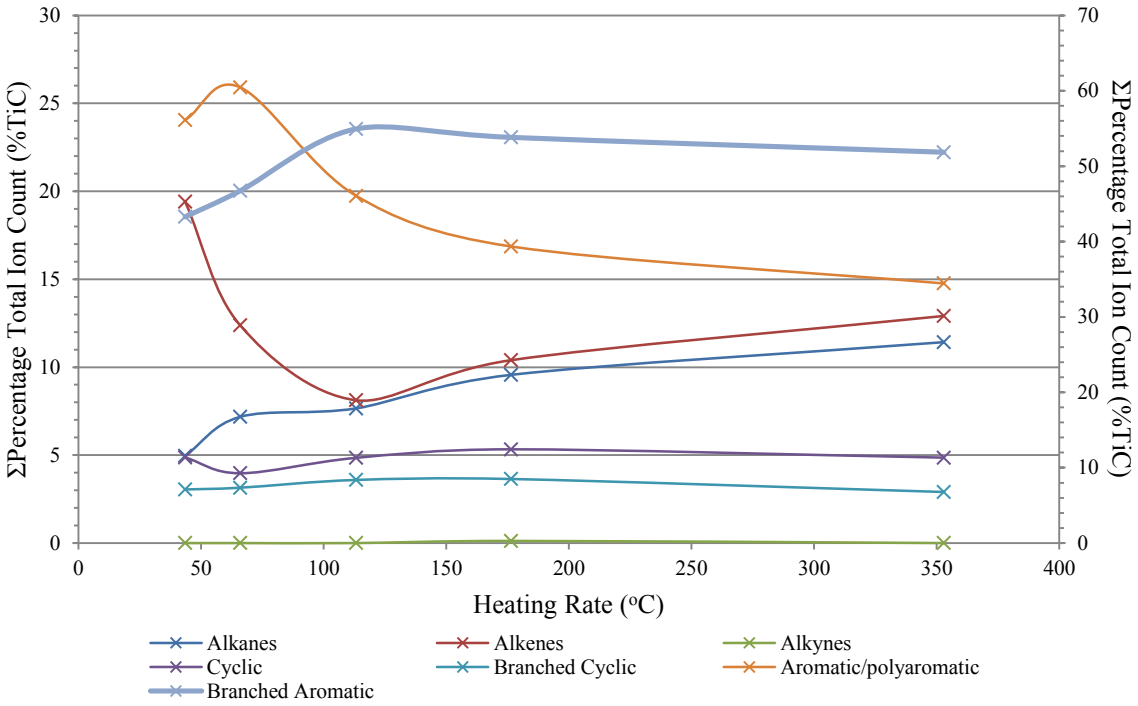


Figure 6-63 Speciated oil constituents with increasing heating rate for 440W ratio experiments semi quantified by %TiC (branched aromatic structures relate to right hand y-axis)

These radicals subsequently combine to form short chain alkenes. This is shown in Figure 6-58 to clearly be the case, as evidence by markedly increased proportions of Benzene, Naphthalene, Azulene and Tetradecene.

As heating rates increase beyond 113°C/min the proportions of aromatic species decline and a gradual increase in the proportion of alkanes and alkenes is observed. These are most likely formed through the process of bond scission into primary and secondary radicals in the gas phase and the further formation of tertiary radicals. Subsequently, β-scissions are most likely to have led to the formation of shorter chain

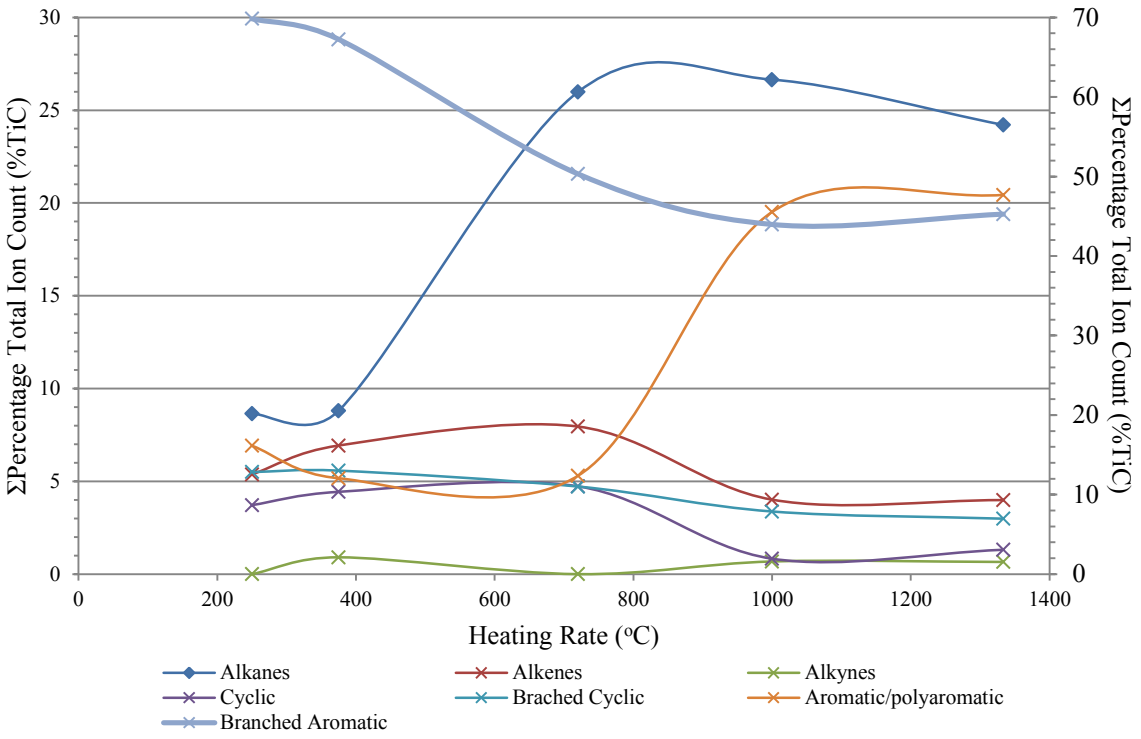


Figure 6-64 Speciated oil constituents with increasing heating rate for 600W ratio experiments semi quantified by %TiC (branched aromatic structures relate to right hand y-axis)

alkanes and alkenes which are less readily condensed, thus supporting the increase in the proportion of gases formed.

Further, it was suggested by Lattimer and Kroenke (1980), that the formation of aliphatic pyrolysates was as a result of hydrogen transfer mechanisms during the dehydrochlorination phase of the decomposition, with aliphatic segments formed by the mechanism shown in Figure 6-65. Further chain scissions would result in the formation of volatile aliphatic species via additional hydrogen transfer mechanisms; see Figure 6-66.

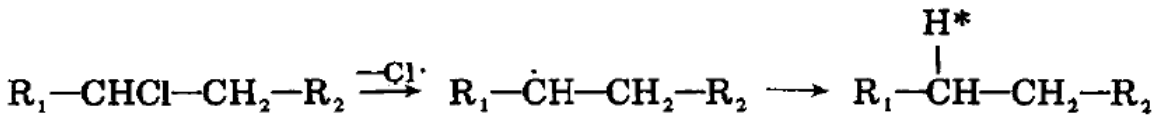


Figure 6-65 Formation of aliphatic segments during the dehydrochlorination of PVC (Lattimer and Kroenke, 1982)

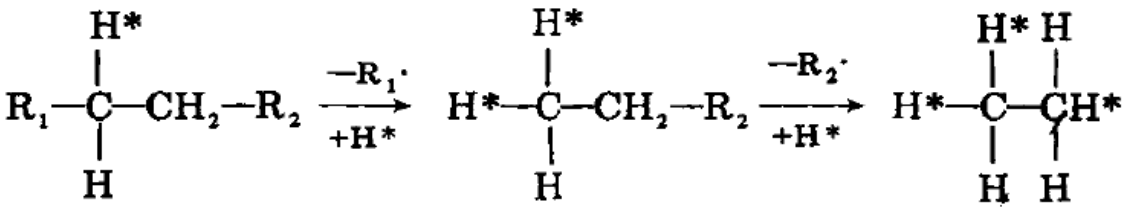


Figure 6-66 Production of volatile aliphatic species (Lattimer and Kroenke, 1982)

This mechanism would support the apparent linkage between the types and quantity of oil formed with the heating rates observed during the dehydrochlorination phase of the decomposition, as the preliminary structure and structural defects are formed on the polymer chain during this phase.

When comparisons are drawn between 440W and 600W experiments, clear differences in the species formed are observed. At 600W a propensity towards the formation of branched aromatic species is observed for heating rates of approximately 200-400^{o}C/min, with 67-69%TiC abundance. However, between a heating rate of 400^{o}C/min and 720^{o}C/min a dramatic shift in the distribution of products occurs with substantial increases in the formation of alkanes, from 8.8%TiC to 26.0%TiC. With this, a considerable decrease in the formation of branched aromatic structures (67.25 to 50.32%TiC) occurred. When the heating rate is further increased a considerable increase in aromatic/polyaromatic structures (5.29 to 19.51%TiC) can be seen. With this a marked decrease in alkenes and cyclic structures arises.

The changes observed are most probably due to the rates of polymer decomposition which occur as a result of increased energy input as represented by increased heating rates. This also increases the radical density in the gas phase and likelihood of secondary reactions, resulting in the formation of unsaturated hydrocarbon species. Alongside this, volatiles are likely to be released from the liquid phase as condensation and dehydrogenation reactions persist.

Nevertheless, the speciation observed, oil yield and heating rate patterns observed strongly support the argument that the strength of the electromagnetic field plays a significant part in the species found within the oil. This is twofold, with initial introduction of defects into the polymer chain during the dehydrochlorination phase and the possible heating of gas phase radicals due to higher radical density as heating rates increase. This allows for greater conversion of microwave energy to heat increasing molecular movement in response to the alternating magnetic field. This is reflected in Figure 6-38 as a significantly increased point of maximum temperature in relation to the observed following plateau.

6.4.2.2.4 Calorific Value

The calorific value of all oils produced from the microwave pyrolysis process was examined by bomb calorimetry. It was found that higher heating values ranged from 36.71MJ/Kg to 39.79MJ/Kg. This established that the oils produced had similar calorific values to heavy fuel oil. However, no correlation with an experimental factor could be established. This is reflective of the composition of oils, with the high degree of aromatic species (low C:H ratio) determining the overall energy released under combustion conditions.

6.4.3 Conclusions

It has been identified that the most appropriate means of microwave pyrolysis of PVC is by utilising a carbon based additive to induce a microwave response within the PVC. This results in the formation of oils and gas of varying properties dependent upon experimental conditions.

It was found that even though the carbon additive followed a predictable response to increasing microwave power, upon addition of PVC an unpredictable behaviour occurred. This was most likely a result of the presence of multiple dielectrically responsive species. There were changes in their dielectric properties in response to temperature as well as an increase in the Wagner effect due to increasing interfacial boundaries occurring with differing electrical properties. Further to this, the presence of electrical discharges and the formation of plasmas from the surface of carbon particles undoubtedly had an effect on the distribution and proportions of pyrolysis products. Such anomalies are a recognised occurrence in microwave heating but it was not possible to measure them by the techniques employed within this investigation.

Nevertheless, it was possible to identify key relationships behind product quantities and compositions which are dependent upon resulting pyrolysis conditions. Key findings during the decomposition of PVC were:

- Higher temperatures are achievable with lower heating rates during the dehydrochlorination phase of the decomposition, as chlorine stays bound within the residual polymer matrix; resulting in more dielectrically responsive species remaining to higher temperatures. This assisted the heating process.
- Low heating rates and high maximum temperatures favoured the production of oils, with 72wt.% oil yield achievable.
- Heating rates experienced by the PVC during the dehydrochlorination phase of PVC decomposition determined product distributions and composition.

- High heating rates during the dehydrochlorination phase favoured gas production with a maximum of 67wt% achievable.
- The oil composition can be altered significantly by optimising parameters to adjust the heating rate.

Chapter Seven

7 Conclusions and Discussions

The investigation of the microwave induced pyrolysis of ABS and PVC has proved successful in establishing key parameters and identification of fundamental differences between the thermal and microwave decomposition processes. The microwave reactor designed for use in this study was suitable to enable the investigation of key parameters and recording the resultant thermal profiles, heating rates and product yields; whilst maintaining independent variables at constant values.

7.1 Reactor Design and Methodology

During experimentation the design of the reactor applied was found to have significant advantages over previously reported systems. Most significant of these was the means of temperature measurement, as this was of upmost importance in the microwave decomposition process. The direct measurement of sample surface temperature gave significant advantages, allowing for:

- Establishing a representative measurement of the sample temperature inside the reactor : this is of upmost importance as it has enabled recording of heating rates in excess of 1000^{o}C/min which otherwise could not have been established by external reactor measurements, or through the use of thermocouples.
- Observation of hot spotting: due to the nature of infrared measurement, hot spotting and localised thermal runaway have been observed and recorded as the radiation emitted is registered by the IR thermometer. This is often seen as sharp spikes in thermal profiles. This has given a greater understanding of the processes occurring during the microwave decomposition, allowing for the heating rates during hot spotting to be recorded and correlated into the decomposition process.
- Identification of non uniformities in temperature: the method of temperature measurement along with visible changes in sample, have allowed for the determination of thermal gradients across samples and identification of progressive decomposition reactions; as observed in the dehydrochlorination of PVC.

The advantages offered by the temperature measurement method are also tempered by disadvantages. The limitation of surface temperature measurement means that for greater sample masses, with increasing bed depth, a true temperature of the decomposition could not be derived. Also, the inability to establish the change in emissivity of the sample introduced an error into temperature measurements of approximately 10% of full scale during the phase of decomposition.

Nevertheless, this method of measurement still gave greater capability to the system than that offered by the use of thermocouples and fibre optic probes. The non-intrusive nature of the method enabled the observation of the material without interfering with the electromagnetic field and the decomposition process. It also facilitated the investigation of significantly greater temperatures (<=1000^{o}C) than previously explored or reported in the research community.

The equipment and methods used further allowed for the accurate establishment of product yields, attributable to the complete condensation of organic species via liquid nitrogen condensation and the ease of collection from reactor components.

Nevertheless, the microwave reactor design did suffer from a number of limitations:

- Inability to stir/agitate sample during decomposition(although this would have prevented temperature measurement).
- Inability to measure microwave field density/energy usage; forward and reverse power.
- Limited capability in adjustment of applied microwave power.

Further limitations of the microwave reactor design were surrounding the inability to stop the microwave reaction at a given temperature. This was largely as a result of the heating rates observed being in the high hundreds to thousands of degree Celsius per minute. This meant that any temperature that was attempted to be stopped at, would be highly inaccurate with significant overrun seen due to the response of the infrared detector and the time taken to stop the microwaves input. This is not only the limitation of this microwave reactor system, but also of many others. This surrounds the nature of microwave heating. As a sample volumetrically heats, the mechanism of thermal conduction which would normally be relied upon during conventional pyrolysis is no longer a significant factor and temperature measurement appears to be always the limitation during microwave experimentation involving solid phase reactions. This is less so during a liquid heating applications as stirring and the conduction of heat results in a more even distribution of heating.

This effect is less of a problem during the heating of solids of low dielectric response, however a system that contains carbon/char has an extremely high dielectric. For example cellulose, can be heated with a reasonable degree of control as demonstrated by Fan *et al.* (2013). However, this has always been performed with a small sample size and the temperature of the sample monitored on the external surface of the reactor. Hence, there is no guarantee that the temperature observed is representative of the total sample mass. As such, the results gained are liable to questioning as to their degree of accuracy.

The alternative to the system used would be similar to that proposed by Ludlow-Palafox and Chase (2001) in which a large fluidised carbon bed was used and the total mass heated and then the sample of plastic introduced to the system. However this lends itself to the limitations as the method of temperature measurement was liable to error resulting from the use of thermocouples. These are subject to induction of current within them and false temperature readings given. Further to this the heating of a carbon mass does not directly explore the nature of the decomposition of a polymer after initiation of a decomposition reaction as the large sample load of carbon will absorb all the microwaves entering the cavity limiting the possibility of interaction with plastic decomposition products. This largely amounts to a thermal process rather than a microwave induced decomposition.

Nevertheless, it would be desirable to engineer the current microwave reactor setup so that more precise control of temperature could be achieved. This would most likely encompass the use of heat feedback system in which multiple temperature measurement points were used to derive sample temperature. This would also have to incorporate the use of an inducing material with a significantly lower dielectric than that of carbon but equally it must not partake in the reaction undergone chemically remaining essentially inert. This would most likely take the form of giant ionic structures such as silicon carbide, in which the imperfections of the crystalline structure of the points at which a dipole moment is present. However, as of yet the research community has not identified such a material with the use of the highly responsive silicon carbide and carbon dominating a research field. Otherwise the use of materials that can act as a co pyrolysis are used, such as metals, waste engine oils, cellulosic biomass etc. However, these do not lend themselves to understanding possible fundamental decomposition of a single polymer of plastic as their decomposition products will interact with those of the pyrolysis material disguising or even the eliminating the possible products that might be achieved from a single plastic waste stream. This is not conducive with investigating the fundamental microwave decomposition of plastics.

7.2 Decomposition of Acrylonitrile-co-Butadiene-co-Styrene

From the examination of ABS and it was quickly determined that the polymer underwent decomposition of predictable fashion when exposed to thermal degradation. As a result the products formed largely consisted of monomer units which were styrene acrylonitrile and butadiene. It was further seen that combinations of these monomers can also arise. Hence, it was quickly concluded that the decomposition process of ABS was a free radical driven process in which end chain and random scissions take place simultaneously. Upon the microwave decomposition of ABS it was quickly ascertained that an additive was required as the di electric of the polymer was not sufficient to

undergo any significant degree of heating. As such, carbon/char additive was trialled in varying proportions with the polymer.

The overall behaviour of the carbon additive was found to be predictable in its response to microwave radiation but also to not partake in the chemical reactions occurring during the decomposition of the polymer itself, with no evidence of catalytic activity. This was proven through a combination of py-GC/MS and TGA. In this the ratios of each individual chemical components during the thermal decomposition of ABS were not seen to vary in relation to increasing proportions of carbon/ char additive.

The investigation into the combination of Char and ABS quickly determined that below a critical portion of char the initiation of the ABS decomposition could not occur. This was typically less than to 0.5 grams or equivalent material. This was concluded to be as a result of the proportion of carbon being insufficient to overcome the thermal losses from the reactor, hence an equilibrium state was achieved below that of the decomposition temperature of ABS.

It was found that the microwave decomposition of ABS could not be achieved without the assistance of a carbon additive.

- With carbon addition it was found that the initial decomposition of the plastic occurred at 150-160^{o}C. At which point the dielectric of the material changes and the plastic undergoes sudden and complete decomposition.
- The amount of carbon receptor used in the process was found to be critical for the time required to reach the point at which the decomposition occurred.
- The carbon had little/no influence on the heating rates achieved during the decomposition phase.
- The creation of radical species during the ABS decomposition assisted in the further breakdown of the plastic, as a result of their charge imbalance and subsequent increased dielectric properties.
- Microwave power was critical in influencing the yield of char, oil and gas, with a critical power threshold required to be overcome to achieve greater yields of gas.
- Lower microwave power favoured the formation of oil.
- (i.e. almost complete decomposition of the ABS was feasible).
- Lower temperatures favoured cleavage of monomer units, allowing for the recovery of oil containing substantially greater levels of styrene than that of a thermal process, 39.5 %TiC as compared to 34.5%TiC respectively. Indicating a favourable reaction pathway to exist under microwave conditions.

- Maximum temperatures toward 550^{o}C pushed oil distributions to heavier fractions and for C_7 to C_9 components to disappear, indicating the shift to significant cracking and radical condensation mechanisms taking place.
- With carbon added it was found that the initial decomposition of the plastic, occurred at 150-160^{o}C. At which point the dielectric of the material changes and the plastic undergoes sudden and complete decomposition.
- The amount of carbon receptor used in the process was found to be critical in the time required to reach the point at which the decomposition was attained
- This had little/no influence on the heating rates achieved during the phase of decomposition.
- The creation of radical species during the decomposition assisted in the further decomposition of the plastic, as a result of their charge imbalance and subsequent increased dielectric properties.
- Microwave power was critical in discerning the yield of char, oil and gas, with a critical power threshold required to be overcome to achieve greater yields of gas.
- Lower microwave power favours the formation of oil.
- Char formation was found to be consistent, with no greater than 2wt.% formed under all experimental conditions.
- Oil composition was found to change with maximum temperature.
- Lower temperature favoured cleavage of monomer units, allowing for the recovery of oil containing substantially greater levels of styrene than that of a thermal process, 39.5 %TiC as compared to 34.5%TiC respectively. Indicating a favourable reaction pathway to exist under microwave conditions.
- Maximum temperatures toward 550^{o}C pushed oil distributions to heavier fractions and for C_7 to C_9 components to disappear, indicating the shift to significant cracking and radical condensation mechanisms taking place.

The microwave decomposition of ABS demonstrated significant advantages over that of a thermal process, with the possibility of favourable recovery of monomer units. It also allowed for the adjustment of power to push the process towards the production of gaseous compounds, demonstrating the versatility of the microwave decomposition process. This is a significant finding which could create a step-change in the recyclability of used/waste ABS.

During the microwave decomposition of ABS the variation of yields (char, oil and gas) was not significant in that ratio experiments displayed a maximum difference in oil percentage of approximately 20% and gas percentage in the order of 18%. This was found to be largely a result of the decomposition of ABS mainly correlating to the maximum temperature of the reactor. This

indicated that material remaining within a reactor underwent cracking at higher temperatures to produce more gas. As maximum temperature was expected to be correlated to heating rate it was further postulated that heating rate would show a significant relationship with oil and gas yield.

However, this was not seen. This may be evidence that the method of temperature measurement was insufficient to ascertain the heating rates over the critical decomposition period or that the combination of maximum temperature and heating rate have a significantly more complicated relationship than what could be examined by the current microwave setup. This is most likely to coincide with the interdependent relationship of materials dielectric properties, heating rate and temperature achieved. As the dielectric properties are a function of temperature and the amount of energy that's the sample was able to absorbed from the microwaves passing is a function that of the dielectric properties then the overall temperature is a function of dielectric properties. Which both in turn affect heating rate. To derive which of these parameters has a significant effect is not possible with current technology and would require the ability to control each of these parameters independently whilst still maintaining microwave input into the reaction chamber.

The microwave decomposition process did display significant differences in the oil composition as compared to thermal process. The major difference observed was a significant shift from the lighter organic species to those of heavier organic species. However, it could not be determined if this was a result of the differing experimental setups e.g. py-GC/MS verses the microwave configuration. It is distinctly possible that the lighter organic species were lost during the ratio rotary evaporation of the oil samples. Nevertheless, the wider product distribution displayed in the microwave process indicates that a far more random process of decomposition had arisen possibly as a result of increased residence time of components in the energy rich reaction zone, cracking arising and increased numbers of secondary reactions. This would be less common in the py-GC/MS experimentation due to the rapid movement of reaction products away from the reaction zone.

Nevertheless, the microwave process did demonstrate significant advantages over that of a thermal process in that the versatility of the changes in heating rate provided significant shifts in the production of oil and gas. This has the larger implications to an industrial process in which the ability to favour gas over of oil may be preferable. However, the largely unpredictable nature of the interaction of microwaves with a combination of char additive and plastic, then the resulting heating rate and product distribution, mean that significant amounts of time and effort would be required in the set-up of each reactor; as each microwave cavity, the power input, reactor shape, specific plastic type etc. would have a significant effect on the overall pyrolysis process.

7.3 Decomposition of Polyvinylchloride

The decomposition of polyvinylchloride proved to be interesting with respect to the overall decomposition process, with the two phase decomposition resulting from the chlorine content of the polymer. This presented a process with significant implications for industrial use with a microwave process demonstrating potential as a pre-treatment for the removal of chlorine. This is of great use when it comes to the incineration of PVC, in which the elimination of chlorine reduces the corrosive gases that may be produced, decreases the potential for formation of dioxins but also provides a potentially beneficial process in which the recovery of chlorine in the form of hydrochloric acid can be achieved reducing the overall burden and energy demand required in the initial production of hydrochloric acid.

This is also interesting with respect to a pyrolysis process in which chlorine acts as a significant contaminant if a one step process is undertaken. The microwave process demonstrated that the removal of chlorine is possible and there is significant evidence to demonstrates that and little or no chlorine is incorporated into the oil products. This means that it may be potentially easier to recycle mixed plastic types that contain PVC by the method of pyrolysis which would otherwise have not been possible. The microwave pyrolysis process of PVC also displayed significant linkages between maximum achieved temperature and heating rates attained during the pyrolysis process and the yields of oil and gas. This is a significant finding as it indicates that a microwave process follows a similar pathway to that of a purely thermal process, demonstrating that the microwave heating does not affect the underlying chemistry. However, when we compare the results of the oil composition from the microwave process to that of the thermal degradation process significant differences arise, yet again relating to heating rate and the overall product distribution. This display is a similar trend to that of the ABS decomposition in which the versatility of the microwave decomposition process in adjustment of heating rates potentially significant industrial application.

Nevertheless, the limitations of the observations that can be achieved through current microwave setup mean that a full understanding of the processes occurring are not possible. For a deeper understanding it would be required that the energy absorbed by the sample could be measured at any given point during the experiment and the rate of decomposition could be more accurately determined. This is a current feature of all microwave experimentation throughout the academic community in which the containment of the electromagnetic field and the interactions it has with materials that are required in sensors which would otherwise prove useful in measuring such parameters as temperature, heating rate, rate of mass loss, heat flow within the sample.

The decomposition of PVC demonstrated, during dehydrochlorination:

- PVC underwent two phases of decomposition: (i) dehydrochlorination; (ii) decomposition of remaining 'polyene' structure.
- It was possible to heat PVC under microwave irradiation without the addition of a microwave receptor to approximately 250^{o}C, due to the dipole moment resulting from the presence of Cl on the polymer backbone.
- High heating rates during dehydrochlorination resulted in lower maximum temperatures.
- Higher temperatures are achievable with lower heating rates during the dehydrochlorination phase of the decomposition because the chlorine stays bound within the residual polymer matrix; resulting in more dielectrically responsive species remaining to higher temperatures. Aiding in the heating process.
- Increased sample mass aided in achieving greater levels of dehydrochlorination, with a maximum of 95.85wt.% chlorine removed from the polymer, with a remaining 2.37wt.% found within the residue.
- Dehydrochlorination efficiency of the polymer demonstrated 4 to 6 times the theoretical energy essential for the dissociation of HCl from the polymer, with 607.1kJ/mol required as compared to that of 124.0 – 276.4 kJ/mol
- During the microwave dehydrochlorination process the evolution of benzene and aromatic species is suppressed and the formation of alkane and alkenes are enhanced, indicating a differing reaction pathway being followed during the microwave decomposition process

During the carbon assisted microwave decomposition process it was found that:

- Low heating rates and high maximum temperature favoured the production of oils, with 72wt.% oil yield achievable.
- Heating rates experienced during the dehydrochlorination phase of PVC decomposition determined product distributions and composition.
- High heating rates during the dehydrochlorination phase favoured gas production with a maximum of 67wt% achievable.
- Oil composition can be altered significantly by optimising parameters to adjust heating rate. Lower heating rates produce a wider product distribution with greater proportions of components found at boiling points under 350^{o}C. The converse occurs at greater heating rates.

Of significant importance has been the discovery that PVC undergoes a wave amplitude specific interaction with microwaves at 2.45MHz and 600W applied power. It is not possible to establish the specific mechanism behind this, however it has been proposed that the possibility of spin wave excitation, Maxwell Wagner or Wigner energy based mechanism may underlie the observed effect.

7.4 Concluding Comments

The microwave decomposition process appears material dependent, with the polymer structure and mechanism of decomposition of significant importance in the progression of the decomposition observed. This was clearly demonstrated by PVC which heated readily as a result of the dipole moment caused by chlorine. However, upon removal of the chlorine from the polymer structure, the system stabilises and decomposition does not continue. It is only after the addition of a microwave receptor, (carbon char in this study) followed by the continual input of microwave power to heat the carbon receptor, that it is possible to thermally crack the residual polymer structure. Similarly, ABS will only undergo complete decomposition in the presence of the carbon receptor and with the application of microwave energy. Once the temperature exceeds 160^{o}C, the decomposition of butadiene can occur and rapid disassembly of the ABS ensues.

The microwave process studied has demonstrated a clear potential over that of the traditional thermal process, with the ability to:

- preferential remove halogen species
- change product yields by adjusting power input
- adjust product composition to favour monomer recovery
- reduced processing times
- enhance significantly the energy efficiency of the process due to the direct application of energy to the targeted material.

Chapter Eight

8 Future Work

From the research performed it has been found that the microwave decomposition process shows significant differences to that of a thermal process. However, it was not possible to fully understand the differences identified by the methods employed and due to limitations of the technology applied. Thus, the following points require further examination and testing:

- A more detailed analysis of the oils produced to determining their full boiling point range, their molecular weight distribution, pour point, vapour pressure, viscosity, water content and wax content.
  - To ascertain a more detailed characterisation of oils produced during the pyrolysis process it would be preferable to use HPLC-SEC, GCMS MS, simulated distillation using SIMDIS GC, reometry to measure the viscosity, Karl Fisher to determine the water content and other extraction technologies such as supercritical CO_2 to examine wax contents.
- Analyse the gases produced for their composition, density, gross heating value and net heating value.
  - In the examination of gases the adjustment of the condensation system would be required so that products with boiling points of greater than 40° C would be condensed and yet those below this point would remain in the gas phase. These maybe collected through such techniques as gas sampling bags or live gas analysis through continuous GC sampling.
- Perform an energy balance of the process from the extra data gathered.

The further examination of plastics and their decomposition process and products should be undertaken:

- The dielectric properties of ABS and PVC in relation to temperature and during their decomposition. This would be best achieved by measurement of forward/reverse power of the microwave, weight loss and temperature during the decomposition process.
- Determination of the progression of decomposition reactions by FT-IR and/or MS, to help develop a fundamental understanding of the decomposition mechanisms and product formation pathways.
  - To determine the progression of the decomposition reactions by FT-IR it would be necessary to configure the microwave with a heated transfer line to the FTIR. This would allow for the transfer of gases without condensation and resulting in the production of a

gram Schmidt FT-IR plot. This would then allow for the analysis and determination of functional groups within the gases contained. In a similar vein the same could be achieved for MS sampling in which much more detail could be achieved giving an indication of the components contained within the gas. This would then further require analysis of gas using GC-FID to determine the quantities of each component are present.

- Examine the factors of polymer chain length, particle size and increased sample load on the decomposition process and product distributions.
  - It would be important to examine polymer chain length as it may have a significant effect on the product distribution from each individual plastic. Hence, without performing this, it would not be possible to determine if the same plastic would exhibit the same behaviour under similar microwave conditions. In the same line of thinking this would also apply to particle size and increasing product load within a reactor. From this information it would then be possible to begin to build a model of which the change in each parameter could be used to predict the products outcome.
- Explore the effects of microwave decomposition on plastics of differing polymer structure.
  - As this investigation was limited to PVC and the ABS it will also be of significant interest to determine the effects of other polymer structures on the products produced and their reaction to microwaves. As such, it would be of interest to test phalate based polymers, simple polymers, such as polyethylene or the halogenated polymers, such as bromine based polymer and fluorine based polymer. This would require significant investment both money and time to achieve.
- Explore the effect of multiple plastics and their interaction during the microwave decomposition process.
  - Once the product distribution and reactions to varying parameters of each polymer were established it could be taken upon with confidence to explore a mixed polymer pyrolysis process and understand the potential interactions undergone in such a pyrolysis process. It is also necessary to determine the effect of non plastic additives such as carbon black, UV protection agents, reinforcing materials etc.
- Examine waste plastics and their decomposition in comparison to pure polymers.
  - As a differing investigation it would also be of interest to examine other potential microwave absorbers, which do not take part in a microwave decomposition reaction with plastics; hence a screening exercise of materials with high dielectric properties to medium dielectric properties would be necessary. It may also prove interesting to look at materials which may have a potential catalytic effect on the decomposition of plastic such as metaliferous additives and their effect on the overall product distributions.
- Evaluate the change in particle size of the carbon additive.

It is not possible to ascertain a full understanding of the decomposition of the plastics without further refining the design of the microwave used to investigate the decomposition processes, as such the following must be achieved:

- The design and building a Microwave Thermal Gravimetric Analysis (MTGA) system so that the changing properties of the plastic can be examined during the decomposition process and the weight/temperature/field strength relationships identified.
    - In order to achieve all of this significant refinement of the microwave reactor would be required. To ascertain a greater understanding of the dynamics and kinetics of the decomposition process a microwave with the ability to measure the absorption of power the change in field density, the rate of mass loss, and more accurate temperature within the sample on both a gross scale and microscopic scale.
- Examine ABS and PVC over microwave powers of much smaller intervals and over a greater range to ascertain if further amplitude specific reactions occur.
- Examine methods of reducing hot spotting by sample agitation and/or modification of the microwave field for more even field density.
- Explore alternative avenues of temperature measurement.

Further steps should also be taken to explore the additional factors of:

- The dielectric properties of carbon additive over differing temperatures.
- The effect of sample pre-heating.
    - The effect of sample pre-heating is likely to have a significant effect on the decomposition of any plastic. This is as it has a similar effect to an additive in that it allows the plastic to achieve such temperatures that its dielectric increases so that it responds to the microwaves. It might be possible that this has an advantage over that of an additive but then again it might improve the energy intensive and less attractive.
- Examine the effect of differing carrier gas flow rates and type.
    - It would also be interesting to examine the effect of differing carrier gas type such as hydrogen, which may act as a hydrogen donator decreasing number of secondary reactions occurring during the decomposition process through eliminating radical species. Other gas types such as argon with their increased weight and higher heat capacity may affect the overall reaction kinetics and hence product distribution. In a similar vein the use of vacuum pyrolysis would also decrease the density of radical species during the pyrolysis process potentially eliminating secondary reactions and attaining a less complex oil.
- Explore the effect of vacuum pyrolysis.

- The use of differing dielectric additives.

Once these tests have been performed it would then be possible to model the potential commercial viability and scale up of the microwave process.

9 References

A.P.M.E 2011. Plastics - The Facts 2011: An analysis of European plastics production, demand and waste data 2011 Brussels, Belgium: Association of Plastics Manufacturers Europe.

Achaw, O.-W. & Afrane, G. 2008. The evolution of the pore structure of coconut shells during the preparation of coconut shell-based activated carbons. *Microporous and Mesoporous Materials,* 112, 284-290.

Achilias, D. S., Antonakou, E., Roupakias, C., Megalokonomos, P. & Lappas, A. 2008. Recycling techniques of polyolefins from plastic wastes. *Global Nest Journal,* 10, 114-122.

Aguado, J., Serrano, D. & San Miguel, G. 2007. European trends in the feedstock recyling of palstic wastes. *Global Nest Journal,* 9, 12-19.

Aguado, J., Serrano, D. P. & Escola, J. M. 2008. Fuels from Waste Plastics by Thermal and Catalytic Processes: A Review. *Industrial & Engineering Chemistry Research,* 47, 7982-7992.

Aguado, J., Serrano, D. P., Escola, J. M., Garagorri, E. & Fernández, J. A. 2000. Catalytic conversion of polyolefins into fuels over zeolite beta. *Polymer Degradation and Stability,* 69, 11-16.

Aguado, J. a. S., D. 1999. *Feedstock recycling of plastic wastes,* Cambridge, Royal Society of Chemistry.

Ahmed, A. & Siores, E. 2001. Microwave joining of 48% alumina–32% zirconia–20% silica ceramics. *Journal of Materials Processing Technology,* 118, 88-94.

Ahmed, I. I. & Gupta, A. K. 2009. Hydrogen production from polystyrene pyrolysis and gasification: Characteristics and kinetics. *International Journal of Hydrogen Energy,* 34, 6253-6264.

Al-Salem, S. M., Lettieri, P. & Baeyens, J. 2009. Recycling and recovery routes of plastic solid waste (PSW): A review. *Waste Management,* 29, 2625-2643.

Al-Salem, S. M., Lettieri, P. & Baeyens, J. 2010. The valorization of plastic solid waste (PSW) by primary to quaternary routes: From re-use to energy and chemicals. *Progress in Energy and Combustion Science,* 36, 103-129.

Allred, R. & Busselle, L. 2000. Tertiary recycling of automotive plastics and composites. *Journal of Thermoplastic Composite Materials,* 13, 92-101.

Ambrose, C. A., Hooper, R., Potter, A. K. & Singh, M. M. 2002. Diversion from landfill: quality products from valuable plastics. *Resources, Conservation and Recycling,* 36, 309-318.

Andrady, A. L. & Neal, M. A. 2009. Applications and societal benefits of plastics. *Philosophical Transactions of the Royal Society B: Biological Sciences,* 364, 1977-1984.

Apme, A. O. P. M. I. E. 2011. Plastics - the Facts 2010: An analysis of the European plastics production, demand and recovery for 2010. [Accessed 29/07/12].

Appleton, T. J., Colder, R. I., Kingman, S. W., Lowndes, I. S. & Read, A. G. 2005. Microwave technology for energy-efficient processing of waste. *Applied Energy,* 81, 85-113.

Arena, U. & Mastellone, M. L. 2000. Defluidization phenomena during the pyrolysis of two plastic wastes. *Chemical Engineering Science,* 55, 2849-2860.

Armaroli, T., Trombetta, M., Alejandre, A. G., Solis, J. R. & Busca, G. 2000. FTIR study of the interaction of some branched aliphatic molecules with the external and internal sites of H-ZSM5 zeolite. *Physical Chemistry Chemical Physics,* 2, 3341-3348.

Arostegui, A., Sarrionandia, M., Aurrekoetxea, J. & Urrutibeascoa, I. 2006. Effect of dissolution-based recycling on the degradation and the mechanical properties of acrylonitrile–butadiene–styrene copolymer. *Polymer Degradation and Stability,* 91, 2768-2774.

Audisio, G., Silvani, A., Beltrame, P. L. & Carniti, P. 1984. Catalytic thermal degradation of polymers: Degradation of polypropylene. *Journal of Analytical and Applied Pyrolysis,* 7, 83-90.

Aurell, J. 1977. Effects of varying combustion conditions on PCDD/F formation. *Chemosphere,* 8, 455.

Ávila, A. F. & Duarte, M. V. 2003. A mechanical analysis on recycled PET/HDPE composites. *Polymer Degradation and Stability,* 80, 373-382.

Aznar, M. P., Caballero, M. A., Sancho, J. A. & Francés, E. 2006. Plastic waste elimination by co-gasification with coal and biomass in fluidized bed with air in pilot plant. *Fuel Processing Technology,* 87, 409-420.

Baden Fuller, A. 1979. *Microwaves: An introduction to microwave theory and technique,* Oxford and New York, Pergamon Press.

Bai, X., Isaac, D. H. & Smith, K. 2007. Reprocessing acrylonitrile–butadiene–styrene plastics: Structure–property relationships. *Polymer Engineering & Science,* 47, 120-130.

Balart, R., Sánchez, L., López, J. & Jiménez, A. 2006. Kinetic analysis of thermal degradation of recycled polycarbonate/acrylonitrile–butadiene–styrene mixtures from waste electric and electronic equipment. *Polymer Degradation and Stability,* 91, 527-534.

Ballice, L. 2001. A kinetic approach to the temperature-programmed pyrolysis of low- and high-density polyethylene in a fixed bed reactor: determination of kinetic parameters for the evolution of n-paraffins and 1-olefins. *Fuel,* 80, 1923-1935.

Ballschmiter, K., Niemczyk, R., Schäfer, W. & Zoller, W. 1987. Isomer-specific identification of polychlorinated benzenes (PCBz) and -biphenyls (PCB) in effluents of Municipal waste incineration. *Fresenius' Journal of Analytical Chemistry,* 328, 583-587.

Bansal, N. P. & Singh, J. P. 2012. *Innovative Processing and Synthesis of Ceramics, Glasses, and Composites VI: Proceedings of the Symposium Held at the 104th Annual Meeting of The American Ceramic Society, April 28-May1, 2002 in Missouri, Ceramic Transactions*, John Wiley & Sons, Incorporated.

Behnisch, J. & Zimmermann, H. 1988. Proof of the kinetic reaction mechanism of PVC degradation using TA. *Journal of Thermal Analysis and Calorimetry,* 33, 191-196.

Beyler, C. L. & Hirschler, M. M. 2002. Thermal decomposition of polymers. NFPA.

Bilali, L., Benchanaa, M., El Harfi, K., Mokhlisse, A. & Outzourhit, A. 2005. A detailed study of the microwave pyrolysis of the Moroccan (Youssoufia) rock phosphate. *Journal of Analytical and Applied Pyrolysis,* 73, 1-15.

Bockhorn, H., Hentschel, J., Hornung, A. & Hornung, U. 1999a. Environmental engineering: Stepwise pyrolysis of plastic waste. *Chemical Engineering Science,* 54, 3043-3051.

Bockhorn, H., Hornung, A. & Hornung, U. 1998. Stepwise pyrolysis for raw material recovery from plastic waste. *Journal of Analytical and Applied Pyrolysis,* 46, 1-13.

Bockhorn, H., Hornung, A., Hornung, U., Jakobströer, P. & Kraus, M. 1999b. Dehydrochlorination of plastic mixtures. *Journal of Analytical and Applied Pyrolysis,* 49, 97-106.

Bockhorn, H., Hornung, A., Hornung, U. & Schawaller, D. 1999c. Kinetic study on the thermal degradation of polypropylene and polyethylene. *Journal of Analytical and Applied Pyrolysis,* 48, 93-109.

Bradshaw, S., Van Wyk, E. & De Swardt, J. 1998. Microwave heating principles and the application to the regeneration of granular activated carbon. *Journal of the South African Institute of Mining and Metallurgy(South Africa),* 98, 201-210.

Bren, U., Krzan, A. & Mavri, J. 2007. Microwave Catalysis through Rotationally Hot Reactive Species†. *The Journal of Physical Chemistry A,* 112, 166-171.

Brydson, J. A. 1999. *Plastics Materials[*Butterworth-Heinemann Limited.

Buekens, A. & Cen, K. 2011. Waste incineration, PVC, and dioxins. *Journal of Material Cycles and Waste Management,* 13, 190-197.

Buekens, A. & Huang, H. 1998. Comparative evaluation of techniques for controlling the formation and emission of chlorinated dioxins/furans in municipal waste incineration. *Journal of Hazardous Materials,* 62, 1-33.

Bur, A. J. 1985. Dielectric properties of polymers at microwave frequencies: a review. *Polymer,* 26, 963-977.

Cai, H. Y., Güell, A. J., Dugwell, D. R. & Kandiyoti, R. 1993. Heteroatom distribution in pyrolysis products as a function of heating rate and pressure. *Fuel,* 72, 321-327.

Calex Uk 2013. Emissivity Data Table. Calex Electronics Limited, Leedon House, Billington Road, Leighton Buzzard, Bedfordshire LU7 4TN.

Cerqueira, H. S., Ayrault, P., Datka, J. & Guisnet, M. 2000. Influence of coke on the acid properties of a USHY zeolite. *Microporous and Mesoporous Materials,* 38, 197-205.

Cha, C. Y., Kim, B. I., Lumpkin, R. E. & Quinga, E. M. Y. 1993. ELECTROMAGNETIC ENHANCEMENT OF CHEMICAL REACTIONS (Devolatilization of Char and Coal). *Fuel Science and Technology International,* 11, 1175-1202.

Chen, M., Siochi, E. J., Ward, T. C. & Mcgrath, J. E. 1993. Basic ideas of microwave processing of polymers. *Polymer Engineering & Science,* 33, 1092-1109.

Christmann, W., Kasiske, D., Klöppel, K. D., Partscht, H. & Rotard, W. 1989. Combustion of polyvinylchloride - an important source for the formation of PCDD/PCDF. *Chemosphere,* 19, 387-392.

Clark, D. E. & Sutton, W. H. 1996. Microwave processing of materials. *Annual Review of Materials Science,* 26, 299-331.

Clark, G. L. & Rhodes, H. D. 1940. Practical Evaluation of Commercial Rubber Carbon Blacks by X-Ray Diffraction. *Industrial & Engineering Chemistry Analytical Edition,* 12, 66-71.

Conner, W. C., Tompsett, G., Lee, K.-H. & Yngvesson, K. S. 2004. Microwave Synthesis of Zeolites: 1. Reactor Engineering. *The Journal of Physical Chemistry B,* 108, 13913-13920.

Corma, A. 1995. Inorganic solid acids and their use in acid-catalyzed hydrocarbon reactions. *Chemical Reviews,* 95, 559-614.

Council, A. P. 1999. Development of hydrocarbons for use in plastics recycling. *Technical Paper.*

Cullis, C. F. & Hirschler, M. M. 1983. The significance of thermoanalytical measurements in the assessment of polymer flammability. *Polymer,* 24, 834-840.

Damgaard, A., Riber, C., Fruergaard, T., Hulgaard, T. & Christensen, T. H. 2010. Life-cycle-assessment of the historical development of air pollution control and energy recovery in waste incineration. *Waste Management,* 30, 1244-1250.

Darwent, B. 1970. *Bond Dissociation Energies in Simple Molecules,* Washington, U.S. National Bureau of Standards.

Das, S., Mukhopadhyay, A., Datta, S. & Basu, D. 2009. Prospects of microwave processing: An overview. *Bulletin of Materials Science,* 32, 1-13.

Day, M., Shen, Z. & Cooney, J. D. 1999. Pyrolysis of auto shredder residue: experiments with a laboratory screw kiln reactor. *Journal of Analytical and Applied Pyrolysis,* 51, 181-200.

Del Remedio Hernández, M., García, Á. N. & Marcilla, A. 2007. Catalytic flash pyrolysis of HDPE in a fluidized bed reactor for recovery of fuel-like hydrocarbons. *Journal of Analytical and Applied Pyrolysis,* 78, 272-281.

Denison, R. A. 1996. ENVIRONMENTAL LIFE-CYCLE COMPARISONS OF RECYCLING, LANDFILLING, AND INCINERATION: A Review of Recent Studies. *Annual Review of Energy and the Environment,* 21, 191-237.

Di Cortemiglia, M. P. L., Camino, G., Costa, L. & Guaita, M. 1985. Thermal degradation of ABS. *Thermochimica Acta,* 93, 187-190.

Diaz, A. F. & Felix-Navarro, R. M. 2004. A semi-quantitative tribo-electric series for polymeric materials: the influence of chemical structure and properties. *Journal of Electrostatics,* 62, 277-290.

Domínguez, A., Menéndez, J. A., Fernández, Y., Pis, J. J., Nabais, J. M. V., Carrott, P. J. M. & Carrott, M. M. L. R. 2007. Conventional and microwave induced pyrolysis of coffee hulls for the production of a hydrogen rich fuel gas. *Journal of Analytical and Applied Pyrolysis,* 79, 128-135.

Dong, D., Tasaka, S., Aikawa, S., Kamiya, S., Inagaki, N. & Inoue, Y. 2001. Thermal degradation of acrylonitrile–butadiene–styrene terpolymer in bean oil. *Polymer Degradation and Stability,* 73, 319-326.

Drouzas, A. E. & Schubert, H. 1996. Microwave application in vacuum drying of fruits. *Journal of Food Engineering,* 28, 203-209.

Dupont, C., Chiriac, R., Gauthier, G. & Toche, F. 2014. Heat capacity measurements of various biomass types and pyrolysis residues. *Fuel,* 115, 644-651.

Durka, T., Stefanidis, G., Gerven, T. & Stankiewicz, A. 2010. On the accuracy and reproducibility of fiber optic (FO) and infrared (IR) temperature measurements of solid materials in microwave applications. *Measurement Science Technology,* 21.

Dyke, P. H., Foan, C. & Fiedler, H. 2003. PCB and PAH releases from power stations and waste incineration processes in the UK. *Chemosphere,* 50, 469-480.

Encinar, J. M. & González, J. F. 2008. Pyrolysis of synthetic polymers and plastic wastes. Kinetic study. *Fuel Processing Technology,* 89, 678-686.

Environment-Agency 2008. Technical Report No. 223-4598, Waste Facts *In:* Agency, E. (ed.). UK: Environment Agency.

European Commision 2000. Green Paper - Environemntal Issues of PVC. *In:* Comission, E. (ed.). Brussels, Belgium.

Evans, S. & Marsh, H. 1971. The chemistry of formation of semi-cokes from aromatic systems using mass-spectrometry—I: Carbonisation of single substances and mixtures thereof. *Carbon,* 9, 733-746.

Fan, J., De Bruyn, M., Budarin, V. L., Gronnow, M. J., Shuttleworth, P. S., Breeden, S., Macquarrie, D. J. & Clark, J. H. 2013. Direct Microwave-Assisted Hydrothermal Depolymerization of Cellulose. *Journal of the American Chemical Society,* 135, 11728-11731.

Fang, C. S. & Lai, P. M. C. 1996. MICROWAVE REGENERATION OF SPENT POWDER ACTIVATED CARBON. *Chemical Engineering Communications,* 147, 17-27.

Faravelli, T., Pinciroli, M., Pisano, F., Bozzano, G., Dente, M. & Ranzi, E. 2001. Thermal degradation of polystyrene. *Journal of Analytical and Applied Pyrolysis,* 60, 103-121.

Fătu, D., Geambaş, G., Segal, E., Budrugeac, P. & Ciutacu, S. 1989. On the thermal decomposition of the copolymer ABS and of nylon polyamide. *Thermochimica Acta,* 149, 181-187.

Flammersheim, H. J. & Opfermann, J. 1999. Formal kinetic evaluation of reactions with partial diffusion control. *Thermochimica Acta,* 337, 141-148.

Fletcher, T. H., Kerstein, A. R., Pugmire, R. J. & Grant, D. M. 1990. Chemical percolation model for devolatilization. 2. Temperature and heating rate effects on product yields. *Energy & Fuels,* 4, 54-60.

Fossey, J., Lefort, D. & Sorba, J. 1995. *Free radicals in organic chemistry*, Wiley.

Galema, S. A. 1997a. *Microwave Chemistry,* Cambridge, ROYAUME-UNI, Royal Society of Chemistry.

Galema, S. A. 1997b. Microwave chemistry. *Chemical Society Reviews,* 26, 233.

Gao, Z., Amasaki, I. & Nakada, M. 2003. A thermogravimetric study on thermal degradation of polyethylene. *Journal of Analytical and Applied Pyrolysis,* 67, 1-9.

Gasner, L. L., Denloye, A. O. & Regan, T. M. 1986. MICROWAVE AND CONVENTIONAL PYROLYSIS OF A BITUMINOUS COAL. *Chemical Engineering Communications,* 48, 349-354.

Gentil, E., Clavreul, J. & Christensen, T. H. 2009. Global warming factor of municipal solid waste management in Europe. *Waste management & research : the journal of the International Solid Wastes and Public Cleansing Association, ISWA,* 27, 850-860.

Giugliano, M., Cernuschi, S. & Ghezzi, U. 1989. The emission of dioxins and related compounds from the incineration of municipal solid wastes with high contents of organic chlorine (PVC). *Chemosphere,* 19, 407-411.

Green, L. E., Schmauch, L. J. & Worman, J. C. 1964. Simulated Distillation by Gas Chromatography. *Analytical Chemistry,* 36, 1512-1516.

Gudzinowicz, B. J., Gudzinowicz, M. J. & Martin, H. F. 1976. *Fundamentals of integrated GC-MS*, Dekker.

Gulab, H., Jan, M. R., Shah, J. & Manos, G. 2010. Plastic catalytic pyrolysis to fuels as tertiary polymer recycling method: Effect of process conditions. *Journal of Environmental Science and Health Part A,* 45, 908-915.

Gupta, S., Mohan, K., Prasad, R., Gupta, S. & Kansal, A. 1998. Solid waste management in India: options and opportunities. *Resources, Conservation and Recycling,* 24, 137-154.

Hayes, B. L. 2002. *Microwave synthesis: chemistry at the speed of light*, CEM Pub.

Hernandez, M., Garcia, A. & Marcilla, A. 2006. Catalytic flash pyrolysis of HDPE in a fluedized bed reactor for recovery of fuel like hydrocarbons. *Journal of Analytical and Applied Pyrolysis,* 78, 272-281.

Herrero, M. A., Kremsner, J. M. & Kappe, C. O. 2007. Nonthermal Microwave Effects Revisited: On the Importance of Internal Temperature Monitoring and Agitation in Microwave Chemistry. *The Journal of Organic Chemistry,* 73, 36-47.

Hill, J. M. & Marchant, T. R. 1996. Modelling microwave heating. *Applied Mathematical Modelling,* 20, 3-15.

Hirschler, M. M. 1986. Thermal decomposition (STA and DSC) of PVC compounds under a variety of atmospheres and heating rates. *European Polymer Journal,* 22, 153-160.

Hokuto Electronics Corporation, T. 2012. *New Super High Efficiency Magnetron 2M303* [Online]. http://www.hokuto.co.jp/00eng/e5500_sm/e5585_sm_inform_2m303.html: Toshiba Hokuto Electronics Corporation. [Accessed 15/07/12 2012].

Hopewell, J., Dvorak, R. & Kosior, E. 2009. Plastics recycling: challenges and opportunities. *Philosophical Transactions of the Royal Society B: Biological Sciences,* 364, 2115-2126.

Hosler, D., Burkett, S. L. & Tarkanian, M. J. 1999. Prehistoric Polymers: Rubber Processing in Ancient Mesoamerica. *Science,* 284, 1988-1991.

Houska, C. R. & Warren, B. E. 1954. Ray Study of the Graphitization of Carbon Black. *Journal of Applied Physics,* 25, 1503-1509.

Howell, S. G. 1992. A ten year review of plastics recycling. *Journal of Hazardous Materials,* 29, 143-164.

Huang, Y. F., Kuan, W. H., Lo, S. L. & Lin, C. F. 2008. Total recovery of resources and energy from rice straw using microwave-induced pyrolysis. *Bioresource Technology,* 99, 8252-8258.

Hübschmann, H. 2001. *Handbook of GC/MS: Fundamentals and Applications,* Federal Republic of Germany, Wiley-VCH.

Ito, M., Ushida, K., Nakao, N., Kikuchi, N., Nozaki, R., Asai, K. & Washio, M. 2006. Dechlorination of poly(vinyl chloride) by microwave irradiation I: A simple examination using a commercial microwave oven. *Polymer Degradation and Stability,* 91, 1694-1700.

Ivan Diaz-Loya, E., Allouche, E. N., Eklund, S., Joshi, A. R. & Kupwade-Patil, K. 2012. Toxicity mitigation and solidification of municipal solid waste incinerator fly ash using alkaline activated coal ash. *Waste Management,* 32, 1521-1527.

Jesch, R. L. & Mclaughlin, R. H. 1984. Dielectric Measurements of Oil Shale as Functions of Temperature And Frequency. *Geoscience and Remote Sensing, IEEE Transactions on,* GE-22, 99-105.

Jiang, G., Nowakowski, D. J. & Bridgwater, A. V. 2010. Effect of the Temperature on the Composition of Lignin Pyrolysis Products. *Energy & Fuels,* 24, 4470-4475.

Jiménez, A., Berenguer, V., López, J. & Sánchez, A. 1993. Thermal degradation study of poly(vinyl chloride): Kinetic analysis of thermogravimetric data. *Journal of Applied Polymer Science,* 50, 1565-1573.

Kaminsky, W. 1991. Recycling of polymeric materials by pyrolysis. *Makromolekulare Chemie. Macromolecular Symposia,* 48-49, 381-393.

Kaminsky, W. 1992. Possibilities and limits of pyrolysis. *Makromolekulare Chemie. Macromolecular Symposia,* 57, 145-160.

Kaminsky, W., Menzel, J. & Sinn, H. 1976. Recycling of plastics. *Conservation & Recycling,* 1, 91-110.

Kaminsky, W., Predel, M. & Sadiki, A. 2004. Feedstock recycling of polymers by pyrolysis in a fluidised bed. *Polymer Degradation and Stability,* 85, 1045-1050.

Kaminsky, W., Schlesselmann, B. & Simon, C. M. 1996. Thermal degradation of mixed plastic waste to aromatics and gas. *Polymer Degradation and Stability,* 53, 189-197.

Kang, H.-Y. & Schoenung, J. M. 2005. Electronic waste recycling: A review of U.S. infrastructure and technology options. *Resources, Conservation and Recycling,* 45, 368-400.

Kantarelis, E., Donaj, P., Yang, W. & Zabaniotou, A. 2009. Sustainable valorization of plastic wastes for energy with environmental safety via High-Temperature Pyrolysis (HTP) and High-Temperature Steam Gasification (HTSG). *Journal of Hazardous Materials,* 167, 675-684.

Kappe, C. O. 2013. How to measure reaction temperature in microwave-heated transformations. *Chemical Society Reviews,* 42, 4977-4990.

Kappe, C. O. & Dallinger, D. 2006. The impact of microwave synthesis on drug discovery. *Nat Rev Drug Discov,* 5, 51-63.

Katz, J. D. 1992. Microwave sintering of ceramics. *Annual Review of Materials Science,* 22, 153-170.

Kelen, T., Bàlint, G., Galambos, G., Tüdo, Amp, X030b & S, F. 1969. Polymer degradation by elimination—I. Thermal degradation of poly(vinyl chloride) and kinetic treatment of the process. *European Polymer Journal,* 5, 597-616.

Kimrey, H. D. & Janney, M. A. 1988. *Design principles for high-frequency microwave cavities*.

Kiran Ciliz, N., Ekinci, E. & Snape, C. E. 2004. Pyrolysis of virgin and waste polypropylene and its mixtures with waste polyethylene and polystyrene. *Waste Management,* 24, 173-181.

Kiselev, S. I., Sankey, J. C., Krivorotov, I. N., Emley, N. C., Schoelkopf, R. J., Buhrman, R. A. & Ralph, D. C. 2003. Microwave oscillations of a nanomagnet driven by a spin-polarized current. *Nature,* 425, 380-383.

Kpere-Diabo, T. 2009. *Plastic catalytic degradation study of the role of external catalytic surface, catalytic reusability and temperature effects.* Doctor of Philosophy, university College London.

Krieger-Brockett, B. 1994. Microwave Pyrolysis of Biomass. *Research on Chemical Intermediates* [Online], 20. Available: http://booksandjournals.brillonline.com/content/10.1163/156856794x00054.

Kriegsmann, G. A. 1992. Thermal runaway in microwave heated ceramics: A one dimensional model. *Journal of Applied Physics,* 71, 1960-1966.

Kubrakova, I. V. 2002. Microwave radiation in analytical chemistry: the scope and prospects for application. *Russian chemical reviews,* 71, 283-294.

Kuhnert, N. 2002. Microwave-Assisted Reactions in Organic Synthesis—Are There Any Nonthermal Microwave Effects? *Angewandte Chemie International Edition,* 41, 1863-1866.

Kumar, S., Panda, A. K. & Singh, R. 2011. A review on tertiary recycling of high-density polyethylene to fuel. *Resources, Conservation and Recycling,* 55, 893-910.

Lam, S. S., Russell, A. D., Lee, C. L. & Chase, H. A. 2012. Microwave-heated pyrolysis of waste automotive engine oil: Influence of operation parameters on the yield, composition, and fuel properties of pyrolysis oil. *Fuel,* 92, 327-339.

Larhed, M., Moberg, C. & Hallberg, A. 2002. Microwave-Accelerated Homogeneous Catalysis in Organic Chemistry. *Accounts of Chemical Research,* 35, 717-727.

Lattimer, R. P. & Kroenke, W. J. 1980. The formation of volatile pyrolyzates form poly(vinyl chloride). *Journal of Applied Polymer Science,* 25, 101-110.

Lattimer, R. P. & Kroenke, W. J. 1982. Mechanisms of formation of volatile aromatic pyrolyzates from poly(vinyl chloride). *Journal of Applied Polymer Science,* 27, 1355-1366.

Lattimer, R. P., Pausch, J. B. & Meuzelaar, H. L. C. 1983. Pyrolysis studies of chlorinated poly(vinyl chloride). *Macromolecules,* 16, 1896-1900.

Lea, W. R. 1996. Plastic incineration versus recycling: a comparison of energy and landfill cost savings. *Journal of Hazardous Materials,* 47, 295-302.

Lee, K.-H. 2006. Pyrolysis of municipal wastes seperated by difference of specific gravity. *Journal of Analytical and Applied Pyrolysis,* 79, 362-367.

Lewis, I. C. 1982. Chemistry of carbonization. *Carbon,* 20, 519-529.

Lewis, I. C. 1987. Chemistry of pitch carbonization. *Fuel,* 66, 1527-1531.

Lidström, P., Tierney, J., Wathey, B. & Westman, J. 2001. Microwave assisted organic synthesis—a review. *Tetrahedron,* 57, 9225-9283.

Ludlow-Palafox, C. & Chase, H. A. 2001. Microwave-Induced Pyrolysis of Plastic Wastes. *Industrial & Engineering Chemistry Research,* 40, 4749-4756.

Ludlow-Palafox, C. & Chase, H. A. 2006. Microwave Pyrolysis of Plastic Wastes. *Feedstock Recycling and Pyrolysis of Waste Plastics.* John Wiley & Sons, Ltd.

Lundin, L. & Marklund, S. 2008. Distribution of Mono to Octa-chlorinated PCDD/Fs in Fly Ash from a Municipal Solid-Waste Incinerator. *Environmental Science & Technology,* 42, 1245-1250.

Mamleev, V., Bourbigot, S., Le Bras, M., Duquesne, S. & Sestak, J. 2000. Modelling of nonisothermal kinetics in thermogravimetry. *Physical Chemistry Chemical Physics,* 2, 4708-4716.

Manos, G., Garforth, A. & Dwyer, J. 2000. Catalytic Degradation of High-Density Polyethylene over Different Zeolitic Structures. *Industrial & Engineering Chemistry Research,* 39, 1198-1202.

Mantaux, O., Lorriot, T., Chibalon, L., Aurrekoetxea, J., Puerto, A., Arostegi, A. & Urrutibeascoa, I. 2004. Recycling study of end of life products made of ABS resin. *Journal of material science and technology,* 20, 125-128.

Marand, E., Baker, K. R. & Graybeal, J. D. 1992. Comparison of reaction mechanisms of epoxy resins undergoing thermal and microwave cure from in situ measurements of microwave dielectric properties and infrared spectroscopy. *Macromolecules,* 25, 2243-2252.

Marchant, T. R. & Pincombe, A. H. 1994. Microwave heating of materials with temperature-dependent wavespeed. *Wave Motion,* 19, 67-81.

Marcilla, A. & Beltrán, M. 1995. Thermogravimetric kinetic study of poly(vinyl chloride) pyrolysis. *Polymer Degradation and Stability,* 48, 219-229.

Marongiu, A., Faravelli, T., Bozzano, G., Dente, M. & Ranzi, E. 2003. Thermal degradation of poly(vinyl chloride). *Journal of Analytical and Applied Pyrolysis,* 70, 519-553.

Maskan, M. 2000. Microwave/air and microwave finish drying of banana. *Journal of Food Engineering,* 44, 71-78.

Mattila, H., Virtanen, T., Vartiainen, T. & Ruuskanen, J. 1992. Emissions of polychlorinated dibenzo-p-dioxins and dibenzofurans in flue gas from co-combustion of mixed plastics with coal and bark. *Chemosphere,* 25, 1599-1609.

Mba-Polymers 1998. Development of hydrocyclones for use in plastic recycling. *American Plastics Council*.

Mcneill, I. C., Memetea, L. & Cole, W. J. 1995. A study of the products of PVC thermal degradation. *Polymer Degradation and Stability,* 49, 181-191.

Menéndez, J. A., Inguanzo, M. & Pis, J. J. 2002. Microwave-induced pyrolysis of sewage sludge. *Water Research,* 36, 3261-3264.

Menéndez, J. A., Juárez-Pérez, E. J., Ruisánchez, E., Bermúdez, J. M. & Arenillas, A. 2011. Ball lightning plasma and plasma arc formation during the microwave heating of carbons. *Carbon,* 49, 346-349.

Mersiowsky, I., Stegmann, R. & Ejlertsson, J. 1999. Long term behaviour of poly(vinyl chloride) products under soil buried and landfill conditions. *Plastics, Rubber and Composites,* 28, 321-326.

Mersiowsky, I., Weller, M. & Ejlertsson, J. 2001. Fate of Plasticised PVC Products under Landfill Conditions: A Laboratory-Scale Landfill Simulation Reactor Study. *Water Research,* 35, 3063-3070.

Miklavc, A. 2001. Strong Acceleration of Chemical Reactions Occurring Through the Effects of Rotational Excitation on Collision Geometry. *ChemPhysChem,* 2, 552-555.

Miranda, M., Pinto, F., Gulyurtlu, I., Cabrita, I., Nogueira, C. A. & Matos, A. 2010. Response surface methodology optimization applied to rubber tyre and plastic wastes thermal conversion. *Fuel,* 89, 2217-2229.

Miranda, R., Pakdel, H., Roy, C. & Vasile, C. 2001a. Vacuum pyrolysis of commingled plastics containing PVC II. Product analysis. *Polymer Degradation and Stability,* 73, 47-67.

Miranda, R., Yang, J., Roy, C. & Vasile, C. 1999. Vacuum pyrolysis of PVC I. Kinetic study. *Polymer Degradation and Stability,* 64, 127-144.

Miranda, R., Yang, J., Roy, C. & Vasile, C. 2001b. Vacuum pyrolysis of commingled plastics containing PVC I. Kinetic study. *Polymer Degradation and Stability,* 72, 469-491.

Miskolczi, N., Bartha, L., Deák, G. & Jóver, B. 2004. Thermal degradation of municipal plastic waste for production of fuel-like hydrocarbons. *Polymer Degradation and Stability,* 86, 357-366.

Miura, M., Kaga, H., Sakurai, A., Kakuchi, T. & Takahashi, K. 2004. Rapid pyrolysis of wood block by microwave heating. *Journal of Analytical and Applied Pyrolysis,* 71, 187-199.

Mølgaard, C. 1995. Environmental impacts by disposal of plastic from municipal solid waste. *Resources, Conservation and Recycling,* 15, 51-63.

Monsef-Mirzai, P., Ravindran, M., Mcwhinnie, W. R. & Burchill, P. 1995. Rapid microwave pyrolysis of coal: Methodology and examination of the residual and volatile phases. *Fuel,* 74, 20-27.

Montaudo, G. & Puglisi, C. 1991. Evolution of aromatics in the thermal degradation of poly(vinyl chloride): A mechanistic study. *Polymer Degradation and Stability,* 33, 229-262.

Moriwaki, S., Machida, M., Tatsumoto, H., Kuga, M. & Ogura, T. 2006a. A study on thermal runaway of poly(vinyl chloride) by microwave irradiation. *Journal of Analytical and Applied Pyrolysis,* 76, 238-242.

Moriwaki, S., Machida, M., Tatsumoto, H., Otsubo, Y., Aikawa, M. & Ogura, T. 2006b. Dehydrochlorination of poly(vinyl chloride) by microwave irradiation. *Applied Thermal Engineering,* 26, 745-750.

Muto, H. & Takizawa, Y. 1992. Potential health risk via inhalation/ingestion exposure to polychlorinated dibenzo-p-dioxins and dibenzofurans. *Bulletin of Environmental Contamination and Toxicology,* 49, 701-707.

National-Scientific-Company. 2013. *Fused quartz properties & usage guide* [Online]. Quakertown, Ohio, U.S.A: National Scientific Laboratory. Available: http://www.quartz.com/gedata.html [Accessed 27.04.13 2013].

Osada, F. & Yoshioka, T. 2009. Dechlorination of polyvinyl chloride in NaOH/ethylene glycol solution by microwave heating. *Journal of Material Cycles and Waste Management,* 11, 19-22.

Ozawa, T. 1993. Industrial standardization of thermal analysis in Japan. *Journal of Thermal Analysis and Calorimetry,* 40, 1379-1398.

Panda, A. K., Singh, R. K. & Mishra, D. K. 2010. Thermolysis of waste plastics to liquid fuel: A suitable method for plastic waste management and manufacture of value added products—A world prospective. *Renewable and Sustainable Energy Reviews,* 14, 233-248.

Parfitt, J. 2002. Analysis of household waste composition and factors driving waste increases, WRAP for strategy unit. *Government Cabinet Office, London, UK.*

Perdan, S. 2005. Introduction to Sustainable Development. *Sustainable Development in Practice.* John Wiley & Sons, Ltd.

Pert, E., Carmel, Y., Birnboim, A., Olorunyolemi, T., Gershon, D., Calame, J., Lloyd, I. K. & Wilson, O. C. 2001. Temperature Measurements during Microwave Processing: The Significance of Thermocouple Effects. *Journal of the American Ceramic Society,* 84, 1981-1986.

Pincombe, A. H. & Smyth, N. F. 1991. Microwave Heating of Materials with Low Conductivity. *Proceedings of the Royal Society of London. Series A: Mathematical and Physical Sciences,* 433, 479-498.

Polli, H., Pontes, L. a. M., Araujo, A. S., Barros, J. F. & Fernandes, V. J., Jr. 2009. Degradation behavior and kinetic study of ABS polymer. *Journal of Thermal Analysis and Calorimetry,* 95, 131-134.

Qian, K., Killinger, W. E., Casey, M. & Nicol, G. R. 1996. Rapid Polymer Identification by In-Source Direct Pyrolysis Mass Spectrometry and Library Searching Techniques. *Analytical Chemistry,* 68, 1019-1027.

Raia, J. C., Villalanti, D. C., Subramanian, M. & Williams, B. 2000. Application of High-Temperature Simulated Distillation to the Residuum Oil Supercritical Extraction Process in Petroleum Refining. *Journal of Chromatographic Science,* 38, 1-5.

Rao, K. J., Vaidhyanathan, B., Ganguli, M. & Ramakrishnan, P. A. 1999. Synthesis of Inorganic Solids Using Microwaves. *Chemistry of Materials,* 11, 882-895.

Retsch. 2012. *Cryomill* [Online]. Retsch. [Accessed 24/06/12 2012].

Robinson, J., Kingman, S., Irvine, D., Licence, P., Smith, A., Dimitrakis, G., Obermayer, D. & Kappe, C. O. 2010. Understanding microwave heating effects in single mode type cavities-theory and experiment. *Physical Chemistry Chemical Physics,* 12, 4750-4758.

Russell, N. V., Beeley, T. J., Man, C. K., Gibbins, J. R. & Williamson, J. 1998. Development of TG measurements of intrinsic char combustion reactivity for industrial and research purposes. *Fuel Processing Technology,* 57, 113-130.

Saad, A. L. G., Sayed, W. M., Ahmed, M. G. M. & Hassan, A. M. 1999. Preparation and properties of some filled poly(vinyl chloride) compositions. *Journal of Applied Polymer Science,* 73, 2657-2670.

Saha, B., Maiti, A. & Ghoshal, A. 2006. Model-free method for isothermal and non-isothermal decomposition kinetics analysis of PET sample. *Thermochimica Acta,* 444, 46-52.

Sakai, S., Hiraoka, M., Takeda, N. & Shiozaki, K. 1993. Coplanar PCBs and PCDDs/PCDFs in municipal waste incineration. *Chemosphere,* 27, 233-240.

Salema, A. A. & Ani, F. N. 2011. Microwave induced pyrolysis of oil palm biomass. *Bioresource Technology,* 102, 3388-3395.

Salema, A. A. & Ani, F. N. 2012. Pyrolysis of oil palm empty fruit bunch biomass pellets using multimode microwave irradiation. *Bioresource Technology,* 125, 102-107.

Santos, T., Costa, L., Valente, M., Monteiro, J. & Sousa, J. 2010. 3D electromagnetic field simulation in microwave ovens: a tool to control thermal runaway. *COMSOL.* Paris.

Scheirs, J. & Kaminsky, W. 2006. *Feedstock Recycling and Pyrolysis of Waste Plastics: Converting Waste Plastics into Diesel and Other Fuels*, Wiley.

Schlomann, E., Green, J. J. & Milano, U. 1960. Recent Developments in Ferromagnetic Resonance at High Power Levels. *Journal of Applied Physics,* 31, S386-S395.

Schlomann, E., Joseph, R. I. & Bady, I. 1963. Spin Wave Instability in Hexagonal Ferrites With a Preferential Plane. *Journal of Applied Physics,* 34, 672-681.

Sekine, Y. & Fujimoto, K. 2003. Catalytic degradation of PP with an Fe/activated carbon catalyst. *Journal of Material Cycles and Waste Management,* 5, 107-112.

Serrano, D. P., Aguado, J., Escola, J. M. & Garagorri, E. 2001. Conversion of low density polyethylene into petrochemical feedstocks using a continuous screw kiln reactor. *Journal of Analytical and Applied Pyrolysis,* 58–59, 789-801.

Shang, H., Snape, C. E., Kingman, S. W. & Robinson, J. P. 2006. Microwave treatment of oil-contaminated North Sea drill cuttings in a high power multimode cavity. *Separation and Purification Technology,* 49, 84-90.

Shapi, M. M. 1991. TG and DSC studies of some thermal properties and stability aspects of poly(acrylonitrile butadiene styrene), polystyrene and poly(acrylonitrile styrene) plastics. *Thermochimica Acta,* 175, 25-34.

Shent, H., Pugh, R. J. & Forssberg, E. 1999. A review of plastics waste recycling and the flotation of plastics. *Resources, Conservation and Recycling,* 25, 85-109.

Siddiqui, M. N. & Redhwi, H. H. 2009. Pyrolysis of mixed plastics for the recovery of useful products. *Fuel Processing Technology,* 90, 545-552.

Sigma-Aldrich. 2013. *Poly(acrylonitrile-co-butadiene-co-styrene)* [Online]. Sigma-Aldrich. Available: http://www.sigmaaldrich.com/catalog/product/aldrich/180882?lang=en&region=GB [Accessed 29th March 2013 2013].

Sparks, M. 1965. Ferromagnetic Resonance Porosity Linewidth Theory in Polycrystalline Insulators. *Journal of Applied Physics,* 36, 1570-1573.

Stadler, A., Yousefi, B. H., Dallinger, D., Walla, P., Van Der Eycken, E., Kaval, N. & Kappe, C. O. 2003. Scalability of Microwave-Assisted Organic Synthesis. From Single-Mode to Multimode Parallel Batch Reactors. *Organic Process Research & Development,* 7, 707-716.

Starnes Jr, W. H. 2002. Structural and mechanistic aspects of the thermal degradation of poly(vinyl chloride). *Progress in Polymer Science,* 27, 2133-2170.

Steeman, P. a. M., Gondard, C. & Scherrenberg, R. L. 1994. A broad-band dielectric study of poly(vinyl chloride): Effect of molar mass and processing conditions on space-charge mechanisms. *Journal of Polymer Science Part B: Polymer Physics,* 32, 119-130.

Strauss, C. & Trainor, R. 1995. Developments in Microwave-Assisted Organic Chemistry. *Australian Journal of Chemistry,* 48, 1665-1692.

Stromberg, R. R., Straus, S. & Achhammer, B. G. 1959. Thermal decomposition of poly(vinyl chloride). *Journal of Polymer Science,* 35, 355-368.

Sturm, G. S. J., Verweij, M. D., Van Gerven, T., Stankiewicz, A. I. & Stefanidis, G. D. 2012. On the effect of resonant microwave fields on temperature distribution in time and space. *International Journal of Heat and Mass Transfer,* 55, 3800-3811.

Suhl, H. 1956. The Nonlinear Behavior of Ferrites at High Microwave Signal Levels. *Proceedings of the IRE,* 44, 1270-1284.

Sutton, W. H., Brooks, M. H. & Chabinsky, I. I. 1988. *Microwave processing of materials*.

Suzuki, M. & Wilkie, C. A. 1995. The thermal degradation of acrylonitrile-butadiene-styrene terpolymei as studied by TGA/FTIR. *Polymer Degradation and Stability,* 47, 217-221.

Tang, L. & Huang, H. 2005. Plasma Pyrolysis of Biomass for Production of Syngas and Carbon Adsorbent. *Energy & Fuels,* 19, 1174-1178.

Tawansi, A., Zidan, H. M. & Eldumiaty, A. H. 1998. Electron Spin Resonance, Magnetic and Optical Properties of MnCl2 Filled PVC Films. *Polymer Testing,* 17, 211-224.

Thostenson, E. T. & Chou, T. W. 1999. Microwave processing: fundamentals and applications. *Composites Part A: Applied Science and Manufacturing,* 30, 1055-1071.

Tong, H. Y. & Karasek, F. W. 1984. Flame ionization detector response factors for compound classes in quantitative analysis of complex organic mixtures. *Analytical Chemistry,* 56, 2124-2128.

Troitskii, B. B., Troitskaya, L. S., Myakov, V. N. & Lepaev, A. F. 1973. Mechanism of the thermal degradation of poly(vinyl chloride). *Journal of Polymer Science: Polymer Symposia,* 42, 1347-1361.

Tsang, W. 1990. Mechanisms for the Formation and Destruction of Chlorinated Organic Products of Incomplete Combustion. *Combustion Science and Technology,* 74, 99-116.

Tsuchiya, Y. & Sumi, K. 1969. Thermal decomposition products of polypropylene. *Journal of Polymer Science,* 7, 1599-1607.

Tu, W. & Liu, H. 2000. Continuous Synthesis of Colloidal Metal Nanoclusters by Microwave Irradiation. *Chemistry of Materials,* 12, 564-567.

Tukker, A. 1996. A PVC substance flow analysis for Sweden. Part II:Mass flows and emissions by PVC chain section.

Tukker, A. 2002. Plastic waste feedstock recycling, chemical recycling and incineration. *Rapara Review Reports*.

Turner, I. W. & Jolly, P. C. 1991. COMBINED MICROWAVE AND CONVECTIVE DRYING OF A POROUS MATERIAL. *Drying Technology,* 9, 1209-1269.

Uchida, S., Kamo, H., Kubota, H. & Kanaya, K. 1983. Reaction kinetics of formation of hydrochloric acid in municipal refuse incinerators. *Industrial & Engineering Chemistry Process Design and Development,* 22, 144-149.

Ungár, T., Gubicza, J., Ribárik, G., Pantea, C. & Zerda, T. W. 2002. Microstructure of carbon blacks determined by X-ray diffraction profile analysis. *Carbon,* 40, 929-937.

Van Der Peyl, G. J. Q., Linnartz, T. C. T., Van Rossum, C. a. J. J. & Zeelenberg, M. 1991. Identification of polar monomers in poly acrylate dispersions with pyrolysis-gas chromatography/mass spectrometry. *Journal of Analytical and Applied Pyrolysis,* 19, 279-283.

Vasile, C., Brebu, M. A., Karayildirim, T., Yanik, J. & Darie, H. 2006. Feedstock recycling from plastic and thermoset fractions of used computers (I): pyrolysis. *Journal of Material Cycles and Waste Management,* 8, 99-108.

Villalanti, D. C., Raia, J. C. & Maynard, J. B. 2006. High-temperature Simulated Distillation Applications in Petroleum Characterization. *Encyclopedia of Analytical Chemistry.* John Wiley & Sons, Ltd.

Von Hippel, A. R. 1966. *Dielectric Materials and Applications: Papers by Twenty-two Contributors*, MIT Press.

Vyazovkin, S. 1996. A unified approach to kinetic processing of nonisothermal data. *International Journal of Chemical Kinetics,* 28, 95-101.

Wagner, J. C. & Green, A. E. S. 1993. Correlation of chlorinated organic compound emissions from incineration with chlorinated organic input. *Chemosphere,* 26, 2039-2054.

Wallace, M., Attwood, D., Day, R. & Heatley, F. 2006a. Investigation of the microwave curing of the PR500 epoxy resin system. *Journal of Materials Science,* 41, 5862-5869.

Wallace, M., Attwood, D., Day, R. J. & Heatley, F. 2006b. Investigation of the microwave curing of the PR500 epoxy resin system. *Journal of Materials Science,* 41, 5862-5869.

Wan, J. 1993. Microwaves and chemistry: The catalysis of an exciting marriage. *Research on Chemical Intermediates,* 19, 147-158.

Wang, C. a. F., R. 2005. Simulated distillation system for ASTM D2887, based on the Agilent 6890 GC [Accessed 08/07/2012].

Wang, Z., Guo, Q., Liu, X. & Cao, C. 2007. Low Temperature Pyrolysis Characteristics of Oil Sludge under Various Heating Conditions. *Energy & Fuels,* 21, 957-962.

Will, H., Scholz, P., Ondruschka, B. & Burckhardt, W. 2003. Multimode Microwave Reactor for Heterogeneous Gas-Phase Catalysis. *Chemical Engineering & Technology,* 26, 1146-1149.

Williams, E. A. & Williams, P. T. 1997. The pyrolysis of individual plastics and a plastic mixture in a fixed bed reactor. *Journal of Chemical Technology & Biotechnology,* 70, 9-20.

Williams, P. T. & Williams, E. A. 1998. Interaction of Plastics in Mixed-Plastics Pyrolysis. *Energy & Fuels,* 13, 188-196.

Williams, P. T. & Williams, E. A. 1999. Fluidised bed pyrolysis of low density polyethylene to produce petrochemical feedstock. *Journal of Analytical and Applied Pyrolysis,* 51, 107-126.

Wollny, V., Dehoust, G., Fritsche, U. R. & Weinem, P. 2001. Comparison of Plastic Packaging Waste Management Options: Feedstock Recycling versus Energy Recovery in Germany. *Journal of Industrial Ecology,* 5, 49-63.

Wu, C.-H., Chang, C.-Y., Hor, J.-L., Shih, S.-M. & Chen, L.-W. 1994. Pyrolysis kinetics of waste PVC at high conversion. *The Chemical Engineering Journal and the Biochemical Engineering Journal,* 55, 87-92.

Xia, D. K. & Picklesi, C. A. 2000. Microwave caustic leaching of electric arc furnace dust. *Minerals Engineering,* 13, 79-94.

Xiao, C., Allen, L., Biddle, M. B. & Fisher, M. M. Electrostatic separation and recovery of mixed plastics. Society of plastics engineers (SPE) annual recycling conference (ARC), 1999.

Yan, H., Huang, X., Zhonghua, L., Huang, H., Xue, R. & Chen, L. 1997. Microwave synthesis of LiCoO2 cathode materials. *Journal of Power Sources,* 68, 530-532.

Yang, S., Rafael Castilleja, J., Barrera, E. V. & Lozano, K. 2004. Thermal analysis of an acrylonitrile–butadiene–styrene/SWNT composite. *Polymer Degradation and Stability,* 83, 383-388.

Yarlagadda, P. K. D. V. & Chai, T. C. 1998. An investigation into welding of engineering thermoplastics using focused microwave energy. *Journal of Materials Processing Technology,* 74, 199-212.

Yatsun, A., Konovalov, P. & Konovalov, N. 2008. Gaseous products of microwave pyrolysis of scrap tires. *Solid Fuel Chemistry,* 42, 187-191.

Zhao, H.-Y., Cao, Y., Sit, S., Lineberry, Q. & Pan, W.-P. 2012. Thermal characteristics of bitumen pyrolysis. *Journal of Thermal Analysis and Calorimetry,* 107, 541-547.

Zhao, L. & Yao, K. L. 2000. Effect of inter-site electron-electron interaction on the spin-wave excitation in quasi-one-dimensional organic magnetic polymer. *Journal of Physics: Condensed Matter,* 12, 5735.

Zhao, X., Song, Z., Liu, H., Li, Z., Li, L. & Ma, C. 2010. Microwave pyrolysis of corn stalk bale: A promising method for direct utilization of large-sized biomass and syngas production. *Journal of Analytical and Applied Pyrolysis,* 89, 87-94.

Zheng, Y., Yanful, E. K. & Bassi, A. S. 2005. A Review of Plastic Waste Biodegradation. *Critical Reviews in Biotechnology,* 25, 243-250.

Zhou, L., Wang, Y., Huang, Q. & Cai, J. 2006. Thermogravimetric characteristics and kinetic of plastic and biomass blends co-pyrolysis. *Fuel Processing Technology,* 87, 963-969.

Zia, K. M., Bhatti, H. N. & Ahmad Bhatti, I. 2007. Methods for polyurethane and polyurethane composites, recycling and recovery: A review. *Reactive and Functional Polymers,* 67, 675-692.

Zlotorzynski, A. 1995. The Application of Microwave Radiation to Analytical and Environmental Chemistry. *Critical Reviews in Analytical Chemistry,* 25, 43-76.

Zong, L., Zhou, S., Sgriccia, N., Hawley, M. C. & Kempel, L. C. 2003. A review of microwave-assisted polymer chemistry (MAPC). *J Microw Power Electromagn Energy,* 38, 49-74.

Zou, J.-Z., Zeng, X.-R., Xiong, X.-B., Tang, H.-L., Li, L., Liu, Q. & Li, Z.-Q. 2007. Preparation of vapor grown carbon fibers by microwave pyrolysis chemical vapor deposition. *Carbon,* 45, 828-832.

Zuo, W., Tian, Y. & Ren, N. 2011. The important role of microwave receptors in bio-fuel production by microwave-induced pyrolysis of sewage sludge. *Waste Management,* 31, 1321-1326.

10 Appendix A

Experiments were undertaken to examine the microwave decomposition of polypropylene and polyethylene Terephthalate using the same experimental setup has ABS and PVC. However due to the decomposition kinetics of these plastics it was found that every polarisation of products took place within the condensing system resulting in blockage and experimental failure. As such the current microwave setup was deemed not practical for the investigation of these polymers. In order to investigate these it would be necessary to design such experimental apparatus with larger gas-flow apertures so that blockages did not occur and the four product distribution could then be analysed in a similar vein to that of ABS and PVC. However, for those a re-polymerised polymers and it would be necessary to undertake such techniques as GPC FT-IR and HPLC to fully determine the product distribution has GC techniques are likely to be able to cope with the higher molecular weight compounds produced.

11 Appendix B

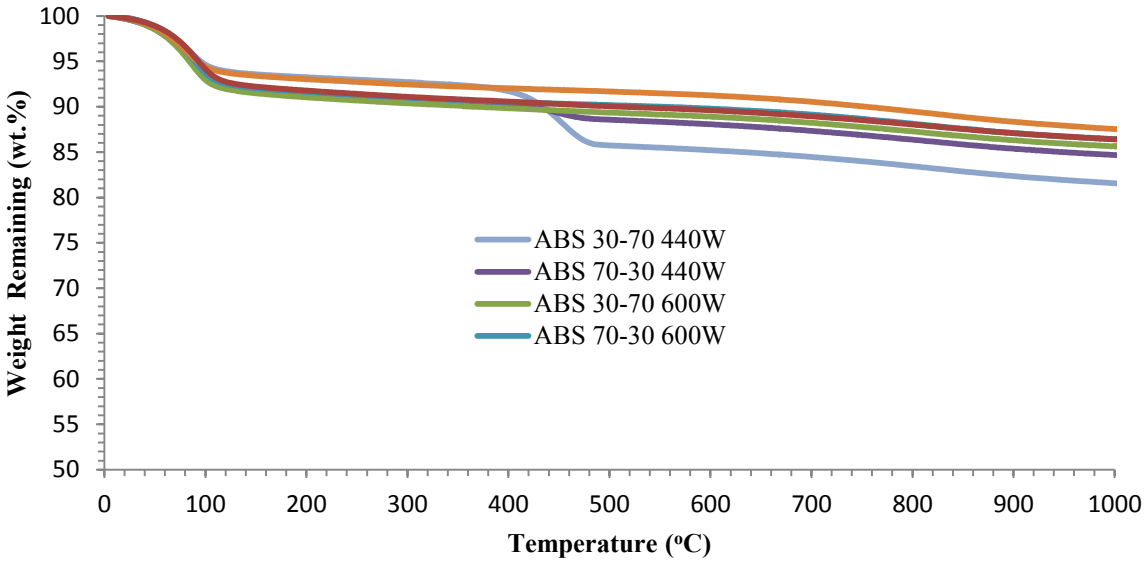


Figure 11-1 Thermal Degradation Profiles of ABS Chars Post Experiments for the Powers of 440W, 600W and 850W

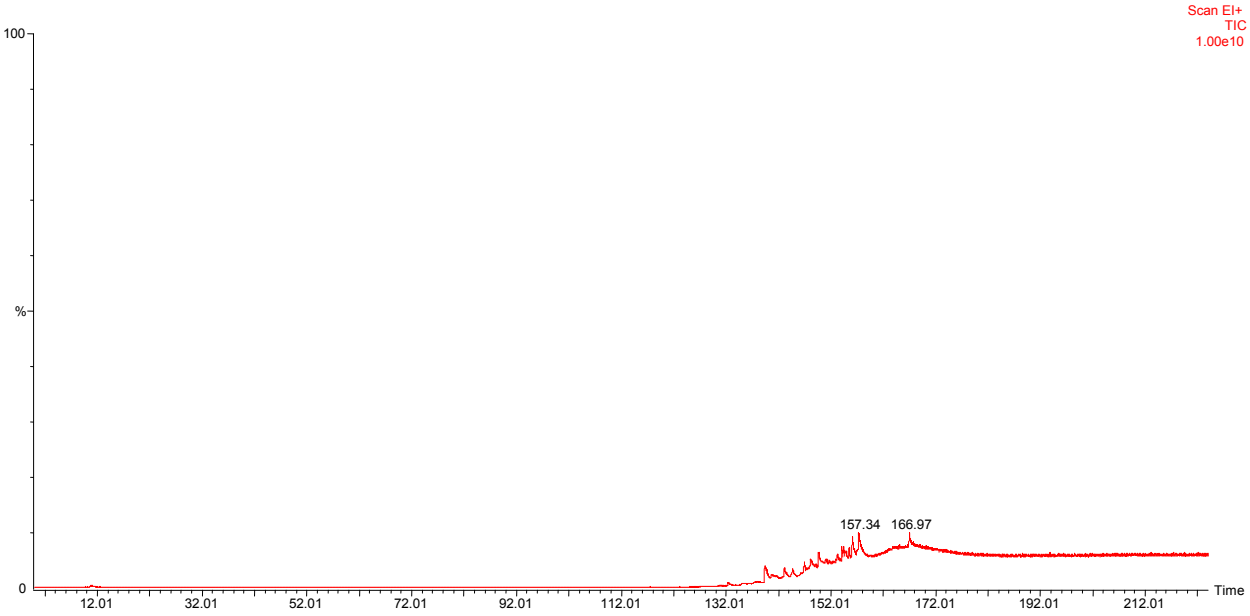


Figure 11-2 Typical py-GC/MS (0-1000°C at 10,000°C/min) of ABS char residue after microwave exposure

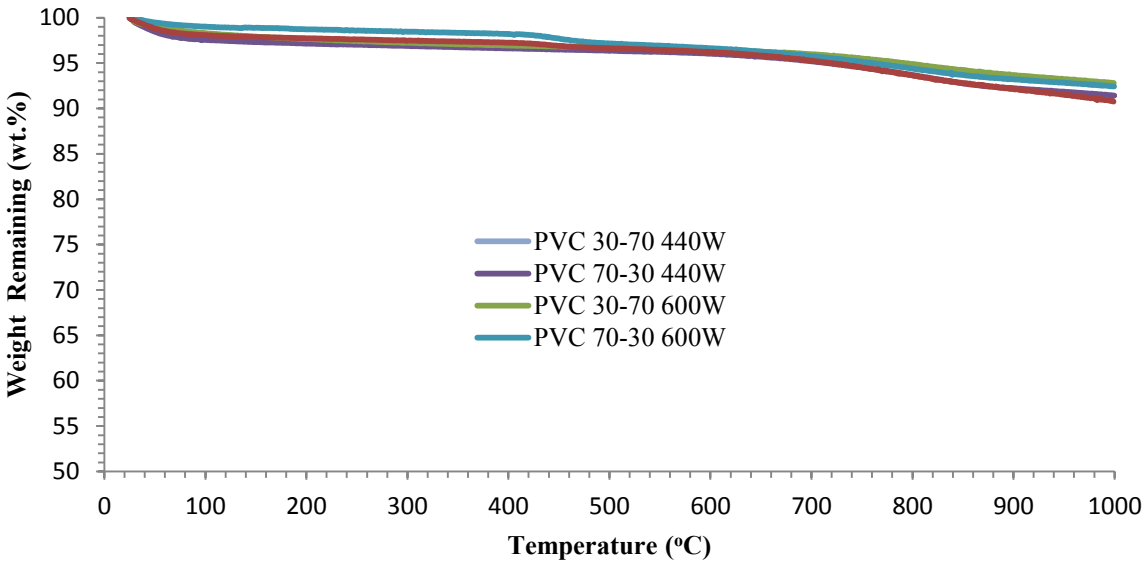


Figure 11-3 Thermal Degradation Profiles of PVC Chars Post Experiments for the Powers of 440W, 600W and 850W



Figure 11-4 Typical py-GC/MS (0-1000oC at 10,000°C/min) of ABS char residue after microwave exposure